The Relationship Between Programmed Cell Death And The Cell Cycle In The Tobacco BY-2 Cell Line

Craig Brailsford Orchard

September 2004

Cardiff School of Biosciences
Cardiff University
Museum Avenue
Cardiff
CF10 3TL

ProQuest LLC
789 East Eisenhower Parkway
P.O. Box 1346
Ann Arbor, MI 48106-1346

Acknowledgements

I would like to thank both the University of Wales and University College Worcester for the funding of my PhD. I would also like to thank my supervisors Dennis Francis, Hilary Rogers, and Robert Herbert without whose support this thesis would not have been completed. Special thanks go to Mike O'Reilly for his technical help over the past few years. A big thank you to all my friends who have believed in me including Jon, Jim, Ben, Dan, Kerry, Stef, to name but a few. I would especially like to thank my parents, Keith and Linda, for their support both financially and emotionally. This thesis is dedicated to all of above, but in particular Mererid, my partner and above all else my closest friend.

Contents

2. Materials And Methods

4. 1-Methylcyclopropene Ameliorates Both Ethylene-Induced And Wild-Type Mortality Levels

5. Expression Of The Mutated *Arabidopsis* Ethylene Receptor, *etr1-1*, In The Tobacco BY-2 Cell Line

7. General Discussion

Abbreviations

1-MCP	-	1-Methylcyclopropene:
2, 4-D	-	2, 4-Dichlorophenoxyacetic acid.
2xYT	-	Medium used to grow *Agrobacterium* (see appendix I).
At	-	*Arabidopsis thaliana.*
AT	-	Ataxia teleangiectasia
Atetr1	-	Mutated version of the *Arabidopsis* ETR1 gene.
Atetr1-1	-	Mutated version of the *Arabidopsis* ETR1 gene.
Atetr^e	-	*Atetr1* expressing.
ATM	-	Ataxia-teleangniectasia mutated
ATP	-	Adenosine Triphosphate.
ATR	-	Ataxia-teleangniectasia related
AVG	-	Aviglycine.
BSA	-	Bovine serum albumen.
BY-2	-	Tobacco Bright Yellow var. 2 cell line.
CAK	-	CDK-activating kinases.
CDK	-	Cyclin dependent kinase.
CKI	-	CDK Inhibitor.
cDNA	-	Complementary DNA.
CTAB	-	Hexadecyltrimethylammonium bromide.
CTD	-	Carboxy-terminal domain.
d	-	Day
dH_2O	-	Distilled water.
DMSO	-	Dimethylsulfoxide.
DNA	-	Deoxyribonucleic acid.
dNTPs	-	Deoxyribonucleotide triphosphates.
DTT	-	Dithiothreitol.
dUHP	-	Distilled ultra high purity water.
EDTA	-	Ethylene diaminetetraacetic acid.
EtBr	-	Ethidium bromide.
EREBP	-	Ethylene responsive binding protein
ETR	-	Ethylene receptor.
EV	-	Empty vector
FDA	-	Fluorescein diacetate.
g	-	Grammes.
G1	-	Gap 1.
G2	-	Gap 2.
GA	-	Gibberellic acid.
h	-	Hour
HCl	-	Hydrochloric acid.
HEPES	-	N-[2-hydroxyethyl]piperazine-N'-[2-ethanesulfonic Acid.
HR	-	Hypersensitive response.
HU	-	Hydroxyurea.
IR	-	Ionising radiation.

M	-	Molar.
mg	-	Milligrammes.
µg	-	Microgrammes.
µm	-	Micrometre
µM	-	Micromolar
mM	-	Millimolar.
mins	-	Minutes
M (Phase)	-	Mitosis phase of the cell cycle.
M&S	-	Murashige and Skoog basal salts.
mV	-	Millivolts
nm	-	Nanometres.
NaAc	-	Sodium acetate.
NBD	-	2, 5-Norbornadiene
OD	-	Optical density
OH	-	Hydroxy.
Os	-	*Oryza sativa*.
PAGE	-	Polyacrylamide gel electrophoresis.
PBS	-	Phosphate buffered saline solution.
PCD	-	Programmed cell death.
PCR	-	Polymerase chain reaction.
pgr	-	Plant growth regulator
PVDF	-	Polyvinylidene difluoride.
PI	-	Propidium iodide.
PMSF	-	Phenylmethylsulfonyl fluoride.
Rb	-	Retinoblastoma protein.
RNA	-	Ribonucleic acid.
ROS	-	Reactive oxygen species
SAG	-	Senescence associated gene.
SDS	-	Sodium laureth sulphate. Also known as sodium dodecyl sulphate.
SEVAG	-	24:1 chloroform: isoamyl alcohol.
S (Phase)	-	Synthesis phase
TAE	-	Tris, acetic acid, and EDTA (see appendix I).
Taq	-	DNA polymerase from *Thermophillus aquaticus*.
TBE	-	Tris, boric acid, and EDTA (see appendix I).
TBS	-	Tris buffered saline solution (see appendix I).
TdT	-	Deoxynucleotidyl transferase
TBY-2	-	Tobacco bright yellow var. 2 cell line.
TE	-	Tris, EDTA (see appendix I)
TEMED	-	N, N, N, N – Tetramethylethylenediamine.
Thiamine HCl	-	Thiamine hydrochloride.
Thr	-	Threonine
Tris	-	Tris[hydroxymethyl]aminomethane.
Tyr	-	Tyrosine.
Ub	-	Ubiquitin.
UHP	-	Ultra-high purity water.
UV	-	Ultraviolet light.
WT	-	Wild-type.
Zm	-	*Zea mays*

Abstract

Ethylene is an established plant growth regulator linked with programmed cell death (PCD). To investigate the relationship between the cell cycle and PCD, ethylene was used to see if it induced mortality in a cell cycle specific manner. Tobacco BY-2 cultures synchronized with aphidicolin were treated with ethylene. Cell cycle progression and mortality, measured at hourly intervals, showed distinct peaks of mortality at the G2/M boundary and S-phase. In conjunction with this, DNA fragmentation increased at G2/M. Furthermore, ethylene caused a significant reduction in cell size of the cycling population. Simultaneous addition of silver nitrate with ethylene ameliorated ethylene-induced G2/M mortality, although a toxic effect of silver alone was evident. Due to the toxicity of silver, 1-MCP, an alternative chemical for blocking ethylene receptors was used. 1-MCP neither affected the BY-2 cell cycle nor mortality levels. In addition, 1-MCP ameliorated ethylene-induced G2/M mortality. To balance the chemical approaches to blocking ethylene receptors, tobacco BY-2 cells were transformed with *Atetr1* that encodes a dominant insensitive form of the *Arabidopsis* ETR1 ethylene receptor. *Atetr1* expression caused a massive perturbation to the tobacco BY-2 cell cycle, especially in S-phase, and resulted in high levels of mortality throughout the cell cycle. Ethylene treatment caused a doubling of G2 duration but did not affect temporal distribution of mortality. However, ethylene treatment generated a peak of mortality in S-phase. These results suggest that ethylene induces PCD at G2/M through the known ethylene signaling pathway. Furthermore, it confirms that 1-MCP and *Atetr1* result in ethylene insensitivity.

To examine the G2/M transition, *Spcdc25*, a positive regulator of G2/M in fission yeast was transformed into the tobacco BY-2 cell line. This resulted in premature entry into mitosis, a shortened cell cycle, and reduced cell size. This was similar to *Spcdc25* over-expression in fission yeast and suggests the presence of a CDC25-like phosphatase in plants.

Chapter 1

Introduction

1. Introduction

In this thesis the work reported is about the extent to which programmed cell death is cell cycle specific using the tobacco BY-2 cell line as a model system. In order to provide background information between cell cycle regulation and exit into programmed cell death (PCD) a number of subject areas are covered in this introduction.

In the opening section, a general model of cell cycle regulation is presented and emphasis placed on the genes/proteins that regulate key transitions of the cell cycle. This includes a closer inspection of cell cycle checkpoints – brakes that prevent cells from proliferating until damage to DNA is repaired or DNA replication is normalised. In the next section emphasis is then given to PCD and its occurrences in development and pathogen attack. Apoptosis is described as well as mitochondrial involvement and the role of caspases in PCD is reviewed. This section ends with the role of the plant growth regulator ethylene in PCD. The penultimate section is an overview of the tobacco BY-2 cell line, the model system employed in my research. Finally, the aims of the research reported here, on the transition between cell proliferation and PCD, are stated in relation to the hypothesis that exit into PCD occurs predominantly in late G2.

1.1. The Eukaryotic Cell Cycle

The basic mechanisms and logic of cell cycle control are highly conserved in eukaryotes and therefore to a large extent so are the key genes that mediate cell cycle progression and control (Novak *et al.*, 1998; Potuschak and Doerner, 2001).

The mitotic cell cycle, the focus of this thesis, consists of alternating rounds of DNA replication (synthesis or S-phase) and chromosome segregation (mitosis or M-phase) interrupted by gaps known as G1 (the interval before S phase) and G2 (the interval

between S-phase and M-phase) (Fig. 1.1). Each phase, and the processes therein, are regulated to ensure that the daughter cells are competent for the next division. The main focus of regulation is at phase transitions and is achieved by cyclin-dependent kinases (CDKs) and their corresponding regulatory cyclin proteins. These complexes, originally identified in *Xenopus* eggs, are phospho-regulated by a series of proteins; primarily serine-threonine kinases and phosphatases (Russell and Nurse, 1986; Russell and Nurse, 1987).

There are two major transition points in the cell cycle: G1/S and G2/M (Van't Hof, 1974). Checkpoints exist at these transition points, ensuring cell viability throughout the cell cycle. If a problem occurs, these checkpoints ensure that cells are either repaired before progressing or exit into PCD if it is irresolvable (see section 1.2). The checkpoint at the G1/S transition ensures that cells are able to undergo DNA replication, and the G2/M checks that cells are able to commit to mitotic division (O'Connell *et al.*, 2000; Francis and Sorrell, 2001).

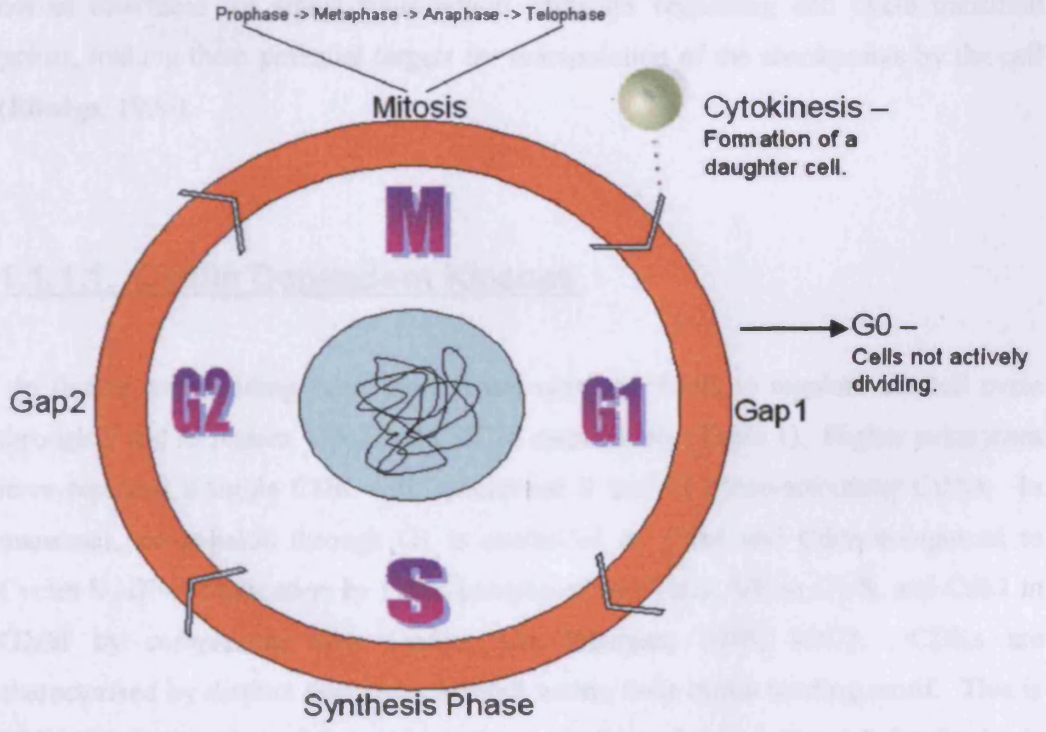

Figure 1.1. The Cell Cycle and its Component Phases. The cycle is divided into several phases an initial gap (G1), synthesis of DNA (S), a second gap (G2) and the final mitotic nuclear and cellular division (M) to result in two identical daughter cells

1.1.1. CDKs and Cyclin Complexes

Cyclin-dependent kinases (CDKs) and cyclins that perform specific roles at particular phases of the cell cycle have been characterised in many model eukaryotic species. Numerous review papers have been written on this subject in yeast (Nasmyth, 1996; Stern and Nurse, 1996), animals (Morgan, 1995; Pines, 1996) and plants (DeVeylder *et al.*, 1997; Burssens *et al.*, 1998) and see table 1 and 2.

There is a single cell cycle CDK in *Saccharomyces cerevisiae* (CDC28) and *Schizosaccharomyces pombe* (Cdc2); whereas several (Elledge, 1996) are known to be involved in both plant and mammalian cell cycles (Burssens *et al.*, 1998) that are specialised for different transitions. Cyclins are the activating subunit for CDKs and are therefore essential for both kinase activity and substrate specificity (Elledge, 1996). The CDK-cyclin complex is negatively and positively regulated by phosphorylation, cyclin-dependent kinase inhibitors (CKIs) that have an inhibitory binding effect, and other proteins that might modify specificity or accessibility to regulators (Patra and Dunphy, 1996). All proteins that affect CDK/cyclin activity can act as interfaces for signal transduction pathways regulating cell cycle transition points, making them potential targets for manipulation of the checkpoints by the cell (Elledge, 1996).

1.1.1.1. Cyclin Dependent Kinases

In fission and budding yeast there exists only one CDK to regulate the cell cycle through S and M phases, Cdc2 and CDC28 respectively (Table 1). Higher eukaryotes have replaced a single CDK with specialised S and M phase-activating CDKs. In mammals, progression through G1 is controlled by Cdk4 and Cdk6 complexed to Cyclin D, DNA replication by Cdk2 complexed to Cyclin A/E in G1/S, and Cdk1 in G2/M by complexing with Cyclin A/B (Morgan, 1995; 1997). CDKs are characterised by distinct sequences located within their cyclin binding motif. This is PSTAIRE in the case of *S. pombe* and mammalian *cdc2* (see Fig. 1.2 for the basic structure of plant CDKs).

Plants contain a diverse group of CDKs (see Table 1) including those containing the PSTAIRE motif, known as CDK-a, and plant specific CDKs characterised by the variant motifs PPTALRE or PPTTLRE (Huntley and Murray, 1999; Mironov *et al.*, 1999; Joubes *et al.*, 2000; Umeda *et al.*, 1999). Both sequences form the basis of the plant specific CDK-b group with the proteins falling into two sub-groups on the basis of the above mentioned variant motif. The CDK-b1 CDKs all contain the PPTALRE sequence and the CDK-b2 CDKs have the sequence P(S/P)TTLRE. The exception to this is rice Cdc2Os3, this has the CDK-b1 motif but still belongs to the CDK-b2 group (Hirt *et al.*, 1993; Fobert *et al.*, 1996; Umeda *et al.*, 1999; Kidou *et al.*, 1994; Magyar *et al.*, 1997; Huntley and Murray, 1999). C-type plant CDKs are characterised by the presence of the PITAIRE motif but as yet their function is not known (Joubes *et al.*, 2000). In tobacco BY-2 cells the expression of C-type cyclins has been shown to be high in late M-phase and early S-phase, indicating a role in G1 (Breyne *et al.*, 2001). E-type cyclins have been identified in Alfalfa and show highest homology to CDK8 in humans, a regulator of RNA polymerase II activity, and can be identified by the SPTAIRE motif. CDK-fs, another type of CDK unique to plants, are mitotic kinases with both mRNA and kinase activity reaching a peak in mitosis (Meszaros *et al.*, 2000).

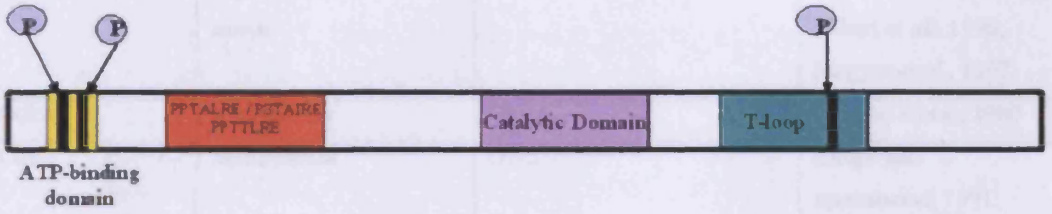

Figure 1.2. Basic Structure of Plant CDKs. Phosphorylation sites are denoted by P. Phosphorylation sites in the ATP-binding domain are T14 and Y15, targets of WEE1 and CDC25. The phosphorylation site in the T-loop, T167, is the target of CAK. Adapted from *Sorrell et al.*, 2001.

Plant CDK-as fall into three subgroups, CDK-a1, -a2, and -a3 with each subgroup showing an expression pattern involving either G1/S or G2/M (Mironov *et al.*, 1999). In tobacco BY-2 cells CDK-a1s show a mitotic accumulation of transcript, CDK-a2s show an increase in S-phase and decreases in M-phase, and CDK-a3s are expressed during S-phase and decrease during G2 (Breyne *et al.*, 2002)

However, the expression pattern of CDK-bs at the transcriptional, translational, and protein level is dependent on cell cycle phase (Mironov *et al.*, 1999). CDK-b1 transcripts in *Arabidopsis* accumulate during S, G2, and M phase whereas CDK-b2 is specific to G2 and M (Segers *et al.*, 1996). Due to this, CDK-b2 is commonly used as a marker of proliferative activity (Sorrell *et al.*, 2002).

Cyclin-Dependent Kinase	**Species**	**Spatial Functionality/ Characteristics**	**Reference**
CDC28 (PSTAIRE)	Budding yeast - *S. cerevisiae*	Involved in G1/S and G2/M	Piggott *et al.*, 1982.
Cdc2 (PSTAIRE)	Fission yeast – *Schizosaccharomyces pombe*	Involved in G1/S and G2/M	Nurse and Thuriaux, 1980.
CDK-a (PSTAIRE)	Plant – Widely identified	Involved in G1/S and G2/M	Mironov *et al.*, 1999; Segers *et al.*, 1998.
CDK-b1 (PPTALRE)	Plant – *A. thaliana, A. majus, N. tabacum, M. sativa*	Expressed S to M	Mironov *et al.*, 1999; Segers *et al.*, 1998; Fobert *et al.*, 1996; Magyar *et al.*, 1997.
CDK-b2 (PPTTLRE)	Plant – *A. thaliana, A. majus, O. sativa, M. sativa*	Probably expressed G2 and M only	Mironov *et al.*, 1999; Segers *et al.*, 1998; Fobert *et al.*, 1996; Magyar *et al.*, 1997.
Cdk1	Mammalian	G2/M	Lee and Nurse, 1980
Cdk2	Mammalian	G1/S	Ellege and Spottswood, 1991.
Cdk4	Mammalian	G1	Matsushime *et al.*, 1992.
Cdk6	Mammalian	G1	Meyerson and Harlow, 1994.

Table 1.1. Cyclin-dependent kinases and their spatial functionality in eukaryotes.

CDK Regulation -

CDK activity is not only reliant on cyclin binding but also on a number of other factors as well (Fig. 1.3). CDK-activating kinases (CAKs) phosphorylate a threonine residue within the CDK T-loop to cause CDK activation (Fig. 1.2). In some organisms CAKs can also activate RNA polymerase II by phosphorylation of the carboxy-terminal domain (CTD) of the largest RNA polymerase sub-unit, although this is not the case in yeast. In plants CAKs have been found that both lack and contain this extra function. Cak1At, an *Arabidopsis* CAK homologue, lacks the ability to phosphorylate *Arabidopsis* RNA polymerase II but can phosphorylate human CDK2. This can be compared to the rice CAK OsR2 which is able to carry out the T-loop phosphorylation of Cdc2Os1 (CDK-a) and human CDK2, as well as RNA polymerase II. Another example of regulation is by the cyclin-dependent kinase inhibitors (CKIs). In plants these are known as ICKs and are proteins that mask the ATP binding domain of Cdc2 kinase (Wang *et al.*, 1997). Both the *Arabidopsis* ICK1 and ICK2 block CDK activity and cell division when *Arabidopsis* is treated with abscisic acid (Zhou *et al.*, 2002) (Fig. 1.3).

The 'next' level of regulation occurs through the phosphorylation/dephosphorylation of conserved threonine and tyrosine residues, Thr14 and Tyr15 respectively. Inhibitory regulators (phosphorylators) of these residues are the kinases Myt1 and Wee1 with Cdc25 phosphatase acting as the counterbalance (dephosphorylator) (Fig. 1.3). *wee1* has been identified in both maize (Sun *et al.*, 1999) and *Arabidopsis* (Sorrell *et al.*, 2002) although *cdc25* has yet to be identified in plants. In cell cultures of *Nicotiana plumbaginifolia*, cells depleted of cytokinin arrested in G2 and CDK was phosphorylated on Thr14 and Tyr15. Addition of cytokinin to the medium accelerated these arrested cells into G2 with a concomitant dephosphorylation of CDK. The phosphorylated CDK could also be dephosphorylated by *Sp*Cdc25 phosphatase (John, 1998; Zhang *et al.*, 1996). The data were consistent with the idea that cytokinins regulate an extra-cellular signaling pathway that ends in the de-phosphorylation of CDKs by plant-like CDC25 phosphatases.

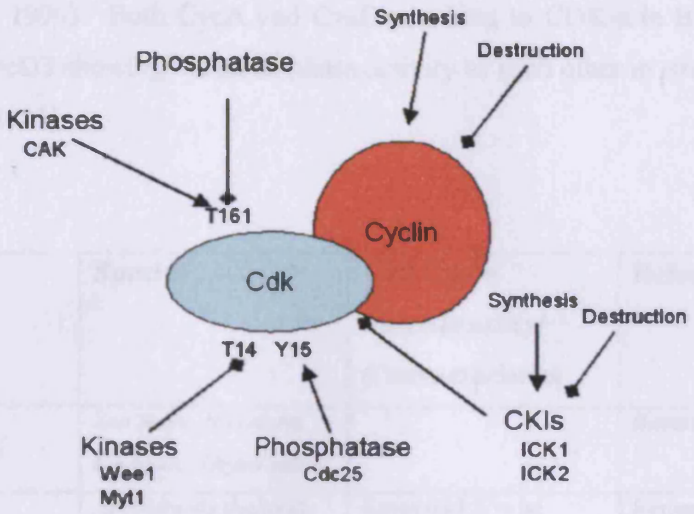

Figure 1.3. Regulation of CDK-Cyclin complexes in Plants. Arrowheads represent activating events and square ends represent inhibitory events. Regulatory genes known to perform the indicated functions in plants are listed where known. Both cyclins and some CKIs are regulated by synthesis and ubiquitin-mediated proteolysis. Adapted from King *et al.*, 1996. Checkpoint pathways could act to promote inhibitory pathways or inhibit activating pathways to cause cell cycle arrest

1.1.1.2. Cyclins

Cyclins interact with CDKs to regulate their activity, substrate specificity, and sub-cellular localisation. All major classes of cyclins from mammalian studies are represented in plants including A-, B-, and D-type (known as CycA, CycB, and CycD respectively). Several sub-groups exist within these and are categorised on the basis of sequence homology (see Table 2). Both *CycA* and *CycB* are expressed in a cell cycle dependent manner and peak around S/M and G2/M respectively (Fig. 1.4). Within the CycA sub-types the expression pattern is slightly different with expression of the sub-types shown to be sequential (Reichheld *et al.*, 1996). *CycD* genes are expressed similarly to their mammalian counterparts, exhibiting a cell cycle independent pattern of transcription based on mitogen induction (Soni *et al.*, 1995; Sorrell *et al.*, 1999; Riou-Khamlichi *et al.*, 1999). Expression levels of D-type cyclins generally remain constant in actively dividing cells (Sorrell *et al.*, 1999; Dahl *et al.*, 1995; Fuerst *et al.*, 1996; Soni *et al.*, 1995). Two exceptions to this are the tobacco CycD2;1 and CycD3 cyclins which accumulate during mitosis in BY-2 cell cultures

(Sorrell *et al.*, 1999). Both CycA and CycD can bind to CDK-a in BY-2 cells with CycD2 and CycD3 showing the same phase activity as each other in *Arabidopsis* cells (Healy *et al.*, 2001).

Cyclin	**Species**	**Cell Cycle Functionality/ Characteristics**	**Reference**
CycA1	*Zea mays, Nicotiana tabacum, Oryza sativa*		Renaudin *et al.*, 1996
CycA2	*Arabidopsis thaliana, Zea mays, Nicotiana tabacum, Medicago sativa*	Expressed S to M	Renaudin *et al.*, 1996
CycA3	*Catheus roseus, Nicotiana tabacum, Antirrhinum majus*		Renaudin *et al.*, 1996
CycB1	*Arabidopsis thaliana*	Expressed at G2/M transition	Day and Reddy, 1998
CycB2	*Medicago sativa*	Expressed at G2/M transition	Day and Reddy, 1998
CycD1	*Arabidopsis thaliana, Antirrhinum majus, Helianthus tuberosus*		Renaudin *et al.*, 1996; Soni *et al.*, 1995
CycD2	*Arabidopsis thaliana, Nicotiana tabacum*	Involved in G1/S, sucrose induced	Sorrell *et al.*, 1999; Soni *et al.*, 1995
CycD3	Widely identified	Involved in G1/S. AtCycD3 is induced by cytokinin. Several sub-groups exist dependent on different inducers	Riou-Khamichi *et al.*, 1999
CycD4	*Arabidopsis thaliana*	Sucrose induced	De Veylder *et al.*, 1999

Table 1.2. Functionality of cyclins within the cell cycle in plants

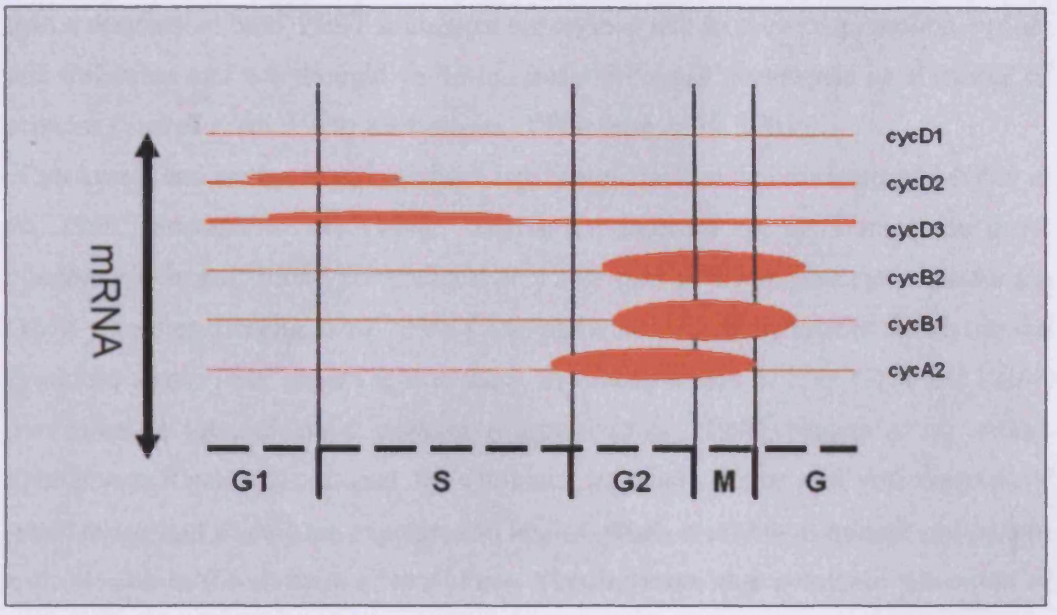

Figure 1.4. Plant Cyclin Expression Through the Cell Cycle. Width of red line denotes level of activity at the particular point in the cell cycle indicated at the bottom of the diagram. Adapted from Mironov *et al.*, 1999.

Cyclin Regulation –

Regulation of cyclins usually occurs by gene expression and protein turnover. The breakdown of CycA and CycB cyclins occurs at specific points during M-phase and is dependent on a destruction box motif that is the target for ubiquitin-dependent proteolysis (Renaudin *et al.*, 1998; Glotzer *et al.*, 1991). Genschik *et al* (1998) showed that in *Arabidopsis* CycA and CycB degradation was due to this destruction box by fusing the reporter gene GFP (green fluorescence protein) to the amino termini of these genes. A reduction in the rate of degradation was also noted when mutations were introduced into the conserved residues of the destruction box. The ubiquitin proteolysis pathway is highly conserved in all eukaryotes and is involved in auxin signaling, jasmonic acid signaling, photomorphogenesis, and floral development as well as the cell cycle in plants (Plesse *et al.*, 1998). Attachment of ubiquitin to proteins leads to subsequent degradation by a multi-catalytic protease complex called the 26S proteasome (Vierstra, 2003).

CycD genes deviate from CycA and CycB as they contain PEST sequences rather than a destruction box. PEST sequences are regions rich in glutamate, proline, serine, and threonine and are thought to be the basis for rapid proteolysis in a variety of proteins (Sorrell *et al.*, 1999; Rechateiner, 1998; Soni *et al.*, 1995).

Cytokinins and auxins have both been implicated in plant cell cycle control (Gray *et al.*, 1998; Jacqmard *et al.*, 1994). Auxins are essential for G1/S transition in *N. plumbagnifolia* suspension cultures and play a co-operative role with cytokinin for the G2/M transition (Zhang *et al.*, 1996). In particular, inhibitor studies involving the cytokinin zeatin have shown that it plays an essential role in both G1/S and G2/M transitions in tobacco BY-2 cultures (Laureys *et al.*, 1998; Nagata *et al.*, 1994). *Arabidopsis* CycD3 is induced by cytokinin in whole plants and cell cultures of *Arabidopsis* and when over-expressed in leaf ex-plants it is able to initiate and sustain cell division in the absence of cytokinin. This indicates that cytokinin activation of CycD3 is required for G1/S transition in *Arabidopsis* (Riou-Khamlichi *et al.*, 1999). Sucrose is also implicated in the regulation of D-type cyclins including *A. thaliana* CycD4;1, CycD2 (early G1 expression), and CycD3 (late G1 expression).

Thus far, the genes/proteins involved in phase transitions of the cell cycle have been reviewed. Fig. 1.5 gives an overview of the cell cycle progression discussed thus far. However, for cells to undergo these transitions they need to acquire competence to do so. Critically, brakes are applied on the cell cycle if competence is flawed due, for example, DNA damage. These brakes are more usually referred to as checkpoints, that prevent G2/M, and G1/S until DNA damage is repaired or DNA replication is normalised.

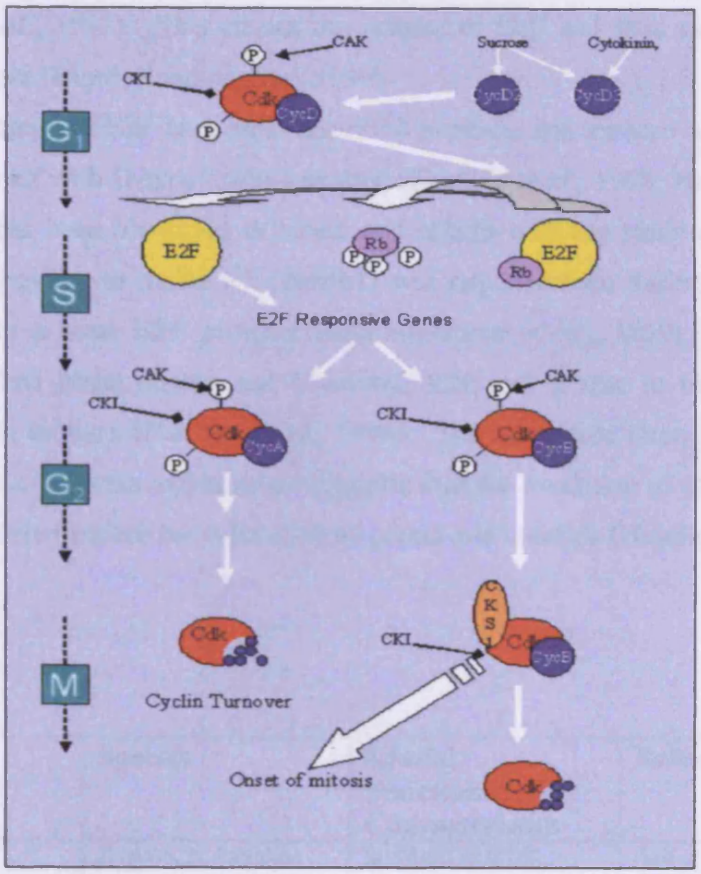

Figure 1.5. Basic overview of CDK-Cyclin regulation. Effects of regulators on the different CDK-Cyclin complexes and subsequent progression through the cell cycle induced by them. Adapted from Huntley and Murray (1999).

1.1.2. G1/S Specific Controls

The G1/S transition and the checkpoint controls that exist for progression to take place are not as well known in plants as those in mammalian systems but as with the majority of cell cycle research, parallels can be drawn to elucidate mechanisms (Table 1.3).

In animal cells, for progression into S-phase, the activation of E2F transcription factors is required. To ensure this does not occur prematurely, E2F is bound to the retinoblastoma protein (Rb) (Harbour and Dean, 2000). Transcription of the E2F regulated genes is inactivated due to histone deacetylases binding to their promoters during E2F-Rb interaction (Magnaghi-Jaulin *et al.*, 1998). In mammalian cells E2F is re-activated by hyper-phosphorylation of Rb by cyclinD-CDK4/6 complexes

(Ezhevsky *et al.*, 1997). This causes the release of E2F and thus stimulating E2F responsive genes (Huntley and Murray, 1999).

Plant homologues of E2F have been identified in maize and tobacco with both being shown to interact with D-type cyclins *in vitro* (Huntley *et al.*, 1998; Nakagami *et al.*, 1999). E2F has been identified in wheat and alfalfa with the study on wheat E2F showing that binding to maize Rb (*Zm*Rb1) was dependent on different residues to that present in animal E2F proteins (Ramirez-Parra *et al.*, 1999). Interestingly however, ZmRb1 binds human and *Drosphila* E2F and is able to transcriptionally activate E2F in humans (Huntley *et al.*, 1998). The conserved interactions of G1/S regulators between plants and animals suggests that the evolution of the Rb pathway may have occurred before the separation of plants and animals (Huntley and Murray, 1999).

Regulator	**Species**	**Spatial Functionality/ Characteristics**	**References**
Rb	*Z. mays, N. tabacum*	Involved in G1/S, phosphorylated by CDK-a/CycD3 kinase in vitro	Ach *et al.*, 1997; Huntley *et al.*, 1998; Nakagami *et al.*, 1999
E2F	*M. sativa*	Up-regulated in early S phase, expressed in proliferating cultured cells and in differentiated tissues. Binds and is probably activated by Rb.	Inze D, Gutierrez C, and Chua N-H, 1999; Gutierrez C, 1998; Ramirez-Parra *et al.*, 1999
CKI	*Arabidopsis thaliana*	ICK1 binds both CDK-a and CycD3 and is induced on abscisic acid treatment, further CKI genes exist	Wang *et al.*, 1998; Mironov V *et al.*, 1999
Cks	*Arabidopsis thaliana*	Role in both mitotic and endoreduplication cycles	De Veylder *et al.*, 1997; Jacqmard *et al.*, 1999
Msi1	*Arabidopsis thaliana, L. esculentum*	Rb binding protein, possibly part of histone deacetylase complexes, may be involved in G1/S	Ach, Taranto, and Gruissem, 1997
Cak	*O. sativa, Arabidopsis thaliana*	Activates CDKs by T-loop phosphorylation	Umeda *et al.*, 1998; Yamaguchi *et al.*, 1998
Mcm3	*Nicotiana tabacum Arabidopsis thaliana*	Involved in DNA synthesis although only *A. thaliana* Mcm3 shows S-phase specific	Dambrauskas *et al.*, 2003; Stevens *et al.*, 2002

		expression.	
DP	*Arabidopsis thaliana*, *Triticum monococcum*	Dimerises with E2F to activate transcription factors in G1/S	Magyar *et al.*, 2000; Ramirez-Parra and Gutierrez, 2000)

Table 1.3. Other homologues of mammalian cell cycle regulators in plants

1.1.3. Cdc25 and the G2/M DNA Damage Checkpoint

The G2/M (DNA damage) checkpoint is still poorly understood in plants but the knowledge is catching up fast following the completion of the *Arabidopsis* genome project. More information is now available about plant homologues to checkpoint genes in yeasts and animals. The checkpoint will be mainly discussed from the point of mammalian systems and plant homologues stated where known.

Unfortunately *Cdc25*, a positive regulator of the G2/M Checkpoint, has yet to be identified in plants although, as stated earlier, *Wee1* has. A single *cdc25* gene exists in *S. pombe*, and it is a multigene family in mammalian cells. This is composed of *CDC25A*, *CDC25B*, and *CDC25C* (Sadhu *et al.*, 1990; Galaktionov and Beach, 1991; Nagata *et al.*, 1991). The CDC25 proteins share approximately 40-50% amino acid identity with the highest homology in the C-terminal catalytic domain.

*Sp*Cdc25's amino acid sequence is closest in homology to *HsCDC25C* and carries out the same function, being important at the G2-M transition (Hoffman *et al.*, 1993). Cdc25B is also functional at this transition with Cdc25A being important for regulation of G1-S phase transition (Jinno *et al.*, 1994; Lammer *et al.*, 1998).

In the case of damage inflicted during the G2 phase of the cell cycle, arrest occurs before the onset of mitosis (Rhind and Russell, 1998). In fission yeast, arrest of cells in G2 is dependent on inhibitory tyrosine phosphorylation of Cdc2 carried out by Wee1 and Mik1 kinases. When *S. pombe* is irradiated, the rate of tyrosine dephosphorylation is reduced, suggesting that the regulation of Cdc2 by Cdc25 is an important part of the mechanism underlying the DNA damage checkpoint by which Cdc2 inhibition and G2 arrest occurs (Rhind *et al.*, 1998). Chk1 (checkpoint kinase 1) (Cds1 in fission yeast) is a kinase involved in cell cycle arrest. Cdc25 is a target for Chk1 and is phosphorylated and thus inactivated by it when DNA damage occurs (Walworth *et al.*, 1993; Funari *et al.*, 1997). Furthermore, fission yeast which express activated Cdc2 but lack Cdc25 were shown to be responsive to Wee1 but insensitive

to Chk1 and irradiation, suggesting that Cdc25 and not Wee1 is a target of the DNA damage checkpoint (Funari *et al.*, 1997). However, another study showed that Chk1 can act as a Wee1 kinase in the DNA damage checkpoint, phosphorylating it at Y15 and thus inhibiting Cdc2 activity (O'Connell *et al.*, 1997). It is therefore likely that regulation of both Wee1 and Cdc25 by Chk1 is important for the DNA damage checkpoint (Releigh and O'Connell, 2000).

Phosphorylation of Cdc25 by Chk1 occurs on Ser-216 (fission yeast) and creates a binding site for 14-3-3 proteins (Peng *et al.*, 1997) with binding being high during interphase and low during mitosis. The 14-3-3 protein masks this phosphorylated residue and prevents other phosphatases accessing this site. Destruction of the 14-3-3 binding site leads to premature entry into mitosis and an inability to arrest in response to damaged or unreplicated DNA. This was found to be due to 14-3-3s playing an important role in controlling intracellular distribution of Cdc25. In fission yeast, the 14-3-3 Rad24 escorts Cdc25 from the nucleus due to the nuclear export signal (NES) with *rad24* mutants preventing export of both proteins from the nucleus (Lopez-Girona *et al.*, 1999). This escort however is not required for the DNA damage checkpoint (Lopez-Girona *et al.*, 2001). Recently a plant 14-3-3, GF 14-3-3ω, has been found to bind with *Sp*Cdc25 and rescue checkpoint defects in yeast (Sorrell *et al.*, 2003). Recently an *Arabidopsis* gene that encodes a *cdc25*-like phosphatase has been identified although it lacks the regulatory domain (D.A. Sorrell, D. Francis, H.J. Rogers, and J.R. Dickinson, unpublished data). Further work, however, is required to see if it functions properly as a plant CDC25.

Upstream from Cdc25 and Chk1 are the sensor proteins for DNA damage. These are ATM/ATR (Ataxia-teleangniectasia mutated/related) in humans and RAD3 in fission yeast (Elledge, 1996; Weinert, 1998). Ataxia teleangiectasia (AT) is a rare inherited disorder in which ATM is non-functional. This causes chromosomal instability and sensitivity to ionising radiation (Savitsky *et al.*, 1995). Cells in which ATM is non-functional are unable to activate cell cycle checkpoints when exposed to ionising radiation (Meyn, 1999). ATR is similar in function to ATM but is affected by UV instead of ionising radiation (Hirao *et al.*, 2000). In fission yeast, RAD3 fulfils the role of both ATR and ATM (Bentley *et al.*, 1996). To support the hypothesis that this system exists in plants (Fig. 1.6), an *Arabidopsis* ATM homologue has been cloned (Garcia *et al.*, 2001) and found to be essential for meiosis and somatic response to

DNA damage in *Arabidopsis* (Garcia *et al.*, 2003). Once ATR/ATM is activated in response to DNA damage, the signal is passed on to Chk1, however a plant Chk1 has yet to be identified.

The high amount of functional conservation between mammalian and yeast DNA damage checkpoints, and the identification of key components from it in plants, indicates that this functional conservation is likely to extend to plants and that both Cdc25-like and Chk1-like proteins exist in plants but not necessarily with structural homology. A plant Chk1 homologue would provide the link to the downstream regulators *At*WEE1 (Sorrell *et al.*, 2002) and a putative CDC25 acting on *At*CDC2a/b. *At*WEE1 and CDC25 in turn may be regulated in plants by 14-3-3 proteins as they are in other systems, given that an *Arabidopsis* 14-3-3 protein interacts with *Sp*Cdc25 (Sorrell *et al.*, 2003).

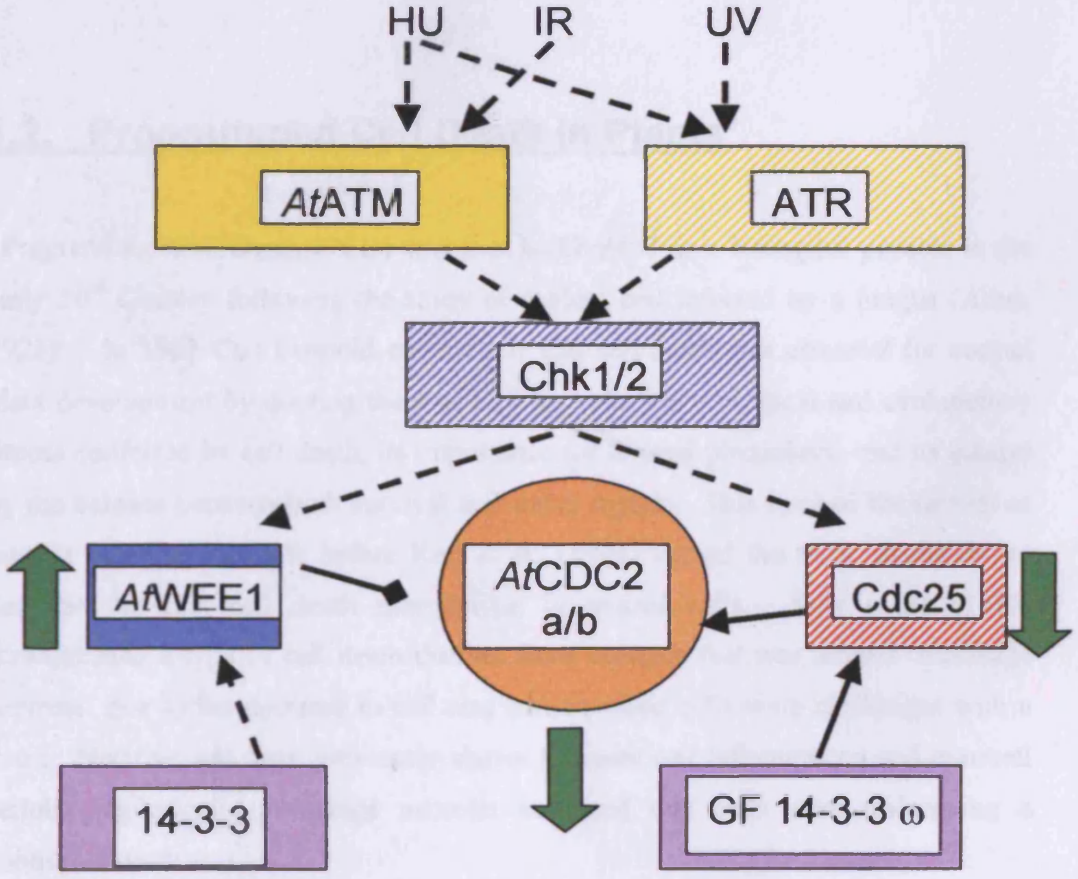

Figure 1.6. Putative *Arabidopsis* model of DNA damage checkpoint control. Filled boxes indicate components that are known. Shaded boxes indicate proteins not yet found but are thought to exist due to mammalian/yeast models. Straight lines represent known effects whereas dotted lines are hypothetical links. Green arrows denoted change in activity when the checkpoint is activated. Hydroxyurea (HU), ionising radiation (IR), and ultraviolet radiation (UV) are used as examples of DNA damage checkpoint elicitors. Adapted from Francis, 2003.

Checkpoints function to protect proliferative cells under stress conditions. However, when DNA damage is catastrophic, checkpoint control can be overridden and a different set of molecular controls activated that steer the damaged cell into programmed cell death. Exit into PCD in late G2 and late G1 is well-characterised in animal systems (Hirao *et al.*, 2000; Tanaka *et al.*, 2000).

1.2. Programmed Cell Death In Plants

Programmed Cell Death (PCD) was first highlighted as a biological process in the early 20th Century following the study of a plant cell infected by a fungus (Allen, 1923) In 1961 Carl Leopold emphasised that cell death was essential for normal plant development by quoting the evidence for selective ecological and evolutionary fitness conferred by cell death, its importance for normal physiology, and its control by the balance between both survival and death signals. This marked the revival of interest in PCD a decade before Kerr *et al.* (1971) coined the term 'apoptosis' to describe the first cell death morphotype in animal cells. Kerr *et al.* (1971) distinguished a type of cell death distinct from necrosis that was termed 'shrinkage necrosis' due to the decrease in cell size caused when cells were challenged with a toxin. Necrosis had been previously shown to cause cell inflammation and eventual cellular explosion. Shrinkage necrosis indicated that cells were undergoing a controlled death.

PCD differs from necrosis as it is a controlled and active process requiring changes in the genome to minimise the loss of nutrients and damage to surrounding tissue. This can happen in a variety of ways depending on the type of PCD occurring (Jones, 2001). Evidence that some forms of cell death were directed by an active program

was primarily found by Yoshio Yoshida who worked on leaf senescence. Yoshida (1962) showed that a nucleus was required for cellular disassembly and that inhibitors of protein translation inhibited leaf senescence.

PCD in plants fulfils a number of essential functions (Fig. 1.7) and can be placed into two distinct groups, developmental and non-developmental. Examples of developmental programmed cell death are senescence, aleurone layer development, and xylogenesis. This is not a comprehensive list but highlights the main areas in which PCD affects development. Non-developmental PCD involves response to pathogens (biotic stress) and abiotic stress (temperature, drought, UV etc.)

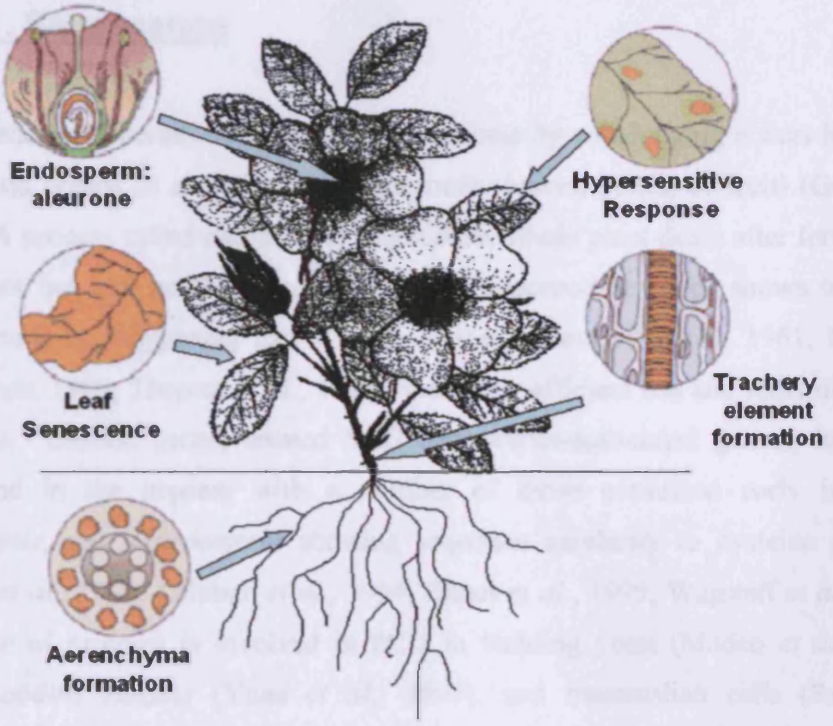

Figure 1.7. Examples of Programmed Cell Death in Plants. *Adapted from Biochemistry and Molecular Biology of Plants (2001).*

In this section examples of developmental and non-developmental processes will be discussed in further detail and the evidence suggesting they involve PCD discussed. The role of the plant growth regulator ethylene in PCD, a focus of this thesis, will be highlighted under developmental PCD. Furthermore, a description of the morphological features of apoptosis is discussed as a reference point against which

plant PCD can be compared and the potential molecular mechanisms of PCD in plants is discussed. This section is not intended to be encyclopaedic but is designed to give a broad introduction to PCD from which the rest of the thesis can expand where necessary.

1.2.1. Developmental PCD

1.2.1.1. Senescence

Senescence is generally referred to as the process by which aging occurs in various tissues and organs as a plant matures (normally leaves, petals, or fruit) (Greenberg, 1996). A process called monocarpic senescence, whole plant death after fertilisation, also exists but will not be discussed here. Senescence has been shown to require nuclear activity, suggesting that it is an active process (Yoshida, 1961; Ness and Woolhouse, 1980; Thomas *et al.*, 1992), providing efficient use and redistribution of resources. Several genes, termed SAG (senescence-associated genes), have been implicated in the process with a number of those expressed early in maize, *Arabidopsis*, and *Alstroemeria* showing sequence similarity to cysteine proteases (Hensel *et al.*, 1993; Lohman *et al.*, 1994; Smart *et al.*, 1995; Wagstaff *et al.*, 2002). This type of protease is involved in PCD in budding yeast (Madeo *et al.*, 2002), *Caenorhabditis elegans* (Yuan *et al.*, 1993), and mammalian cells (Rudel and Bokoch, 1997) thus there is a good indication in its involvement with the senescence process. The majority, but not all (Gewies and Grimm, 2003) of cysteine proteases involved in regulating mammalian and yeast PCD belong to a sub-family known as caspases (see 1.2.4.2), and have yet to be identified in plants. RNase (Green, 1994; Blank and McKeon, 1991) and lipoxygenases (Rouet-Mayer *et al.*, 1992) have also been linked to senescence as the activity/expression of these enzymes increases during senescence. Other SAGs include SAG12; a protease (involved in protein degradation), ACS6; an ACC synthase gene (involved in ethylene production), and

SAG17; a metal-binding protein (involved in ROS scavenging) (Buchanan-Wollaston, 1997; Weaver *et al.*, 1997).

Plant growth regulators have also been implicated in senescence. Mutants of *Arabidopsis* that lack ethylene perception show delayed senescence (Grbic and Bleeker, 1995). Cytokinins may also be involved: a reduction in their levels in mature leaves may act as a contributing factor to the onset of senescence. This is thought to be due to cytokinins repressing genes involved in senescence. To support this, expression of a number of genes upregulated during senescence, including *SAG12,* are known to be affected by cytokinin levels (Gan and Amasino, 1995; Teramoto *et al.*, 1995).

1.2.1.2. Reproduction

Cell death occurs throughout plant reproductive processes. Male sex determination in maize results from the selective death of female reproductive primordia so that the male floral structures (stamens) can develop. The *TASSELSEED2* gene has been implicated in this and thought to be due to the production of a steroid-like molecule that provokes a cell suicide process (DeLong *et al.*, 1993).

PCD also plays an important role in seed germination in plants. Following seed germination cereal aleurone cells produce large amounts of α- and β-amylases. These hydrolyse starch to supply energy for the developing embryos before the aleurone cells undergo PCD (Fath *et al.*, 2000). In barley aleurone protoplasts, the PCD occurs in a gibberellic acid (GA)-dependent manner due to down-regulation by GA of enzymes that scavenge reactive oxygen species (ROS). This results in the protoplasts dying from ROS-induced injury to their structural components (Fath *et al.*, 2001). Evidence also exists that ethylene induces PCD in endosperm development as inhibition of ethylene action/synthesis inhibits aleurone cell death (Young and Gallie, 1999;2000).

1.2.1.3. Xylogenesis

Classic examples of developmental PCD occur during xylogenesis and phloem formation (nutrient conducting tubes) that form the vascular system. Both undergo autolysis as they mature. In cultured parenchyma cells, cells from which xylem and phloem develop, differentiation can be induced by auxin (Fukuda, 1992). Induction of differentiation has also been shown *in vivo* as a result of wounding. The purpose of this form of PCD is to ensure that water and nutrients can be distributed throughout the plant and that mechanical support is provided. Xylogenesis *in vitro* is an active process, requiring RNA and protein synthesis and thus satisfying various PCD criteria (Fukuda and Komamine, 1983).

A number of genes have now been implicated in xylogenesis including those for endonucleases (Thelen and Northcote, 1989), important because developing xylem cells show evidence of nuclear fragmentation (Mittler *et al.*, 1995). Because increases in nucleases occur during tracheary element differentiation it is unclear whether the DNA fragmentation is due to PCD-specific endonucleases.

Interestingly, inhibition of cysteine protease activity has been shown to suppress nuclear loss and therefore implies a role for cysteine proteases in the nuclear degradation observed in xylogenesis (Watanabe and Fukuda, 1995).

1.2.1.4. Ethylene-Induced PCD

Ethylene is a gas and endogenous regulator of growth and development in higher plants including programmed cell death (PCD) events (Young and Gaille, 1999). Changes in ethylene affect developmental PCD events such as abscission, organ senescence, xylogenesis, and aerenchyma formation (Fukuda, 1996; He *et al.*, 1996). Environmentally induced PCD events affected by ethylene include wounding, pathogen invasion (Ohtsubo *et al.*, 1999) and adaptation to events like water-logging (Drew *et al.*, 2000).

The first *Arabidopsis* mutant identified with ethylene insensitivity was designated *etr* (ethylene receptor mutated) due to the lack of ethylene response compared to the wild type plant (Bleecker *et al.*, 1988). These include inhibition of

cell elongation, promotion of seed germination, enhancement of peroxidase activity, acceleration of leaf senescence, and suppression of the feedback mechanism of ethylene synthesis by ethylene. Genetic analysis of the *Arabidopsis etr* mutant confirmed that ethylene insensitivity was due to a dominant mutation at a locus designated *ETR1* (Bleecker *et al*, 1988). Whilst ETR1 was the first ethylene receptor to be identified in plants, there have now been a number of receptor-encoding genes identified through additional screens for ethylene insensitive seedlings showing high sequence homology. These include ETR2, ERS1, EIN4, and ERS2 (Hua *et al.*, 1995,1998; Sakai *et al.*, 1998) and form the basis of the ETR1 receptor family. Schaller and Bleecker (1995) showed that *ETR1* encodes an ethylene receptor and that the N-terminal hydrophobic domain has high affinity to ethylene when expressed in yeast. Rodriguez *et al* (1999) showed that the ethylene binding domain of ETR1 consists of three putative membrane spanning sub-domains modelled as alpha helices. The *etr1-1* mutation, a point mutation located in the second of the three sub-domains, abolishes ethylene binding (Schaller and Bleecker, 1995) and removes the capacity of the receptor to co-ordinate the copper ion located in the N-terminal hydrophobic domain of ETR1, a requirement for ethylene binding (Rodriguez *et al.*, 1999).

The ETR1 receptor family acts in conjunction with CTR1, a Raf-like kinase, to suppress response pathways in the absence of ethylene (Clark *et al.*, 1998). Ethylene binding converts receptors to a non-signaling state (Hall *et al.*, 1999). Genetic analysis of other *Arabidopsis* ethylene insensitive mutants indicated that the genes responsible are integrated into a linear stress response pathway (Roman *et al.*, 1995). These include the *ETR1* family members as well as *EIN2*, *EIN3*, *EIN5*, *EIN6*, and *EIN7* amongst others (Ecker JR, 1995; McGrath and Ecker, 1998; Sakai *et al.*, 1998) (Fig. 1.8).

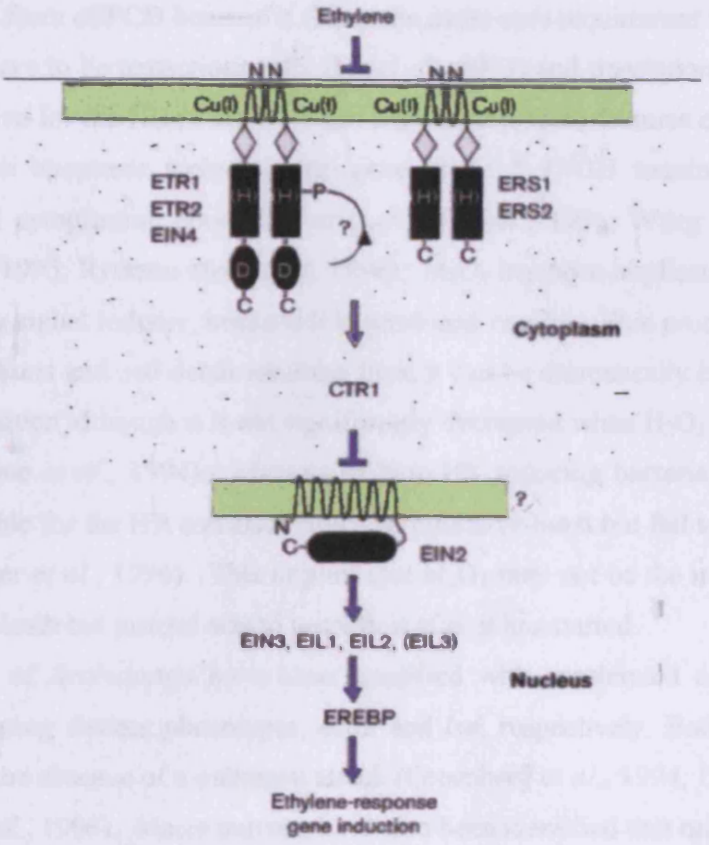

Figure 1.8. The ethylene signal transduction pathway in plants: based on currently known *Arabidopsis* genes. Ethylene perception occurs through the receptors, ETR1, ERS1, ETR2, EIN4, and ERS2. In the absence of ethylene, a response is repressed through activation of CTR1. In the presence of ethylene, CTR1 action is repressed and EIN2 is activated. This is turn activates the transcription factor EIN3. Subsequently EREBP transcription factors (ethylene responsive binding proteins) bind to promoters of ethylene regulated genes. Adapted from Chang and Shockley, 2002.

1.2.2. Non-Developmental PCD

1.2.2.1. Pathogenesis

Cellular interactions with a number of pathogens cause activation of defences that limit pathogen spread at the site of infection. This is described as the resistance response and normally results in the induction of localised cell death known as the hypersensitive response (HR). This is regarded as an important defence mechanism

whereby the nutrient supply to the pathogen becomes limited. The HR can be classified as a form of PCD because it shares the same core requirement with all other forms, cells have to be transcriptionally (He *et al.*, 1993) and translationally (Keen *et al.*, 1981) active for the HR to arise. It can also exhibit some features characteristics of mammalian apoptosis including the generation of 3'-OH termini, membrane blebbing, and cytoplasmic condensation (Levine *et al.*, 1996; Wang *et al.*, 1996; Mittler *et al.*, 1995; Ryerson and Heath, 1996). H_2O_2 has been implicated in the HR, especially as a signal inducer, because it is produced rapidly. This process is termed the oxidative burst and cell death resulting from it can be dramatically increased with H_2O_2 up-regulation although it is not significantly decreased when H_2O_2 production is blocked (Levine *et al.*, 1994). Mutants of Non-HR inducing bacteria containing a gene responsible for the HR can also induce an oxidative burst but fail to activate cell death (Glazener *et al.*, 1996). This implies that H_2O_2 may not be the major factor in inducing cell death but instead acts to amplify it after it has started.

HR mutants of *Arabidopsis* have been identified with accelerated cell death and lesions simulating disease phenotypes, *acd2* and *lsd*, respectively. Both can exhibit active HR in the absence of a pathogen attack (Greenberg *et al.*, 1994; Dietrich *et al.*, 1994; Jabs *et al.*, 1996). Maize mutants have also been identified that mimic a disease phenotype resulting in cell death (Walbot, 1991; Johal *et al.*, 1995).

1.2.3. Apoptosis

It is important that mammalian apoptosis is described because links are often made between PCD in plants and animals when symptoms of mammalian apoptosis occur during plant cell death. The importance of this is highlighted by a number of apoptosis symptoms occurring in plant PCD. As mentioned above, the first symptom of apoptosis observed was cell shrinkage due to a loss of water. This leads to compaction of the cytoplasm. Membrane blebbing occurs leading to formation of apoptotic bodies (apoptosis comes from the Greek for 'falling away' and was first used by Kerr *et al.*, 1972). Chromatin condenses along the margin of the nucleus. DNA is fragmented into 50Kb and 300Kb stretches, representing chromatin loops detached from the nuclear matrix (Brown *et al.*, 1993). This is usually followed by

double-strand fragmentation of DNA at internucleosomal linker regions yielding multiples of 180-200bp known as DNA laddering due to the pattern visible upon gel electrophoresis (Wyllie, 1987). This fragmentation of DNA also leads to the generation of 3'-OH termini. The mitochondria can also play an important role and this is highlighted upon in section 1.2.4.1. It is important to note that not all of the above mentioned symptoms always occur during apoptosis (Nagata, 2000). In particular different cell types may show different symptoms of apoptosis and symptoms shown may vary with the elicitor used (Oberhammer *et al.*, 1993). It is important that mammalian PCD is understood in relation to plant PCD and is highlighted in both developmental and non-developmental PCD in plants. The previous sections on these types of PCD highlight at least one of the above mentioned mammalian symptoms of PCD being involved.

1.2.4. Molecular Mechanisms of PCD

1.2.4.1. The Role of Mitochondria

In mammalian systems, the importance of the mitochondria in PCD has long been known (Green, 2000; Ferri *et al.*, 2001). A role for mitochondria is not always assured in PCD but in the majority of cases it acts to both mediate and amplify the cell-stress signals from throughout the cell. In mammalian cells, intracellular communication of the cell death signal to the mitochondria involves translocation of proteinaceous signals. The Bcl-2 family of proteins Bax, Bid, Bad, Bim, Bcl-2 and Bcl-X_L play an important role in this. Both Bcl-2 and Bcl-X_L reside in the outer mitochondrial membrane (OMM) and inhibit cytochrome *c* release. Their pro-apoptotic counterparts, Bax, Bid, Bam, and Bad, reside in the cytosol but are translocated to the OMM by cell death signaling. Bad forms a complex with Bcl-X_L to form a pro-apoptotic complex (Zha *et al.*, 1996; Gross *et al.*, 1999) (Fig. 1.9). This affects the voltage-dependent anion channel (VDAC) which results in cytochrome c release (Shimizu *et al.*, 1999).

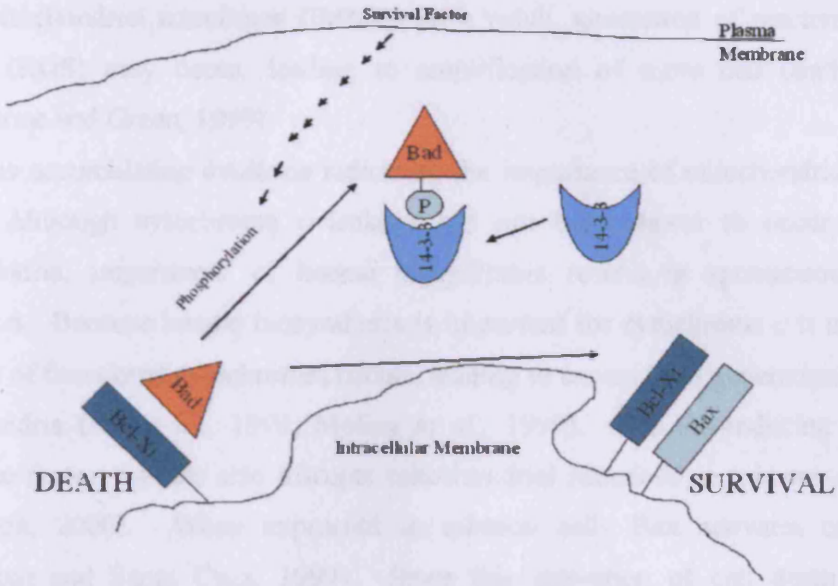

Figure 1.9. Promotion and Inhibition of Cell Death Via the Formation of Ion-Conducting Channels Effecting Mitochondrial Membrane Permeability In Mammalian Cells. Represented by BCL-2/Bax regulation in mammalian systems. Non-phosphorylated Bad heterodimerizes with membrane bound Bcl-X_L. Phosphorylation of Bad leads to its release from Bcl-X_L and allows it to complex with a protein 14-3-3. 14-3-3 sequesters Bad in the cytosol until it is required. This in turn allows Bcl-X_L molecules to homodimerize or heterodimerize with Bax to promote cell survival. Adapted from Zha *et al.* (1996).

Mitochondria may initiate PCD in response to changes in cellular pH, calcium, and other metabolites such as those important for energy distribution; NADH, NADPH, ATP, ADP, and creatine phosphate (Vander Heiden *et al.*, 2000).

When the permeability of the OMM is increased, factors effecting cell death are released. Good examples of these are cytochrome *c*, apoptosis inducing factor (AIF) and Smac/DIABLO. Apoptosis-associated release of Smac/DIABLO is dependent on caspase activation and is blocked by Bcl-2 (Adrain *et al.*, 2001). Cytochrome *c* has been shown to regulate the activity of the initiator caspase, procaspase-9 by mediation through Apaf-1 (Green *et al.*, 2000). Caspase-9 then goes on to activate the effector caspases responsible for cellular disassembly. It is therefore assumed that Smac/DIABLO is a caspase activated event downstream of cytochrome *c* release (Adrain *et al.*, 2001). AIF, a large protein, acts quite differently from cytochrome *c* by entering the nucleus and activating fragmentation of chromatin DNA into 50Kb fragments (Susin *et al.*, 1999). Disruption of the OMM and cytochrome *c* leakage may also lead to inhibition of electron flow from complex III and complex IV in the

inner mitochondrial membrane (IMM). As a result, generation of reactive oxygen species (ROS) may occur, leading to amplification of more cell death signals (Blackstone and Green, 1999).

There is accumulating evidence indicating the importance of mitochondria in plant PCD. Although cytochrome *c* leakage has not been shown to occur in plant mitochondria, impairment of haeme biosynthesis results in spontaneous lesion formation. Because haeme biosynthesis is important for cytochrome *c* it is thought that loss of functional cytochromes occurs, leading to excess ROS generation from the mitochondria (Hu *et al.*, 1998; Molina *et al.*, 1999). The HR-inducing bacterial virulence factor, harpin, also disrupts mitochondrial functions in tobacco cells (Xe and Chen, 2000). When expressed in tobacco cells Bax activates cell death (Lacomme and Santa Cruz, 1999). Since this activation of cell death requires mitochondrial targeting of Bax, it suggests at least some level of evolutionary conservation between cell death mechanisms in plants and other eukaryotes. A plant homologue of Bax inhibitor-1 has also been identified in *Arabidopsis* (*At*BI-1) and has been shown to be up-regulated during wounding and pathogen attack. It has also been shown to rescue Bax-induced cell death in yeast (Sanchez *et al.*, 2000). In plants, mitochondria are not the only organelles responsible for ROS production, plastids also participate in cell death signaling. An example of this is the plastid localised (chloroplast) protein DS9 which was found to be repressed with the onset of TMV activated cell death in tobacco leaves (Seo *et al.*, 2000). Over-expression of *DS9* led to a delay in cell death activation by TMV with suppression leading to acute HR cell death. Thus the role of mitochondria in plant PCD may be somewhat more complex than in animal cells.

1.2.4.2. Caspases And Cysteine Proteases

Caspases play an important role in PCD in other higher eukaryotes and are a part of the cysteine protease family of proteins (Green, 2000). Caspases cleave after specific aspartate residues and have the active site motif QACXG (where X is R, Q, or G) (Cohen, 1997). Although there are no direct homologues of caspases in plants, caspase-like protease activity has been associated with a number of types of plant

PCD (de Pozo and Lam, 1998; Korthout *et al.*, 2000). Metacaspases, caspase-related proteases, have been identified in *Arabidopsis* and can be categorised into two types both showing some but not all of the domains found in caspases (Uren *et al.*, 2000). It is, however, normal for cysteine protease activity to be associated with plant PCD, especially with regards to senescence (Wagstaff *et al*, 2002; Buchanan-Wollaston, 1996; Hensel *et al.*, 1993). Interestingly, poly-(ADP-ribose) polymerase (PARP), a specific substrate for caspase 3 during apoptosis in mammalian cells, has been found to be involved in H_2O_2-induced PCD in plant cells (Amor *et al.*, 1998). PARP is associated with DNA repair and DNA replication in mammalian systems (de Murcia and Menissier-de Murcia, 1994; Griffin *et al.*, 1995) with activation of PARP depleting NAD and inducing oxygen radicals (Nosseri *et al.*, 1994; Heller *et al.*, 1995).

Another large group of cysteine proteases distinct from caspases have also been implicated in PCD in mammalian cells. These cysteine proteases are involved in the deubiquitination process and are thus known as deubiquitination enzymes (DUBs). Ubiquitin regulates the turnover of proteins in a cell. Ubiquitination, the attachment of ubiquitin to a protein, is an important function in eukaryotes as it sequesters proteins from interacting with their substrates (similar to phosphorylation) (Baek *et al.*, 2001), or degradation via the 26S proteosome when four or more Ubiquitin (Ub) moieties are attached (Chau *et al.*, 1989). Activation of DUBs is thought to be due to cytokines and this activation by cytokines has been shown for at least three examples, DUB1, DUB2, and DUB2A (Zhu *et al.*, 1996; Zhu *et al.*, 1997; Baek *et al.*, 2001). Many cellular processes are controlled by Ub post-translational modification including cell cycle response through cyclin/CDK inhibitors (Glotzer *et al.*, 1991), DNA repair, and stress response (Hershko and Ciechanover, 1998; Kim *et al.*, 2003). Over-expression of DUB1 has been shown to arrest cells in G1/S, suggesting it has an effect on an important regulator of the G1/S transition of the cell cycle. However, no symptoms of apoptosis were observed (Zhu *et al.*, 1996). In contrast, *UBP41* over-expression has been shown to elicit all features of apoptosis in human cells with an inability to arrest cells in G2/M (Gewies and Grimm, 2003). In *Arabidopsis* 27 sequences matching DUBs have been identified through research (Yan *et al.*, 2000). However their role in plant PCD remains to be established.

The existence of other cysteine proteases apart from caspases involved in mammalian PCD suggests that it is not necessarily important that no structural

homologues of caspases have been found in plants, and the plant cysteine proteases associated with PCD may be playing other roles.

1.3. PCD And The Cell Cycle -

The overall aim of the project has been to test the general hypothesis that exit into PCD is cell cycle specific. Ideally, this work is best done on a cell line that is free of developmental constraints. Another advantage would be the ability to synchronise the cell line so that as many of the cells as possible can be studied in specific windows of the cell cycle. The tobacco TBY-2 cell line fulfils these criteria better than any other plant cell line. In the following section there is a brief outline of the historical advantages of this cell line.

1.4. The Tobacco BY-2 Cell Line

The HeLa cell line has played an important role in the understanding of molecular and cellular biology of mammalian cells since it was first used in the 1960s (Willmer, 1965). The success of using this cell line led plant scientists to create various cell lines including soybean (Gamborg, 1970), *Acer pseudoplatanus* (Simpkins *et al.*, 1970), and *Catharanthus roseus* (*Vinca rosea*) (Misawa and Samejima, 1978). None of these however have shown the same level of growth rates and homogeneity that the tobacco Bright Yellow var. 2 (BY-2) cell line has exhibited (Nagata, 1992). In fact, the BY-2 cell line has a number of unique qualities that have made it highly desirable for investigating molecular and cellular plant biology (Nagata, 1992; Nagata and Kumagai, 1999). Plant cell cultures are especially important since core mechanisms such as PCD and the cell cycle will share fundamental similarities to those in whole plant development (McCabe and Leaver, 2000). Since the interaction of PCD and the cell cycle at the molecular level is the focus of this thesis it is important that the right system is used to investigate it.

1.4.1. History of the BY-2 Cell Line –

The TBY-2 cell line was established from seedling callus of *Nicotiana tabacum* L. cv. Bright Yellow 2 in the Central Research Institute of the Japan Tobacco and Salt Public Corporation. It was identified as the most proliferative out of cell lines established from 40 species of *Nicotiana* and three species of *Populus* (Kato *et al.*, 1972). Due to the high growth rates and lack of nicotine production it was developed as raw material for cigarette production (Kato *et al.*, 1976) but was stopped as the cells were found to suffer from high levels of proteination (Kato, 1982).

1.4.2. Merits of the BY-2 Cell Line –

As mentioned above the BY-2 cell line exhibits a high level of synchronisation especially when compared to other cell lines. The majority of plant cell lines synchronised have attained mitotic index peaks in the region of 10-20%. This, however, still leaves 80-90% of cells somewhere else in the cell cycle. Recently two *Arabidopsis* cell lines, MM1 and MM2d, have been developed which are subcultured at 7d intervals (Menges and Murray, 2002). Unfortunately the peak value of cells observable in mitosis was only 13% and is not comparable to those observed in BY-2 cells (Menges and Murray, 2002). The only advantage of MM1 and MM2d is that *Arabidopsis* is the model genetic research tool and due to this its genome has been completely sequenced (The *Arabidopsis* Genome Initiative, 2000). This makes it comparatively easy to look at expression patterns and functions of putative genes.

The BY-2 cell line can be synchronised with aphidicolin, a reversible inhibitor of DNA polymerase α. Routinely aphidicolin induces a mitotic peak of 40-50% (Francis *et al.*, 1995; Herbert *et al.*, 2000; Sorrell *et al.*, 2001) but it can be as high as 80% (Nagata *et al.*, 1982). The growth rate of the cell line is also rapid with 2-3ml of stationary culture reaching another stationary phase within 7 days (at 27°C), making sub-culturing a consistent weekly event (Fig. 1.10). Hence, the BY-2 cell line is still the optimum system for investigating core cellular mechanisms with regards to the cell cycle since in a synchronised state it attains the highest recorded mitotic peaks.

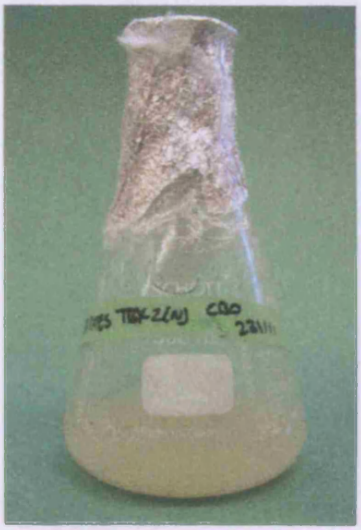

Figure 1.10. Tobacco BY-2 cells after 7 days of growth in liquid modified Linsmaer and Skoog medium at 27°C, 130rpm.

1.5. Aims of the Work Presented in this Thesis

The basis of work in this thesis was to try and elucidate mechanisms of cell cycle-linked programmed cell death in plants through the use of the tobacco BY-2 cell line. Using this cell line, mechanisms of PCD were studied in a system free of developmental constraint. Areas of particular interest were:

- The effect of ethylene, a known inducer of PCD, on the cell cycle and occurrence of mortality in the cell cycle.
- The ability of ethylene inhibitors to ameliorate effects of ethylene. This includes the use of 1-MCP, a relatively new development in ethylene signaling inhibition.
- To see if transformation with *Atetr1*, a gene encoding a dominant insensitive form of the *Arabidopsis* ETR1 receptor, could inhibit ethylene sensitivity in the same fashion as chemical inhibitors.
- Transformation of tobacco BY-2 cells with the mitotic inducer, *Spcdc25*, to see if it affected the G2/M transition. This transition plays an important role in response to DNA damage in yeast and mammalian cells, resulting in PCD if cells are unable to progress.

Chapter 2

Materials And Methods

2. Materials And Methods

2.1. Plant Material

The tobacco BY-2 cell line was cultured in modified Linsmaier and Skoog medium (Linsmaier and Skoog, 1965) supplemented with sucrose (3%), myoinositol, KH_2PO_4, thiamine HCl, and 2,4-D. Cells were cultured at 27°C, 130 rpm in the dark and subcultured at 7 day intervals. Cells were subcultured by transferring 2 ml into 95 ml of fresh medium in a 300 ml Duran flask.

2.2. Plasmid Transformation Of The Tobacco BY-2 Cell Line

Transformation of tobacco BY-2 cells was achieved using a modified version of the method described by An (1985). Isolated colonies of *Agrobacterium tumefaciens* strain LB4404 containing the appropriate binary vector (see Table 2.1) were picked from fresh 2xYT plates containing the appropriate antibiotic selection (see Table 2.1) and cultured overnight in 7 ml 2xYT (without antibiotic) in 50 ml conical flasks at 30°C with shaking. Aliquots (4ml) of 6 day old stationary phase BY-2 cells containing 20 μM of Acetosyringon (Sigma-Aldrich) (freshly added) were co-cultivated with 100 μl of *Agrobacterium* culture in 90mm Petri dishes sealed with Nescofilm for two days at 27°C in the dark without shaking. Cells were washed with 1 litre of BY-2 medium using a cell dissociation sieve fitted with a 100 μm mesh (Sigma-Aldrich) and re-suspended in 5ml BY-2 medium containing 250 μg/ml Timentin (Melford laboratories). Aliquots (2.5ml) were plated onto solidified BY-2

medium (0.8% agar; Sigma) supplemented with 250 μg/ml Timentin and the selective antibiotic (Table 2.1). Plates were sealed with micropore tape and incubated at 27°C in the dark. Isolated antibiotic-resistant calli (each individual callus was considered as an independent clone) appeared after 2-4 weeks, and were harvested and grown for a further two weeks on fresh plates. Calli were then transferred to 50 ml BY-2 medium supplemented with 250 μg/ml Timentin and a selective antibiotic. These were incubated at 27°C and 130 rpm in the dark until the cultures reached stationary phase (2-4 weeks). Cultures were subsequently maintained as described for wild-type BY-2 cultures using medium supplemented with both 250 μg/ml Timentin and the selective antibiotic. Timentin was omitted after the first sub-culture. Cultures were subjected to at least four rounds of sub-culturing before being used experimentally.

Vector	**Transgene**	**Antibiotic Selection: *E. coli***	**Antibiotic Selection: *Agrobacterium***	**Antibiotic Selection: Tobacco BY-2**	**Notes on Vector**
pBinHygTX:*Cdc25*	*Cdc25sp*	Kanamycin	Kanamycin	Hygromycin	Has an attenuated version of the *CaMV35S* promoter.
pBINHygTX	*None*	Kanamycin	Kanamycin	Hygromycin	As above
pHK1001:*etr1-1*	*etr1*	Spectinomycin	Spectinomycin/ Kanamycin	Kanamycin	*CaMV35S* promoter; supplied by H. Klee, University of Florida

Table 2.1. Details of transgene vectors and antibiotic selection used to transform tobacco BY-2 cells by *Agrobacterium*.

2.3. Synchronisation And Mitotic Index Measurements

Aphidicolin, a reversible inhibitor of DNA polymerase α, was used to synchronise the cells using a modified version of the Nagata *et al*, 1992 protocol. In the presence of this inhibitor, any cell replicating its nuclear DNA is arrested and all other cells are unable to enter S-phase. Hence, a 24 h exposure to, and subsequent removal of, aphidicolin will cause the vast majority of cycling cells to accumulate in late G1 and then be released into S-phase.

At the end of stationary phase (7 days following subculture), 20 ml of culture was transferred to 95ml of fresh medium containing aphidicolin dissolved in dimethylsulphoxide (DMSO; 5 μg/ml, Sigma) and cells were incubated in the same conditions as above for 24 hours. Immediately following the 24 hour incubation, cells were washed with 1 litre of fresh BY-2 medium in 100 ml aliquots using a sintered glass filter funnel (Baird and Tatlock No. 1). The flow rate of the washing medium was regulated by a Hoffman clamp attached to silicon tubing connected to the bottom of the funnel. To achieve a high level of mitotic synchrony the wash procedure was of exactly 15 mins in duration. The cells were resuspended in 95 ml of fresh medium and returned to the conditions above.

Following release from aphidicolin, 100 μl of cell suspension was taken at hourly intervals for 24 h, and mixed immediately with 5 μl Hoechst stain (Bisbenzimide Sigma, 100 μg/ml in 2% (v/v) Triton X-100). The mitotic index (the sum of prophase, metaphase, anaphase, and telophase mitotic figures as a percentage of all cells) was measured for a minimum of 300 cells per slide on random transects across the coverslip on each of the slides per sampling time per treatment. Cells and mitotic figures were visualised using a fluorescence microscope (Olympus BH-2, UV, λ=420nm). So that further analysis of cell size could be carried out, digital images were taken of each slide using a Fujifilm HC-300Z digital camera attachment for the microscope and saved as JPEGs.

2.4. Ceil Viability And Mortality Index

Following release from aphidicolin, mortality indices were scored every hour for the duration of the experiment. Cells (50 µl) were diluted 1:1 in solution containing fluorescein diacetate (FDA) (Sigma, 200 µg/ml) and propidium iodide (PI) (Sigma, 120 µg/ml) in 3% (w/v) sucrose and incubated on ice (20 min) (Harris and Oparka, 1994). A minimum of 300 cells were scored as dead (red) or alive (green) on random transects across the coverslip on each slide for every hour per released cell culture.

2.5. Ethylene, Silver Nitrate, 1-MCP And Mevinolin Treatment Of Tobacco BY-2 Cell Lines

Ethylene (SIB Analytical, Sandwich, Kent, UK) was administered to the headspace of TBY-2 cultures through a layer of Nescofilm as previously described (Herbert *et al*, 2001) to achieve a final concentration of 17700 µl/l. The ethylene was injected at 3.5 h following the release from aphidicolin, which coincides with the end of S-phase (Francis *et al.*, 1995; Herbert *et al.*, 2001). Both the injection time and amount of ethylene used were based on preliminary experiments carried out (Herbert *et al.*, 2001). These preliminary experiments showed that mortality for 17700µl/l of ethylene injected at 3.5 h after release from aphidicolin was 21.07±5.8%, significantly higher than that produced for 12400 µl/l (7.20±0.96%), but not much less than the mortality induced by 35000 µl/l of ethylene (24.92±5.6%). An injection point of 3.5 h was chosen as opposed to 0 h as it was shown to have a greater effect on the rise of the mitotic peak. Due to the low solubility of ethylene in water, the concentration in the medium is calculated using Boyles law to be below 73 µmol/l at 25°C. Therefore ethylene was re-administered at every sampling point to ensure it was kept present in the medium.

Silver is a well-established inhibitor of ethylene action and acts by inhibiting the binding of ethylene to its receptors (Drew *et al.*, 1981). Silver nitrate was added 3.5 h after the removal of aphidicolin and transfer of cells to fresh medium, giving a final

concentration of 1.2 μM. (Herbert *et al*, 2001). This concentration was chosen as it had been previously used in studies on aerenchyma formation in maize (Drew *et al.*, 1981).

1-Methylcyclopropene (1-MCP) is an inhibitor of ethylene action by the same process as silver (Serek *et al.*, 1994). Addition of 3.2 g 1-MCP (kindly supplied by Rohm-Haas in 0.14% powder formulation) to cell cultures occurred 3.5 h after release from aphidicolin with the 1-MCP treated flask being subsequently sealed with Nescofilm to restrict loss of 1-MCP in its gaseous (natural) form. Due to the gaseous nature of 1-MCP and its low solubility in water (10 ppb in 1 ml of H_2O), it was re-administered at every sampling point to ensure its presence in the medium.

Mevinolin (Sigma) is an inhibitor of cytokinin production (Laureys *et al.*, 1998). Addition of 10μM mevinolin, previously shown by Laureys *et al.* (1998) to reduce the mitotic index peak by 50% tobacco BY-2 cell cultures, occurred to *Spcdc25* 3* and EV2 cell cultures 0 h after release from aphidicolin.

2.6. Mitotic Cell Size Measurements

Mitotic cell size measurements were carried out using Sigmascan® (Sigma), an image analysis program. A line was traced around the contour of cells undergoing mitosis so that their area could be determined. To ensure measurements were accurate, a graticule was used as a distance reference point from which Sigmascan® could calculate the area of a cell. Data obtained was recorded into Microsoft® Excel.

2.7. Growth Rate Measurements

Cells were taken at stationary phase of the cultures in 2.5 ml aliquots and resuspended in 95 ml of fresh medium. Two ml of cells were aliquoted from the culture every 24 h for a period of 7 days (or until stationary phase was reached) and cell density measured using a spectrophotometer (λ=550nm). Where absorbance readings were in excess of 1.0, samples were diluted to ensure an accurate measurement.

2.8. Detection Of 3'-OH DNA Termini

The Apoptag® apoptosis detection kit (Intergen) utilising fluorescein-labelled antibodies specific to 3'-OH breaks in nuclear DNA was used. Cells from the 3.5 h ethylene and control treatments were sampled every 2 h. At each sampling time, 1ml of cells was removed, centrifuged at 1000 rpm (MSE Centaur 2) (10 min) and the supernatant discarded. Cells were resuspended in 1% (v/v) paraformaldehyde in Phosphate Buffered Saline (PBS) and stored at 4°C for a maximum of 48 h. Cells (70 µl) were placed on alcohol-cleaned slides, a coverslip applied and the slide placed on dry ice until the coverslip became heavily frosted (5-10 min); it was then removed using a razorblade. The preparation was allowed to dry at room temperature and the procedure outlined in the Apoptag manual for indirect fluorescence was subsequently followed (Fig 2.1). The reaction buffer in the Apoptag® kit is designed to add digoxigenin-labelled nucleotides via the enzyme terminal deoxynucleotidyl transferase (TdT) to 3'-OH ends of double-stranded or single-stranded DNA. DNA fragments labelled with the digoxigenin nucleotide are then allowed to bind to an anti-digoxigenin antibody that is conjugated to a fluorescein reporter molecule. The counter-staining procedure outlined in the Apoptag® manual was modified in that the cells were mounted in PBS containing PI (120 µg/ml). Cells were visualised using a fluorescence microscope (Olympus BH-2, UV, λ = 420 nm). At each sampling time, the number of green (antibody labelled) or red (PI-stained) nuclei were scored and the results expressed as % labelled. Images were captured using a digital camera attachment (Fujitsu HC-300Z) for the microscope.

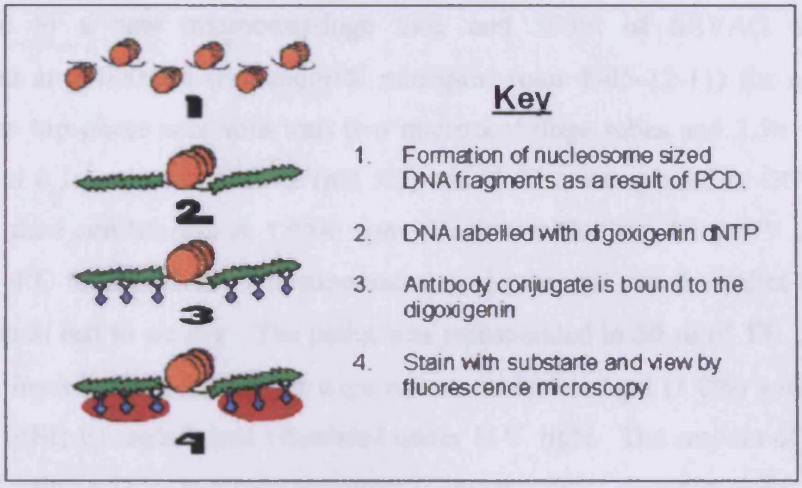

Figure 2.1. Apoptag® fluorescence labelling for DNA 3'-OH termini detection. Adapted from The Complete Apoptag® Manual, Intergen.

2.9. DNA Extraction

Cells (50 ml) were harvested from tobacco BY-2 cultures and spun at 3000 rpm for 5 mins to form a pellet. The supernatant was discarded and approximately 0.5 g of the material ground to a fine pellet using liquid nitrogen and a pestle and mortar. This was transferred to a polypropylene tube (50 ml; Falcon) with 2x CTAB buffer (15 ml) preheated to 60°C and gently mixed. The tube was subsequently incubated at 60°C for 20 mins. SEVAG (15 ml) was added and the samples placed on a rocker for 30 mins ensuring that the screwcap was additionally sealed with Nescofilm to prevent leakage. Samples were then spun at 8000 rpm for 10 mins at 4°C. The top layer was placed in a fresh 50 ml polypropylene tube (Falcon) and mixed with 30 ml of pre-cooled (-20°C) Ethanol. This was placed at -20°C for at least one hour until precipitation was visible. The sample was then centrifuged at 3750 rpm (Beckman Coulter Allegra™ 21R, rotor F2402H) for 30 mins at 4°C. The supernatant was discarded and the pellet air dried. 500 µl of TE was added and the sample heated to 60°C to mix. This was transferred to a 1.5 ml microcentrifuge tube and 5 µl of RNase (40 mg/ml) was added and incubated at 37°C for one hour. 500 µl of phenol/chloroform was added and gently mixed with the sample then centrifuged at 13000 rpm (Eppendorf® minispin; rotor F-45-12-11) for 5 mins. The top phase was

transferred to a new microcentrifuge tube and 500µl of SEVAG added and centrifuged at 13000rpm (Eppendorf® minispin; rotor F-45-12-11) for a further 5 mins. The top phase was split into two microcentrifuge tubes and 2.5x volume of ethanol and 0.1x volume of NaAc (pH 5.2) added. This was placed at -20°C for one hour and then centrifuged at 13000 rpm (Beckman Coulter Allegra™ 21R, rotor F2402H), 4°C for 20 mins. The supernatant was removed and the pellet formed by centrifugation left to air dry. The pellet was resuspended in 50 µl of TE. To ensure DNA had been extracted, samples were run on an agarose gel (1.0%) with ethidium bromide (EtBr; 10 mg/ml) and visualised under U.V. light. The amount of DNA was quantified using a U.V. spectrophotometer (Genequant®). Samples were stored at -20°C until further need.

2.10. DNA Amplification

DNA amplification was carried out via the Polymerase Chain Reaction (PCR; Fig 2.2). For this the Reddymix™ PCR Master Mix system (ABgene) was used. This contains all the reagents necessary for DNA amplification including dNTPS (0.2 mM), Thermoprime plus DNA polymerase (1.25u), MgCl (1.5 mM), and loading buffer for gel electrophoresis. For a total reaction volume of 50 µl, 45 µl of Reddymix™, 1 µl of forward primer (10 µM), 1 µl of reverse primer (10 µM), 2 µl of DNA, and 1 µl of sterile dH_2O was used. Table 2.2 shows the primers used for each gene of interest and the annealing temperatures used. The PCR program followed for DNA amplification was 94°C for 1 min, annealing temperature for 1 min, 72°C for 1 min (repeated for 40 cycles), and 72°C for 7 mins. PCR products were run on an agarose gel (1.0%) with EtBr (10 mg/ml) and visualised under U.V light.

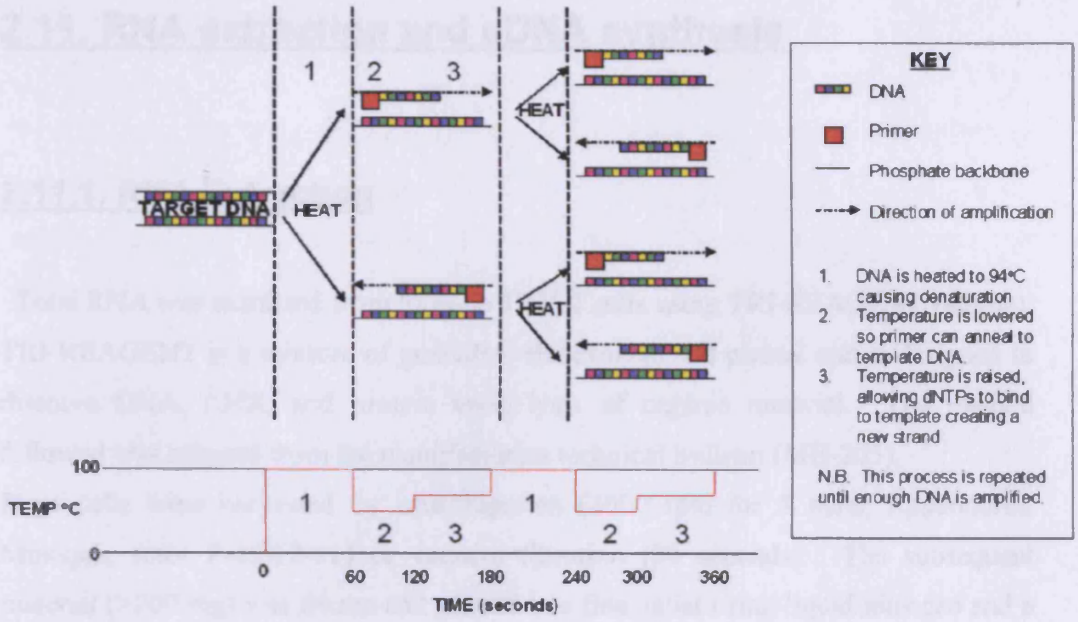

Figure 2.2. DNA Amplification via the Polymerase Chain Reaction. Short oligonucleotides known as primers with homology to the target gene are used to amplify regions.

Primer Pair	Annealing Temperature (°C)	Target Gene	Oligonucleotide Sequence	Product size (bp)
Cdc25:P2 Cdc25:P7	60	*SpCdc25*	5' – TTCCATGCTAATGTATTCAGAG 5' – ATGGTGGTGACGGGTGAC	718
CaMV35sF ETR1R	60	*Atetr1*	5' – GACCCTTCCTCTATATAAGG 5' – CGGTTCTCGAATGCGTAG	338
ETR1F ETR1R	60	*Atetr1*	5' – GATTGCGTATTTTTCGATTCCTC 5' – CGGTTCTCGAATGCGTAG	161

Table 2.2. Primers used for DNA amplification using PCR.

2.11. RNA extraction and cDNA synthesis

2.11.1. RNA Extraction

Total RNA was extracted from tobacco TBY-2 cells using TRI-REAGENT (Sigma). TRI-REAGENT is a mixture of guanidine thiocyanate and phenol and is designed to dissolve DNA, RNA, and protein upon lysis of organic material. The method followed was adapted from the manufacturers technical bulletin (MB-205).

Plant cells were harvested by centrifugation (3000 rpm for 5 mins; Eppendorf® Minispin, rotor F-45-12-11) or vacuum filtration (30 seconds). The subsequent material (>200 mg) was frozen and ground to a fine pellet using liquid nitrogen and a pestle and mortar pre-cooled to -20°C. Tri-Reagent (2 ml; Sigma) was added and grinding resumed until a homogenous paste was formed. Equal amounts of paste were transferred to two 1.5 ml microcentrifuge tubes, vortexed, and left to stand at room temperature for 5 mins. Samples were subsequently centrifuged at 1200 rpm (Beckman Coulter Allegra™ 21R, rotor F2402H) 4°C, for 10 mins and the supernatant transferred to fresh microcentrifuge tubes leaving the solid plant material behind. Chloroform (0.2ml) was added to each tube, vortexed for 15 seconds, and left to stand at room temperature. Samples were then centrifuged at 1200 rpm (Beckman Coulter Allegra™ 21R, rotor F2402H), 4°C for 15 mins. The top layer containing RNA was transferred to fresh microcentrifuge tubes (1.5ml) and isopropanol (0.5 ml) added. This was left to stand at room temperature for 10 mins and centrifuged at 12000 rpm (Beckman Coulter Allegra™ 21R, rotor F2402H), 4°C for 10 mins. The supernatant was removed and ethanol (1 ml) added to wash the pellet formed by the previous centrifugation. The samples were vortexed for 15 seconds and centrifuged at 12000 rpm (Beckman Coulter Allegra™ 21R, rotor F2402H), 4°C for 10 mins. The supernatant was carefully removed and the pellet air dried for 30 mins. The pellet was resuspended in dUHP H_2O (50 µl) with samples initially split into two microcentrifuge tubes recombined into one, giving a final volume of 100µl. Samples were stored at -70°C.

2.11.2. DNase Treatment

To 100 µl of each RNA preparation 10 µl of 10x DNase buffer and 3 µl of DNase added. Preparations were incubated at 37°C for 1 hour. 0.2 ml of DNase activation reagent was added and samples incubated at room temperature for 2 mins. The samples were centrifuged at 13000rpm (Eppendorf® minispin; rotor F-45-12-11) for 1 minute to pellet the inactivation reagent and the supernatant carefully transferred to a fresh microcentrifuge tube. Treated RNA was stored at -70°C.

Quantity and quality of RNA was estimated by spectrophotometry and by running on an agarose gel. The RNA extracts (10ml) were mixed with 2ml of loading buffer and run on an electrophoresis gel (1% agarose, 10mM EtBr). To minimise RNA degradation the gel tank, tray, and combs were treated with RNase Zap® (Albion). The RNA was visualised under UV light and photographed using a Gene Genius Bioimaging System and Gene Snap® software package (Syngene).

2.11.3. cDNA Synthesis

To ensure that direct comparison between samples could occur, equal amounts of RNA from each sample were reverse transcribed. cDNA synthesis was carried out in a PCR machine using the Gibco BRL Life Technologies reagents unless otherwise stated . 5 µg of DNase treated RNA was added to microcentrifuge tubes (0.5 ml) and made up to 20 µl with sterile dH_2O. 1 µl of oligo (dt)-15 (50 µg/ml; Promega) was added and samples incubated at 70°C for 10 mins. Samples were then cooled at 4°C for 10 mins. 5x 1st strand buffer (6 µl), 0.1M DTT (dithiothreitol; 2 µl), and 10 mM dNTPs (1 µl) were added and incubated at 42°C for 2 mins. M-MLV RNase H- Reverse Transcriptase (1 µl; Promega) was added and the samples incubated for a further 50 mins at 42°C. This enzyme lacks RNase H activity, eliminating degradation of RNA templates. The samples were heated to 70°C for 15 mins to inactivate the reverse transcriptase and reactions stored at -20°C. Mock reactions, important for ensuring no genomic DNA contamination, were also carried out following the above procedure. For this sterile dH_2O was substituted for Superscript II reverse transcriptase.

2.12. cDNA Amplification And Semi-Quantitative PCR

2.12.1. cDNA Amplification

cDNA was subject to PCR amplification for confirmation of transgene expression in transformed lines and for analysis of gene expression through the cell cycle. Amplification was carried out using Qiagen Hotstar® PCR reagents. For a reaction mix total of 25 µl the following was used. cDNA (0.5 µl), 2.5x Buffer (2.5 µl), 10 µM forward primer (1 µl), 10 µM reverse primer (1 µl) (see Table 6), 10 mM dNTPs (0.5 µl), Hotstar® Taq (DNA polymerase; 0.125 µl (5u/µl)), and sterile dH_2O (19.4 µl). Where possible a master mix was always used to reduce pipetting error and a negative control (sterile dH_2O substituted for cDNA) always used to ensure no water contamination. A positive control was used when available. Samples were placed in a PCR machine for amplification (Applied Biosystems Geneamp PCR system 2700). Each step in the PCR cycling stage was for 1 min with the annealing temperature varying between primer pairs (Table 2.3). Results were visualised by running samples on an agarose gel (1%) containing EtBr (10 mg/ml) for 20 mins at 120 millivolts.

Primer Pair	Reference	Target Gene	Oligonucleotide Sequence	Product Size (bp)	Tm (°C)
PUV2 PUV4		18S riboso-mal RNA	5' – TTCCATGCTAATGTATTCAGAG 5' – ATGGTGGTGACGGGTGAC	459	60
Cdc25 P2 Cdc25 P7		*S. pombe Cdc25*	5' – TTAGGTCCCCTTCTCCGATG 5' – GCGCGTCGACCATTAACGTCTGGGGAA GC	718	60
H4F H4R	Dambru-skas *et al.*, 2003	*Histone H4*	5' – GGCACAGGAAGGTTCTGAGGGATAACA 5' – TAACCGCCGAAACCGTAGAGAGTCC	196	60

Table 2.3. Primer Details for Gene Expression Analysis.

2.12.2. Semi-Quantitative PCR

Semi-quantitative PCR was carried out on tobacco BY-2 wild-type (WT) and *Spcdc25*-expressing cell lines. Samples (4 ml) were taken during synchrony experiments every hour in conjunction with mitotic index and mortality readings and immediately frozen at -70°C. RNA was extracted and used to synthesise cDNA (see 2.11). So that a semi-quantitative result could be obtained, samples from each hour of the same synchrony experiment were subjected to PCR with a range of cycle numbers. This was to determine a cycle number that would show an exponential increase or decrease in expression levels of the gene of interest (Fig. 2.3). For this, a composite cDNA sample from each synchrony experiment was prepared by mixing together 5 µl of each of the individual samples. Once a cycle number had been determined, PCR was carried out in triplicate on all cDNA samples from the same synchrony experiment. Samples were visualised using a 1% agarose gel with EtBr (10 mg/ml) and ethidium bromide fluorescence of PCR products recorded using a Gene Genius Bioimaging System and Gene Tools® software package (Sygene). This was carried out for all genes of interest. To ensure that results were due to a change in expression levels rather than an error during cDNA amplification, 18S ribosomal cDNA was amplified as a control. To equilibrate results, the EtBr fluorescence obtained from the gene of interest was divided by the EtBr fluorescence obtained for 18S amplification.

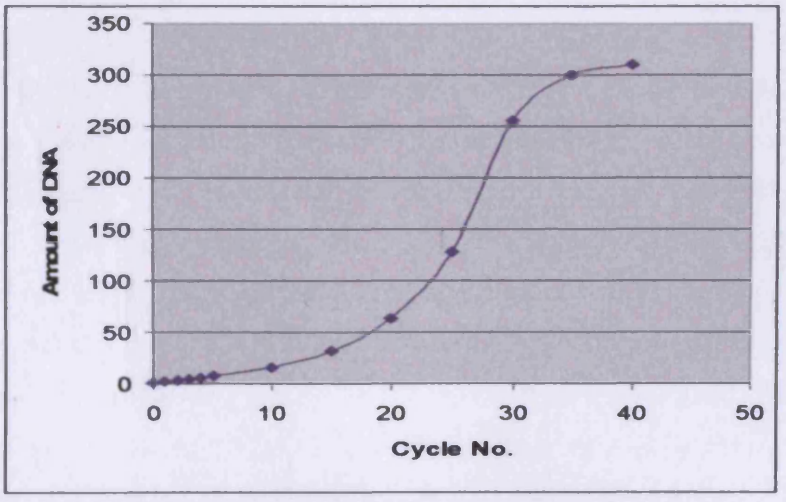

Figure 2.3. Graphical representation of the amount of DNA amplification with regards to cycle number in a PCR reaction. To carry out semi-quantitative PCR a cycle number within the exponential curve of the reaction is chosen to ensure up- and down-regulation of the target gene can be visualised.

2.13. Protein Extraction And Western Blotting

2.13.1. Protein Extraction

Cells, 15 ml in polypropylene tubes (Falcon), were harvested from tobacco BY-2 cultures in stationary phase (7 days old) and spun at 3000 rpm (MSE centaur 2) for 5 mins to form a pellet. The supernatant was discarded with the subsequent material frozen and ground to a fine pellet using liquid nitrogen and a pestle and mortar. Approximately 1 g of the ground pellet was transferred to 1.5 ml microcentrifuge tube and resuspended in 1 ml lysis buffer on ice. The suspension was centrifuged at 13000 rpm (Beckman Coulter Allegra™ 21R, rotor F2402H) 4°C for 30 mins and the supernatant transferred to a fresh microcentrifuge tube on ice. 1 µl of extract was transferred to 1 ml Coomassie® Protein Assay Reagent (Bradford assay; Sigma) and concentration of total extracted proteins measured with a UV-spectrophotometer λ = 595nm (Smartspec™3000, Bio-Rad Laboratories Ltd) against a standard curve (Fig. 2.4). Samples were stored at -70°C after being frozen in liquid nitrogen until further use.

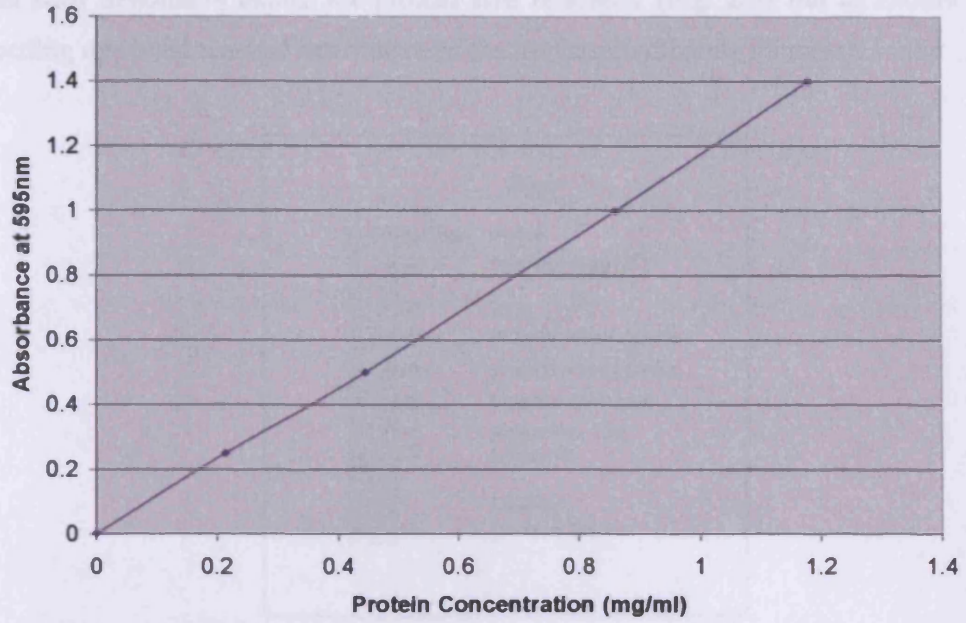

Figure 2.4. Standard curve for protein concentrations measured against absorbance using known amounts of bovine serum albumen (BSA).

2.13.2. SDS-PAGE Gel

To separate proteins into their respective molecular weights an SDS-PAGE gel was used. Gels consisted of a two-layered system of a stacking gel (where samples are loaded) and a resolving gel (where the proteins are resolved). To make the gel the Biorad Mini-PROTEAN II kit was used and the protocol described in QIAGENnews (Issue No. 5, 2000) adapted for use. Two glass plates separated by 1.5 mm were assembled according to the manufacturers instructions. The resolving gel mixture was made (see Appendix II) and 3 ml was poured between the glass plates leaving a 2-3 cm (a third of the height of the glass plates) gap at the top. 200 µl of butan-1-ol was applied to the surface of this layer using a syringe to exclude oxygen and to ensure a level transition point between the two gels. After polymerisation had occurred the butan-1-ol was removed by syringe and any excess with filter paper. The stacking gel mixture was made (see Appendix II) and poured onto the resolving gel until it reached the top of the glass plates. Before polymerisation could occur a plastic comb was inserted at the top of the gel to create wells for running the samples in. Once the gel had set, 25 µl of protein samples were aliquoted into microcentrifuge tubes and 5 µl of 5x loading buffer added. Samples were placed onto the SDS-PAGE

gel with Seablue™ ladder for protein size reference (Fig. 2.5) run at 150mv until loading dye band reached the bottom of the gel (approximately 45 mins).

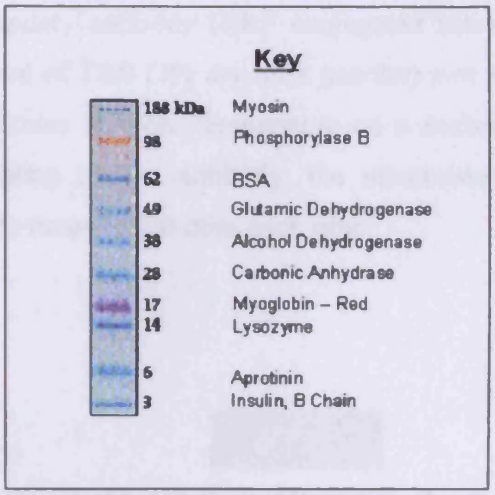

Figure 2.5. Seablue® Plus 2 Protein standard (Invitrogen). Molecular weights of protein standards are shown in kilo-Daltons (kDa).

2.13.3. Western Blotting and Detection

Five pieces of filter paper and a piece of PVDF membrane were cut out to the size of the SDS-PAGE gel. The PVDF membrane was pre-wetted in methanol and then incubated with the filter paper in the tank-blotting transfer buffer with the filter paper. The SDS-PAGE gel, PVDF membrane, and filter paper were then placed in a plastic support and arranged as shown in Fig. 2.6. The apparatus was assembled into the transfer tank (Bio-Rad) containing the tank-blotting transfer buffer and 100mV applied for 1 hour. After transfer had been completed the orientation of the gel was marked on the membrane and Ponceau S staining was carried out (see Section 2.13.4). This was to ensure that the transfer of protein to the membrane had been successful. After Ponceau S staining the membrane was placed in a small tray with 20ml of Tris Buffered Saline (TBS) supplemented with dry milk powder (3%) (Premier Brands UK Limited). This was incubated at room temperature on a rocker for 30 mins. The membrane was rinsed twice in TBS and then washed for 5 mins. The membrane was then subjected to the primary antibody (anti-*Sp*Cdc25 antibody supplied by Dr. S.

Moreno, 1:1000 dilution) diluted in 15ml of TBS (3% dry milk powder; Premier Brands UK Limited) for 1 hour at room temperature on a rocker. The membrane was rinsed twice in TBS and then left for a further 15 mins in TBS. The TBS was removed and the secondary antibody (HRP conjugated anti-rabbit, DACO, 1:1000 dilution) diluted in 20ml of TBS (3% dry milk powder) was added. The membrane was incubated for 30 mins at room temperature on a rocker. To ensure minimal background contamination by the antibody, the membrane was washed in TBS (0.05% Tween 20) eight times for 20 mins each time.

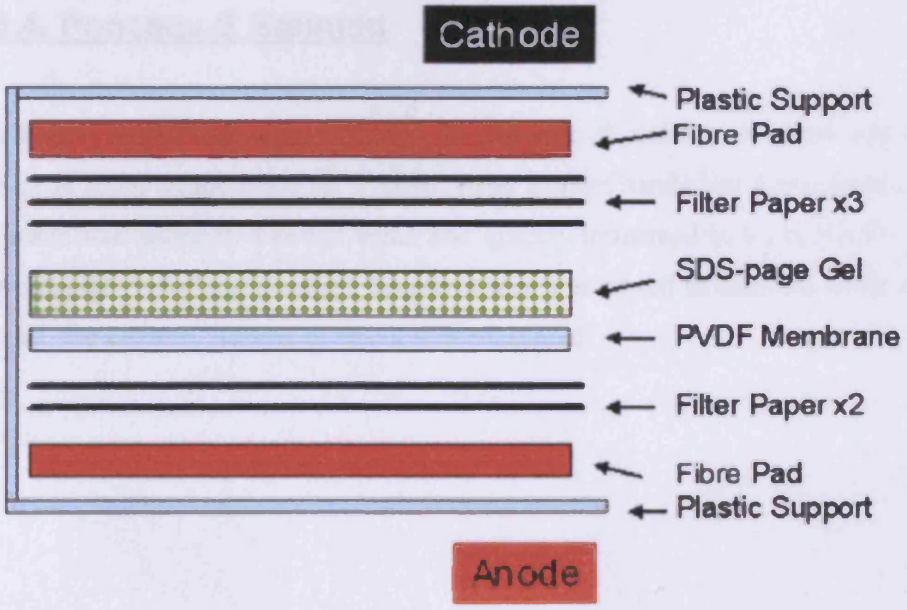

Figure 2.6. Arrangement of SDS-PAGE gel, PVDF membrane, and filter paper for protein transfer onto the membrane. Cathode and anode denote direction of current once transfer is taking place.

For detection of the proteins the Amersham ECL western blotting detection protocol (RPN 2108) was used. This detection kit makes use of a horseradish peroxidase (HRP) conjugated secondary antibody that, in conjunction with a chemiluminescent substrate, luminol, generates a signal that can be detected on film. The PVDF membrane was placed on SaranWrap™ (DOW Chemical Company) and 2.5 ml of reagent 1 and 2 was placed on top of it. This was allowed to incubate at room

temperature for 1 min and then removed. The membrane was then wrapped in SaranWrap® and exposed to chemiluminescent radiograph film (Hyperfilm ECL; Amersham) in the dark room. The orientation of the membrane was marked by using a fluorescent star. The film was exposed for varying lengths of time, changing the film each time, to ensure that a clear result could be obtained. After exposure the film(s) were placed in developing solution for 1 min, dipped in acetic acid (1.5%) briefly, and then fixed for 5-10 mins in fixing solution. Following the fixing of the film it was rinsed in water for 10 mins and then air-dried.

2.13.4. Ponceau S Staining

The PVDF membrane was immersed in Ponceau S staining solution and left to incubate at room temperature for 5 mins. After protein bands had been visualised the membrane was rinsed in distilled water and quickly immersed in 0.1M NaOH. Once the protein bands had disappeared the membrane was rinsed in distilled water for 2-3 mins and the western blotting protocol was continued.

Chapter 3

Ethylene Induces Cell Death At The G2/M Boundary With PCD Characteristics

3. Ethylene Induces Cell Death At The G2/M Boundary With PCD Characteristics

3.1. Introduction

In yeast and mammalian systems, some forms of PCD have been shown to exhibit a tight link to cell cycle checkpoints (Hirao *et al.*, 2000; Tanaka *et al.*, 2000). There is particular emphasis on the G2/M transition and this has been described as the DNA damage checkpoint (Rhind and Russell, 1998; Lopez-Girona *et al.*, 1999; Hirao *et al.*, 2000). As described in the thesis introduction, transitions between phases of the cell cycle depend upon CDK-cyclin complexes. In fission yeast, positive regulation of this complex at the G2/M checkpoint is carried out by Cdc25 phosphatase and negative regulation by Wee1 kinase (Russell and Nurse, 1986, 1987). Cdc25 is also the target of a molecular network that checks DNA integrity prior to the G2/M transition. If DNA damage is detected then Cdc25 is inactivated, Cdc2 cannot be dephosphorylated, and cells are held in G2 (Rhind and Russell, 1998; Lopez-Girona *et al.*, 1999). From this point two options exist. If the cell can repair the DNA damage, Cdc25 is reactivated and the cells can progress into mitosis (Lopez-Girona *et al.*, 1999). If the damage is too extensive, cells exit into PCD (Lane, 1992; Hirao *et al.*, 2000).

It was therefore interesting to test the hypothesis that in plants, exit into PCD is cell cycle specific. For this purpose the tobacco BY-2 cell line was used. This cell line is highly sychronisable with aphidicolin and therefore an extremely desirable system due to its uniformity and lack of developmental constraints (see section 1.4).

As discussed in section 1.2. , ethylene is a plant growth regulator known to be involved in certain PCD events in plants including endosperm development, xylogenesis, and organ senescence (He *et al.*, 1996; Young and Gallie, 1999, 2000; Fukada, 1996; Grbic and Bleecker, 1995). It has also been established that the ethylene signaling pathway is a stress response pathway involved in wounding and pathogen attack (Penninckx *et al.*, 1998; Watanabe *et al.*, 2001). In each of these

cases the outcome is cell death. PCD in mammalian systems has been described as an active and controlled process requiring *de novo* gene transcription (Ellis *et al.*, 1993) and as described in section 1.2. has certain characteristics defining it. In response to ethylene binding, the transcription factors known as EREBPs (ethylene responsive binding proteins) are known to increase and in turn have been shown to up-regulate a number of PR (pathogenesis related) genes (Eyal *et al.*, 1992; Mee Park *et al.*, 2001). This provides a link between ethylene causing cell death and *de novo* gene transcription, indicating plants share some PCD features of animal systems in response to ethylene.

In this study I report cell cycle specific death in tobacco BY-2 cell cultures and two associated features of PCD accompanying it, reduced cell size and generation of 3-'OH termini at the G2/M checkpoint in response to ethylene treatment.

3.2. Materials And Methods

Details of materials and methods are fully described in chapter 2.

See page 33 for synchronisation and mitotic index measurements, page 34 for cell viability and mortality index measurements, page 34 for ethylene and silver nitrate treatments, and page 36 for 3'-OH termini DNA detection.

3.3. Results

3.3.1. Ethylene and Ethylene+Silver Treatments Affect the Component Phases but not the Overall Length of the Cell Cycle.

A number of experiments were carried out using ethylene at 3.5 h to determine the length of the component phases of the cell cycle. An appreciable effect of the ethylene treatment was to delay the initial rise of the first mitotic index peak (Fig. 3.1a). This was due to an increase in the length of G2 to 6 h compared with 5 h in controls. Cell cycle duration is calculated from the distance in time between the two peaks of the mitotic index and its component from the mitotic index data generated using the formula described by Quastler and Sherman (1959). Using this formula, G2 + ½M = the interval between the *y*-axis and the 50% intercept of the initial rise of the mitotic index; S-phase = 50% intercept of the ascending and descending limbs of the mitotic peak; and M-phase = from where the curve begins to rise taken as the first mitotic index value above zero, to where it begins to plateau. G1 is calculated by the difference.

Since S-phase was confirmed by northern blotting (data not shown; see Herbert *et al.*, 2001) and from the mitotic index data to be approximately 3.5 h in controls, this meant that the addition of ethylene was given after the majority of cells had finished DNA replication. However, ethylene had no significant effect on cell cycle duration with the interval between two peaks being 14 h, identical to the WT control (Fig. 3.1a).

In the ethylene + silver nitrate experiments the silver ions would be expected to block the action of ethylene. This treatment had a small effect on G2, lengthening it by 0.5 h compared to controls, and caused an increase in the duration of M-phase to 3 h compared with 2 h for control (Fig 3.1b). S-phase remained unchanged at 3.5 h. As with the ethylene treatment, cell cycle duration remained unaltered at 14 h (Fig. 3.1b).

To examine whether the silver ions used in conjunction with the ethylene were having a detrimental effect of their own, further experiments were conducted. This involved the addition of silver nitrate (1.2 μM) at 3.5 h independent of ethylene

treatment. The silver treatment caused an even greater delayed rise into mitosis than that exhibited during ethylene treatment, 6-7 h after release from aphidicolin (Fig 3.1c). However, again overall cell cycle duration was not affected by the silver treatment with S-phase reduced by 0.5 h, M-phase reduced to 1 h and G1 duration reduced to 2 h (3.5 h in control). The most significant change was an increase in G2 to 8h (5 h in control; Fig. 3.1c).

The proportion of cycling cells is estimated as the area beneath the mitotic index curves. The proportion of cycling cells was greatest in control experiments ($15.27cm^2$) followed by ethylene ($7.18cm^2$), ethylene + silver ($5.28cm^2$), and silver alone ($3.72cm^2$) (Fig 3.1). Thus the silver treatment caused the largest reduction in the population of cycling cells. This was the most dramatic effect caused by the silver ions on the cell cycle. Cell cycle duration did not alter in any of the treatments relative to the control.

(a)

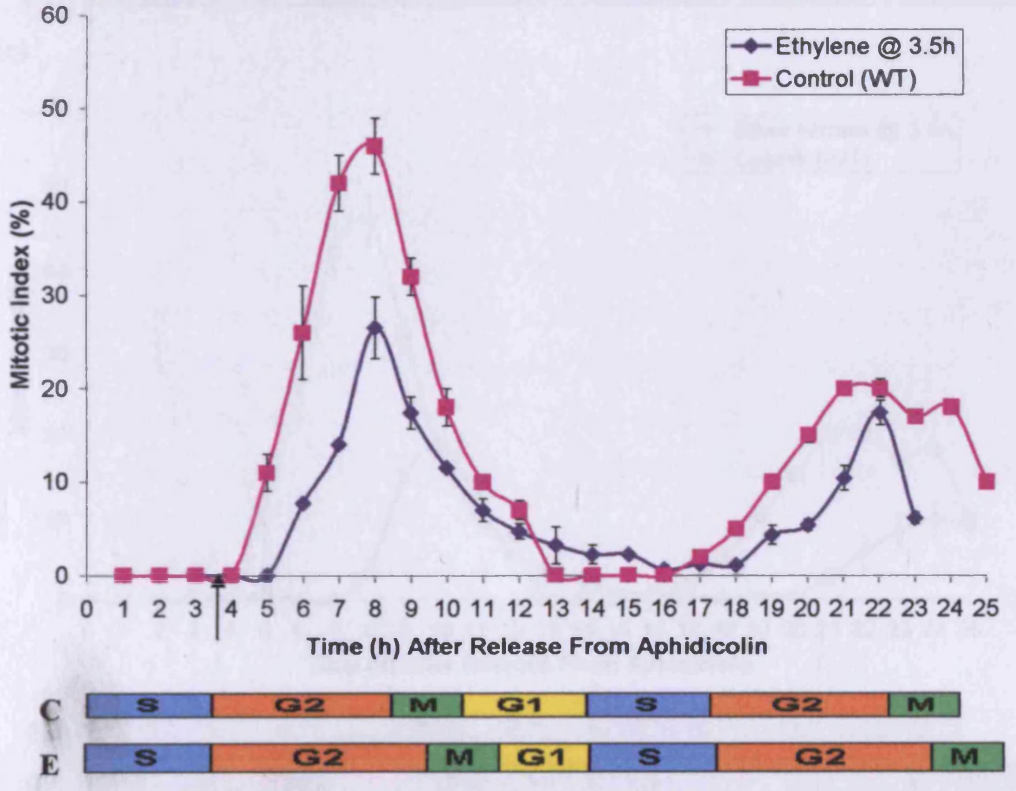

(b)

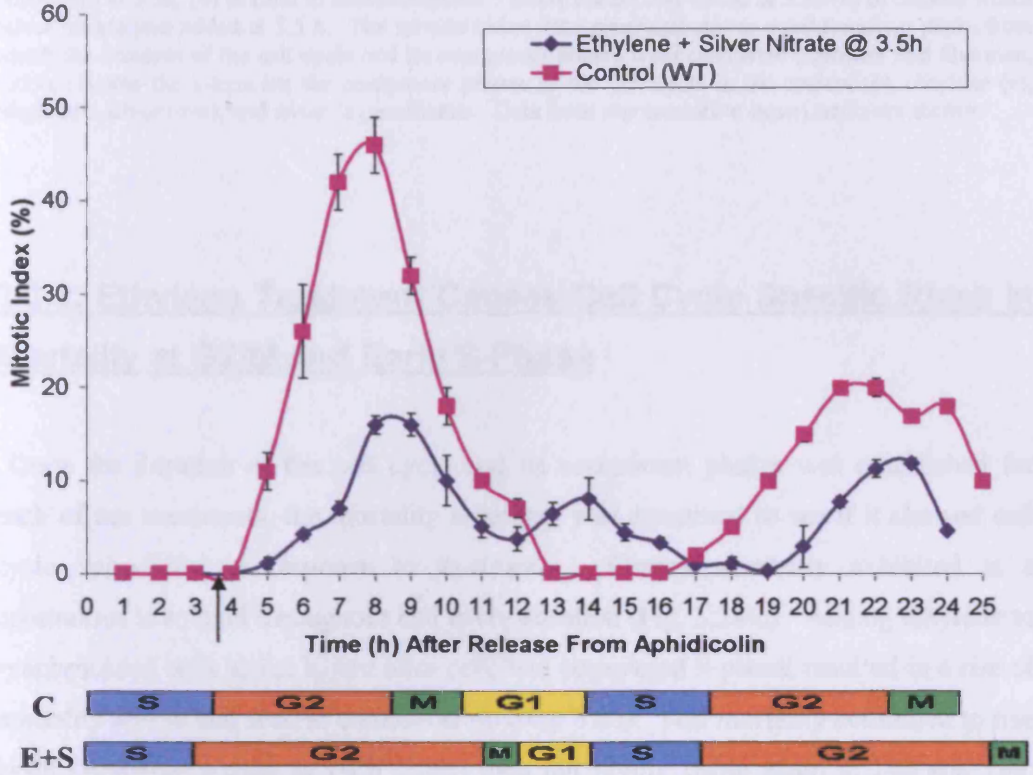
Ethylene + Silver Nitrate @ 3.5h
Control (WT)
Mitotic Index (%)
Time (h) After Release From Aphidicolin
C
E+S
S
G2
M
G1

(c)

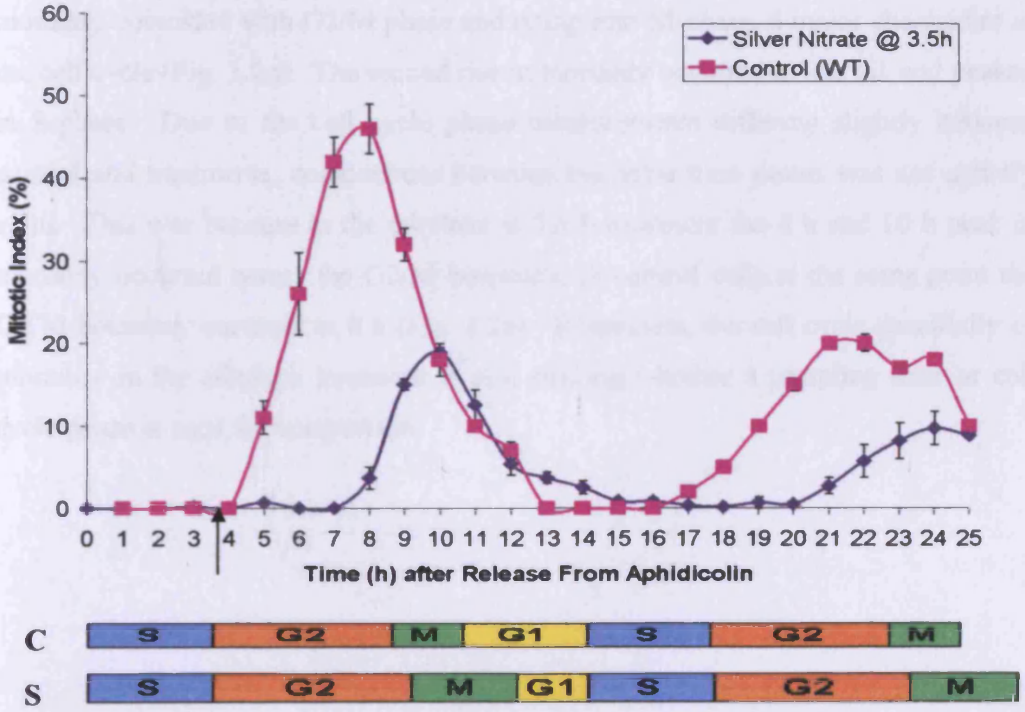
Silver Nitrate @ 3.5h
Control (WT)
Mitotic Index (%)
Time (h) after Release From Aphidicolin
C
S
G2
M
G1

Figure 3.1. The mitotic index of tobacco BY-2 cells plotted against time after the release from a 24h synchronization treatment with aphidicolin in controls or in (a) cells to which ethylene was added (arrow up) at 3.5h, (b) in cells to which ethylene + silver nitrate was added at 3.5h (c) in cells to which Silver nitrate was added at 3.5 h. The mitotic index data generated curves exhibiting two peaks from which the duration of the cell cycle and its component phases were calculated (Quastler and Sherman, 1959). Below the x-axis are the component phases of the cell cycle in the control (c), ethylene (e), ethylene + silver (e+s), and silver (s) treatments. Data from representative experiments are shown.

3.3.2. Ethylene Treatment Causes Cell Cycle Specific Rises in Mortality at G2/M and Early S-Phase

Once the duration of the cell cycle and its component phases was established for each of the treatments, the mortality exhibited was examined to see if it showed cell cycle specificity in response to treatments. Control mortality exhibited at a continuous low level throughout cell cycle duration (Fig. 3.2a-c). Adding ethylene to synchronized cells at 3.5 h, just after cells had completed S-phase, resulted in a rise of mortality above that seen in controls at 4h (Fig. 3.2a). This mortality continued to rise before reaching a peak at 10 h (25%) then fell before rising again at 14h and 16h. Aligning the cell cycle phases below the *x*-axis indicated that the largest incidences of mortality coincided with G2/M phase and rising into M-phase, a major checkpoint in the cell cycle (Fig. 3.2a). The second rise in mortality occurred in late G1 and peaked in S-phase. Due to the cell cycle phase measurements differing slightly between control and treatments, comparisons between the same time points was not entirely valid. This was because in the ethylene at 3.5 h treatment the 8 h and 10 h peak in mortality occurred across the G2/M boundary, in control cells at the same point the G2/M boundary occurred at 8 h (Fig. 3.2a). Regardless, the cell cycle specificity of mortality in the ethylene treatment is still striking whether a sampling time or cell cycle phase is used for comparison.

(a)

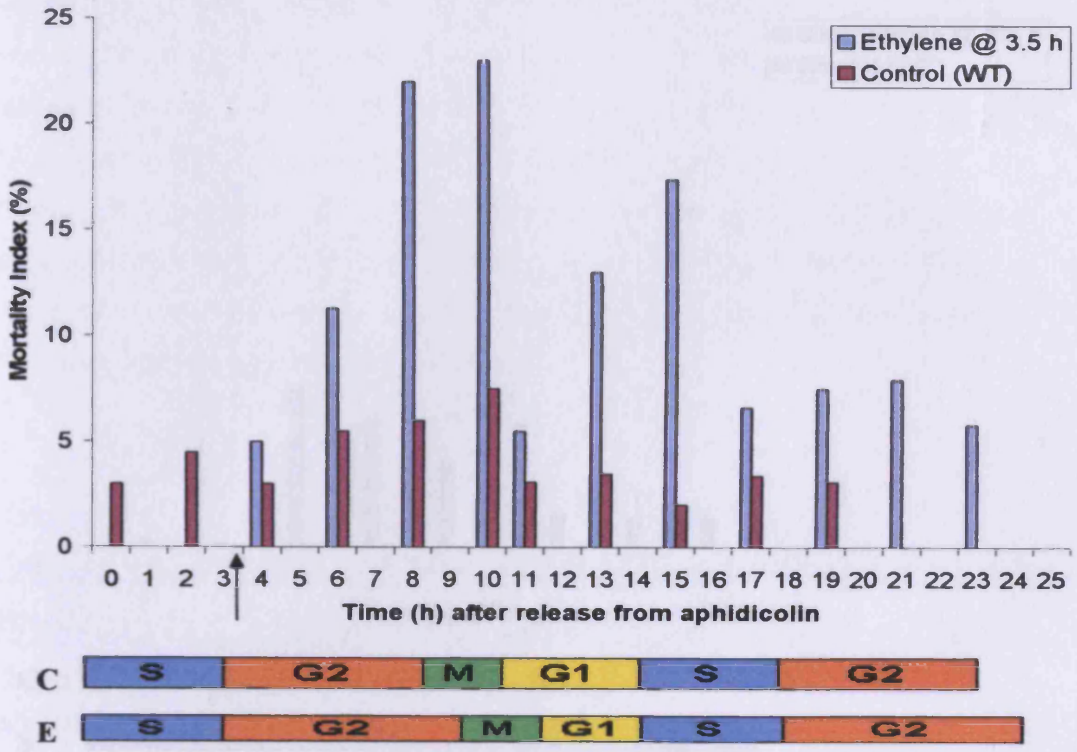
Ethylene @ 3.5 h
Control (WT)
Mortality Index (%)
0 5 10 15 20 25
0 1 2 3 4 5 6 7 8 9 10 11 12 13 14 15 16 17 18 19 20 21 22 23 24 25
Time (h) after release from aphidicolin
C
E
S
G2
M
G1
S
G2

(b)

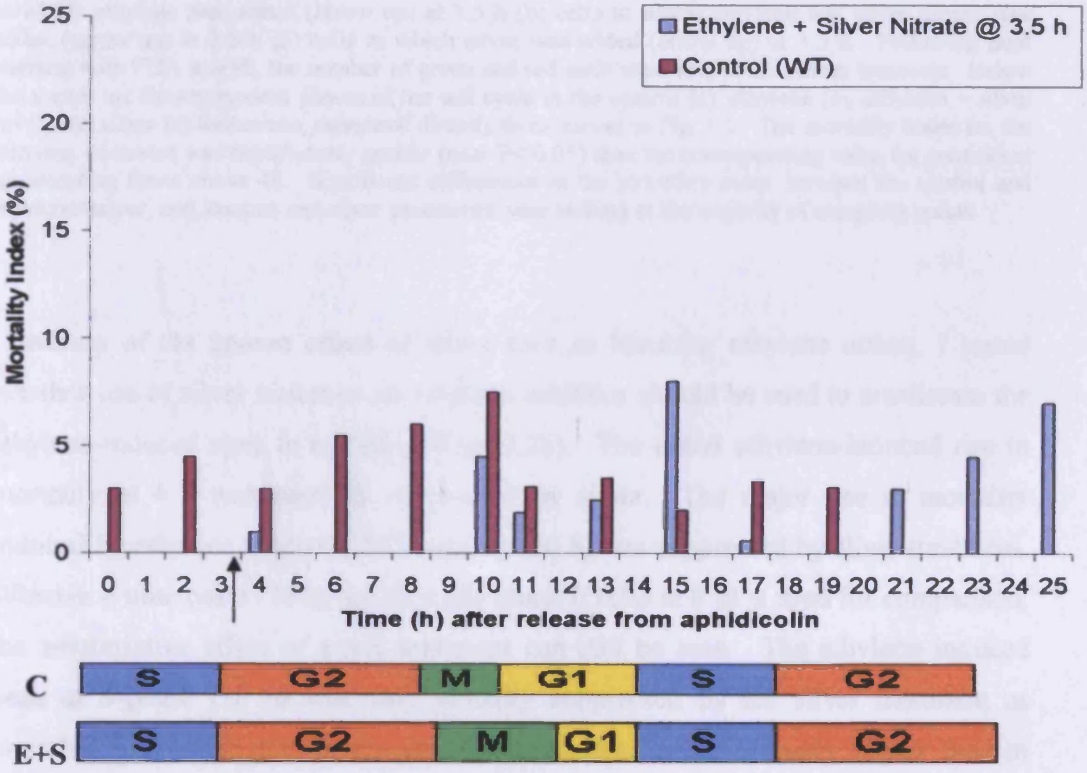
Ethylene + Silver Nitrate @ 3.5 h
Control (WT)
Mortality Index (%)
0 5 10 15 20 25
0 1 2 3 4 5 6 7 8 9 10 11 12 13 14 15 16 17 18 19 20 21 22 23 24 25
Time (h) after release from aphidicolin
C
E+S
S
G2
M
G1
S
G2

(c)

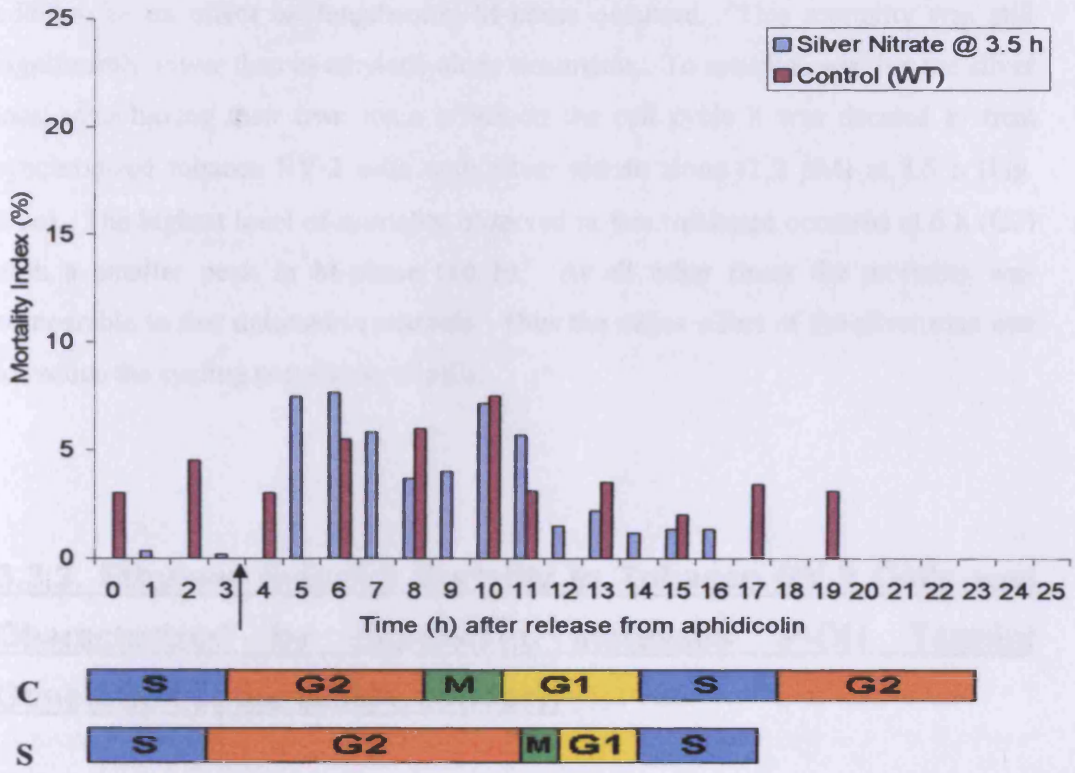

Figure 3.2. The mortality index (%) following the release from aphidicolin in controls and in (a) cells to which ethylene was added (arrow up) at 3.5 h (b) cells to which ethylene and silver nitrate was added (arrow up) at 3.5 h (c) cells to which silver was added (arrow up) at 3.5 h. Following dual staining with FDA and PI, the number of green and red cells were scored at random transects. Below the x-axes are the component phases of the cell cycle in the control (c), ethylene (e), ethylene + silver (e+s), and silver (s) treatments, measured directly from curves in Fig. 1.1. The mortality index for the ethylene treatment was significantly greater (min. $P< 0.05$) than the corresponding value for controls at all sampling times above 4h. Significant differences in the mortality index between the control and ethylene+silver, and, control and silver treatments were lacking at the majority of sampling points.

Because of the known effect of silver ions in blocking ethylene action, I tested whether use of silver nitrate as an ethylene inhibitor should be used to ameliorate the ethylene-induced rises in mortality (Fig. 3.2b). The initial ethylene-induced rise in mortality at 4 h was partially suppressed by silver. The major rise in mortality induced by ethylene at the G2/M boundary (10 h) was suppressed by silver treatment. Whether a time point (10 h) or cell cycle phase (G2/M at 8 h) is used for comparison, the ameliorative effect of silver treatment can still be seen. The ethylene induced peak at S-phase (16 h) was only partially suppressed by the silver treatment as mortality was lower than in the ethylene treatment but significantly higher than in

control (Fig. 3.2b). The silver treatment induced a rise in mortality in M-phase in addition to its effect on lengthening M-phase occurred. This mortality was still significantly lower than in ethylene-alone treatments. To establish whether the silver ions were having their own toxic effect on the cell cycle it was decided to treat synchronized tobacco BY-2 cells with silver nitrate alone (1.2 μM) at 3.5 h (Fig. 3.2c). The highest level of mortality observed in this treatment occurred at 6 h (G2) with a smaller peak in M-phase (10 h). At all other times the mortality was comparable to that detected in controls. Thus the major effect of the silver ions was to reduce the cycling population of cells.

3.3.3. Ethylene Induced Mortality in Tobacco BY-2 Cells was Characterized by Significant Increases 3'-OH Termini Generation at the G2/M Boundary.

As explained in chapter 1, when cells undergo apoptosis, DNA strand breaks can occur. During this study DNA laddering, the visualization of the broken strands of DNA, was not detected and it was therefore thought that the maximum level of mortality (25%, see Fig 3.2a) may not have been enough to resolve laddering on an agarose gel. Thus, detection of 3'-OH termini, exposed when DNA strand breaks occur, was carried out using the Apoptag® 3'-OH termini detection kit to see if DNA fragmentation was occurring in ethylene treated cells. The indirect fluorescence technique utilized by the Apoptag® kit labels the 3'-OH termini with digoxygenin nucleotides which are then subsequently labelled with fluorescein-conjugated antidigoxygenin. This results in a green/blue fluorescence in the nuclei of cells exhibiting the feature (Fig. 3.3c).

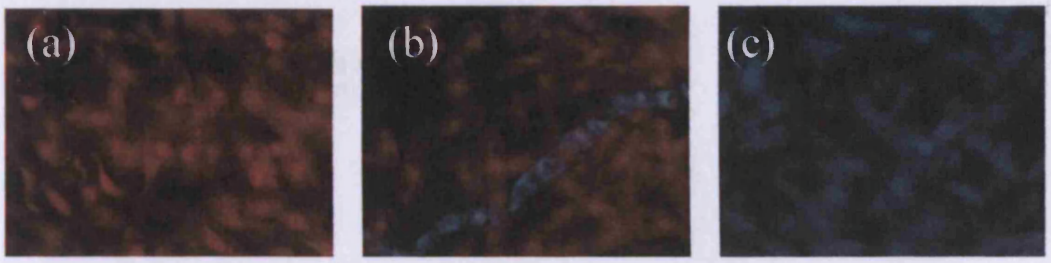

Figure 3.3. Photographs of cells which have undergone Apoptag® treatment for 3'-OH termini detection. Once cells had been labelled with the fluorescein probe, counterstaining occurred with PI. (a) cells exhibiting no 3'-OH termini (red stained) (b) cells exhibiting 3'-OH termini in a chain (blue stained) and background cells showing no 3'-OH termini (red stained) (c) all cells exhibiting the presence of 3'-OH termini (blue stained); taken from an ethylene treatment experiment.

Nuclear DNA exhibiting 3'-OH termini was detected in control and ethylene treatments. No difference in the percentage of nuclear fragmentation was detected before ethylene treatment at 3.5h in control and ethylene experiments. After ethylene treatment a subsequent increase in ethylene treated cells exhibiting 3'-OH termini occurred but was not mirrored in the control. The occurrence of 3'-OH in ethylene treated cells dramatically increased between 6 and 8 h. This was a greater than 7-fold increase in the percentage of ethylene treated cells exhibiting the 3'-OH termini when the cells were undergoing mitosis (Fig. 3.4). This rise in and peak of the occurrence of 3'-OH termini also corresponded with the rise and peak in mortality observed at the G2/M transition.

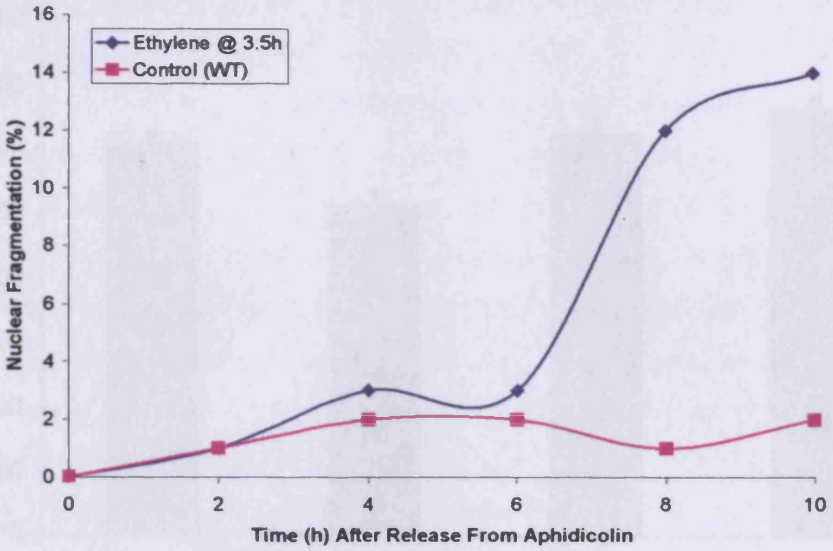

Figure 3.4. The percentage of cells that generated 3'-OH termini (nuclear fragmentation) in tobacco BY-2 cells plotted against time after the release from a 24h synchronization with aphidicolin in control (red line) or in cells to which ethylene was added (arrow up) at 3.5h (blue line) following labelling of 3'-OH termini with fluorescein using the Apoptag® kit.

3.3.4. Ethylene Induced Mortality in the Tobacco BY-2 Cell Line Causes a Reduction in Mitotic Cell Size

Mitotic cell areas were measured using image analysis to determine whether ethylene, ethylene + silver nitrate, or silver nitrate had any effect on this parameter. Mitotic cell area was used to ensure that all measured cells were in the same stage of the cell cycle (M-phase). Using a two-sample t-test, chosen because most treatments indicated normal distribution, a significant reduction in mitotic cell areas of ethylene treated cells cf. control was observed (Fig. 3.5). Significant differences could not be detected in ethylene + silver and silver cf. control ($P<0.05$) with both being similar to that observed in control (Fig. 3.5).

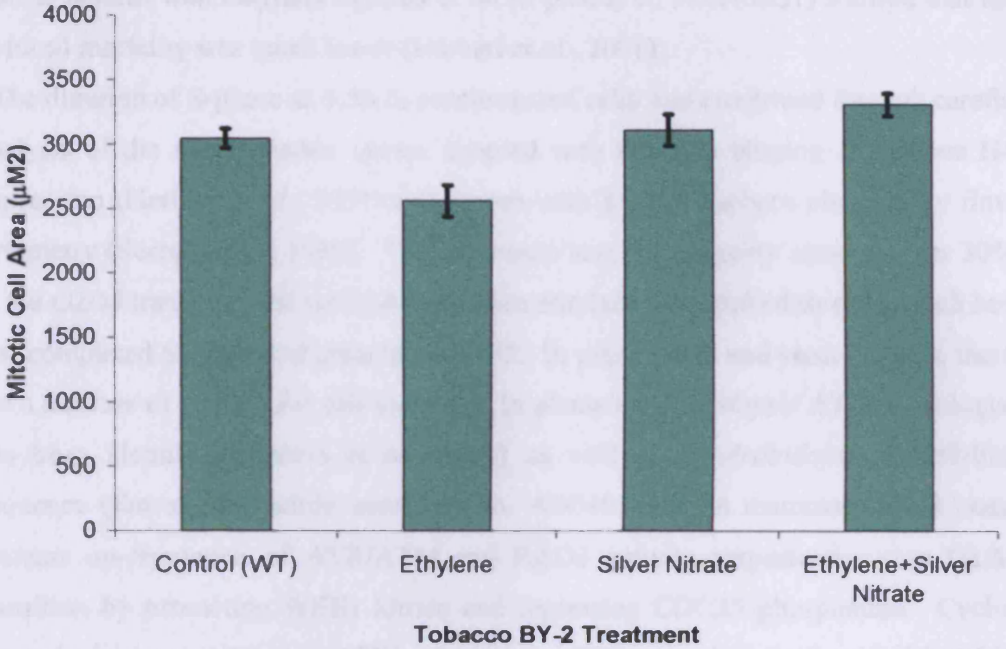

Figure 3.5. The mitotic cell areas of control (WT) cells (mean = 3046µm^2; n = 125), ethylene treated cells (mean = 2562µm^2: n = 124), ethylene + silver nitrate treated cells (mean = 3472µm^2; n = 94), and silver nitrate treated cells (mean = 3115µm^2: n = 51). The vertical lines (black) represent ±SE.

3.5. Discussion

The data reported in this chapter confirm the hypothesis that ethylene treatment resulted in increased levels of mortality in the tobacco BY-2 cell line in a cell cycle specific pattern (see also, Herbert *et al.*, 2001). When ethylene was added to cells that had just completed S-phase (3.5 h), a substantial peak of mortality was detected at G2/M, a major checkpoint in the cell cycle, and another in the next S-phase. Moreover, the cell death in the tobacco BY-2 cells shows some features of apoptosis including DNA fragmentation and reduced cell size. These features were prominent in the ethylene treatment, especially at the G2/M transition, and coincides with the highest levels of ethylene-induced mortality observed. However, in the ethylene treatment, the cycling population divided at the same rate as the controls indicating that the level of ethylene used did not cause massive perturbation to the cell cycle.

Earlier studies with ethylene injected at 0h (S-phase) cf. 3.5h (S/G1) showed that the induced mortality was much lower (Herbert *et al.*, 2001).

The duration of S-phase as 3.5h in synchronized cells was confirmed through careful analysis of the mitotic index curves coupled with northern blotting of Histone H4 expression (Herbert *et al.*, 2001) and agrees with a 3.5 h S-phase obtained by flow cytometry (Sorrell *et al.*, 1999). The maximum level of mortality observed was 30% at the G2/M transition and was induced when ethylene was applied to cells which had just completed S-phase and entered early G2. In mammalian and yeast systems, there are a number of sensors for cell viability. In plants an *Arabidopsis* ATM homologue has been identified (Garcia *et al.*, 2000) as well as an *Arabidopsis* RAD3-like sequence (Entrez Nucleotide accession no. AB040133). In mammalian and yeast systems up-regulation of ATR/ATM and RAD3 activity respectively, stop G2/M transition by promoting WEE1 kinase and repressing CDC25 phosphatase. Cyclin dependent kinase inhibitors (CKIs; known as ICKs in plants) also inhibit CDK activity by masking the ATP binding domain of Cdc2 kinase (Wang *et al.*, 1997). Both *Arabidopsis* ICK1 and ICK2 have been shown to stop CDK activity and cell division in response to the plant growth regulator, abscisic acid (Zhou *et al.*, 2002). I suggest that in the tobacco BY-2 system, ethylene initiates the ethylene stress response pathway (see section 1.2.1.4; Fig. 1.8) and that this pathway directly or indirectly activates inhibition of the CDK/cyclin complex by one of the methods mentioned above. However, if DNA damage is catastrophic exit into cell death occurs. In the ethylene treatment of tobacco BY-2 cells, delayed entry of viable cells into mitosis by 1h occurred and could be a result of a lag in which the cells recover from DNA damage inflicted by ethylene. Notably in fission yeast and mammalian systems, the DNA damage checkpoint causes cells to arrest in G2 (Rhind and Russell, 1998). In the 3.5h ethylene treatment, one third of tobacco BY-2 cells failed to satisfy this hypothesized DNA checkpoint at the G2/M transition and exited the cell cycle into death. The increase in 3'-OH termini by ethylene is interpreted as evidence for damage at the level of nuclear DNA. Moreover, reduced cell size, another associated feature of PCD, was induced by ethylene at G2/M.

In fumonisin B1-induced cell death, ethylene signaling was found to be essential in plants (Asai *et al.*, 2000). This is also the case for a number of developmental cell death events (see section 1.2.1). It would be interesting to identify a change in regulation of proteins that interact directly with the CDK/cyclin complex. This would

help elucidate the mechanism of ethylene induced cell death and cell cycle interaction downstream of the ethylene responsive binding factors. So far this has not been achieved but it is interesting to note that a putative GCC box, a *cis* element present in many ethylene-regulated pathogen-related genes (Wang *et al.*, 2002), exist in the sequence of *Oryza sativa* *At*ATM-like protein (Entrez Nucleotide accession no. NM_183488).

A second peak of ethylene-induced mortality was also observed in S-phase. In yeast and vertebrates, a major cell cycle checkpoint for DNA damage operates in late G1 (Tanaka *et al.*, 2000). This checkpoint is important because it checks the competency of cells to undergo DNA synthesis. Hence the observed rise in mortality in S-phase may be a consequence of the failure of 20% of cells to satisfy this DNA damage checkpoint, exiting into cell death. In support of this hypothesis, the level of mortality rose in late G1 until reaching the S-phase peak. Further study into 3'-OH termini occurrence would be required to see if this mortality bore hallmarks of a PCD process. The ethylene-induced peak of mortality at G2/M was suppressed by silver ions, which fits with their known effect of blocking ethylene action (Drew *et al.*, 1981). At all sampling times, the level of mortality in the ethylene+silver treatment was reduced compared with that in the ethylene treatment. However, the ethylene+silver treatment resulted in a significant increase in mortality at M- and S-phase compared with the controls. Silver is a toxic metal (Woolhouse, 1983) and is perhaps exerting a toxic effect at mitosis as was found when synchronized tobacco BY-2 cells were treated with zinc at 100 μM (Francis *et al.*, 1995). This was partly confirmed by the data from the silver treatment, which indicated a rise in mortality in M-phase, which was not detected in the ethylene treatment. Notably the silver+ethylene and silver treatments reduced the population of rapidly cycling cells to a greater extent than ethylene. Whether in response to toxic metals dying tobacco BY-2 also exhibit apoptotic symptoms has to be resolved.

The concentration of ethylene used in these experiments (17700 μl/l) was chosen because it induced measurable, but not overwhelming, levels of mortality (maximum 30%) in this system. Clearly, cells in a plant are never exposed to such high concentrations of gaseous ethylene. So, what is the physiological relevance of the data reported here? First, as emphasized earlier, although this much ethylene was released into the head-space of the flask, only a very small proportion would enter the

liquid phase given the extremely low solubility of this gas in water. Hence on this basis, the amount of ethylene taken up by the tobacco BY-2 cells would be much more similar to that in the whole plant. Second, concentrations of ethylene lower than 17700 µl/l had a negligible effect on mortality. Thirdly, the concentration of silver nitrate used (1.2 µM) is known to inhibit ethylene action in whole plant studies (Drew *et al.*, 1981). This concentration of silver ions was sufficient to ameliorate ethylene-induced mortality, most notably in cells sampled at G2/M of the cell cycle. Clearly, if unusually large amounts of ethylene had entered the tobacco BY-2 cells, then 1.2 µM silver nitrate would have been ineffective in ameliorating ethylene action. Fourth, in the ethylene treatment, a substantial population of viable cells divided at the same rate as controls. Again, if unusually large amounts of ethylene reached the cells then massive mortality or profound cell cycle perturbation, or both, would be likely. Fifth, a clear parallel exists with metal toxicity studies particularly regarding the concentration required to produce a given degree of inhibition in cultured cells (Davies *et al.*, 1991). For example, inhibitory concentrations of metals used in studies utilizing plant cells in the culture are much greater than those used in whole plant work (Steffens *et al.*, 1986). Finally, ethylene is integral to normal plant development and is therefore more relevant than other compounds such as camptothecin, an anti-cancer drug (Hsiang *et al.*, 1985) that plant cells would not come into contact with naturally.

Various groups have shown how plant growth regulators (pgrs) interface with the G2/M and G1/S phase checkpoints of the plant cell cycle (Zhang *et al.*, 1996; Wang *et al.*, 1997; Riou-Khamlichi *et al.*, 1999; Francis and Sorrell, 2000). The work reported here has demonstrated how another pgr, ethylene, induced cell death maximally, at G2/M in the tobacco BY-2 cell line. Some characteristics of apoptosis such as nuclear blebbing and DNA laddering were not detected. However, it should be noted that DNA laddering is not always a feature of plant cells undergoing PCD (Jones and Dangl, 1996; Buckner *et al.*, 2000). A programmed mechanism acting through the ethylene receptors is favoured in order to explain the cell-cycle specific cell death observed here, given the generation of 3'-OH ends, nuclear shrinkage and the isolation of dead/dying cells adjacent to living ones.

3.6. Summary

The data reported in this chapter are summarised as follows:

- Ethylene induced high mortality at the G2/M boundary.
- Ethylene treatment resulted in a mortality peak in S-phase.
- Ethylene caused a one hour delay in the rise of the mitotic index.
- DNA fragmentation (3'-OH termini) was detected in ethylene treated cells.
- Simultaneous addition of silver nitrate ameliorated the effects of ethylene
- Silver nitrate exhibited a toxic side-effect.
- Ethylene treatment resulted in a reduced cell size phenotype.

Other ways of ameliorating ethylene-induced cell death were sought in the literature and 1-methylcyclopropene (1-MCP) was identified as a useful chemical inhibitor. 1-MCP has a similar mode of action to silver ions, blocking the ethylene binding site of ethylene receptors (Sisler *et al.*, 1996a-b). Due to the inherent mortality observed when using silver ions, 1-MCP was obtained in the hope it would provide a greater insight into the effect of ethylene on the tobacco BY-2 cell cycle. The results from this work are reported in the next chapter.

Chapter 4

1-Methylcyclopropene Ameliorates Both Ethylene-Induced And Wild-Type Mortality Levels

4. 1-Methylcyclopropene Ameliorates Both Ethylene-Induced And Wild-Type Mortality Levels

4.1. Introduction

1-Methylcyclopropene (1-MCP) is an ameliorator of ethylene action in the same fashion as silver ions. 1-MCP blocks ethylene action by attaching to the ethylene binding sites of ethylene receptors (Sisler *et al.*, 1996a-b). Because 1-MCP is gaseous it is formulated as a 0.14% soluble powder (1-methylcyclopropene Technical Bulletin, Rohm Haas, 2001). Commercial use of 1-MCP was approved by the EPA (Environment Protection Agency) in the US in 1999 and European registration in 2003 (Watkins and Miller, 2003). The effect of 1-MCP in ameliorating disease in plants has been mixed with incidences of infection found to increase in oranges and strawberries (Porat *et al.*, 1999; Jiang *et al.*, 2001) but decrease in apricots (Dong *et al.*, 2002). Since the pathogens used in these studies were not identical, the results are probably because ethylene sensitivity can be both advantageous and deleterious, depending on the pathogen in question.

1-MCP has been used as a research tool to investigate the effect of ethylene in over fifteen fruits as well as cut flowers and flowering plants (Watkins and Miller, 2003). There are a number of other ethylene inhibitors apart from silver ions (either in nitrate thiosulphate form) and 1-MCP. These include aviglycine (AVG), cobalt chloride, and 2,5-norbornadiene (NBD). Both AVG and cobalt chloride are inhibitors of the ethylene biosynthesis pathway and are toxic when used in high concentrations (Yang, 1980; Murashige and Skoog, 1962; Lai *et al.*, 2000). NBD is an inhibitor of ethylene action but is less effective than silver ions (Buse and Laties, 1993).

In the previous chapter, the effect of silver nitrate on tobacco BY-2 cells was described and data presented showing that it could ameliorate ethylene action. Unfortunately it also exerted a toxic side-effect. Given that 1-MCPs efficacy in ethylene inhibition is a relatively new development, its effectiveness in blocking ethylene action is reported in this chapter together with any toxic side-effects. 1-MCP

was obtained from Rohm-Haas and applied to both tobacco BY-2 cultures after release from 24 h synchronization with aphidicolin and during normal 7 day batch culture growth.

4.2. Materials And Methods

Details of materials and methods are fully described in chapter 2.
See page 33 for synchronisation and mitotic index measurements, page 34 for cell viability and mortality index measurements, page 34 for 1-MCP and 1-MCP+ethylene treatments, and page 35 for growth rate measurements.

4.3. Results

4.3.1. 1-MCP Treatment and 1-MCP+Ethylene Treatment Have no Effect on the Cell Cycle

A number of cell cycle experiments were carried out exposing tobacco BY-2 cells to 1-MCP 3.5 h following release from aphidicolin. In wild-type (WT) cells, this 3.5 h time point coincides with the end of S-phase (chapter 3). Treatment with 3.2 g 1-MCP resulted in a rise in the mitotic index at 4 h and peak at 7h (Fig. 4.2a). This pattern in the rise and peak of the mitotic index was virtually identical to the control (WT) data (Fig. 4.2) with the height of the mitotic peaks also being similar. This was unlike the silver nitrate treatment which caused a substantial reduction in the mitotic peak cf. WT (chapter 3). The second peak for both 1-MCP treated and control experiments occurred at 20 h and meant that cell cycle duration remained unaltered between control and 1-MCP treated cells (13 h; Fig. 4.2). Hence the data are consistent in demonstrating that 1-MCP had very little, if any, effect on the proportion of cycling cells. The cell cycle phases for control tobacco BY-2 cells as calculated from Fig. 4.2 were 2.5 h for S-phase, 4 h for G2, 3 h for M-phase and 3.5 h for G1. 1-MCP treatment 3.5 h after release from aphidicolin had little effect on the cell cycle

phases compared with control, the only differences being a slight lengthening of G2 to 4.5 h and a slight reduction of G1 to 3 h (Fig. 4.2a). Both S-phase and M-phase duration remained the same between control and 1-MCP treated cells (2.5 h and 3 h respectively).

S-phase Confirmed as 2.5 h in Control (WT)

Histone H4 expression is an excellent marker of S-phase. S-phase duration in control (WT) tobacco BY-2 cells, observed in chapter 3, was approximately 3.5 h in duration and identical to published values for S-phase in this cell line (Sorrell *et al.*, 1999; Herbert *et al.*, 2001). Monitoring of histone H4 in the control (WT) for this chapter indicated an S-phase duration of 2.5 h (Fig. 4.1) and was identical to the calculated value.

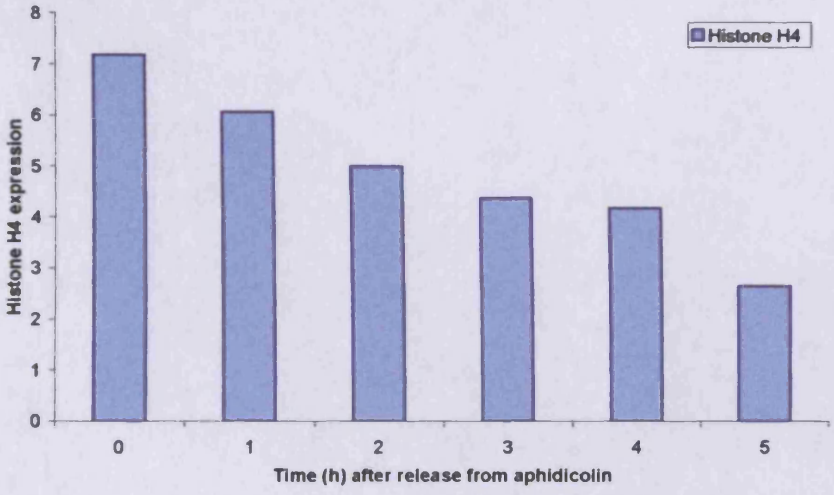

Figure 4.1. Expression of histone H4 following the release of tobacco BY-2 cells from a 24 h synchronisation with aphidicolin in control (WT). RNA was amplified using semi-quantitative PCR and results obtained measuring amplified band intensity. Histone H4 expression was corrected for error using 18S ribosomal RNA expression as a standard.

To test whether 1-MCP was effectively blocking ethylene action, tobacco BY-2 cells were treated with both 1-MCP and ethylene 3.5 h after release from aphidicolin. Unlike 1-MCP treatment, cell cycle duration increased to 14h with mitotic peaks

occurring at 7 and 21 h (Fig. 4.2b). The duration of S-phase was 3 h compared with 2.5 h for both control and the 1-MCP treatment (Fig. 4.2). This may indicate an effect of ethylene on the second S-phase following removal of aphidicolin (note that 1-MCP/ethylene injection occurred at 3.5 h following the completion of the first S-phase). In the 1-MCP+ethylene treatment, M-phase remained unaltered compared with control and 1-MCP treatments (3 h) with G2 being comparable to that of the control (4.5 h) and G1 identical to 1-MCP treated cells (3.5 h). The height of the first mitotic peak for 1-MCP+Ethylene treated cells (Fig. 4.2b) was also similar to that observed in control and 1-MCP treatment (Fig. 4.2a). As with the 1-MCP treatment, the second mitotic peak for 1-MCP+Ethylene showed a significant reduction (21.78% compared with 32.01% for control), and was comparable to the second peak in the 1-MCP treatment. The coincidental rise and fall of the peaks in 1-MCP cf. control suggests that unlike silver nitrate treatments, 1-MCP does not appear to deliver a toxic effect (Fig. 3.1c cf. Fig. 4.2a). The area under the mitotic index curve in control and 1-MCP was 15.91 and 15.54cm^2 respectively. Once again, the first peak of mitotic index in the 1-MCP+ethylene treatment was remarkably similar to the control treatment, although the amplitude of the second peak was 'noisier' cf. control. The area under the mitotic index curve in 1-MCP+ethylene was 15.26cm^2. The comparable areas for silver and silver+ethylene treatments (Fig. 3.1, page 52) were 3.72cm^2 and 5.28cm^2 respectively. Hence there were substantially more cycling cells in the 1-MCP and 1-MCP+ethylene treatment than in the silver and silver+ethylene treatments.

(a)

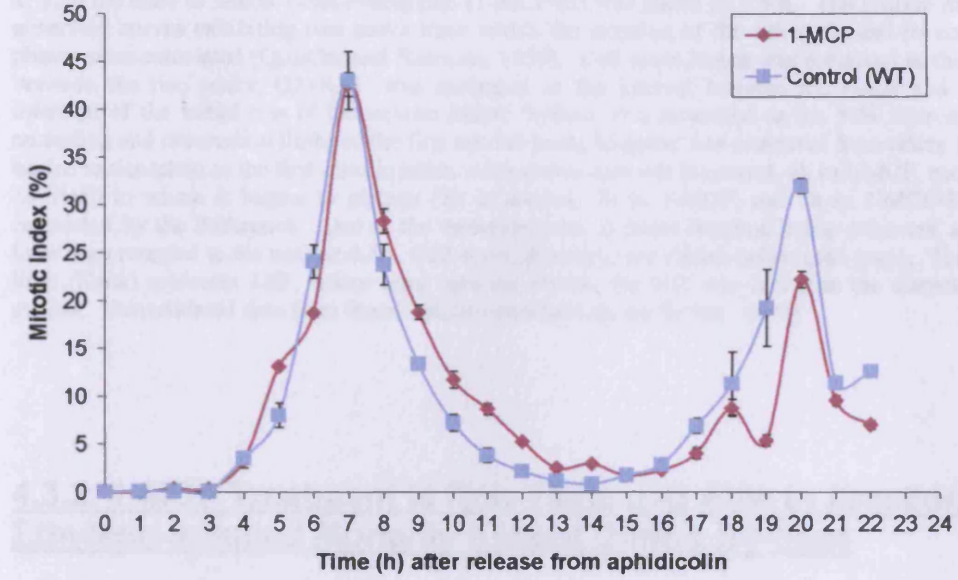
1-MCP
Control (WT)
Mitotic Index (%)
Time (h) after release from aphidicolin


Control
S
G2
M
G1
S
G2
M
1-MCP
S
G2
M
G1
S
G2
M

(b)

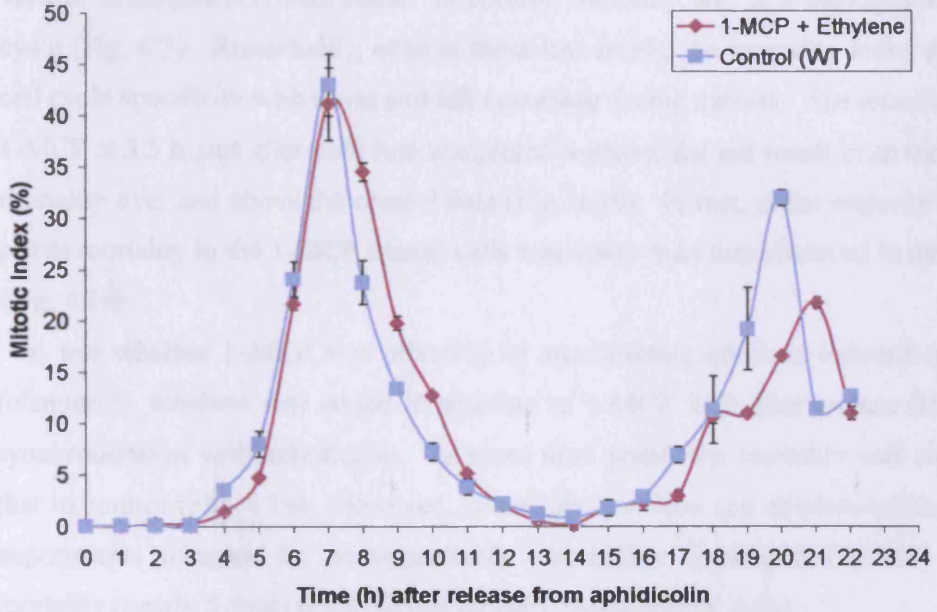
1-MCP + Ethylene
Control (WT)
Mitotic Index (%)
Time (h) after release from aphidicolin


Control
S
G2
M
G1
S
G2
M
1-MCP+E
S
G2
M
G1
S
G2

Figure 4.2. The mitotic index of tobacco BY-2 cells plotted against time after the release from a 24h synchronization treatment with aphidicolin in controls (WT) and (a) cells to which 1-MCP was added at 3.5h (b) cells to which 1-MCP+ethylene (1-MCP+E) was added at 3.5 h. The mitotic index data generated curves exhibiting two peaks from which the duration of the cell cycle and its component phases were calculated (Quastler and Sherman, 1959). Cell cycle length was measured as the interval between the two peaks; G2+½M was measured as the interval between the y-axis and the 50% intercept of the initial rise of the mitotic index; S-phase was measured as the 50% intercept of the ascending and descending limbs of the first mitotic peak; M-phase was measured from where the curve begins to rise taken as the first mitotic index value above zero (4h in control, 4h in 1-MCP, and 4h in 1-MCP+E) to where it begins to plateau (7h in control, 7h in 1-MCP, and 7h in 1-MCP+E); G1 is calculated by the difference. Due to the measurements of phase duration being estimates, all values have been rounded to the nearest 0.5h. Cell cycle phases (h) are shown below each graph. The vertical lines (black) represent ±SE, where error bars are absent, the ±SE was less than the diameter of the symbol. Consolidated data from three replicate experiments are shown. (n=3).

4.3.2. 1-MCP Treatment is Non-Toxic and Able to Ameliorate Ethylene-Induced Mortality Except During S-Phase

Once the duration of the cell cycle and its component phases were established from the mitotic index data, the mortality index (FDA + PI double stain; see p34 of chapter 2) was examined to see whether 1-MCP induced cell cycle specific mortality. By aligning the cell cycle phases below the x-axes, the incidences of mortality can be viewed in conjunction with them. In control, mortality was low throughout the cell cycle (Fig. 4.3). Remarkably, even at these low levels, the mortality index exhibited cell cycle specificity with a rise and fall occurring during mitosis. The introduction of 1-MCP at 3.5 h, just after cells had completed S-phase, did not result in an increase of mortality over and above the control data (Fig. 4.3b). In fact, at the majority of time-points mortality in the 1-MCP treated cells was lower than that observed in the control (Fig. 4.3a).

To test whether 1-MCP was effective in ameliorating ethylene-induced mortality (chapter 3), ethylene was added in addition to 1-MCP 3.5h after release from 24 h synchronization with aphidicolin. At most time points the mortality was similar to that in control (Fig. 4.3b). However, as with the ethylene and ethylene+silver nitrate experiments (chapter 3), an appreciable and highly significant ($P<0.05$) rise in mortality (nearly 5-fold) occurred during early S-phase (Fig. 4.3b).

(a)

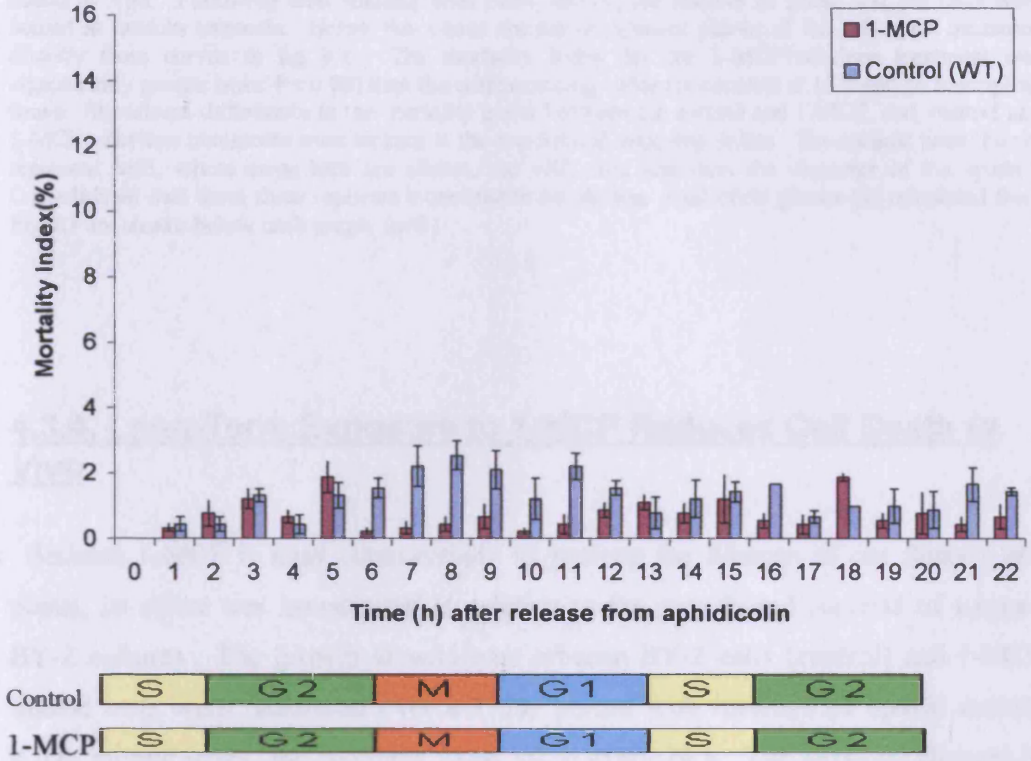
1-MCP
Control (WT)
Mortality Index(%)
0 1 2 3 4 5 6 7 8 9 10 11 12 13 14 15 16 17 18 19 20 21 22
Time (h) after release from aphidicolin
Control
1-MCP
S
G2
M
G1
S
G2

(b)

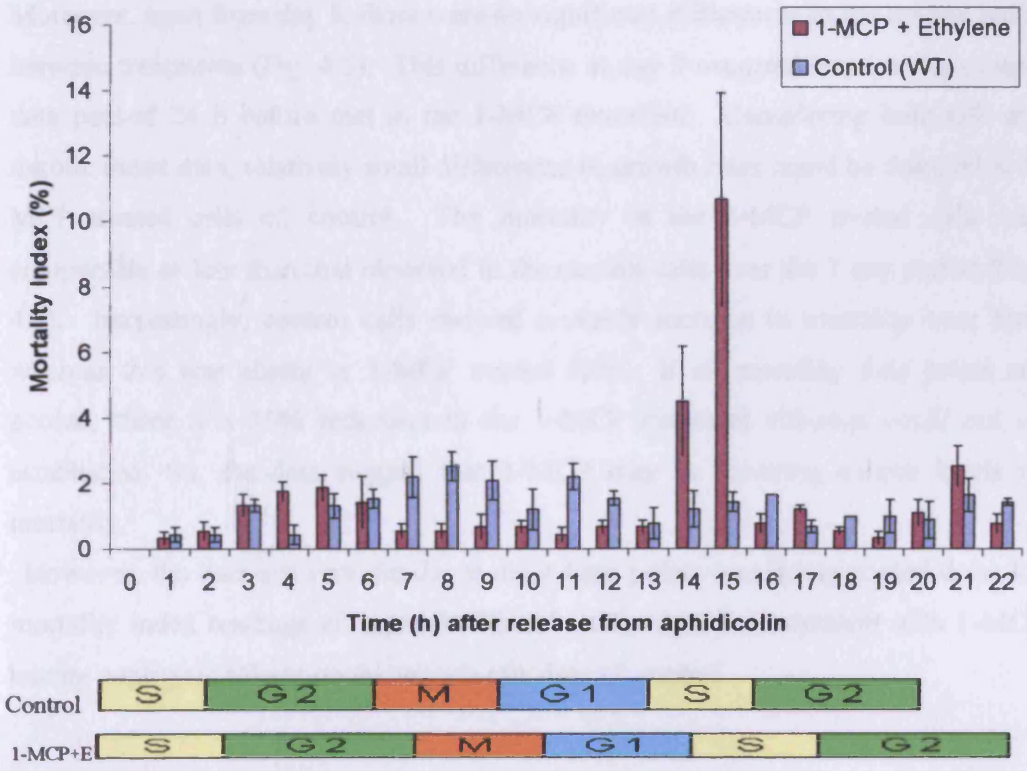
1-MCP + Ethylene
Control (WT)
Mortality Index (%)
0 1 2 3 4 5 6 7 8 9 10 11 12 13 14 15 16 17 18 19 20 21 22
Time (h) after release from aphidicolin
Control
1-MCP+E
S
G2
M
G1
S
G2

Figure 4.3. The mortality index (%) following the release from aphidicolin in control (WT) cells and (a) cells to which 1-MCP was added at 3.5h (b) cells to which 1-MCP+Ethylene (1-MCP+E) was added at 3.5h. Following dual staining with FDA and PI, the number of green and red cells were scored at random transects. Below the x-axes are the component phases of the cell cycle measured directly from curves in fig 4.1. The mortality index for the 1-MCP+ethylene treatment was significantly greater (min. $P< 0.05$) than the corresponding value for controls at 15 h and 16 h sampling times. Significant differences in the mortality index between the control and 1-MCP, and, control and 1-MCP+ethylene treatments were lacking at the majority of sampling points. The vertical lines (black) represent ±SE, where error bars are absent, the ±SE was less than the diameter of the symbol. Consolidated data from three replicate experiments are shown. Cell cycle phases (h) calculated from Fig.4.1 are shown below each graph. (n=3).

4.3.4. Long-Term Exposure to 1-MCP Reduces Cell Death *In Vivo*

Because 1-MCP is used commercially to prolong the lifespan of cut flowers and plants, its effect was investigated in relation to the growth and survival of tobacco BY-2 cultures. The growth of wild-type tobacco BY-2 cells (control) and 1-MCP treated cells were monitored over a 7 day period with readings of optical density (OD), mitotic index, and mortality index taken every 24 h. The temporal changes in OD were virtually identical between control and 1-MCP treated cells (Fig. 4.4). Moreover, apart from day 3, there were no significant differences in the mitotic index between treatments (Fig. 4.5). This difference at day 3 occurred because the control data peaked 24 h before that in the 1-MCP treatment. Considering both OD and mitotic index data, relatively small differences in growth rates could be detected in 1-MCP treated cells cf. control. The mortality in the 1-MCP treated cells was comparable or less than that observed in the control cells over the 7 day period (Fig. 4.6). Interestingly, control cells showed a steady increase in mortality over time whereas this was absent in 1-MCP treated cells. If all mortality data points are pooled, there is a 10% reduction in the 1-MCP treatment although could not be established. So, the data suggest that 1-MCP may be lowering natural levels of mortality.

However, the data are very similar at most time points (excluding pooled data) for mortality index readings cf. control. Therefore the data are consistent with 1-MCP having negligible effects on the growth rate data cf. control.

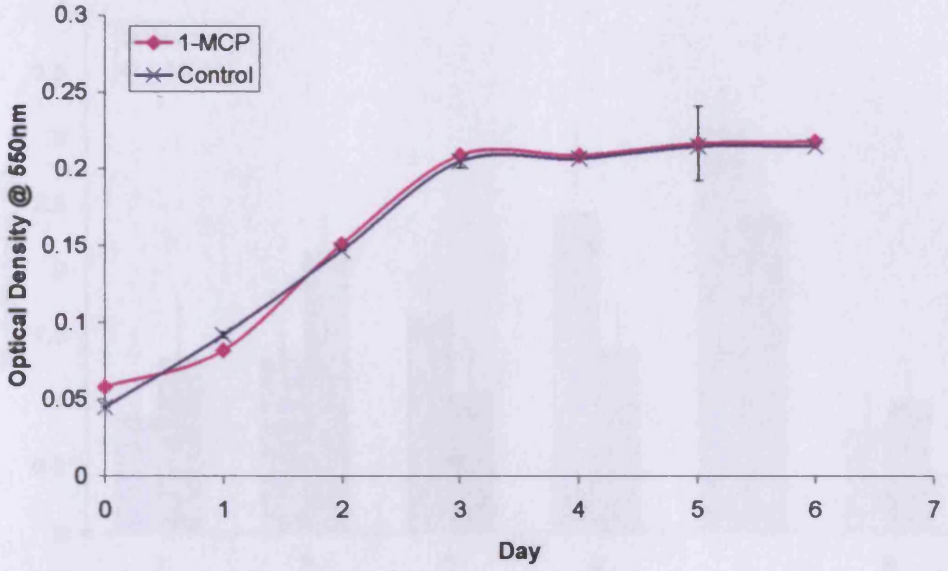

Figure 4.4. The optical density readings over a 7d growth period indicating growth of control (WT) cells (blue line) and 1-MCP + ethylene treated cells (pink line). The vertical lines (black) represent ±SE, where lines are absent the ±SE was less than the diameter of the symbol. (n=9).

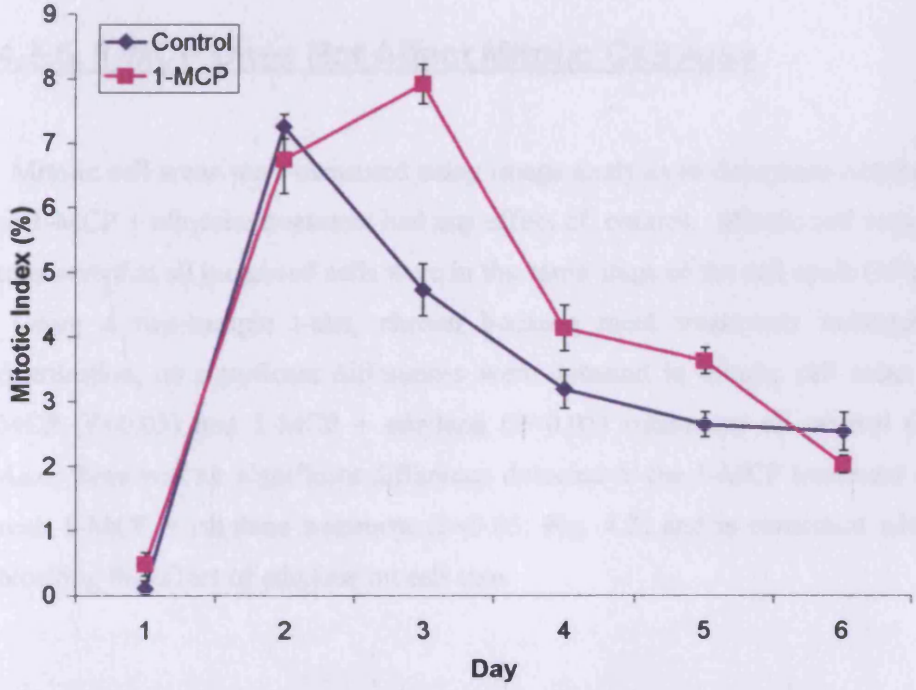

Figure 4.5. The mitotic index (%) over a 7d growth period in control (WT) cells (blue line) and 1-MCP treated cells (pink line). The vertical bars represent ±SE, where lines are absent the ±SE was less than the diameter of the symbol. (n=9)

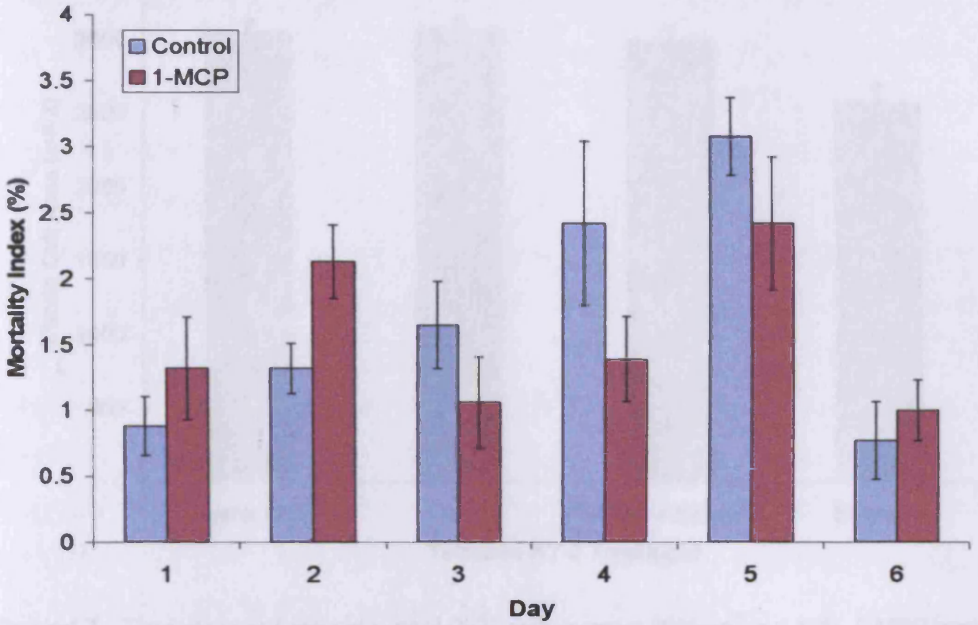

Figure 4.6. The mortality index (%) over a 7d growth period in control (WT) cells (blue bars) and 1-MCP treated cells (red bars). The vertical lines (black) represent ±SE. (n=9).

4.3.5. 1-MCP Does Not Affect Mitotic Cell Area

Mitotic cell areas were measured using image analysis to determine whether 1-MCP or 1-MCP + ethylene treatment had any effect cf. control. Mitotic cell area was used to ensure that all measured cells were in the same stage of the cell cycle (M-phase).

Using a two-sample t-test, chosen because most treatments indicated normal distribution, no significant differences were detected in mitotic cell areas in the 1-MCP ($P<0.05$) and 1-MCP + ethylene ($P<0.05$) treatments cf. control (Fig. 4.7). Also, there was no significant difference detected in the 1-MCP treatment compared with 1-MCP + ethylene treatment ($P<0.05$: Fig. 4.7) and is consistent with 1-MCP blocking the effect of ethylene on cell size.

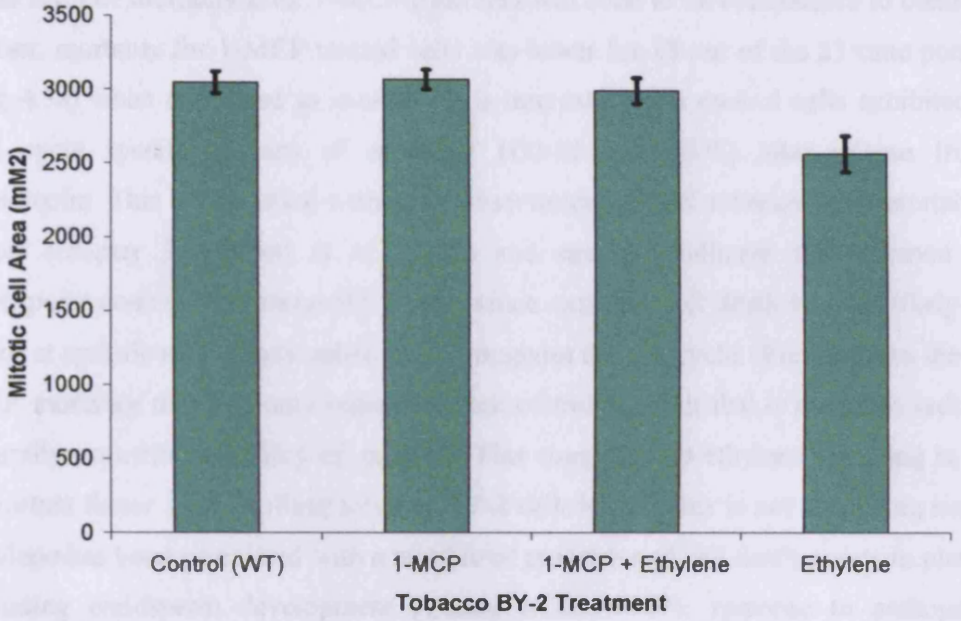

Figure 4.7. The mitotic cell areas of control (WT) cells (mean = 3046μm^2; n = 125), 1-MCP treated cells (mean = 3067μm^2: n = 124), 1-MCP + ethylene treated cells (mean = 3020μm^2; n = 94), and ethylene treated cells (mean = 2562μm^2: n = 51). The vertical lines (black) represent ±SE.

4.4. Discussion

The data from this study confirm the hypothesis that 1-MCP treatment results in little or no effect on tobacco BY-2 cells in terms of the cell cycle, cell size, and cell growth. Following the addition of 1-MCP to cells that had just completed S-phase cell cycle duration, the number of cells cycling, mortality levels, and duration of cell cycle periods all remained similar to that observed in control. Cell cycle duration was unaffected, remaining at 13 h for control and 1-MCP treatment although a slight decrease in the number of cells attaining the second mitotic peak was observed in the 1-MCP treated cells. 1-MCP treatment resulted in a slight lengthening of G2 (4.5 h cf. 4 h control) and a slight reduction of G1 (3 h cf. 3.5 h control) with mitosis and S-phase remaining the same (3 h and 2.5 h respectively). Therefore, unlike silver nitrate treatment (chapter 3), 1-MCP has no effect on cell cycle duration or its component phases.

The level of mortality after 1-MCP treatment was seen to be comparable to control. In fact, mortality for 1-MCP treated cells was lower for 18 out of the 23 time points (Fig 4.3a) when compared to control. It is interesting that control cells exhibited a cell cycle specific pattern of mortality (G2-M and G1/S) after release from aphidicolin. This is consistent with other observations of WT tobacco BY-2 mortality levels (chapter 3; Herbert *et al.*, 2001) and strongly indicates the presence of checkpoint control in tobacco BY-2 cells since exit into cell death is more likely to occur at specific time points rather than throughout the cell cycle. Furthermore, the 1-MCP mortality data not only indicate a lack of toxicity, but that it may also reduce naturally occurring mortality cf. control. This suggests that ethylene signaling is an important factor in controlling tobacco BY-2 cell death. This is not surprising since ethylene has been associated with a number of programmed cell death events in plants including endosperm development (Young *et al.*, 1997), response to pathogens (Ohtsubo *et al.*, 1999), and water-logging (Drew *et al.*, 2000).

When tobacco BY-2 cells were exposed to ethylene and 1-MCP 3.5 h after release from aphidicolin, cell cycle duration was slightly increased to 14 h (13 h in control). S-phase increased to 3 h, mitosis remained the same as control and 1-MCP treated, G2 was the same as the control (4.5h), and G1 was identical to the 1-MCP treatment (3.5 h). There was therefore very little overall change in cell cycle duration and component phases because WT tobacco BY-2 cells regularly take 14 h to complete a cell cycle (see chapter 3; Francis *et al.*, 1995; Herbert *et al.*, 2001). This is consistent with ethylene causing very little effect on the cell cycle and its component phases when 1-MCP was present. Of greatest interest was the slight increase in S-phase. Although this was only by half an hour, no change was observed in the 1-MCP only treatment cf. control. This may suggest ethylene exerting an effect in S-phase independent of the ethylene receptors although no increase was seen in S-phase in ethylene and ethylene + silver nitrate treatments (see chapter 3).

Mortality levels observed in the 1-MCP + ethylene treatment were comparable to those observed in control and 1-MCP treated with the exception of the second G1/S boundary (Fig. 4.3b). Interestingly the characteristic rise in ethylene induced mortality at G2/M was absent. Unlike silver nitrate, 1-MCP seems to completely ameliorate this mortality and therefore strongly indicates that ethylene induced cell death at G2/M is dependent on the ethylene signaling pathway. At the second G1/S boundary, mortality rose appreciably in late G1 (14 h), attaining its peak in early S-

phase (15 h). After the peak in early S-phase, mortality then dropped again to background levels. This same rise in mortality at the G1/S boundary was observed in both ethylene and ethylene + silver nitrate treatments (chapter 3). However, because of the toxicity of silver nitrate it could not be determined whether this G1/S peak in the ethylene + silver nitrate treatment was due to ethylene alone. Because 1-MCP had no toxic effect through the cell cycle, this indicates that the G1/S mortality in the 1-MCP + ethylene treatment must be because of ethylene. Thus, blocking the ethylene signaling receptors ameliorates G2/M induced cell death (as seen by using both silver nitrate and 1-MCP) but ethylene-induced G1/S mortality is unaffected by the presence of an ethylene receptor inhibitor. Furthermore, use of 1-MCP in conjunction with ethylene indicates that ethylene-induced G2/M mortality is activated through the known ethylene signaling pathway (as described in chapter 1). Programmed cell death has been previously defined as something that requires an active process (Jones, 2001). Since cell death induced by ethylene at G2/M is completely ameliorated by 1-MCP, this is evidence that ethylene (through its normal signaling pathway) is a major inducer of cell cycle specific PCD. To see whether the ethylene signaling pathway is important in controlling cell death in general, further research would have to be carried out using 1-MCP with other elicitors of cell death.

The results of growth rate experiments over a 7 day period show that 1-MCP had little effect on the growth of the culture (measured by optical density), the mitotic index, or mortality index. As with the cell cycle data, this is consistent with 1-MCP not having a toxic effect on tobacco BY-2 cells.

In earlier work reported in this thesis, ethylene was shown to decrease mitotic cell size with the presence of silver nitrate ameliorating this effect. Note that mitotic cell areas in the 1-MCP and 1-MCP + ethylene treatments were very similar to the control. The mitotic cell area measurements are therefore consistent with ethylene not exerting an effect on cell size in the presence of ethylene and may indicate an important role for ethylene signaling in cell size regulation. Work in *Arabidopsis* on ethylene and cell elongation may partly explain this since ethylene has been shown to decrease hypocotyl length in the dark (Bleecker *et al.*, 1988) but increase it in the light (Smalle *et al.*, 1997).

4.5. Summary

The data reported in this chapter are summarised as follows:

- 1-MCP and 1-MCP+ethylene treatments had a negligible effect on cell cycle duration and its component phases
- 1-MCP and 1-MCP+ethylene treatments resulted in substantially more cycling cells than silver and silver+ethylene treatments.
- 1-MCP ameliorated ethylene-induced G2/M mortality but was unable to ameliorate ethylene-induced S-phase mortality.
- Long-term exposure to 1-MCP reduced cell death *in vivo*.
- 1-MCP and 1-MCP+ethylene treatments did not affect tobacco BY-2 cell size.

To balance the two chemical approaches already used to investigate the effect of ethylene signaling inhibition on ethylene-induced mortality, a genetic approach was employed. The *Arabidopsis etr1* (ethylene receptor) mutant is the oldest established ethylene signaling mutant (Bleecker *et al.*, 1988) and is ethylene insensitive. Tobacco BY-2 cells were therefore transformed with the gene responsible for this insensitivity (*Atetr1*) to see how it would affect responses to ethylene treatment.

Chapter 5

Expression Of The Mutated Arabidopsis Ethylene Receptor, etr1-1, In The Tobacco BY-2 Cell Line

5. Expression Of The Mutated *Arabidopsis* Ethylene Receptor, *etr1-1*, In The Tobacco BY-2 Cell Line

5.1. Introduction

Arabidopsis thaliana has emerged as a model in which to study growth and development. One major reason is that it exhibits a range of developmental and physiological mutants. This has offered a tremendous opportunity to clone genes that can complement specific mutations.

In *Arabidopsis* the original *etr* (ethylene receptor) mutant was identified by Bleecker *et al.* (1988), exhibiting dominant insensitivity to ethylene. This dominant insensitivity was because of an amino acid conversion of Cys-65 to Tyr in the ETR protein. This affects the ETR1 protein by disrupting both ethylene binding activity and integration of the copper co-factor essential for protein activity (Schaller and Bleecker, 1995; Rodrigeuz *et al.*, 1999). Since a total of four *etr1* mutants are now known to exist, the original mutation is known as *etr1-1*.

Interestingly, members of the ETR1-like subfamily (ETR1 and ERS2) contain a conserved histidine kinase domain. This is unlike other ethylene receptors which lack one or more components required for histidine kinase catalytic activity (Wang *et al.*, 2002). Using a yeast two-hybrid system, the histidine kinase domains of both ETR1 and ERS2 have been shown to interact directly with CTR1, a MAPK kinase directly downstream of the ethylene receptors (Clark *et al.*, 1998). The lack of other ethylene receptors showing this direct interaction with CTR1 suggests that the ETR1 receptor may be important for rapid stress response to ethylene and other factors that activate the ethylene stress response pathway. The presence of a receiver domain as well as the histidine kinase domain suggests homology of the ETR1 receptor to the bacterial 'two-component' regulators (Chang *et al.*, 1993). These regulators are sensors and transducers of signals in response to environmental stimuli in bacteria (Parkinson and Kofoid, 1992).

The original *Arabidopsis etr* mutant showed a similar phenotype to the wild-type indicating the mutation did not interfere with major developmental stresses. It did,

however, exhibit 25% larger rosette leaf area with a 1 to 2 week delay in flowering and senescence of leaves in comparison to wild-type *in vivo*. Seeds carrying the *etr* mutation also showed very low germination rates compared to wild-type under the came conditions. Interestingly, gibberellic acid ameliorated this low germination rate (Bleecker *et al.*, 1988). The *Arabidopsis etr* mutant also lacked a peroxidase response when treated with ethylene compared to a three- to four-fold ethylene-induced increase in wild-type cells. This is important with regards to cell death, as a decrease in peroxidase activity is directly associated with an increase in hydrogen peroxide (H_2O_2) production (Ros Barcelo, 1999), a major factor in active cell death. In wild-type *Arabidopsis* plants, ethylene treatment normally results in a significant decrease in endogenous levels of ethylene due to a feedback mechanism stopping its production (Bleecker *et al.*, 1988). A decrease in endogenously produced ethylene did not occur when the mutant was treated with ethylene, indicating an inhibition of the feedback mechanism

As described in chapter 3, ethylene induced a cell cycle specific increase in cell mortality in the tobacco BY-2 cell line. This effect was ameliorated by silver nitrate. Moreover, as described in chapter 4, another chemical blocker of the ethylene receptor (1-MCP) was also able to block ethylene induced mortality. The availability of *Atetr1-1* enabled me to test whether this dominant negative gene could confer dominant insensitivity to ethylene in the tobacco BY-2 cell line. *Atetr1-1* is thought to confer dominant insensitivity to ethylene by either competing for downstream effectors with wild-type (WT) receptors or by interacting with them (Hall *et al.*, 1999). Hence, the aim of the work reported in this chapter was to transform the tobacco BY-2 cell line with *Atetr1* and examine if it could confer dominant insensitivity to ethylene and ameliorate the cell cycle specific mortality exhibited when wild-type TBY-2 cells are exposed to ethylene (Herbert *et al.*, 2001; see chapter 3).

5.2. Materials And Methods

Details of materials and methods are fully described in chapter 2.
See page 31 for tobacco BY-2 transformation protocol, page 33 for synchronisation and mitotic index measurements, page 34 for cell viability and mortality index measurements, page 34 for ethylene treatment, and page 35 for growth rate measurements.

5.3. Results

Two independent cell lines designated Clone (Cl) 1 and Cl 2 carrying the *Arabidopsis etr1* in the pHK1001 vector were investigated in relation to ethylene treatment, the cell cycle, cell size, and mortality. In conjunction with the two *Atetr1* expressing (*Atetr*^{e}) cell lines the wild type tobacco BY-2 (WT) cell line was used as an experimental control. RT-PCR confirmed expression of *Atetr1* in Cl 1 and Cl 2 (Fig. 5.1.).

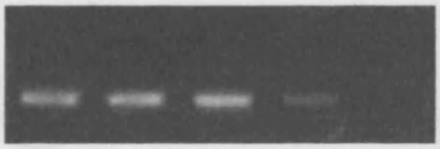

Figure 5.1. RT-PCR analysis of *Atetr1* expression in the tobacco BY-2 cell lines used in this study (product size 161 bp).

5.3.1. *Atetr1* Expression in Tobacco BY-2 Cells Causes a Significant Increase in Cell Cycle Duration and S-phase Length

In the *Atetr*^{e} Cl 1 and Cl 2 cell lines, the mitotic index data gave a similar major peak following the release from aphidicolin at 11h and 10h, respectively (Fig. 5.2). Hence the majority of synchronised cells in the *Atetr*^{e} lines took 2-3 h longer to divide than control (normally 8 h after release from the aphidicolin block).

(a)

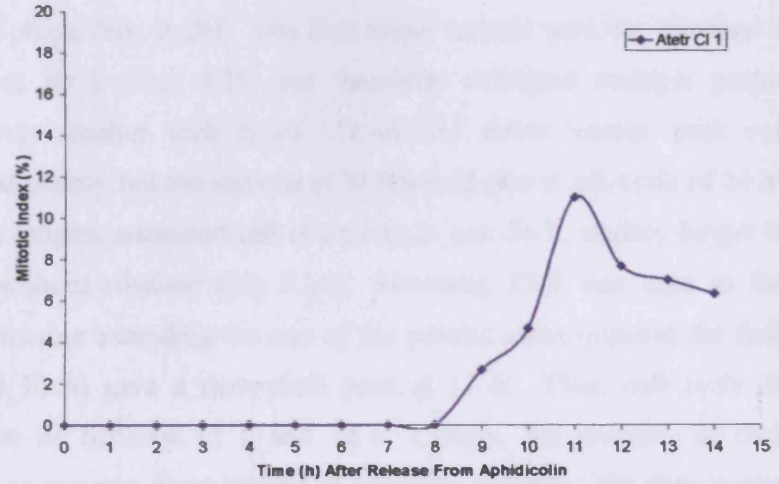

(b)

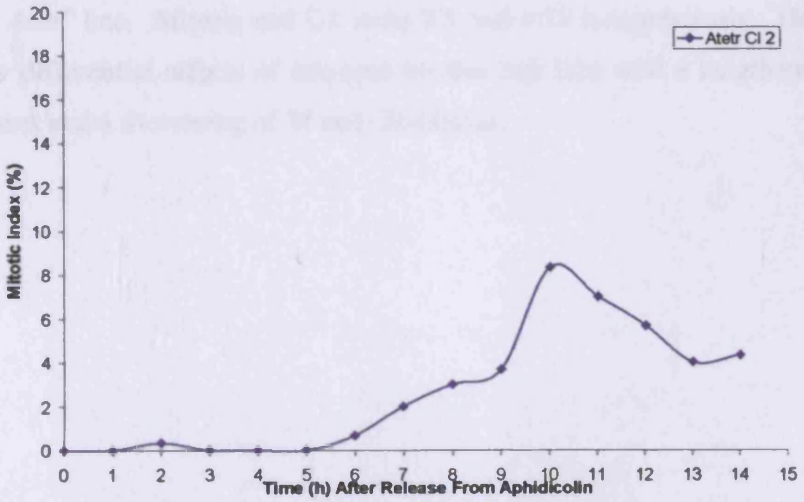

Figure 5.2. The mitotic index of *Atetr*^{e} tobacco BY-2 cells plotted against time after the release from a 24h synchronization treatment with aphidicolin in (a) *Atetr*^{e} Cl 1 cells or in (b) *Atetr*^{e} Cl 2 cells.

At later time points following synchronisation with and release from aphidicolin, the mitotic indices in *Atetr*^{e} Cl 1 exhibited a quartet of peaks, the final one at 33 h being the most substantial (Fig. 5.3a). Thus, maximum cell cycle duration was recorded as 21 h as this was the time period that spanned the most substantial peaks. The smaller peaks could, possibly, represent faster cycling cells albeit smaller populations. Hence the maximum cell cycle length for the *Atetr*^{e} Cl 1 cell line was 50% longer than that for control (21 h cf. 14 h in the control tobacco BY-2 cells).

The calculated component phases (h) for *Atetr*^{e} Cl 1 (control in brackets) were: G2 = 4.25(5), M = 4.5(2), G1 = 4.75 (3.5) and S-phase = 7.5 (3.5). Clearly, the most affected phase was S which doubled in length cf. control.

To see the effect of ethylene on *Atetr*^{e} Cl 1, 17700 µl/l was added about half way through S-phase (Fig. 5.3b). The first major mitotic peak for ethylene treated cells occurred at 10 h (Fig. 5.3b) but thereafter exhibited multiple peaks that were progressively smaller with time. A second major mitotic peak could not be determined exactly but the last one at 34 h would give a cell cycle of 24 h (Fig. 5.3b). Hence the longest estimated cell cycle length was 24 h, slightly longer than that for this line without ethylene (Fig 5.3a). However, 23 h was used as the cell cycle duration because extending the rise of the mitotic index between the first two peaks (10 h and 13 h) gave a theoretical peak at 11 h. Thus, cell cycle duration was assumed to be between 11 h and 34 h. Clearly, the presence of multiple peaks prevented an accurate measurement of cell cycle duration. Ethylene treatment at 3.5 h extended S-phase by 1 h to 8.5 h whilst G2 (7.25 h) was almost double that in the untreated *Atetr*^{e} line. Mitosis and G1 were 2.5 and 4.75 h respectively. Hence there were clear differential effects of ethylene on this cell line with a lengthening of G2 and S-phases and a shortening of M and G1-phases.

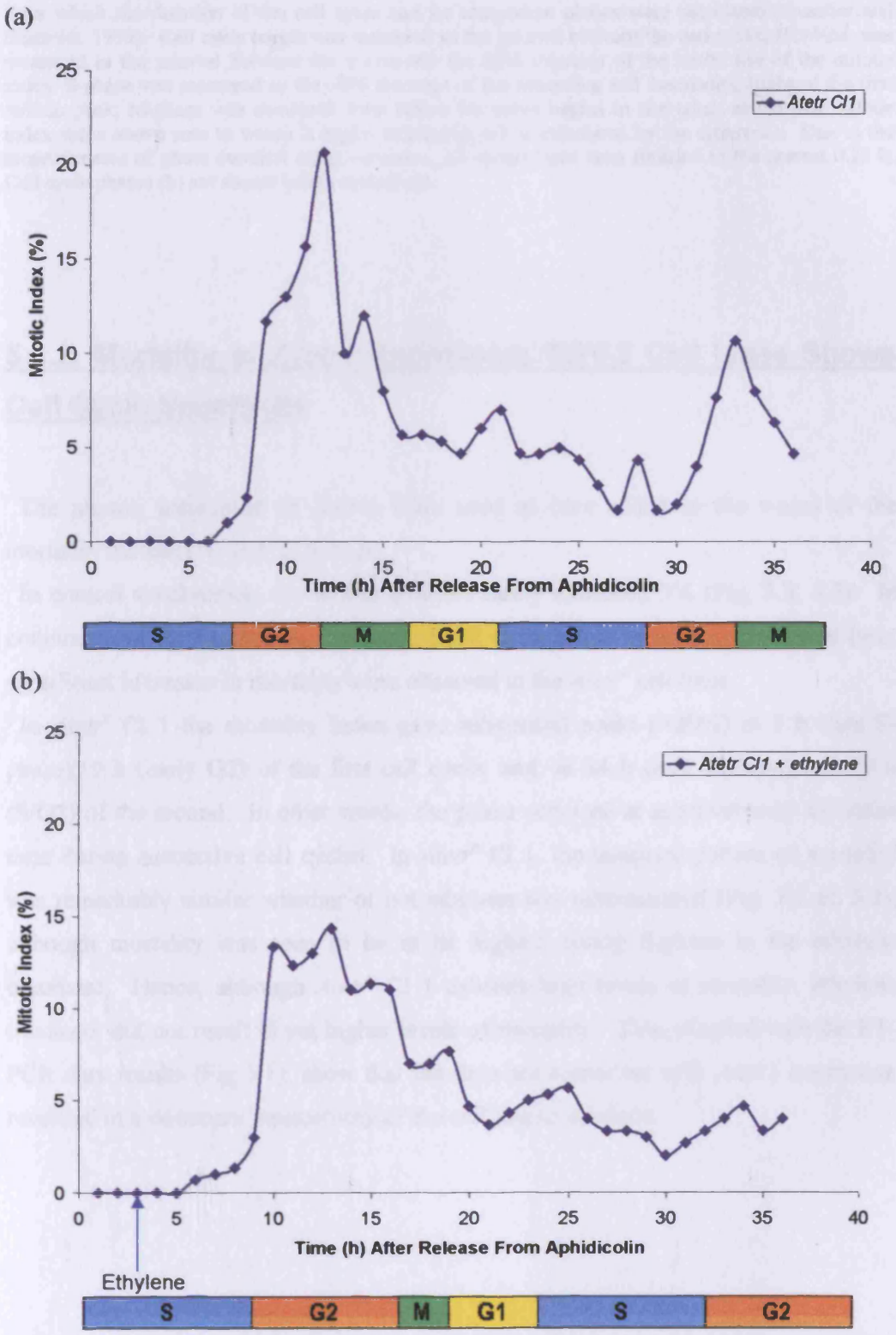

Figure 5.3. The mitotic index of tobacco BY-2 cells plotted against time after the release from a 24 h synchronization treatment with aphidicolin in (a) *Atetr*^{e} Cl 1 cell line (b) *Atetr*^{e} Cl 1 cell line to which ethylene (arrow up) was added at 3.5 h. The mitotic index data generated curves exhibiting two peaks

from which the duration of the cell cycle and its component phases were calculated (Quastler and Sherman, 1959). Cell cycle length was measured as the interval between the two peaks; G2+½M was measured as the interval between the y-axis and the 50% intercept of the initial rise of the mitotic index; S-phase was measured as the 50% intercept of the ascending and descending limbs of the first mitotic peak; M-phase was measured from where the curve begins to rise taken as the first mitotic index value above zero to where it begins to plateau; G1 is calculated by the difference. Due to the measurements of phase duration being estimates, all values have been rounded to the nearest 0.25 h. Cell cycle phases (h) are shown below each graph.

5.3.2. Mortality in *Atetr1* Expressing TBY-2 Cell Lines Shows Cell Cycle Specificity

The phases, calculated as above, were used as bars added to the *x*-axis of the mortality indices (%) in Fig. 5.4a-b.

In control synchronies, the mortality index rarely exceeded 5% (Fig. 3.3; 4.2). In conjunction with the dramatic change in cell cycle duration compared to wild-type, significant increases in mortality were observed in the *Atetr*^{e} cell lines.

In *Atetr*^{e} Cl 1 the mortality index gave substantial peaks (>20%) at 7 h (late S-phase), 9 h (early G2) of the first cell cycle, and, at 24 h (mid S-phase) and 29 h (S/G2) of the second. In other words, the peaks occurred at approximately the same time during successive cell cycles. In *Atetr*^{e} Cl 1, the temporal pattern of mortality was remarkably similar whether or not ethylene was administered (Fig. 5.1 cf. 5.2), although mortality was seen to be at its highest during S-phase in the ethylene treatment. Hence, although *Atetr*^{e} Cl 1 exhibits high levels of mortality, ethylene treatment did not result in yet higher levels of mortality. This, coupled with the RT-PCR data results (Fig 5.1), show that the data are consistent with *Atetr1* expression resulting in a dominant insensitivity of the cell line to ethylene.

(a)

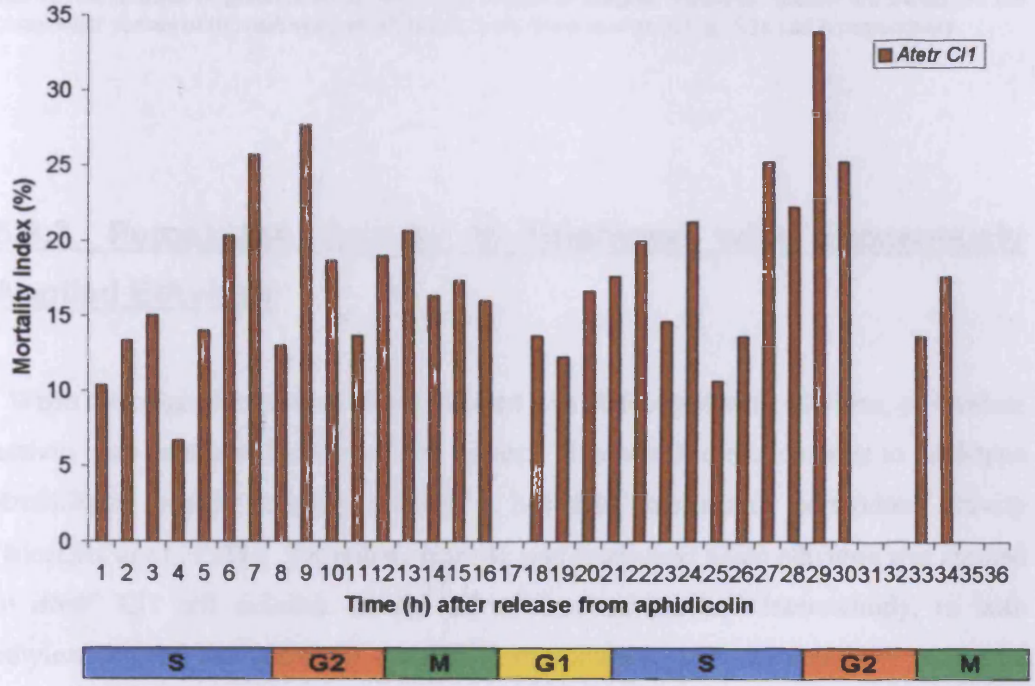
Atetr Cl1
Mortality Index (%)
0 5 10 15 20 25 30 35
1 2 3 4 5 6 7 8 9 10 11 12 13 14 15 16 17 18 19 20 21 22 23 24 25 26 27 28 29 30 31 32 33 34 35 36
Time (h) after release from aphidicolin
S
G2
M
G1
S
G2
M

(b)

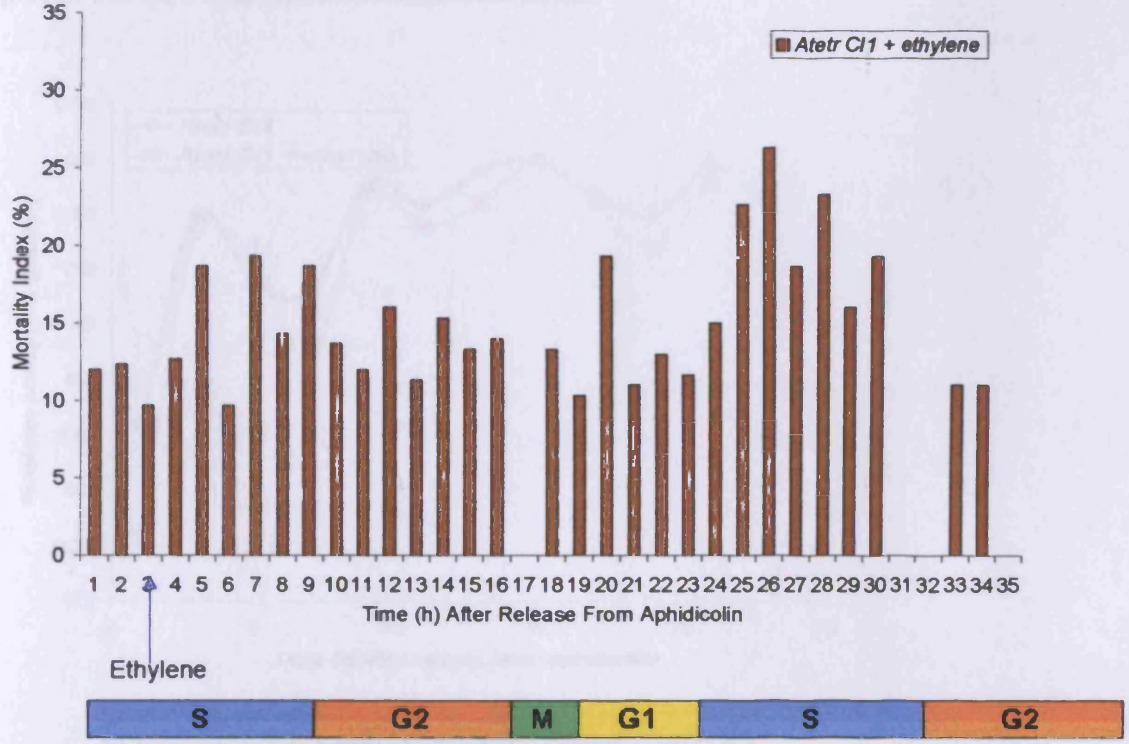
Atetr Cl1 + ethylene
Mortality Index (%)
0 5 10 15 20 25 30 35
1 2 3 4 5 6 7 8 9 10 11 12 13 14 15 16 17 18 19 20 21 22 23 24 25 26 27 28 29 30 31 32 33 34 35
Time (h) After Release From Aphidicolin
Ethylene
S
G2
M
G1
S
G2

Figure 5.4. The mortality index (%) following the release from aphidicolin in (a) *Atetr1*^{e} Cl 1 cells (b) *Atetr1*^{e} Cl 1 cells to which ethylene (arrow up) was added at 3.5 h. Following dual staining with FDA and PI, the number of green and red cells were scored at random transects. Below the *x*-axes are the component phases of the cell cycle measured directly from curves in Fig. 5.3a and b respectively.

5.3.3. Peroxidase Activity is Unaltered with Exogenously Applied Ethylene

When the original *etr1 Arabidopsis* mutant was challenged with ethylene, peroxidase activity was unaffected in the treated leaves. This was in direct contrast to wild-type *Arabidopsis* which normally exhibits a 3-4 fold increase in peroxidase activity (Bleecker *et al.*, 1988). Peroxidase activity was monitored when ethylene was applied to *Atetr*^{e} Cl1 cell cultures during cell cycle experiments. Interestingly, in both ethylene treated and untreated *Atetr*^{e} Cl1 experiments, peroxidase activity decreased before the mortality peaks at 7 h (Fig. 5.4) and was at its lowest when these mortality peaks occurred (Fig. 5.5). The treatment with ethylene resulted in this decrease being greater but the overall pattern remained the same.

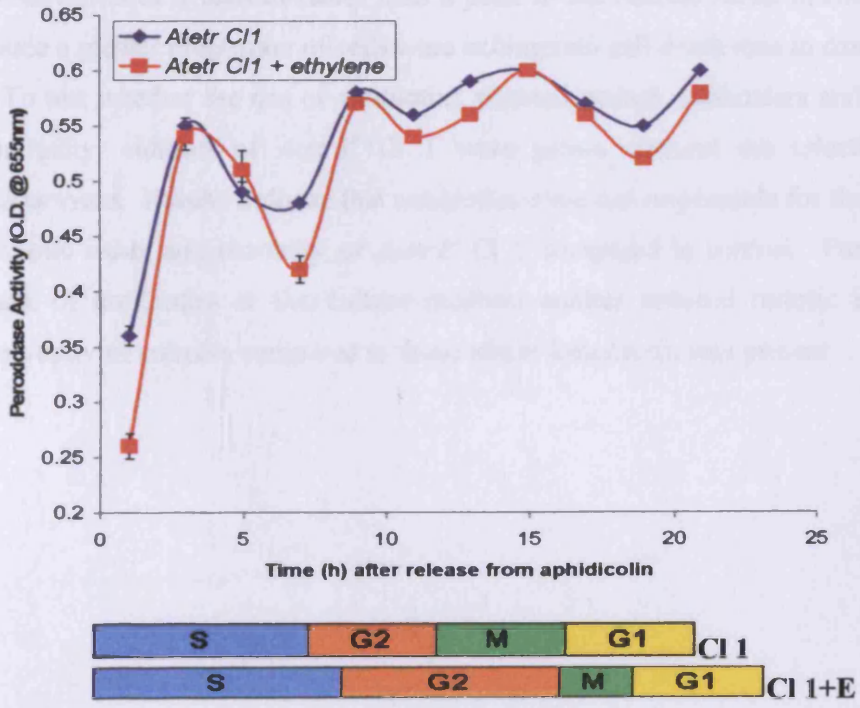

Figure 5.5. The peroxidase activity plotted against time after the release from a 24 h synchronization treatment with aphidicolin in *Atetr*^{e} Cl 1 cells (blue line) and *Atetr*^{e} Cl 1 cells to which ethylene was added at 3.5 h (red line). The vertical lines (black) represent ±SE, where lines are absent the ±SE was less than the diameter of the symbol. Below the *x*-axis are the component phases of the cell cycle in *Atetr*^{e} Cl 1 cells (Cl 1) and *Atetr*^{e} Cl 1 + ethylene cells (Cl 1+E), measured directly from the curves in fig. 5.3a and b respectively. Peroxidase activity was detected using TMBZ-PS, a water soluble analogue of TMBZ, and measured using a spectrophotometer at 655 nm. ($n = 3$)

5.3.4. *Atetr*^{e} Cl 1 Exhibits Increased Mortality and a Delay in Growth *In Vivo*

TBY-2:*Atetr1* expressing cells were investigated over a 7d growth period to see whether *Atetr1* altered cellular growth rates. Over a 7d period *Atetr*^{e} Cl 1 exhibited a delay in growth (using optical density as an indicator) consistent with the longer cell cycle observed after cells were released from aphidicolin (Fig. 5.6). The mitotic index indicates that the number of cells undergoing mitosis was similar to that in controls (Fig. 5.7). However, the mitotic index of *Atetr1*^{e} Cl 1 cells did not attain its peak until day 4 cf. day 2 in control whilst mortality in *Atetr1*^{e} Cl 1 cells was significantly increased compared with control (Fig. 5.8). This may explain the observation of a plateau rather than a peak in the mitotic index in *Atetr*^{e} Cl 1 cells since a greater proportion of cells were exiting into cell death than in controls.

To test whether the use of antibiotics affected growth parameters and the observed mortality, cultures of *Atetr1*^{e} Cl 1 were grown without the selective antibiotic kanamycin. Results indicate that antibiotics were not responsible for the difference in mitotic index and mortality of *Atetr1*^{e} Cl 1 compared to control. Furthermore, the lack of antibiotics in the culture medium neither reduced mitotic index nor the mortality of cultures compared to those where kanamycin was present.

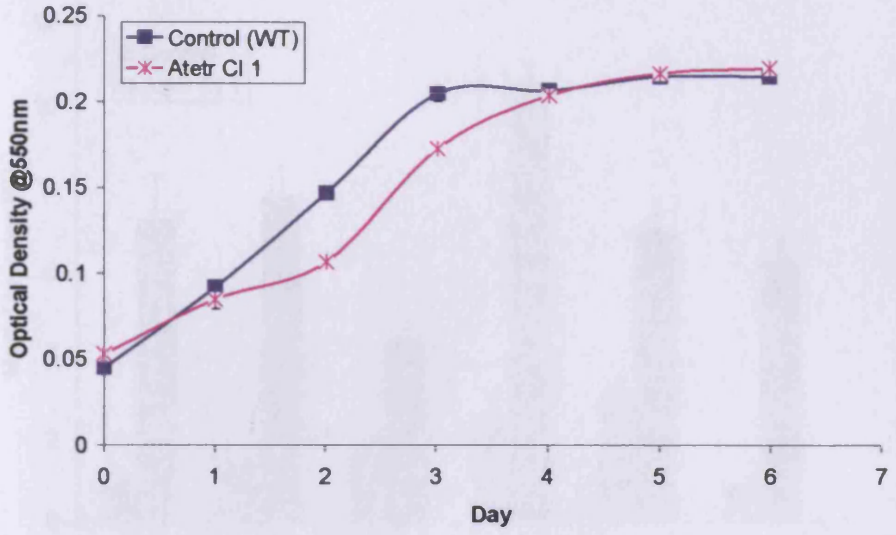

Figure 5.6. The optical density readings over a 7d growth period indicating growth of control (WT) cells (blue line) and *Atetr*^{e} Cl 1 cells (red line). The vertical lines (black) represent ±SE, where lines are absent the ±SE was less than the diameter of the symbol. (n = 9)

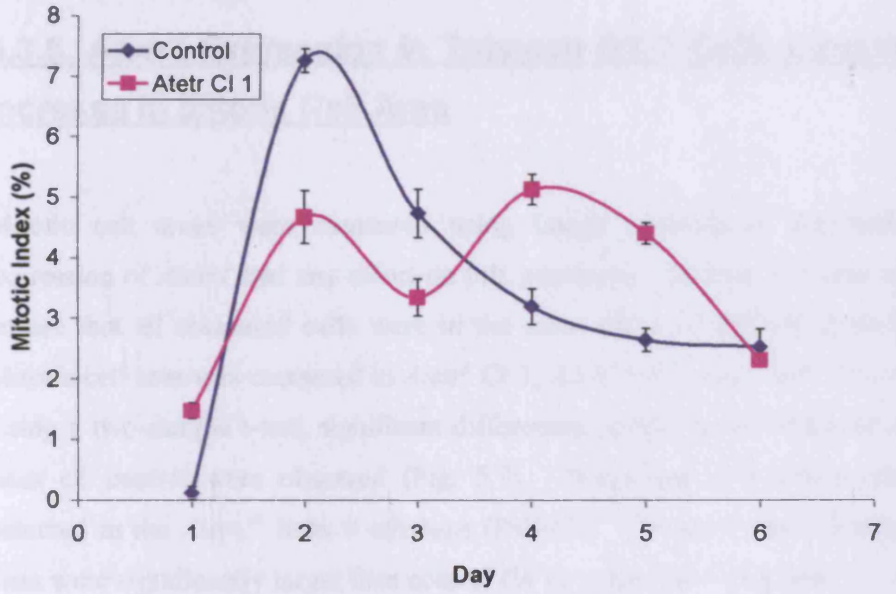

Figure 5.7. The mitotic index (%) over a 7d growth period in control (WT) cells (blue line) and *Atetr*^{e} Cl 1 cells (red line). The vertical bars represent ±SE, where lines are absent the ±SE was less than the diameter of the symbol. (n = 9)

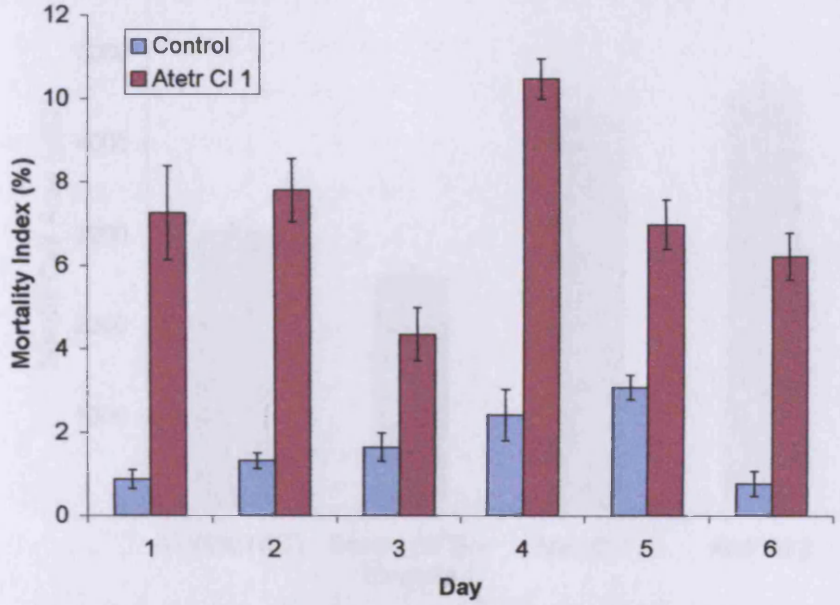

Figure 5.8. The mortality index (%) over a 7d growth period in control (WT) cells (blue bars) and *Atetr*^{e} Cl 1 cells (red bars). The vertical lines (black) represent ±SE. ($n = 9$)

5.3.5. *Atetr1* Expression in Tobacco BY-2 Cells Causes a 50% Increase in Mitotic Cell Area

Mitotic cell areas were measured using image analysis to determine whether expression of *Atetr1* had any effect on this parameter. Mitotic cell area was used to ensure that all measured cells were in the same stage of the cell cycle (M-phase). Mitotic cell area was measured in *Atetr*^{e} Cl 1, *Atetr*^{e} Cl 2, and *Atetr*^{e} Cl 1 + ethylene. Using a two-sample t-test, significant differences in mitotic cell areas of *Atetr1*^{e} cell lines cf. control were observed (Fig. 5.9). Significant differences could not be detected in the *Atetr1*^{e} lines ± ethylene ($P<0.05$). However, the cell areas in these lines were significantly larger than control (WT) or control + ethylene.

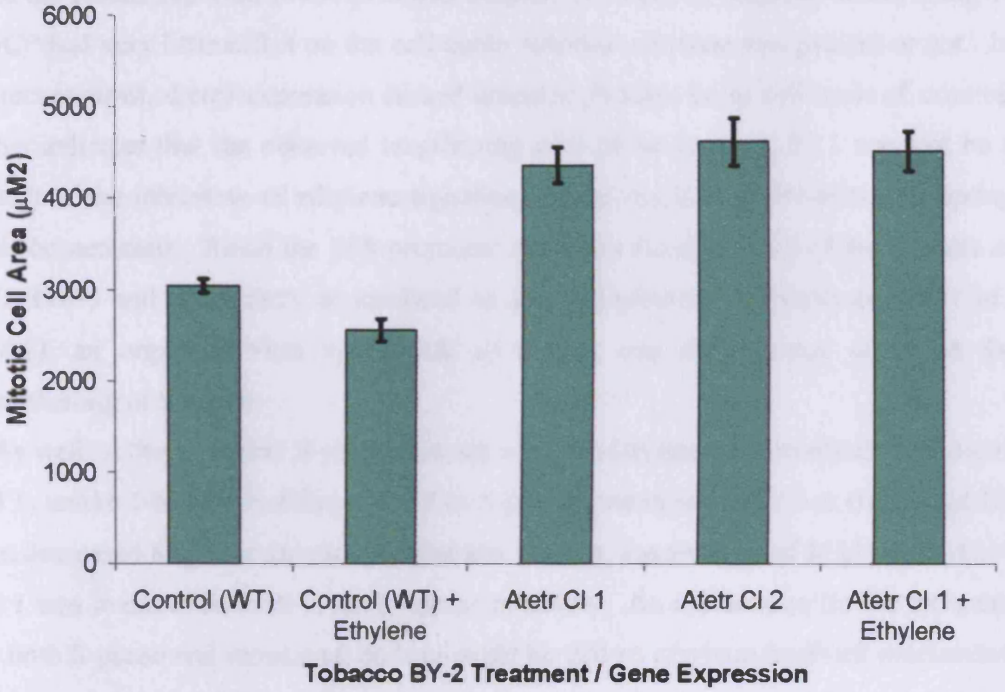

Figure 5.9. The mitotic cell areas of control (WT) cells (mean = 3046µm^2; n = 125), ethylene treated control (WT) cells (mean = 2562µm^2: n = 51), *Atetr*^{e} Cl 1 cells (mean = 4367µm^2; n = 158), *Atetr*^{e} Cl 2 cells (mean = 4629µm^2: n = 35), and *Atetr*^{e} Cl 1 + ethylene cells (mean = 4523µm^2: n = 155). The vertical lines (black) represent ±SE.

5.4. Discussion

Both *Atetr*^{e} lines exhibited a delay into, and peak of, the mitotic index (10 and 11 h; Fig. 5.2) coupled with high levels of mortality (>10%) cf. control. Expression of *Atetr1* increased cell cycle duration by 50% to 21 h and caused significant changes in cell cycle periods cf. control (WT). In *Atetr*^{e} Cl 1, G2 was 4.25 h (5 h in control), mitosis was 4.5 h (2 h in control), G1 was 4.75 h (3.5 h in control) and S-phase 7.5 h (3.5 h in control). The most notable effect of *Atetr1* expression was the doubling of S-phase and mitosis. When ethylene was added to *Atetr*^{e} Cl 1 at 3.5 h after the release from aphidicolin, S-phase and G2 were found to increase cf. untreated cells (8.5 h and 7.25 h respectively) with mitosis decreased to 2.5 h, and G1 showing no change.

In the results reported in the previous chapter, blocking of ethylene action using 1-MCP had very little effect on the cell cycle, whether ethylene was present or not. In direct contrast, *Atetr1* expression caused dramatic changes in the cell cycle cf. control. This indicates that the observed lengthening of S-phase in *Atetr*^{e} Cl 1 may not be a result of the inhibition of ethylene signaling but the result of a side-effect disrupting cell homeostasis. Since the 35S promoter expresses strongest in S-phase (Nagata *et al.*, 1987) and that *At*etr1 is localised to the endoplasmic reticulum (Chen *et al.*, 2002), an organelle vital to the life of a cell, one consequence could be the lengthening of S-phase.

As well as the extended S-phase, mitosis was also lengthened considerably in *Atetr*^{e} Cl 1, unlike 1-MCP (no change in G2 or S-phase) and especially silver (Increased G2 but decreased M-phase duration) treatments. In fact, the duration of M-phase in *Atetr*^{e} Cl 1 was in direct contrast to silver nitrate treatment. An explanation for the increases in both S-phase and mitosis cf. control could be that an ethylene feedback mechanism is disrupted in *Atetr*^{e} Cl 1. Ethylene has been previously shown to inhibit cell division and DNA synthesis in *Pisum sativum* (Apelbaum and Burg, 1971). Furthermore, the original *Arabidopsis etr1* mutant exhibited increased hypocotyl and root length cf. WT *Arabidopsis*, whether ethylene was present or not (Bleecker *et al.*, 1988). The explanation given for the *Arabidopsis etr1* mutant was that although ethylene synthesis rates were not altered by the *etr* mutation, feedback regulation did not occur in these plants (Bleecker *et al.*, 1988). This may also be the case in *Atetr*^{e} Cl 1 but would have to be confirmed by monitoring levels of endogenous ethylene in response to ethylene treatment.

When *Atetr*^{e} Cl 1 was exposed to ethylene at 3.5 h after the release from aphidicolin, both S-phase and G2 increased (8.5 h and 7.25 h respectively). This dramatic lengthening of cell cycle phases in response to ethylene has not been observed for other inhibitors of ethylene action (see chapters 3 and 4). Interestingly, the increase in S-phase duration was similar to that in the 1-MCP + ethylene experiments. This provides more evidence for the effect of ethylene on S-phase being independent of the ethylene signaling receptors, especially when combined with the change in mortality peaks discussed below. The increase in G2 to 7.25 h cf. 4.25 h was the greatest change in cell cycle periods observed as a result of *Atetr*^{e} Cl 1 ethylene treatment. The original *Arabidopsis etr1* mutant was only 80% effective in blocking ethylene binding (Bleecker *et al.*, 1988) and it is therefore possible that ethylene was still exerting an

effect, especially since an increase in G2 occurred when WT tobacco BY-2 cells were challenged with ethylene. However, silver also caused an increase in G2 length. This means that the lengthening of G2 in *Atetr*^{e} Cl 1 may also be independent of the ethylene signaling pathway.

The background mortality observed in the *Atetr*^{e} lines was similar to results in the *Arabidopsis* mutant where seeds showed low germination (high mortality) rates (Bleecker *et al.*, 1988). However, a direct comparison cannot be made since monitoring of mortality in the *Arabidopsis* mutant was not carried out during development. Notably, the highest level of mortality in *Atetr1*^{e} Cl 1 was detected in late S-phase/ early G2. However, in the ethylene treatment, this high level of mortality occurred in mid to late S-phase and correlated with an increase in the duration of both S-phase and G2. This result is surprisingly similar to the response of fission yeast in the DNA replication checkpoint induced by hydroxyurea where cells are held up in a lengthened G2 whilst DNA replication is recovering (Rhind and Russell, 2000).

Although the temporal pattern of mortality was remarkably similar whether or not ethylene was applied, it is interesting to note a peak of mortality occurring mid S-phase of the second cell cycle when the *Atetr*^{e} Cl 1 line was exposed to ethylene. This peak of mortality in mid S-phase was recorded in all ethylene treatments described in this thesis, whether or not an inhibitor of ethylene action has been present.

In conjunction with the 7 h peak of mortality observed when *Atetr*^{e} Cl 1 (±ethylene) was released from aphidicolin, peroxidase activity was reduced. In PCD, peroxidase activity is normally reduced as these enzymes are involved in oxidising H_2O_2 to a harmless alternative (Ros Barcelo, 1999). A reduction in peroxidase activity leads to an increase in H_2O_2 which in turn up-regulates genes involved in the programmed cell death pathway, including the stimulation of ethylene synthesis (Lamb and Dixon, 1997; Levine *et al.*, 1994). In wild-type *Arabidopsis*, exposure to ethylene results in a four-fold increase in peroxidase activity (Bleecker *et al.*, 1988), indicating a dramatic increase in H_2O_2 production. In the *Arabidopsis etr1* mutants exposure to ethylene does not affect peroxidase activity. The lack of increased peroxidase activity in *Atetr1*^{e} Cl 1 in response to ethylene is consistent with the dominant insensitivity of this cell line to exogenously applied ethylene. Furthermore, the lower activity of peroxidase at 7 h detected in ethylene treated *Atetr1*^{e} Cl 1 cf. untreated, occurs in S-phase. Ethylene-induced mortality in S-phase is observed whether an inhibitor is

present or not. This is in conjunction with the reduction in peroxidase activity and the increase in S-phase and G2. This strongly suggests ethylene exerts an effect in S-phase that is independent of the ethylene signaling pathway.

In recent years strong evidence has indicated the involvement of the endoplasmic reticulum (ER) in mammalian programmed cell death (Brekenridge *et al.*, 2003) with ER stress agents causing the release of mitochondrial cytochrome *c* and loss of mitochondrial transmembrane potential (Hacki *et al.*, 2000; Boya *et al.*, 2002); ER Ca^{2+} release associated with activating programmed cell death pathways (Bekenridge *et al.*, 2003); and BCL-2, BAX and BAK proteins, involved in the regulation of apoptosis in mammalian cells, have all been shown to localise to the ER as well as the mitochondria (Nutt *et al.*, 2002). Furthermore, when the capacity of the ER to fold proteins properly is compromised or overwhelmed, a highly conserved unfolded protein response (UPR) pathway is activated. The UPR halts general protein synthesis while up-regulating ER resident chaperones and other regulatory components of the secretory pathway (Travers *et al.*, 2000). This gives cells a chance to correct the environment within the ER (Patil and Walter, 2001). However, if damage is too extensive, the switch from metabolic rest to cell death occurs. This period of metabolic 'rest' has been shown to be as great as 48 h in some cell types (Patil and Walter, 2001). Although evidence of ER involvement in plant PCD is not yet known, the high background mortality in *Atetr1*^{e} lines may be a result of ER localisation of *At*ETR1 (Chen *et al.*, 2002). In support of a putative role for ER in plant PCD, *Arabidopsis* ethylene-responsive binding proteins (*At*EBP) have been found to dominantly suppress Bax-induced cell death in yeast (Pan *et al.*, 2001). Although, again, it is not known whether plants have a system fully equivalent to BCL-BAX (Krishnamurthy *et al.*, 2000; Lam *et al.*, 2001), further research into the relationship between ethylene and ER in plants may prove to be a useful insight into ethylene-induced PCD.

Mean mitotic cell area was significantly larger in the *Atetr*^{e} lines compared with comparable measurements in control. Note that the cell cycle was substantially longer in the *Atetr*^{e} lines and hence a positive relationship exists between mitotic cell area and cell cycle duration. In other words, the longer the cell cycle the larger was the mitotic cell area. However, the mean mitotic cell area was not significantly different in the *Atetr*^{e} Cl 1 in the presence or absence of ethylene. Hence, the data are

also consistent with the dominant insensitivity of these cell lines to exogenous ethylene.

5.5. Summary

The data reported in this chapter are summarised as follows:

- *Atetr1* expression resulted in a 50% increase in cell cycle duration and S-phase length.
- Ethylene treatment resulted in an increase in S-phase length and a doubling of G2 duration.
- *Atetr1* expression resulted in significant increases in mortality, especially at the S/G2 boundary.
- Ethylene treatment resulted in no temporal change in mortality, although mortality was seen to be at its highest during S-phase.
- Peroxidase activity remained unaltered when *Atetr*^{e} Cl 1 was treated with ethylene.
- *Atetr1* expression increased mortality and delayed growth *in vivo*.
- *Atetr1* cell lines show a 50% increase in mitotic cell size.

Other cell cycle work was in progress when these data were collected. This work comprised of the constitutive expression of the mitotic inducer, Spcdc25 in the tobacco BY-2 cell line. I decided to extend my studies of the G2/M transition with this cell line due to a relationship between ethylene-induced cell death and G2/M established in the previous chapters. Work on Spcdc25 expression in tobacco BY-2 cells is reported in the next chapter.

Chapter 6

Expression of Spcdc25 In The Tobacco BY-2 Cell Line Causes Premature Entry Into Mitosis And Nullifies The G2/M Checkpoint

6. Expression Of *Spcdc25* In The Tobacco BY-2 Cell Line Causes Premature Entry Into Mitosis And Nullifies The G2/M Checkpoint

6.1. Introduction

The plant cell cycle is regulated by cyclin-dependent kinases (CDKs) that are themselves, phosphoregulated (Zhou *et al.*, 2002). However, little is known about the genes that exert control over these CDKs in plants, especially at the G2/M transition point of the cell cycle. In fission yeast (*Schizosaccharomyces pombe*), *cdc25* is a positive regulator of the G2/M transition (Russell and Nurse, 1986). It encodes a tyrosine phosphatase that in late G2, dephosphorylates Cdc2 kinase on a tyrosine residue (Y15) near to the NH2 terminus (Russell and Nurse, 1986). Following binding with a B-type cyclin, dephosphorylation of Cdc2, by Cdc25, is the final all-or-nothing signal that triggers Cdc2 kinase activity enabling subsequent entry of a cell from G2 into mitosis (see O'Farrell, 2001). Cdc25 phosphatase competes with Wee1 kinase for the Y15 residue of Cdc2 kinase (Nurse, 1990). When phosphorylated by Wee1 kinase, Cdc2 is unable to exhibit catalytic activity (Russell and Nurse, 1987; Gould and Nurse, 1989). In mammals further negative regulation of cytoplasmic Cdc2 is also provided by MYT1, a membrane-bound dual threonine-tyrosine kinase (Mueller *et al.*, 1995). In humans (Cdc25C) and insects (STRING), Cdc25 has a dual phosphatase activity on Y15 and T14 of the B-type CDC2 that functions in late G2 of the cell cycle (Edgar and O'Farrell, 1989; Sadhu *et al.*, 1990).

In *S. pombe*, over-expression of *cdc25* induced a short cell phenotype. The cells divided prematurely through a shortening of G2 phase but, surprisingly, there was no change in the overall length of the cell cycle (Russell and Nurse, 1986). This was due to G1 compensating for the shortening of G2. Over-expressing Wee1 had the converse effect, resulting in a long cell phenotype (Russell and Nurse, 1987). This suggests strongly that by competing for the same substrate, Wee1 and Cdc25 regulate

cell size at division, although the former is regarded as the main genetic element in this control (Sveiczer *et al.*, 1986).

In plants, a homologue to *wee1* has been identified in *Zea mays* (Sun *et al.*, 1999) and in *Arabidopsis thaliana* (Sorrell *et al.*, 2002) although to date a functional homologue of *cdc25* has not (see discussion). In the absence of a plant homologue, I examined the effects of fission yeast *cdc25* on cell size and development in the tobacco BY-2 cell line.

One of the aims of the work reported here was to examine whether *Spcdc25* results in a shortening of G2 in the plant cell cycle. Evidence for dephosphorylative activity of *Sp*Cdc25 on plant Cdc2 kinase at G2/M was found in cultures of *Nicotiana plumbaginofolia* (Zhang *et al.*, 1996). Also, when these cells were depleted of exogenous cytokinin they arrested in G2 because of inactivation of Cdc2 kinase due to Y15 phosphorylation. Addition of kinetin to these cultures resulted in dephosphorylation of Cdc2 and entry of cells into mitosis (Zhang *et al.*, 1996). These data strongly suggest that there is a cytokinin-mediated signal transduction pathway that regulates the G2/M transition through inactivation of Cdc25-like phosphatases (Zhang *et al.*, 1996). Interestingly, TBY-2 cells exhibited a major peak of zeatin synthesis at the G2/M transition (Redig *et al.*, 1996) that was suppressed by mevinolin treatment (Laureys *et al.*, 1998); mevinolin inhibits the isoprenoid pathway of cytokinin biosynthesis (Crowell and Salaz, 1992). Another aim of the work reported here was to discover whether our *Spcdc25* expressing lines could escape a block imposed by mevinolin thereby providing a further test of the cytokinin regulated model of the G2/M transition of the plant cell cycle.

6.2. Materials And Methods

Details of materials and methods are fully described in chapter 2.

See page 31 for tobacco BY-2 transformation protocol, page for synchronisation and mitotic index measurements, page 34 for cell viability and mortality index measurements, and page 34 for ethylene treatment.

6.3. Results

Three independent cell lines carrying *Spcdc25* under the control of an attenuated version of the BIN-35S CMV promoter, BIN-HYG-TX (Gatz *et al.*, 1992) were investigated in relation to the cell cycle, cell size, and mortality. In conjunction with the three *Spcdc25* expressing lines (denoted as 1*, 2*, and 3*), two empty vector lines (EV1 and EV2) were used as experimental controls. RT-PCR confirmed *Spcdc25* expression in 1*, 2*, 3* and its absence in the empty vector lines (Fig. 6.1a). Western blotting was also used to confirm the presence of *Sp*Cdc25 protein in *Spcdc25* expressing cell lines (Fig. 6.1b). Transformations were carried out on two separate occasions and therefore EV1 is the control for 1* and EV2 for 2* and 3* *Spcdc25* expressing cell lines.

(a)

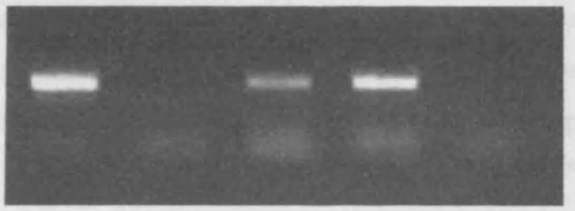

1* EV1 2* 3* EV2

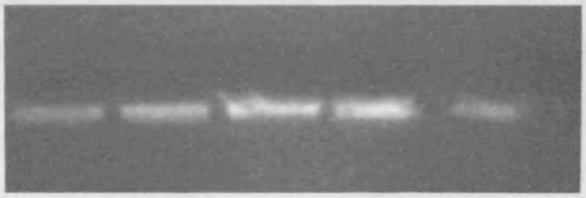

1* EV1 2* 3* EV2

(b)

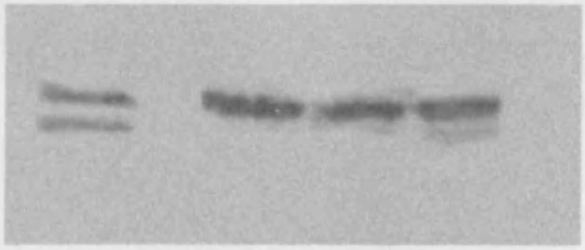

WT * * *

Figure 6.1. (a) RT-PCR analysis of *Spcdc25* expression in the tobacco BY-2 cell lines. Top panel: expression of *Spcdc25* (product size 718 bp), bottom panel: 18S control (product size 459 bp). (b) Western blotting analysis of *Sp*Cdc25 protein in three independent tobacco BY-2 cell lines expressing the gene (indicated with *) and WT.

6.3.1. *Spcdc25* Induces Premature Cell Division Through a Shortening of G2 Phase

Release of TBY-2 cells from an aphidicolin block will start the progression of cells previously held in S-phase, through the cell cycle, with the mitotic index rising as cells traverse G2 and enter mitosis. In 1*, 2*, and 3* cell lines the mitotic index began to rise early by comparison to their respective empty vector counterparts. The most dramatic, 1*, began to rise sharply between 2-3 h and peaked between 3-4 h after release from aphidicolin (Fig. 6.2). This contrasted sharply with EV1, which began to rise between 5-6 h following release and reached the peak of mitoses at 9 h (Fig. 6.2). The overall duration of the cell cycle, the interval between the two peaks, also contrasted with 1* duration being 12 h and EV1, 14 h (comparable to wild type TBY-2 cell cycle duration, see Herbert *et al.*, 2001). For 1* G2 duration was estimated at 0.5 h, mitosis 1 h, G1 7 h, and S-phase at 3.5 h. EV1's G2 duration was 8.5 h, mitosis 2 h, G1 0.5 h, and S-phase 3 h. Hence the *Spcdc25* expressing cell line, 1*, exhibits a shortened cell cycle mainly through a shorter G2 phase compared with EV1 (Fig 6.2).

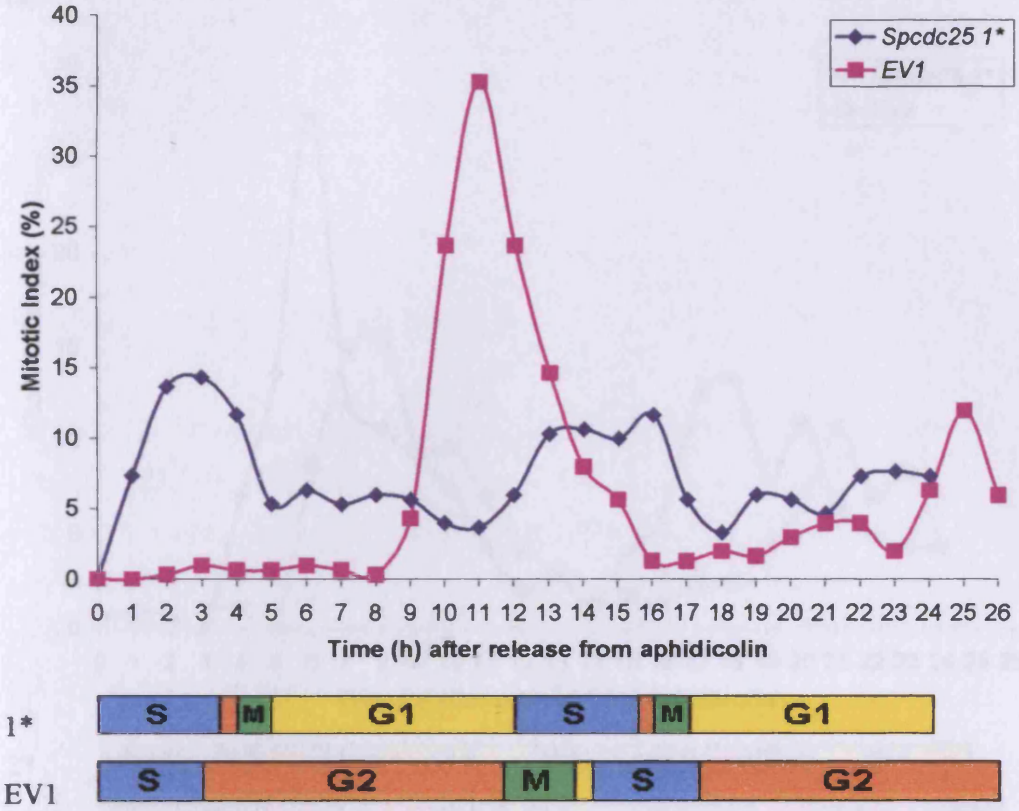

Figure 6.2. The mitotic index (%) of tobacco BY-2 cells plotted against time after the release from a 24h synchronization treatment with aphidicolin in control (EV1) and tobacco BY-2 *Spcdc25* 1*. The mitotic index data generated curves exhibiting two peaks from which the duration of the cell cycle and its component phases were calculated (Quastler and Sherman, 1959). Cell cycle length was measured as the interval between the two peaks; G2+½M was measured as the interval between the *y*-axis and the 50% intercept of the initial rise of the mitotic index; S-phase was measured as the 50% intercept of the ascending and descending limbs of the first mitotic peak; M-phase was measured from where the curve begins to rise taken as the first mitotic index value above zero (1 h in *Spcdc25* 1* and 9 h in EV1) to where it begins to plateau (3 h in *Spcdc25* 1* and 11 h in EV1); G1 is calculated by the difference. Due to the measurements of phase duration being estimates, all values have been rounded to the nearest 0.5 h. Below the *x*-axes are the component phases of the cell cycle in the EV1 (EV1) and *Spcdc25* 1* (1*) cell lines as calculated using the method above.

The cell cycle data for 2* and 3* were consistent with a shorter G2 phase by comparison to EV2 (Fig. 6.3); 4 h and 3.5 h for 2* and 3* respectively cf. 5 h for EV2, with overall cell cycle length reduced in the expressing lines, 12.5 h and 11 h respectively for 2* and 3* cf. 14 h for EV2 (Fig. 6.3).

(a)

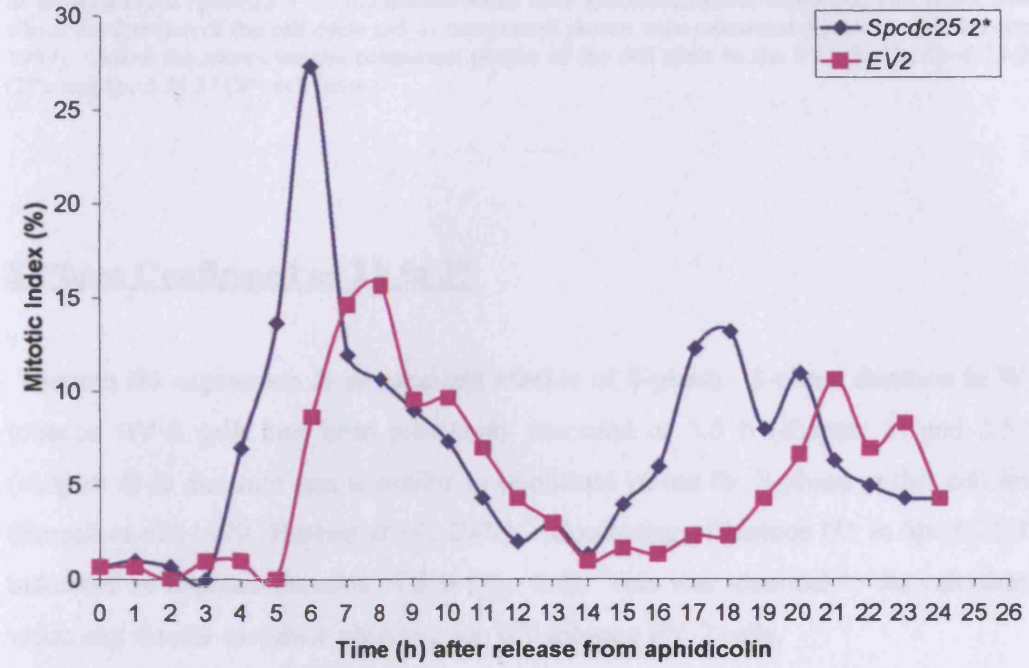
Spcdc25 2*
EV2
Mitotic Index (%)
Time (h) after release from aphidicolin


2*
S G2 M G1 S G2 M G1
EV2
S G2 M G1 S G2 M

(b)

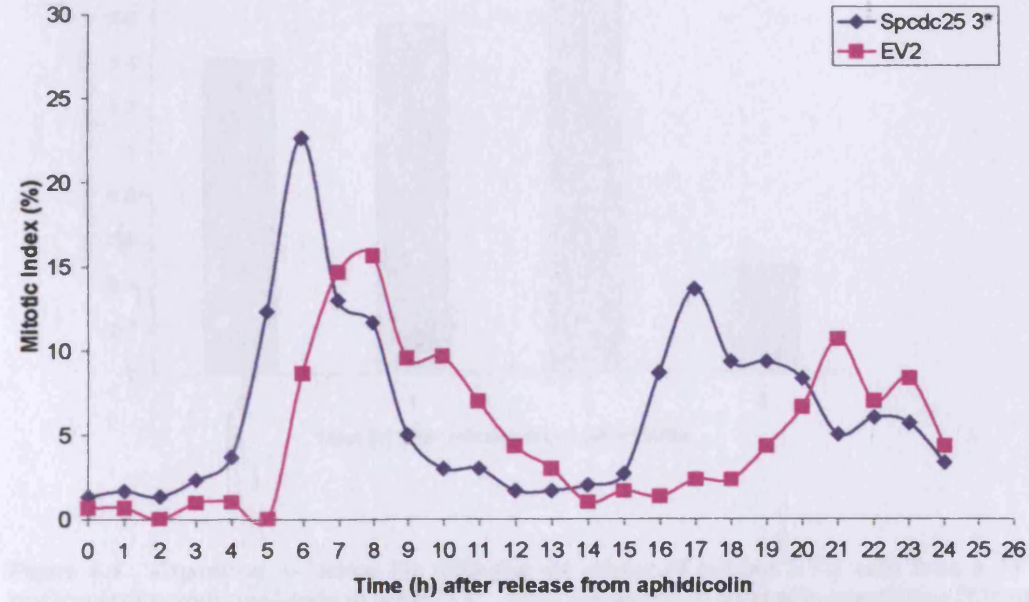
Spcdc25 3*
EV2
Mitotic Index (%)
Time (h) after release from aphidicolin


3*
S G2 M G1 S G2 M G1
EV2
S G2 M G1 S G2 M

Figure 6.3. The mitotic index (%) of tobacco BY-2 cells plotted against time after the release from a 24 h synchronization treatment with aphidicolin in control (EV2) and (a) tobacco BY-2 *Spcdc25* 2* (b) in tobacco BY-2 *Spcdc25* 3*. The mitotic index data generated curves exhibiting two peaks from which the duration of the cell cycle and its component phases were calculated (Quastler and Sherman, 1959). Below the *x*-axes are the component phases of the cell cycle in the EV2 (EV2), *Spcdc25* 2* (2*), and *Spcdc25* 3* (3*) cell lines.

S-Phase Confirmed as 3 h in 3*

Histone H4 expression is an excellent marker of S-phase. S-phase duration in WT tobacco BY-2 cells has been previously recorded as 3.5 h (chapter 3) and 2.5 h (chapter 4) in duration and is similar to published values for S-phase in this cell line (Sorrell *et al.*, 1999; Herbert *et al.*, 2001). Monitoring of histone H4 in *Spcdc25* 3* indicated an S-phase duration of 3 h (Fig. 6.4). This was identical to the calculated value and similar to values observed for WT tobacco BY-2 cells.

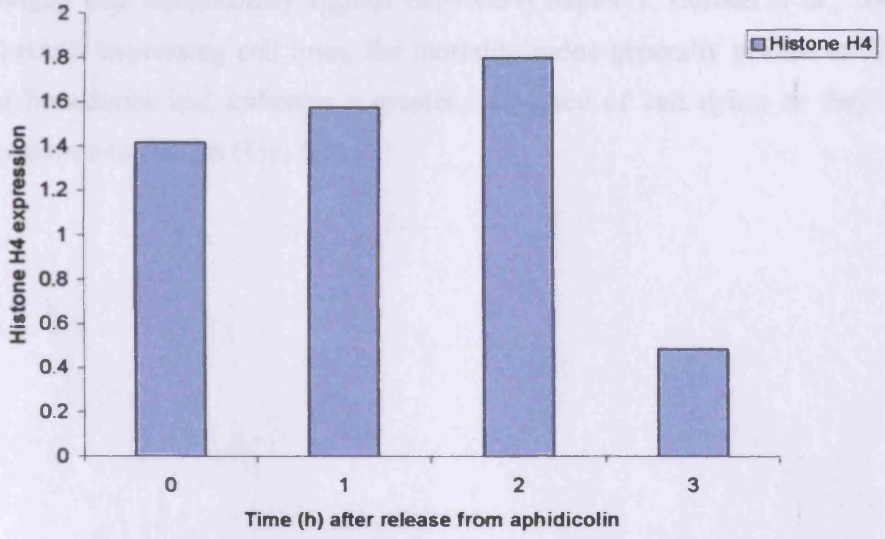

Figure 6.4. Expression of histone H4 following the release of tobacco BY-2 cells from a 24 h synchronization with aphidicolin in *Spcdc25* 3*. RNA was amplified using semi-quantitative PCR and results obtained measuring amplified band intensity. Histone H4 expression was corrected for errors by using 18S ribosomal RNA expression as a standard.

Interestingly, none of the mitotic indices recorded in these experiments exceeded 30%. Characteristically, wild type (WT) TBY-2 cells synchronised with aphidicolin exhibit a mitotic index peak of 45-50% at 7-8 h after aphidicolin release (Herbert *et al.*, 2001; Francis *et al.*, 1995). The lower range of mitotic indices reported here are consistent with a smaller cycling cell population and has been previously noted in TBY-2 transgenic lines (Shaul *et al.*, 1996).

6.3.2. Cell Cycle Specific Mortality is Exhibited by *Spcdc25* Expressing TBY-2 Cell Lines

Remarkably, the TBY-2 cell lines transformed with *Spcdc25* exhibited a cell cycle specific pattern of mortality similar to that exhibited previously in WT when challenged with exogenously applied ethylene (Chapter 3; Herbert *et al.*, 2001). In the *Spcdc25* expressing cell lines, the mortality index generally peaked at S/G2 and G2/M boundaries and indicates a greater frequency of cell dying as they attempt progression into mitosis (Fig. 6.5)

(a)

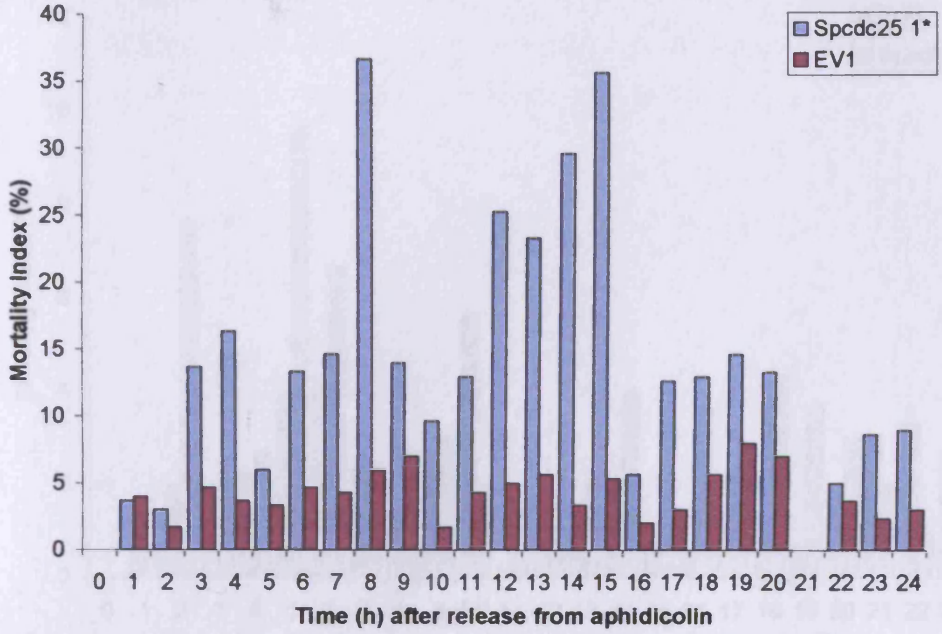
Spcdc25 1*
EV1
Mortality Index (%)
0 5 10 15 20 25 30 35 40
0 1 2 3 4 5 6 7 8 9 10 11 12 13 14 15 16 17 18 19 20 21 22 23 24
Time (h) after release from aphidicolin

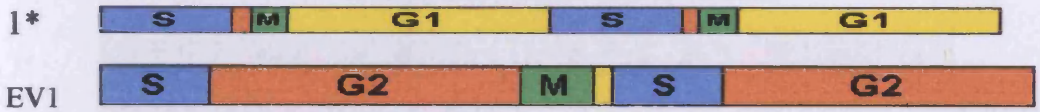
1*
S
M
G1
S
M
G1
EV1
S
G2
M
S
G2

(b)

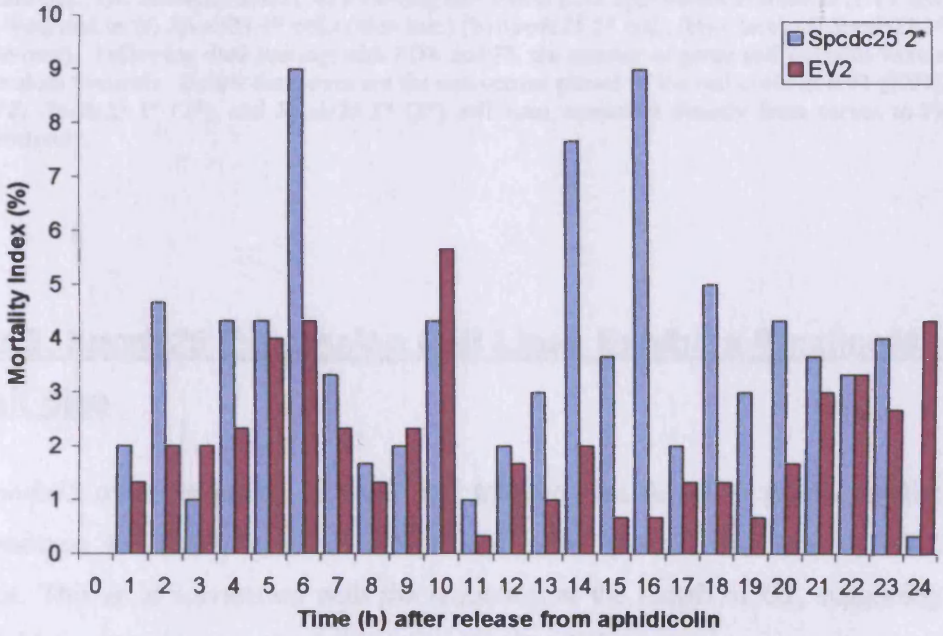
Spcdc25 2*
EV2
Mortality Index (%)
0 1 2 3 4 5 6 7 8 9 10
0 1 2 3 4 5 6 7 8 9 10 11 12 13 14 15 16 17 18 19 20 21 22 23 24
Time (h) after release from aphidicolin

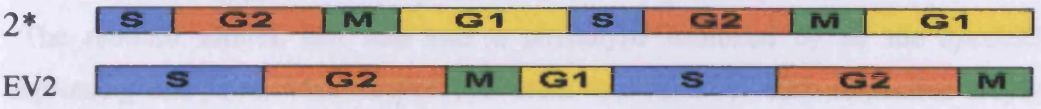
2*
S
G2
M
G1
S
G2
M
G1
EV2
S
G2
M
G1
S
G2
M

(c)

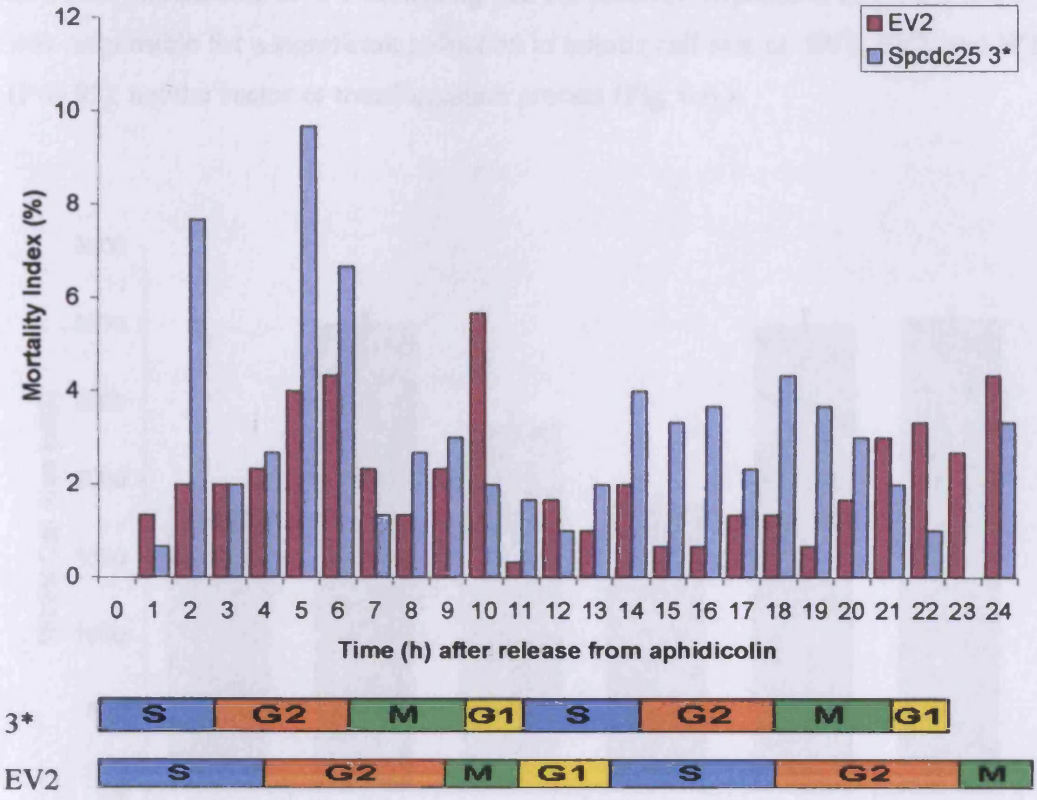

Figure 6.5. The mortality index (%) following the release from aphidicolin in controls (EV1 and EV2; red bars) and in (a) *Spcdc25* 1* cells (blue bars) (b) *Spcdc25* 2* cells (blue bars) (c) *Spcdc25* 3* cells (blue bars). Following dual staining with FDA and PI, the number of green and red cells were scored at random transects. Below the *x*-axes are the component phases of the cell cycle in EV1 (EV1), EV2 (EV2), *Spcdc25* 2* (2*), and *Spcdc25* 3* (3*) cell lines, measured directly from curves in Fig. 6.3 respectively.

6.3.3. *Spcdc25* Expressing Cell Lines Exhibit a Smaller Mitotic Cell Size

Spcdc25 over-expression in yeast and tobacco was found to give a smaller cell phenotype, the same characteristic exhibited in the *Spcdc25* transformed TBY-2 cell lines. This is in correlation with the reduction in the length of G2, suggesting that cells were entering premature division at a reduced size.

The reduced mitotic cell size was a phenotype exhibited by all the *Spcdc25* expressing cell lines, with mitotic cell areas two-thirds of their respective empty

vector transformed control cell lines. The mitotic cell sizes of EV1 and EV2 were, however, comparable to WT indicating that the *Spcdc25* expression in 1*, 2*, and 3* was responsible for a significant reduction in mitotic cell size cf. EV1, EV2, and WT ($P<0.05$), not the vector or transformation process (Fig. 6.6.)

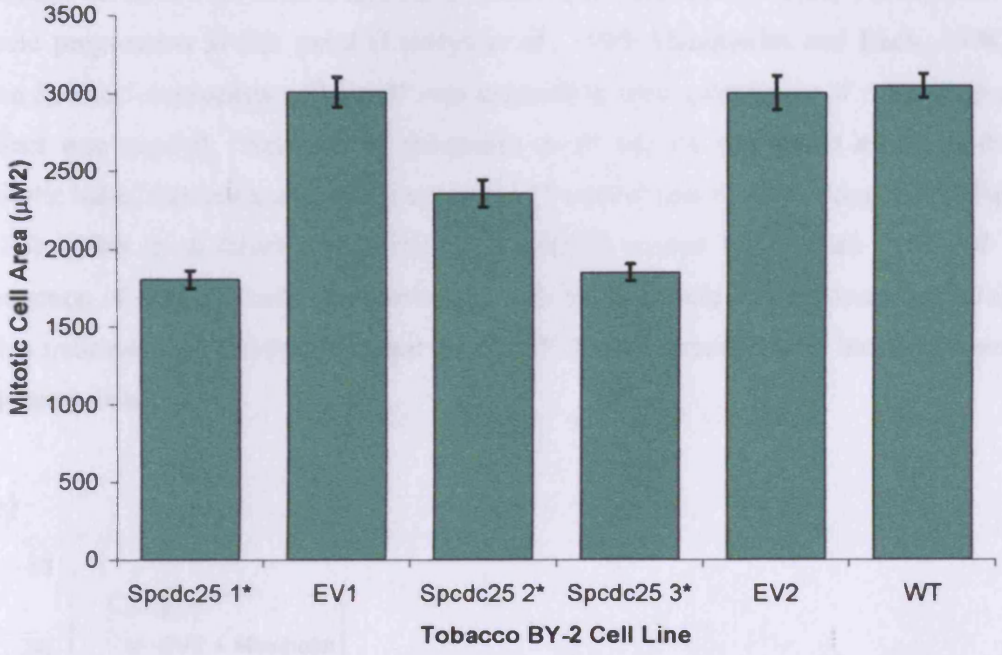

Figure 6.6. The mitotic cell areas of WT cells (mean = 3046μm^2; n = 125), *Spcdc25* 1* cells (mean = 1805μm^2: n = 124), *Spcdc25* 2* cells (mean = 2356μm^2; n = 94), *Spcdc25* 3* cells (mean = 1848μm^2: n = 51), EV1 (mean = 3009μm^2: n = 51), and EV2 (mean = 3002μm^2: n = 51). The vertical lines (black) represent ±SE.

6.3.4. Cytokinin Inhibition in TBY-2 *Spcdc25* Expressing Cell Lines Does Not Restrict Cell Cycle Progression

It has been previously shown that cytokinins are essential for cell cycle progression through G2/M in TBY-2 cells and that mevinolin, a cytokinin inhibitor, will block cell cycle progression at this point (Laureys *et al.*, 1998; Hemmerlin and Bach, 1998). The *Spcdc25* expressing cell line3* was exposed to mevinolin to see if an inhibitory effect was exerted. Addition of mevinolin to 3* had no significant effect on the mitotic index data compared to the untreated 3* control that was ran alongside it (Fig. 6.7b). This is in direct comparison to mevinolin treated EV2 which exhibited a reduction of ~50% in cells progressing through the cell cycle into mitosis (Fig. 6.7a). This indicates that *Spcdc25* expression in TBY-2 cells circumvents a block imposed by mevinolin.

(a)

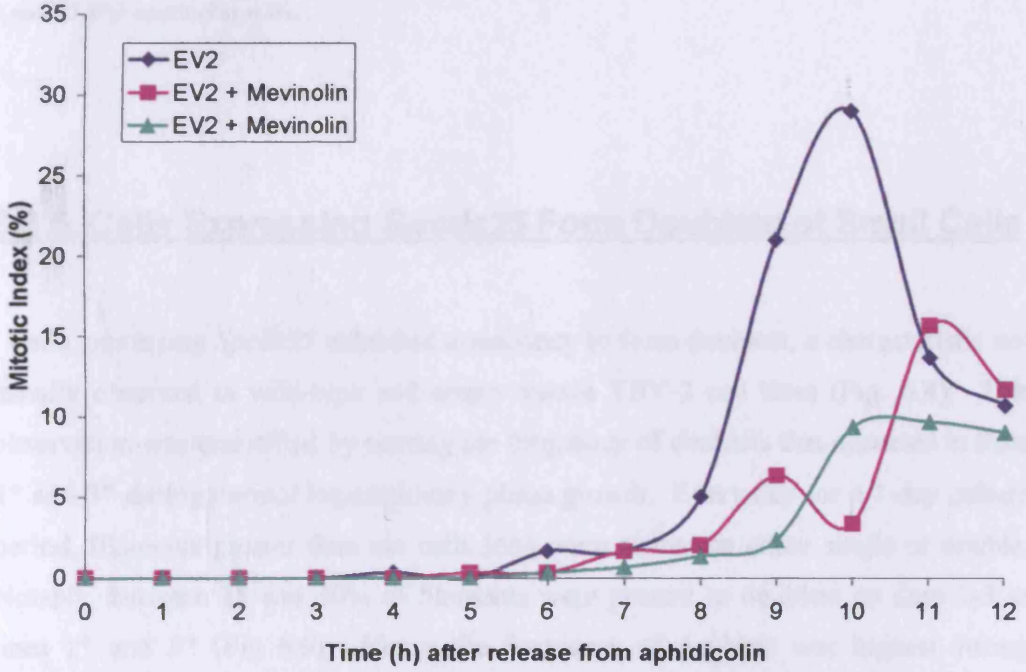

(b)

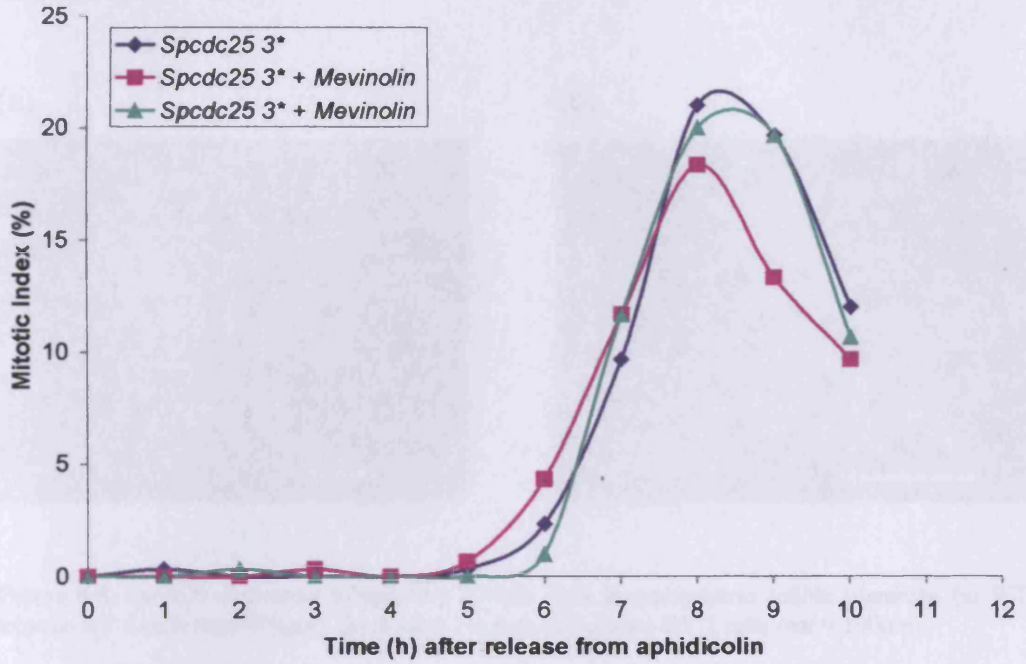

Figure 6.7. The mitotic index (%) of tobacco BY-2 cells plotted against time after the release from a 24 h synchronization treatment with aphidicolin in (a) control (EV2) ± mevinolin at 0 h and (b) in *Spcdc25* 3* ± mevinolin at 0 h

6.3.5. Cells Expressing *Spcdc25* Form Doublets of Small Cells

Cells expressing *Spcdc25* exhibited a tendency to form doublets, a characteristic not usually observed in wild-type and empty vector TBY-2 cell lines (Fig. 6.8). This observation was quantified by scoring the frequency of doublets that occurred in lines 1* and 3* during normal log-stationary phase growth. Every day for a 7-day culture period, filaments greater than six cells long were scored as either single or double. Notably, between 18 and 30% of filaments were present as doublets on days 2-3 in lines 1* and 3* (Fig 6.9). Hence the frequency of doublets was highest during exponential growth of the cell lines. Moreover, in the double filaments the ratio of cell length to cell width was close to unity whereas in the EV and wild type lines the corresponding ratio ranged from 2:1 to 6:1 (data not shown). Hence *Spcdc25*-induced

changes in cell length may predispose changes in the cell division plane (see discussion).

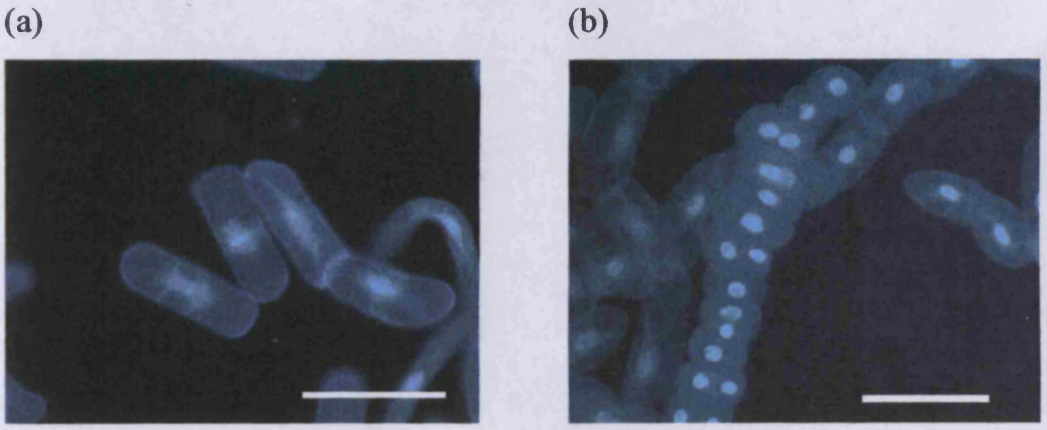

Figure 6.8. *Spcdc25*-expressing tobacco BY-2 cells form in isodiametric double filaments. (a) WT tobacco BY-2 cells (bar=100μm) (b) *Spcdc25*-expressing tobacco BY-2 cells (bar = 100μm).

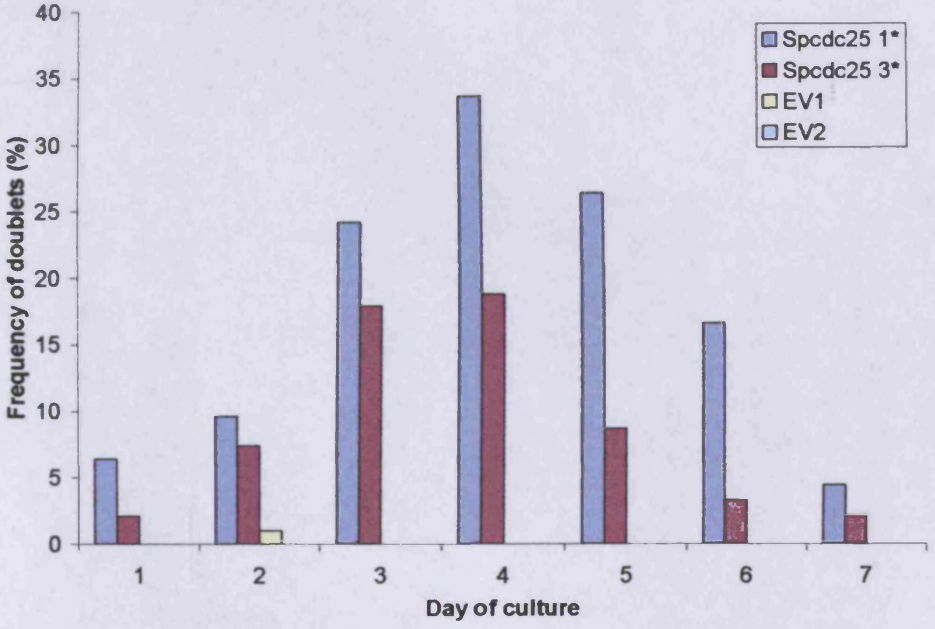

Figure 6.9. The frequency of doublets of tobacco BY-2 cells (double filaments ≥6 cells long) in the *Spcdc25*-expressing line 1* compared with empty vector (EV1) and 3* compared with EV2, during a 7d batch culture of tobacco BY-2 cells at 27°C (n=300).

6.3.6. Ethylene Treatment of *Spcdc25* 1* Results in a Reduction in Mortality

The effect of ethylene on WT tobacco BY-2 cells and *Atetr1* expressing cells in previous chapters indicates that ethylene exerts an effect on the G2/M transition in tobacco BY-2 cells. Since expression of *Spcdc25* was also thought to affect the G2/M transition, *Spcdc25* 1* was challenged with exogenously applied ethylene at 0 h. Interestingly, results did not show an increase in mortality. Instead overall mortality, especially at the peak of mitosis, was reduced cf. the experimental control (untreated *Spcdc25* 1*; Fig 6.10b) and was similar to the results obtained when *Atetr1*-expressing cells were treated with ethylene. The characteristic delay in the rise of mitosis and reduction of the mitotic peak observed in WT treatment were both absent (Fig 6.10b cf. Fig. 3.1a (Chapter 3).

(a)

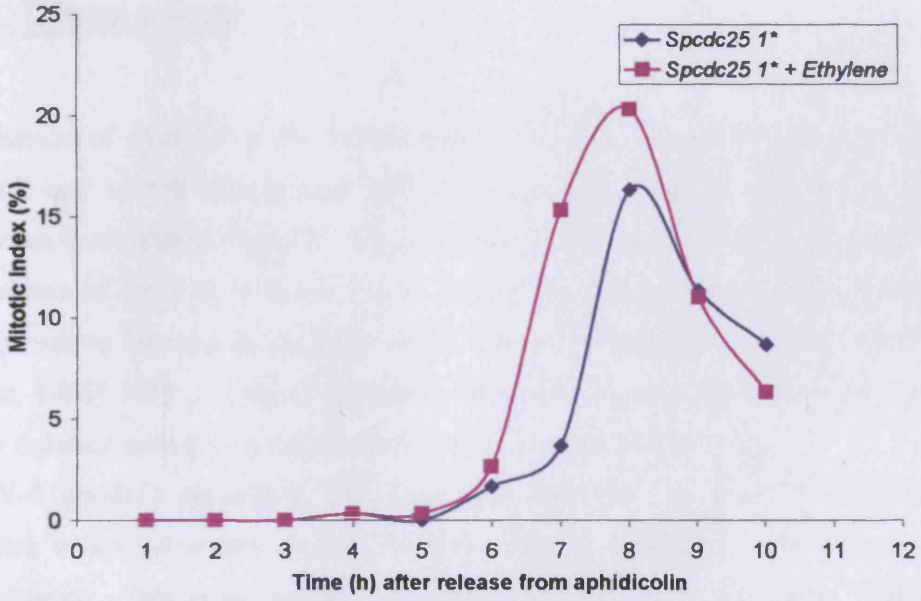

(b)

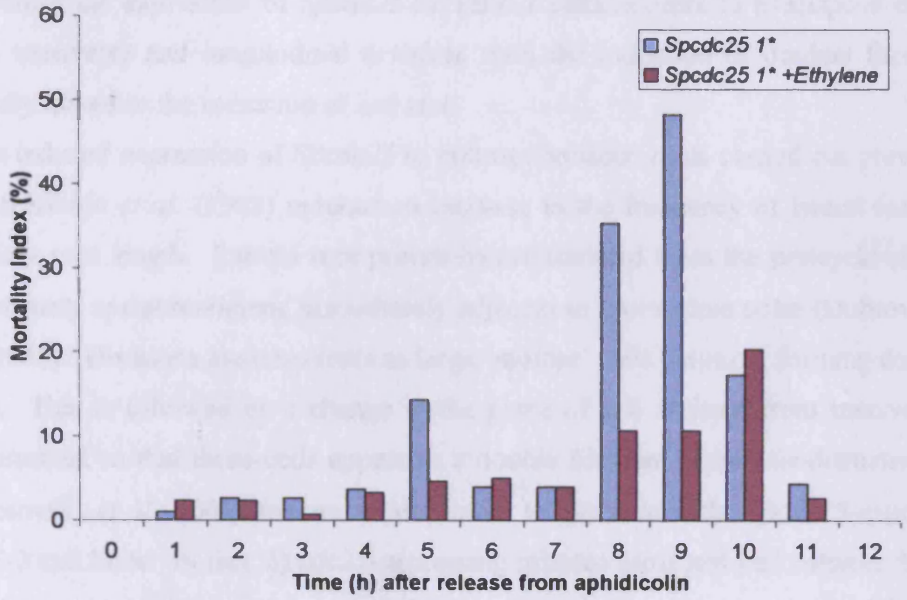

Figure 6.10. The mitotic index (a) and mortality index (b) of *Spcdc25* 1* ± ethylene at 0 h plotted against time after a 24 h synchronisation with aphidicolin

6.4. Discussion

Expression of *Spcdc25* in the tobacco BY-2 cell line has shown that it confers a smaller cell size at mitosis and that premature cell division occurs through the reduction in the duration of G2. This is similar to the results obtained from the over-expression of *Spcdc25* in fission yeast. However, whereas fission yeast exhibited a compensatory increase in duration of G1 due to the reduction in G2 (Russell and Nurse, 1986), TBY-2 *Spcdc25* expressing cell lines showed a 2-3h reduction in cell cycle duration with only a slight compensatory increase in G1 (½-1h).

TBY-2 *Spcdc25* expressing cell lines also exhibited unusual cell morphology, forming near-isodiametric double filaments both in culture and during cell cycle experiments. This is an unusual occurrence in wild-type TBY-2 cells. Normally TBY-2 cells are observed to be 2-6 times longer than wide and filaments normally arise by transverse divisions. In *Spcdc25* expressing cells, reduction in cell size is

mainly achieved by the reduction in cell length, resulting in isodiametric cells. Therefore the expression of *Spcdc25* in TBY-2 cells appears to predispose cells to both transverse and longitudinal division, with the induction of doublet formation directly linked to the reduction of cell size.

The induced expression of *Spcdc25* in cultured tobacco roots carried out previously by McKibbin *et al.* (1998) induced an increase in the frequency of lateral roots per primary root length. Lateral root primordia are initiated from the pericycle close to the primary apical meristem, immediately adjacent to protoxylem poles (Dubrovsky *et al.*, 2001). Divisions are transverse as large 'mother' cells partition, forming daughter cells. This is followed by a change in the plane of cell division from transverse to longitudinal so that these cells appear as a double filament of near-isodiametric cells (Dubrovsky *et al.*, 2001) and are not dissimilar to that seen in the *Spcdc25*-expressing TBY-2 cell lines. In fact, *Spcdc25*-expressing tobacco roots and cell cultures directly correlate, with both exhibiting reduced cell size and a change in the plane of division. Therefore, *Spcdc25* expression may well predispose cells to divide longitudinally.

The levels of mortality exhibited in the *Spcdc25* expressing TBY-2 cell lines were higher than those in the empty vectors and showed cell cycle specificity. Mortality was most notable at the G2/M transition point, indicating that due to the shortened G2 cells may be forced to enter mitosis by *Spcdc25* expression whether they are competent or not, and therefore might exit into cell death due to the negation of a checkpoint that would halt cells from cycling. In fission yeast Russell and Nurse (1986) observed an increase in lethality presumably because of an override of a cell competency (DNA damage) checkpoint.

There is strong evidence that the G2/M transition in the plant cell cycle is cytokinin regulated. Zeatin synthesis peaks in late G2 and mevinolin inhibits this peak, preventing G2/M progression (Redig *et al.*, 1996; Laureys *et al.*, 1998). It is of note that mevinolin also prevents G1/S transition and has been shown to halt cells at both cell cycle transition points in Tobacco BY-2 cells (Hemmerlin and Bach, 1998). It is also known that cytokinin treatment can activate the G2/M transition (John *et al.*, 1993) and both *Spcdc25* and cytokinin can dephosphorylate plant Cdc2 in late G2 (Kumagai and Dunphy, 1992). Since *Spcdc25* expressing TBY-2 cell lines can overcome the mevinolin block, it is possible that the *Spcdc25* expression is compensating for cdc25-like or functionally equivalent phosphatases inhibited by the lack of cytokinin signaling in this treatment. Hence the data support the idea that

G2/M transition mediated by cytokinin involves the induction or promotion of Cdc25 activity. This, of course, relies on the fact that cytokinin indirectly de-phosphorylates Cdc2 at the G2/M transition and that a plant Cdc25-like phosphatase can be identified. In *Arabidopsis* a gene encoding a putative catalytic domain of *Spcdc25* has been identified although it has yet been shown to complement a *S. pombe cdc25*$^{-}$ mutant (D. Francis, H. J. Rogers, J. R. Dickinson, D.A. Sorrell unpublished data; D. Inze, L. DeVeylders, J. Joubes unpublished data). Previous studies using mevinolin on the TBY-2 cell cycle showed increased mortality in relation to treatment (Laureys *et al.*, 1998), however its addition to *Spcdc25*-expressing TBY-2 cell lines didn't effect mortality rates. This supports the link between Cdc25-like phosphatase and cytokinin activity at the G2/M transition in the plant cell cycle and that they are likely to be affecting the same process.

The duration of S-phase is also affected by *Spcdc25* expression in TBY-2 cells, being shorter in each of the expressing lines compared with the empty vectors. In human cells, CDC25A shows its highest expression in late G1 and S-phase (Jinno *et al.*, 1994) indicating that *Spcdc25* expression in tobacco may affect more than the one transition point and/or an increase in the rate of replication fork movement during S-phase (Bryant and Francis, 2000). In this study S-phase duration was calculated using the amplitude of the main peak of mitosis and can be justified since previous work gave an identical S-phase duration whether it was calculated from H4 expression data of the peak amplitude (Herbert *et al.*, 2001)

In the *Spcdc25* expressing TBY-2 cell lines, cell size is approximately two-thirds of that observed in WT and empty vector and is similar to results seen from *Spcdc25* over-expression in fission yeast (Russell and Nurse, 1986). This indicates that cells do not continue to divide at smaller sizes, resulting in mitotic catastrophe, but instead establish a new threshold size for cell division with *Spcdc25* being down-regulated. In the fission yeast cell cycle Cdc25 is normally down-regulated post-translationally with Cdc25 being partitioned from its substrate, Cdc2. This is essential for the fission yeast DNA damage checkpoint to be effective (Kumagai and Dunphy, 1999). During G2 DNA damage prompts the phosphorylation of Cdc25 on serine-216 by Chk2 kinase, causing Cdc25 to exit the nucleus and bind with 14-3-3 proteins whilst the DNA is repaired (Peng *et al.*, 1997; Kumagai and Dunphy, 1999). Using yeast two hybrid screening, an *Arabidopsis* 14-3-3 protein (GF14w) has been identified recently that binds to *Spcdc25* and complements the *S. pombe* DNA damage

checkpoint mutant *rad24*, a gene encoding a 14-3-3 protein (Sorrell *et al.*, 2001; Sorrell *et al.*, unpublished data). When mitotic size control is influenced in fission yeast by such methods as *Spcdc25* over-expression, a G1/S minimum size controller stabilises cell size thereby preventing an ever decreasing cell size (Sveiczer *et al.*, 1996). It is not known whether plants possess G1/S minimum size controllers and clearly other factors may be involved in establishing and maintaining a new threshold size, inactivation and degradation of *Spcdc25* for example (Takizawa and Morgan; Bulavain *et al.*, 2002). Fascinatingly, tobacco BY-2 cultures expressing *Spcdc25* have been observed to revert back to a relatively normal cell cycle length and G2 duration over time compared to empty vector. Therefore *Spcdc25*-expressing cell lines are establishing and maintaining a new cell size threshold although the reason, as discussed above, is as yet unclear and would need further investigation.

It was a surprise to see that treatment of *Spcdc25*-expressing cells with ethylene causing a reduction in mortality rather than increasing it as in WT. Recently, the amount of cytokinin in *Spcdc25*-expressing cells has been monitored and found to be greatly reduced in comparison to WT (D Francis; personal communication) and might explain the reason for the reduction in mortality when cells were exposed to exogenously applied ethylene. This is because cytokinin levels are linked to ethylene biosynthesis in plants, with an increase in cytokinin causing an increase in ethylene. Furthermore, this relationship has been linked to cytokinin inducing ethylene via a post-transcriptional modification of 1-aminocyclopropane-1-carboxylic acid synthase (ACS) (Vogel *et al.*, 1998). ACS activity is the rate limiting step in ethylene biosynthesis (Woeste *et al.*, 1999). It could therefore be that low endogenous levels of cytokinin in *Spcdc25*-expressing cells results in lower amounts of endogenous ethylene and that exogenously applied ethylene may restore levels of ethylene to that in WT tobacco BY-2 cells.

6.5. Summary

The data reported in this chapter are summarised as follows:

- *Spcdc25* expression induced premature cell division and reduced cell cycle duration through a shortening of G2.
- *Spcdc25* cell lines exhibited high levels of mortality, especially at the S/G2 boundary.
- *Spcdc25* expression resulted in a small cell size phenotype
- *Spcdc25* expressing cells overcame a cell cycle block imposed by mevinolin.
- Cells expressing *Spcdc25* formed doublets of small cells
- Ethylene treatment resulted in a reduction of mortality.

Chapter 7

General Discussion

7. General Discussion

The basis of this thesis was to try and elucidate mechanisms of programmed cell death and the cell cycle in plants through the use of the tobacco BY-2 cell line. Because of the merits of this cell line over whole plant studies, it was expected to provide greater insights into the mechanisms of programmed cell death in relation to the cell cycle. Of particular importance was to identify areas both homologous and distinct from other non-plant eukaryotic systems. Two approaches were employed to carry this out. The use of the ethylene and its signaling pathway was chosen as a potential activator of programmed cell death due to its previous associations with the process. To complement this one of the key regulators of fission yeast CDK/cyclin complexes essential for cell cycle phase transitions, Cdc25, was also employed to see how it would affect the cell cycle.

7.1. Ethylene As A Tool For PCD And Cell Cycle Research

Ethylene is an important plant growth regulator and has been known to affect plants since Neljubow noticed it caused leaf abscission in 1901. Furthermore, its role in programmed cell death has been established in a number of plant species and situations. This includes both developmental (endosperm development, senescence etc) and non-developmental (pathogen related) forms of PCD (Grbic and Bleecker, 1995; Fukuda, 1992; Francis, 2003). Research into ethylene and the cell cycle is not as well documented and has mainly focused on the effect of ethylene on events related to phases of the cell cycle, such as DNA synthesis and cell division (Applebaum and Burg, 1972). To my knowledge, the data presented in this thesis are the first to establish a clear link between PCD and the cell cycle in plants. Recently, Kadota *et al.* (2004) have also examined the relationship between elicitor-induced cell death and the cell cycle. As with the ethylene data in this thesis, cryptogein-induced cell death

was found to occur at specific points within the cell cycle, especially at G1 and G2. Furthermore, cell cycle arrest and cell death were only induced by treatment with cryptogein during S or G1 phase (Kadota *et al.*, 2004). This is similar to ethylene treatment of tobacco BY-2 cells where cell death was found to be at its highest in G2 when ethylene was applied at S/G1 (Herbert *et al.*, 2001)

So, is ethylene a useful tool for PCD and cell cycle research? The use of ethylene on synchronized cultures of tobacco BY-2 cells has established that induced cell death occurs mainly at the G2/M boundary. Furthermore, the use of ethylene inhibitors has shown that cell death at G2/M is dependent on the ethylene signaling pathway and that mortality in S-phase is independent of it. Thus, not only has cell cycle specificity of ethylene-induced cell death been established, but also the mechanism by which ethylene exerts cell death at G2/M confirmed. These data lead us one step closer to proving the existence of a plant DNA damage checkpoint, the checkpoint in mammalian and yeast cells that provides the last chance for correction before mitosis or exit into PCD if damage is too extensive (Russell and Nurse, 1986).

7.1.1. The Genetic or Chemical Approach to Understanding Ethylene-Induced PCD?

Two different approaches to blocking ethylene action were used in this thesis, genetic and chemical, with both achieving an increased understanding of the relationship between ethylene-induced PCD and the cell cycle.

Initially silver nitrate was used as the initial ethylene inhibitor since addition of silver ions is an established method of blocking ethylene binding in plants (Drew *et al.*, 1981). Although other ethylene inhibitors such as 2,5-norbornadiene (NBD) have been shown to inhibit ethylene induced PCD (Mergermann and Sauter, 2000), silver nitrate was chosen because it inhibits the ethylene signaling pathway, not ethylene biosynthesis. Silver nitrate was able to successfully ameliorate ethylene-induced mortality (chapter 3) but was also toxic to tobacco BY-2 cells. This meant that the ethylene signaling pathway could be linked to the ethylene-induced cell death, but could not confirm whether it was solely responsible for the cell death arising at G2/M. Due to the toxicity of silver ions 1-MCP, another chemical inhibitor of ethylene

receptors was used. 1-MCP is a potent inhibitor of ethylene action (Sisler *et al.*, 1999) and was found to have several advantages over silver, the most important being a lack of toxicity to tobacco BY-2 cells (chapter 4). Use of 1-MCP confirmed that the ethylene-induced mortality at G2/M was completely dependent on the ethylene signaling pathway due to its lack of toxicity. Furthermore, an ethylene-induced mortality peak in S-phase, seen in both ethylene and ethylene + silver treatments, was not ameliorated by 1-MCP. Hence I conclude that the peak in S-phase was independent of the ethylene signaling pathway. Interestingly, 1-MCP has been shown to reduce reactive oxygen species, including H_2O_2 in pear, although it is unclear whether this is a direct result of blocking the ethylene signaling pathway (Larrigaudiere *et al.*, 2003).

Finally the genetic approach to blocking ethylene signaling using *Atetr1*, the gene responsible for the mutated form of the *Arabidopsis* ETR1 receptor (Bleecker *et al.*, 1988), was employed. Introduction of *Atetr1* into the tobacco BY-2 cells caused massive perturbation to the cell cycle, cell size, and high incidences of mortality throughout the cell cycle. This is similar, but not identical, to observations in the *Arabidopsis* mutant where rosette leaves were 25% larger, flowering and senescence were delayed by 2 weeks, and seeds had very low viability (Bleecker *et al.*, 1988). Using ethylene on *Atetr1*-expressing cells indicated that *Atetr1* conferred ethylene insensitivity (apart from S-phase) but data obtained were less clear-cut than that in previous chapters due to the high background mortality. It was therefore not as successful as 1-MCP in identifying ethylene mortality dependent and independent of the ethylene signaling pathway. Interestingly it did highlight the fact that *Atetr1* expression caused massive perturbation in tobacco BY-2 cells, a fact studies into the *Arabidopsis* mutant did not highlight (Bleecker *et al.*, 1988). Hence, the use of 1-MCP, a chemical approach, was the most successful in identifying and confirming the relationship between ethylene, PCD, and the cell cycle. Due to the effectiveness of 1-MCP it has already become a useful research tool into a variety of ethylene dependent plant processes including senescence and fruit ripening (Watkins and Miller, 2003). However, introduction of *Atetr1*, the genetic approach, provided the most questions for further research into the relationship between ethylene, the cell cycle, and PCD. Recent work into the binding of 1-MCP in the presence of low levels of ethylene may have highlighted a difference between *Atetr1* expression and *1-MCP* treatment. Reid and Celikel (2003) hypothesize that 1-MCP, rather than binding directly to the

ethylene binding site, binds to a site exposed when the receptor is free of ethylene. *Atetr1* has a mutation in the ethylene binding site and may therefore explain the difference in observed results.

Thus, ethylene has proven to be a useful research tool into the interactions between PCD and the cell cycle. Even more interestingly though is the potential for ethylene signaling inhibitors, especially 1-MCP, to provide tighter links between the cell cycle and PCD. Because of its ability to block ethylene signaling without detrimental side-effects, other cell death elicitors could be used in conjunction with it. This would help identify the importance of ethylene signaling in other forms of PCD and whether the ethylene signaling pathway plays an important role in the occurrence of mortality within the cell cycle. 1-MCP has already been used to investigate pathogen-induced disease in strawberries (Porat *et al.*, 1999; Jiang *et al.*, 2001), apricots (Dong *et al.*, 2002) and grapefruit (Mullins *et al.*, 2000).

7.2. The Plant Cdc25: Myth Or Reality?

The existence of a plant Cdc25 has been a topic of hot debate in recent years, especially since the majority of mammalian/yeast cell cycle genes have been identified in plants (Francis, 2003). The roles of CDKs (cyclin dependent kinases) and cyclins have been established in plants for a number of years (Joubes *et al.*, 2000: Huntley and Murray, 1999) and more recently Wee1 (Sun *et al.*, 1999: Sorrell *et al.*, 2002), Cdc25s counterpart in the regulation of CDK/Cyclin complexes. Even ATR and ATM, regulators of CDK/Cyclin complexes in response to DNA damage in mammalian systems have had homologues identified in *Arabidopsis* (Garcia *et al.*, 2000; Culligan *et al.*, 2004). Thus, there are two possibilities as to the existence of a plant Cdc25. Firstly it is present but not yet identified, secondly plants do not have a Cdc25-like protein.

Recently a gene sharing structural homology to the catalytic domain of *Sp*Cdc25 has been identified in *Arabidopsis* (D Francis, personal communication) and at first sounds promising. However, Cdc25 has been recently found to be structurally related to the rodanese superfamily of enzymes in its catalytic domain and that this

superfamily is widely distributed among living organisms (Bordo and Bork, 2002). This putative plant Cdc25 could therefore have no functional homology at all to *Sp*Cdc25. Interestingly, expression of this putative CDC25 in yeast resulted in the same phenotype as *Spcdc25* over-expression (D Francis, personal communication; Russell and Nurse, 1986). Notably, this putative CDC25 was the only one identified in the *Arabidopsis* genome and very recently, its ability to act as a dual-site T14 Y15 phosphatase on phosphorylated CDK has been demonstrated (Landrieu *et al.*, 2004).

Is this plant CDC25 regulated by plant growth regulators? The main contender in this is cytokinin. Cytokinin treatment has already been shown to dephosphorylate plant Cdc2 in late G2 (Zhang *et al.*, 1996) with Cdc25 carrying out this same activity at the same time point in *Xenopus* (Kumagai and Dunphy, 1992). Furthermore, tobacco BY-2 cells expressing *Spcdc25* can overcome cell cycle blocks imposed by mevinolin (an inhibitor of cytokinin; chapter 5) due to lower than normal levels of cytokinin in these cell lines (D Francis, personal communication). This indicates that the role of cytokinin in regulating G2/M transition in *Spcdc25*-expressing tobacco BY-2 cells is replaced by *Sp*Cdc25 and provides strong evidence for the cytokinin signaling cascade being a key player in cell cycle regulation. Thus a model for plant cell cycle regulation using cytokinin to upregulate another plant phosphatase, instead of Cdc25 as the main positive regulator, is proposed (Fig. 7.1).

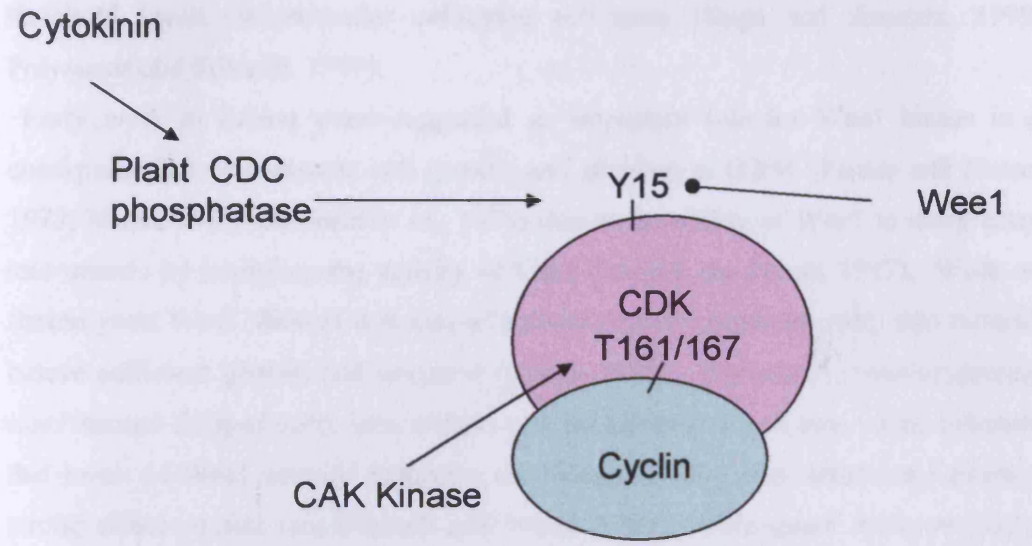

Figure 7.1. Putative model for G2/M cell cycle regulation in tobacco BY-2 cells. Negative regulation is provided by Wee1 kinase that phosphorylates tyrosine 15 of Cdc2. In competition for the same site is a Cdc25-like phosphatase regulated in part by cytokinin levels. CAK kinase phosphorylates Cdc2 at residue threonine 161/167 facilitating binding with Cyclin B.

7.3. Is There A Link Between The Cell Cycle And Cell Size In Plants?

Another interesting finding of this thesis was the positive relationship between cell cycle duration and cell size in tobacco By-2 cells when *Atetr1* and *Spcdc25* were expressed. *Atetr1* expression resulted in a larger cell size phenotype with a longer cell cycle than WT. *Spcdc25* expression caused a smaller cell size phenotype and shorter cell cycle cf. WT. In yeast cells, cell growth occurs in all phases of the cell cycle except M-phase (Mitchison, 1971; Conlon *et al.*, 2001).

To maintain a specific cell size, growth and division must be co-ordinated through the action of cell size checkpoints in G1 and/or G2 (Fantes and Nurse, 1978; Nurse, 1977). This is because cells are able to reach an adequate size before entering S or M phase. Control in fission yeast is primarily at G2/M whereas in budding yeast it is primarily exerted at the G1/S transition (Rupes, 2002). Unfortunately it is still uncertain how these checkpoints work although evidence suggests that it is linked to

threshold levels of particular cell-cycle activators (Daga and Jimenez, 1999; Polymenis and Schmidt, 1999).

Early work in fission yeast suggested an important role for Wee1 kinase in a checkpoint that co-ordinates cell growth and division at G2/M (Fantes and Nurse, 1978; Nurse, 1975; Thuriaux *et al.*, 1978) due to the ability of Wee1 to delay entry into mitosis by inhibiting the activity of Cdc2 (Russell and Nurse, 1987). Work on fission yeast Wee1 showed that loss of activity caused premature entry into mitosis, before sufficient growth had occurred (Nurse, 1975). Conversely, over-expressing *wee1* caused delayed entry into mitosis and an increase in cell size. This indicates that levels of Wee1 activity determine the timing of entry into mitosis and exerts a strong effect on cell size (Russell and Nurse, 1987). Subsequent work on Cdc25 resulted in similar results, with *cdc25-* mutants delaying entry into mitosis with a large cell size, and over-expression of *cdc25* resulting in premature entry into mitosis and a decrease in cell size (Russell and Nurse, 1986). These observations show that at least in fission yeast, both Wee1 and Cdc25 are required for cell-size control.

The small cell size phenotype and premature entry into mitosis when *Spcdc25* was expressed in tobacco BY-2 cells suggests strongly that, in plants, a Cdc25-like protein may also be required for cell size control. In plants, this may be due to the cytokinin transcellular signaling pathway (Fig. 7.1) since regulation of cell size in animals has been linked to growth factors (Conlon and Raffe, 2003). It is therefore likely that *Spcdc25* expression in TBY-2 cells results in premature division at a reduced cell size, a process normally dependent on cytokinin levels (Zhang *et al.*, 1996; Laureys *et al.*, 1998).

The increased cell size and cell cycle duration in *Atetr1*-expressing tobacco BY-2 cells are harder to interpret than the results obtained for *Spcdc25* expression. However, if the presence of ethylene is a requirement for G2/M transition, as is the case with cytokinin (Zhang *et al.*, 1996), a larger cell size phenotype and cell cycle duration would result. Ethylene treatment result in a smaller cell size phenotype, supporting this hypothesis, but blocking of ethylene action with 1-MCP did not result in the same phenotype as *Atetr1* expression. A difference between the *Atetr1* expression and 1-MCP treatment may be elucidated by investigating the effect each one has on the ethylene biosynthesis pathway. In the original *Arabidopsis etr1* mutant, ethylene biosynthesis remained the same, whether exogenous ethylene was applied or not (Bleecker *et al.*, 1988). Thus, it would be interesting to see whether 1-

MCP application results in the same effect. This may help identify whether ethylene is a positive regulator at G2/M, as suggested by ethylene treatment and *Atetr1* expression in tobacco BY-2 cells.

Hence, a link between the cell cycle and cell size in tobacco is likely to be similar to that observed in yeast with the relationship between cell size and cell cycle duration dependent upon cell size checkpoints affected by positive and negative regulators of the cell cycle (Kellog, 2003). If the results of *Atetr1* expression in tobacco BY-2 cells were taken to be more indicative of complete ethylene inhibition than 1-MCP, evidence would strongly suggest checkpoint control at G2/M, similar to that observed in fission yeast (Rupes, 2002). Further research into the relationship between 1-MCP and *Atetr1* expression would have to be carried out to confirm this.

7.4. Concluding Remarks

The major discoveries reported in this thesis are focussed around three main areas. Firstly, ethylene induces cell cycle specific mortality at the G2/M boundary through the known ethylene signaling pathway and that ethylene-induced S-phase mortality was found to be independent of the ethylene signaling pathway. This, in conjunction with the detection of 3'-OH termini, indicates ethylene induced PCD at the G2/M boundary, a cell cycle transition point linked to DNA damage in mammalian and yeast systems. Secondly, the chemical (1-MCP) and genetic (*Atetr1*) approaches to inhibiting ethylene signaling resulted in two completely different cell phenotypes. Both can block ethylene signaling but whereas 1-MCP had no effect on tobacco BY-2 cells, *Atetr1* expression caused massive perturbation to the cell cycle and mortality levels. Thus 1-MCP and *Atetr1* may have different effects downstream of the ethylene receptors. Finally, *Spcdc25* expression in tobacco BY-2 cells resulted in premature entry into mitosis, a shortened cell cycle, and reduced cell size. Results were similar to that observed in fission yeast and indicated a conserved mechanism for cell cycle progression using a CDC25-like phosphatase at G2/M in plants. Furthermore, *Spcdc25*-expressing cells were able to overcome a mevinolin block, indicating *Spcdc25* expression overrides checkpoint control.

7.5. Future Directions

The research in this thesis has lead to a number of areas in which future work could be directed. These include:

- Using 1-MCP in conjunction with other PCD elicitors to see if the induced cell death is dependent on the ethylene signaling pathway. A number of PCD elicitors have already been linked to the ethylene signaling pathway including Fumonisin B1 (Asai *et al.*, 2000).
- Investigating the effects of 1-MCP treatment and *Atetr1* expression on endogenous ethylene/cytokinin levels ± exogenously applied ethylene. It is known that the original *Arabidopsis etr1* mutant showed no change in ethylene biosynthesis when treated with ethylene (Bleecker *et al.*, 1988). It would be interesting to see if inhibition of ethylene biosynthesis occurs in both 1-MCP treatment and *Atetr1* expression in the tobacco BY-2 cell line.
- Examining endogenous levels of ethylene in *Spcdc25* expressing cell lines to see if ethylene biosynthesis is affected by the low levels of cytokinin present. 1-aminocyclopropane-1-carboxylic acid synthase (ACS) activity is the rate-limiting step of ethylene biosynthesis (Woeste *et al.*, 1999) and cytokinin levels have been shown to have a positive relationship with ethylene biosynthesis via posttranscriptional modification of ACS5 (Vogel *et al.*, 1998).
- Expressing both *Spcdc25* and *Atetr1* in the same tobacco BY-2 cell line to see if a normal cell phenotype arises. This is because *Spcdc25* and *Atetr1* expression resulted in exactly the opposite phenotypes.

References

Appendices

References

A

Ach RA, Durfee T, Miller AB, Zambryski PC, Hanley-Bowdoin L, Gruissem W (1997). *RRB1* and *RRB2* encode maize retinoblastoma –related proteins that interact with a plant D-type cyclin and geminivirus replication protein. *Molecular Cell Biology.* **17**: 5077-5086.

Ach RA, Taranto P, Gruissem W (1997). A conserved family of WD-40 proteins binds to the retinoblastoma protein in both plants and animals. *Plant Cell.* **11:** 181-190.

Adrain C, Creagh EM, Martin SJ (2001). Apoptosis-associated release of Smac/DIABLO from mitochondria requires active caspases and is blocked by Bcl-2. *EMBO.* **20:** 6627-6636.

Allen RF (1923). A cytological study of the infection of baart and kenred wheats by puccinia graminis tritici. *Journal of Agricultural Research.* **23:** 131-152.

An GH (1985) High-efficiency transformation of cultured tobacco cells. Plant Physiology **79:** 568-570

Amor Y, Babiychuk E, Inze D, Levine A (1998). The involvement of poly(ADP-ribose) polymerase in the oxidative stress responses in plants. *FEBS Letters.* **440:** 1-7.

Applebaum A, Burg SP (1972). Effect of ethylene on cell division and deoxyribonucleic acid synthesis in *Pisum sativum. Plant Physiology.* **50:** 117-124.

Asai T, Stone JM, Heard JE, Kovtun Y, Yorgey P, Sheen J, Ausubel FM (2000). Fumonisin B1-induced cell death in *Arabidopsis* protoplasts requires jasmonate-, ethylene-, and salicylate-dependent signaling pathways. *Plant Cell.* **12(10):** 1823-1836.

B

Baek K-H, Mondoux MA, Jaster R, Fire-Levin E, D'Amdrea AD (2001). DUB-2A, a new member of the DUB subfamily of hematopoietic deubiquitinating enzymes. *Blood.* **98:** 636-642.

Bell MH, Halford NG, Ormrod JC, Francis D (1993) Tobacco plants transformed with cdc25, a mitotic inducer gene from fission yeast. *Plant Molecular Biology.* **23:** 445-451.

Bentley NJ, Holtzman DA, Flaggs G, Keegan KS, DeMaggio A, Ford JC, Hoekstra M, Carr AM (1996). The *Schizosaccharomyces pombe rad 3* checkpoint gene. *EMBO Journal.* **15:** 6641-6651.

Bestwick CS, Bennett MH, Mansfield JW (1995). *Hrp* mutant of *Pseudomonas syringae pv phaseolicola* induces cell wall alterations but not membrane damage leading to the hypersensitive reaction in lettuce. *Plant Physiology.* **108:** 503-516.

Blackstone NW, Green DR (1999). The evolution of a mechanism of cell suicide. *BioEssays.* **21:** 84-88.

Blank A, McKeon TA (1991). Expression of three RNase activities during natural and dark-induced senescence of wheat leaves. *Plant Physiology.* **97:** 1409-1413.

Bleecker AB, Estelle MA, Somerville C, Kende H (1988) Insensitivity to ethylene conferred by a dominant mutation in *Arabidopsis thaliana. Science.* **241:** 1086-1089

Bordo D, Bork P (2002). The rhodanese/Cdc25 phosphatase superfamily. *EMBO reports.* **3:** 741-746.

Boya P, Cohen I, Zamzami N, Vieira HL, Kroemer G (2002). *Cell Death And Differentiation.* **9:** 465-467.

Breckenridge DG, Germain M, Mathai JP, Nguyen M, Shore GC (2003). Regulation of apoptosis by endoplasmic reticulum pathways. *Oncogene.* **22:** 8608-8618.

Breyne P, Dreesen R, Vandepoele K, DE Veylder L, Van Breusegem F, Callewaert L, Rombauts S, Raes J, Cannoot B, Engler G, Inze D, Zabeau M (2002). Transcriptome analysis during cell division in plants. *Proceedings of the National Academy of Sciences, USA.* **99:** 14825-14830.

Brown, DG, Sun, XM, Cohen GM (1993). Dexamethosone-induced apoptosis involves cleavage of DNA to large fragments prior to internucleosomal fragmentation. *Journal of Biological Chemistry.* **268:** 3037-3039.

Bryant JA, Francis D (2000) Plant growth regulators and the control of S-phase . *In* The Plant Cell Cycle and its Interfaces (Francis D, ed.) Sheffield Academic Press, pp42-56.

Buchanan-Wollaston V (1997). The molecular biology of leaf senescence. *Journal of Experimental Botany.* **48:** 181-199.

Buckner B, Johal GS (2000). Cell death in maize. *Physiologia Plantarum.* **108:** 231-239.

Bulavain DV, Amundson SA, Fornace AJ (2002) p38 and Chk1 kinases: different conductors for the G2/M checkpoint symphony. *Current Opinion in Genetic Development.* **12:** 92-97.

Burssens S, Van Montagu M, Inze D (1998). The cell cycle in *Arabidopsis. Plant Physiology and Biochemistry.* **36 (1-2):** 9-19.

Buse EL, Laties GG (1993). Ethylene-mediated posttranscriptional regulation in ripening avocado (*Persea Americana*) mesocarp discs. *Plant Physiology.* **102:** 417-423.

C

Callard D, Axelos M, Mazzolini L (1996) Novel molecular markers for late phases of the growth cycle of *Arabidopsis thaliana* cell-suspension cultures are expressed during organ senescence. *Plant Physiology.* **112:** 705-715

Chang C, Kwok SF, Bleecker AB, Meyerowitz EM (1993). *Arabidopsis* ethylene-response gene ETR1: similarity of product to two-component regulators. *Science.* **262:** 539-544.

Chang C, Shockey JA (1999). The ethylene-response pathway: signal perception to gene regulation. *Current Opinion in Plant Biology.* **2:** 352-358.

Chau V, Tobias JW, Bachmair A, Marriott D, Ecker DJ, Gonda DK, Varshavsky A (1989). A multiubiquitin chain is confined to specific lysine in a targeted short-lived protein. *Science.* **243:** 1576-1583.

Chen YF, Randlett MD, Findell JL, Schaller GE (2002). Localisation of the ethylene receptor ETR1 to the endoplasmic reticulum of *Arabidopsis. Journal of Biological Chemistry.* **277(22):** 19861-19866.

Clark KL, Larsen PB, Wang X, Chang C (1998). Association of the *Arabidopsis* CTR1 Raf-like kinase with the ETR1 and ERS ethylene receptors. *Proceedings of the National Academy of Sciences, USA.* **95:** 5401-5406.

Cohen GM (1997). Caspases: the executioners of apoptosis. *Journal of Biochemistry.* **326:** 1-16.

Conlon IJ, Dunn GA, Mudge AW, Raff MC (2001). Extracellular control of cell size. *Nature Cell Biology.* **3:** 918-921.

Conlon I, Raffe M (2003). Differences in the way a mammalian cell and yeast cells coordinate cell growth and cell-cycle progression. *Journal of Biology.* **2:** 1-10.

Crowell DN, Salaz MS (1992) Inhibition of growth of cultured tobacco cells at low concentrations of lovastatin is reversed by cytokinin. *Plant Physiology.* **100:** 2090-2095.

Culligan K, Tissier A, Britt A (2004). ATR regulates a G2-phase cell cycle checkpoint in *Arabidopsis thaliana*. *The Plant Cell.* **16:** 1091-1104.

D

Daga R, Jimenez J (1999). Translational control of the Cdc25 cell cycle phosphatase: a molecular mechanism coupling mitosis to cell growth. *Journal of Cell Science.* **112:** 3137-3146.

Dahl M, Meskiene I, Bogre L, Ha DTC, Swoboda I, Hubmann R, Hirt H, Heberle-Bors E (1995). The D-type alfalfa cyclin gene *cycMs4* complements G1 cyclin deficient yeast and is induced in the G1 phase of the cell cycle. *Plant Cell.* **7:** 1847-1857.

Dambrauskas G, Aves SJ, Bryant JA, Francis D, Rogers HJ (2003). Genes encoding two essential DNA replication activation proteins, Cdc6 and Mcm3, exhibit very different patterns of expression in the tobacco BY-2 cell cycle. *Journal of Experimental Botany.* **54:** 699-706.

Day IS, Reddy ASN (1998). Isolation and characterisation of two cyclin-like cDNAs from *Arabidopsis*. *Plant Molecular Biology.* **36:** 451-461.

DeLong A, Calderon-Urrea A, Dellaporta SL. (1993). Sex determination gene *TASSELSEED2* of maize encodes a short-chain alcohol dehydrogenase required for stage-specific floral organ abortion. *Cell.* **74:** 757-768.

Del Pozo O, Lam E (1998). Caspases and programmed cell death in the hypersensitive response of plants to pathogens. *Current Biology.* **8:** 1129-1132.

De Murcia G, Menissier-de Murcia J (1994). Poly(ADP-ribose) polymerase: a molecular nick-sensor. *Trends in Biochemical Science.* **19:** 172-176.

De Veylder L, Segers G, Glab N, Casteels P, Van Montagu M, Inze D (1997). The *Arabidopsis* cks1At protein binds the cyclin-dependent kinases cdc2aAt and cdc2bAt. *FEBS letters.* **412:** 446-452.

De Veylder L, Van Montagu M, Inze D (1997). Cell cycle control in *Arabidopsis*. In *Plant Cell Division*, Francis D, Dudits D, and Inze D., ed., Portland Press, London

De Veylder L, Engler JD, Burssens S, Manevski A, Lesucure B, Van Montagu M, Engler G, Inze D (1999). A new D-type cyclin of *Arabidopsis thaliana* expressed during lateral root primordia formation. *Planta.* 208: 453-462.

Dietrich RA, Delaney TP, Uknes SJ, Ward E, Ryals J, Dangl J (1994). *Arabidopsis* mutants simulating disease response. *Cell.* **77:** 565-577.

Dong L, Zhou H-W, Lurie S (2002). Effect of 1-methylcyclopropene on ripening of 'Canino' apricots and 'Royal Zee' plums. *Postharvest Biology and Technology.* **24:** 135-145.

Drew MC, Jackson MB, Giffard SC, Campbell R (1981). Inhibition by silver ions of gas space (aerenchyma) formation in adventitious roots of *Zea mays* L. subjected to exogenous ethylene or to oxygen deficiency. *Planta.* **153:** 217-224.

Drew MC, He C_J, Morgan PW (2000). Programmed cell death and aerenchyma formation in roots, *Trends in Plant Science.* 5: 123-127.

Dubrovsky JG, Rost TL, Colon-Carmona A, Doerner P (2001) Early primodium morphogenesis during lateral root initiation in *Arabidopsis thaliana. Planta.* **214**: 30-36.

E

Ecker JR (1995). The ethylene signal transduction pathway in plants. *Science.* **268:** 667-675

Edgar BA, O'Farrell PH (1989) Genetic control of cell division patterns in the Drosophila embryo. *Cell.* **67:** 177-187

Elledge SJ, Spottswood MR (1991). A new human p34 protein kinase, CDK2, identified by complementation of a cdc28 mutation in Saccharomyces cerevisiae, is a homolog of Xenopus Eg1. *EMBO Journal.* **10:** 2653-2659.

Elledge SJ (1996). Cell cycle checkpoints: preventing an identity crisis. *Science.* **274:** 1664-1672.

Eyal Y, Sagee O, Fluhr R (1992). Dark-induced accumulation of a basic pathogenesis-related (PR-1) transcript and a light requirement for its induction by ethylene. *Plant Molecular Biology.* **19:** 589-599.

Ezhevsky SA, Nagahara H, Vocero-Akbani AM, Gius DR, Wei MC, Dowdy SF (1997). Hypo-phosphorylation of the retinoblasta protein (pRb) by cyclin D:Cdk4/6 complexes results in active pRb. *Proceedings of the National Academy of Sciences, USA.* **94(20)**: 10699-10704.

F

Fantes PA, Nurse P (1978). Control of the timing of cell division in fission yeast. Cell size mutants reveal a second control pathway. *Experimental Cell Research.* **115:** 317-329.

Fath A, Bethke P, Lonsdale J, Meza-Romero R, Jones R (2000). Programmed cell death in cereal aleurone. *Plant Molecular Biology.* **44:** 245-253.

Fath A, Bethke PC, Jones RL (2001). Enzymes that scavenge reactive oxygen species are down-regulated prior to gibberellic acid-induced programmed cell death in barley aleurone. *Plant Physiology.* **126:** 156-166.

Ferri KF, Kreomer G (2001). Mitochondria – the suicide organelles. *BioEssays.* **23:** 111-115.

Fobert PR, Gaudin V, Lunness P, Coen ES, Doonan JH (1996). Distinct classes of cdc2-related genes are differentially expressed during the cell division cycle in plants. *Plant Cell.* **8:** 1465-1476.

Ford JC, Alkhodairy F, Fotou E, Sheldrick KS, Griffiths DJF, Carr AM (1994) 14-3-3 protein homologs required for the DNA-damage checkpoint in fission yeast. *Science.* **265:** 533-535

Francis D (2003). The interface between cell division and cell death in plants: from division unto death. *Advances in Botanical Research.* **40:** 143-181.

Francis D, Davies MS, Braybrook C, James NC, Herbert RJ (1995). An effect of zinc on M-phase and G1 of the plant cell cycle in the synchronous TBY-2 tobacco cell suspension. *Journal of Experimental Botany.* **46:** 1887-1894.

Francis D, Sorrell DA (2000). The interface between the cell cycle and plant growth regulators. *Plant Growth Regulation.* **33:** 1–12.

Fuerst RAUA, Soni R, Murray JAH, Lindsey K (1996). Modulation of cyclin transcript levels in cultured cells of *Arabidopsis thaliana. Plant Physiology.* **112:** 1023-1033.

Fukuda H. and Komamine A (1981). Relationship between trachery element differentiation and DNA synthesis in single cells isolated from the mesophyll of *Zinnia elegans. Plant Cell Physiology.* **24:** 603-614.

Fukuda H (1992). Trachery element formation as a model system of cell differentiation. *International Review of Cytology.* **136:** 289-332.

Fukuda H (1996). Xylogenesis: initiation, progression, and cell death. *Annual Review of Plant Physiology and Plant Molecular Biology.* **47:** 299-325.

Funari B, Rhind N, Russell P (1997). Cdc25 mitotic inducer targeted by Chk1 DNA damage checkpoint kinase. *Science.* **277:** 1495-1497.

G

Galaktionov K, Beach D (1991). Specific activation of cdc25 tyrosine phosphatase by B-type cyclins: evidence for multiple roles of mitotic cyclins. *Cell.* **67:** 1181-1194.

Gamborg OL (1970). The effects of amino acids and ammonium on the growth of plant cells in suspension culture. *Plant Physiology.* **45:** 372-375.

Gan S, Amasino RM (1995). Inhibition of leaf senescence by autoregulated production of cytokinin. *Science.* **270:** 1966-1967.

Garcia V, Salanoubat M, Choisne N, Tissier A (2000). An ATM homologue from *Arabidopsis thaliana*: complete genome organisation and expression analysis. *Nucleic Acids Research.* **28:** 1692-1699.

Garcia V, Bruchet H, Camescasse D, Granier F, Bouchez D, Tissier A (2003). *AtATM* is essential for meiosis and the somatic response to DNA response in plants. *Plant Cell.* **15:** 119-132.

Gatz C, Frohberg C, Wendenberg R (1992) Stringent repression and homogenous derepression by tetracycline of a modified CaMV 35S promoter in intact transgenic tobacco plants. *Plant Journal.* **2**: 397-404.

Genschik P, Criqui MC, Parmentier Y, Derevier A, Fleck J (1998a). Cell cycle dependent proteolysis in plants: identification of the destruction box pathway and metaphase arrest produced by the proteosome inhibitor MG132. *Plant Cell.* **10:** 2063-2075.

Gewies A, Grimm S (2003). UBP41 is a proapoptotic ubiquitin-specific protease. *Cancer Research.* **63:** 682-688.

Glazener JA, Orlandi EW, Baker CJ (1996). The active oxygen response of cell suspensions to incompatible bacteria is not sufficient to cause hypersensitive cell death. *Plant Physiology.* **110:** 759-573.

Glotzer M, Murray AW, Kirschner MW (1991). Cyclin is degraded by the ubiquitin pathway. *Nature.* **349:** 132-138.

Gould KL, Nurse P (1989). Tyrosine phosphorylation of the fission yeast Cdc2 protein kinase regulates entry into mitosis. *Nature.* **342:** 39-45.

Grbic V, Bleecker AB (1995). Ethylene regulates the timing of leaf senescence in *Arabidopsis*. *Plant Journal*. **8:** 595-602.

Green DR (2000). Apoptotic pathways: paper wraps stone blunts scissors. *Cell*. **102:** 1-4.

Green PJ (1994). The ribonucleases of higher plants. *Annual Review of Plant Molecular Biology*. **45:** 421-245.

Greenberg JT, Guo A, Klessig DF, Aysubel FM (1994). *Cell*. **77:** 551-563.
Gutierrez C (1998). The retinoblastoma pathway in plant cell cycle and development. *Current Opinion In Plant Biology*. **1:** 492-497.

Greenberg JT (1996). Programmed cell death: A way of life for plants. *Proceedings of the National Academy of Sciences, USA*. **93:** 12094-12097.

Griffin RJ, Curtin NJ, Newell DR, Golding BT, Durkacz BW, Calvert AH (1995). *Biochimie*. **77:** 408-422.

Gross A, McDonnell JM, Korsmeyer SJ (1999). Bcl-2 family members and the mitochondria in apoptosis. *Genes & Development*. **13:** 1899–1911.

H

Hacki J, Egger L, Monney L, Conus S, Rosse T, Fellay I, Borner C (2000). Apoptotic crosstalk between the endoplasmic reticulum and mitochondria controlled by Bcl-2. *Oncogene*. **19:** 2286-2295.

Hall AE, Chen QG, Findell JL, Schaller GE, Bleecker AB (1999). The relationship between ethylene binding and dominant insensitivity conferred by mutant forms of the ETR1 ethylene receptor. *Plant Physiology*. **121:** 291-299.

Harbour JW, Dean DC (2000). The Rb/E2F pathway: expanding roles and emerging paradigms. *Genes and Development*. **14:** 2393-2409.

Harris N, Oparka KJ (1994) Plant Cell Biology. 1st edition, Oxford University Press.

Havel L, Durzan DJ. (1996). Apoptosis during diploid parthenogenesis and early somatic embryogenesis of Norway spruce. *International Journal of Plant Science*. **157:** 8-16.

He SY, Huang HC, Collmer A (1993). The *Pseudomonas syringae* pv. *syringae* hairpin$_{Pss}$: a protein that is secreted via the Hrp pathway and elicits the hypersensitive response in plants. *Cell*. **73:** 1255-1266.

He CJ, Morgan PW, Drew MC (1996) Transduction of an ethylene signal is required for cell death and lysis in the root cortex of maize during aerenchyma formation induced by hypoxia. *Plant Physiology.* **112:** 463-472.

Healy JMS, Menges M, Doonan JH, Murray JAH (2001). The *Arabidopsis* D-type Cyclins CycD2 and CycD3 Both Interact *in Vivo* with the PSTAIRE Cyclin-dependent Kinase Cdc2a but Are Differentially Controlled. *Journal of Biological Chemistry.* **276:** 7041-7047

Hemmerlin A, Bach TJ (1998). Effects of mevinolin on cell cycle progression and viability of tobacco BY-2 cells. *Plant Journal.* **14:** 65-74.

Hensel LL, Grbic V, Baumgarten DA, Bleecker AB (1993). Developmental and age-related processes that influence the longevity and senescence of photosynthetic tissues in *Arabidopsis*. *Plant Cell.* **5:** 553-564.

Herbert RJ, Vilhar B, Evett C, Orchard CB, Rogers HJ, Davies MS, Francis D (2001). Ethylene induces cell death at particular phases of the cell cycle in the tobacco TBY-2 cell line. *Journal of Experimental Botany.* **52:** 1615-1623.

Hershko A, Ciechanover A (1998). The ubiquitin system. *Annual Review of Biochemistry.* **67:** 425-479.

Hirao A, Kong YY, Matsuoka S, Wakeham A, Ruland J, Yoshida H, Liu D, Elledge SJ, Mak TW (2000). DNA damage-induced activation by the checkpoint kinase Chk2. *Science.* **287:** 1824-1827.

Hirt H, Pay A, Bogre L, Mesliene I, Herberle-Bors E (1993). *Cdc2MsB*, a cognate *cdc2* gene from alfalfa, complements the G1/S but not the G/M transition of budding yeast *cdc28* mutants. *Plant Journal.* **4:** 61-69.

Hoffman I, Clarke PR, Marcote MJ, Karsenti E, Draetta G (1993). Phosphorylation and activation of human cdc25c by cdc2-cyclin B and its involvement in the self-amplification of MPF at mitosis. *EMBO.* **12:** 53-63.

Hsiang YH, Hertzberg R, Hecht S, Liu LF (1985). Camptothecin induces protein-linked DNA breaks via mammalian DNA topoisomerase I. *Journal of Biological Chemistry.* **260(27):** 14873-14878.

Hu G, Yalpani N, Briggs SP, Johal GS (1998). A porphyrin pathway impairment is responsible for the phenotype of a dominant disease lesion mimic mutant of maize. *Plant Cell.* **10:** 1095-1105.

Hua J, Chang C, Sun Q, Meyerowitz EM (1995) Ethylene insensitivity conferred by *Arabidopsis* ERS gene. *Science.* **269:** 1712-1714.

Hua J, Sakai H, Nourizadeh S, Chen QG, Bleecker AB, Ecker JR, Meyerowitz EM (1998) EIN4 and ERS2 are members of the putative ethylene receptor gene family in *Arabidopsis thaliana*. Cell **94:** 261-271.

Huntley R, Healy S, Freeman D, Lavender P, de Jager S, Greenwood J, Makker J, Walker E, Jackman M Xie Q *et al* (1998). The maize retinoblastoma protein homologue ZmRb-1 is regulated during leaf development and displays conserved interactions with G1/S regulators and plant cyclin D (cycD) proteins. *Plant Molecular Biology.* **37:** 155-169.

Huntley RP and Murray JAH (1999). The plant cell cycle. *Current Opinion In Plant Biology.* 2: 440-446.

I

Inze D, Gutierrez C, Chua N-H (1999). Trends in plant cell cycle research. *Plant Cell.* **11:** 991-994.

J

Jabs T, Dietrich RA, Dangl JL (1996). Initiation of a runaway cell death in an *Arabidopsis* mutant by extracellular superoxide. *Science.* **273:** 1853-1856.

Jacqmard A, De Veylder L, Segers G, Engler JD, Bernier G, Van Montagu M, Inze D (1999). Expression of cks1At in *Arabidopsis thaliana* indicates a role for the protein in both the mitotic and the endoreduplication cycle. *Planta.* **207:** 496-504.

Jiang Y, Joyce DC, Terry LA (2001). 1-Methylcyclopropene treatment affects strawberry fruit decay. *Postharvest Biology and Technology.* **23:** 227-232.

Jinno S, Suto K, Nagata A, Igarashi M, Kanaoka Y, Nojima H, Okayama H (1994). Cdc25A is a novel phosphatase functioning early in the cell cycle. *EMBO Journal.* **13:** 1549-1556.

Johal G, Hulbert SH, Briggs SP (1995). Disease lesion mimics of maize: a model for cell death in plants. *BioEssays.* **17:** 685-692.

John PCL (1998). Cytokinin stimulation of cell division: Essential signal transduction is via Cdc25 phosphatase. *Journal of Experimental Botany.* **49(suppl.):** 91.

Jones AM, Dangl JL (1996). Logjam at the styx, programmed cell death in plants. *Trends in Plant Science.* **1:** 114-119.

Jones AM (2001). Programmed cell death in development and defense. *Plant Physiology.* **125:** 94-97.

Joubes J, Chevalier C, Dudits D, Herberle-Bors E, Inze D, Umeda M, Renaudin JP (2000). CDK-related protein kinases in plants. *Plant Molecular Biology.* 43: 607-620.

K

Kadota Y, Watanbe T, Fujii S, Higashi K, Sano T, Nagata T, Hasezawa S, Kuchitsu K (2004). Crosstalk between elicitor-induced cell death and cell cycle regulation in tobacco BY-2 cells. *The Plant Journal.* **40:** 131-142.

Keen NT, Ersek T, Long M, Bruegger B, Holliday M (1981). Inhibition of the hypersensitive reaction of soybean leaves to incompatible *Pseudomonas* sp by blasticidin S, streptomycin or elevated temperature. *Physiology of Plant Pathology.* **18:** 325-337.

Kellogg DR (2003). Wee1-dependent mechanisms required for coordination of cell growth and cell division. *Journal of Cell Science.* **116:** 4883-4890.

Kerr JFR (1971) Shrinkage necrosis: a distinct mode of cellular death. *Journal of Pathology.* **105:** 13-20.

Kidou S, Umeda M, Uchimiya H (1994). Nucleotide sequence of rice (*Oryza sativa* L.) cDNA homologous to *cdc2* gene. *DNA Sequencing.* **5:** 125-129.

Kim JH, Park KC, Chung SS, Bang O, Chung CH (2003). Deubiquitinating enzymes as cellular regulators. *Journal of Biochemistry.* **143:** 9-18.

King RW, Deshaies RJ, Peters JM, Kirschner MW (1996). How proteolysis drives the cell cycle. *Science.* **274:** 1652-1659.

Korthout HAAJ, Berecki G, Bruin W, van Duijn B, Wang M (2000). The presence and sub-cellular localisation of caspase 3-like proteinases in plant cells. *FEBS Letters.* **475:** 139-144.

Krishnamurthy KV, Krishnaraj R, Chozhavendan R, Christopher FS (2000). The programme of cell death in plants and animals: a comparison. *Current Science in India.* **79:** 1169-1181.

Kumagai A, Dunphy WG (1992) Regulation of the Cdc25 protein during the cell cycle in Xenopus extracts. *Cell.* **70:** 139-151.

Kumagai A, Dunphy WG (1999) Binding of 14-3-3 proteins and nuclear export control the intracellular localisation of the mitotic inducer Cdc25. *Genes and Development.* **13:** 1067-1072.

L

Lacomme C, Santa Cruz S (1999). Bax-induced cell death in tobacco is similar to the hypersensitive response. *Proceedings of the National Academy of Sciences, USA.* **96:** 7956-7961.

Lai C-C, Yeh S-D, Yang J-S (2000). Enhancement of papaya axillary shoot proliferation in vitro by controlling the available ethylene. *Botanical Bulletin of Academia Sinica.* **41:** 203-212.

Lamb C, Dixon RA (1997). The oxidative burst in plant disease resistance. *Annual Review of Plant Physiology and Plant Molecular Biology.* **48:** 251-275.

Lam E, Pontier D, del Pozo O (1999). Die and let live – programmed cell death in plants. *Current Opinion in Plant Biology.* **2:** 502-507.

Lam E, Kato N, Lawton M (2001). Programmed cell death, mitochondria and the plant hypersensitive response. *Nature.* **41:** 848-853.

Lammer C, Wagerer S, Saffrich R, Mertens D, Ansorge W, Hoffman I (1998). The cdc25B phosphatase is essential for the G2/M phase transition in human cells. *Journal of Cell Science.* **111:** 2445-2453.

Landrieu I, da Costa M, De Veylder L, Dewitte F, Vandepoele K, Hassan S, Wieruszeski J-M, Faure J-D, Van Montague M, Inze D, Lippens G (2004). A small CDC25 dual-specificity tyrosine-phosphatase isoforms in *Arabidopsis thaliana*. *Proceedings of the National Academy of Sciences, USA.* **101:** 13380-13385.

Lane DP (1992). Cancer. P53, guardian of the genome. *Nature.* **358(6381):** 15-16.

Larrigaudiere C, Valentines MC, Soria Y, Recasens I (2003). Effect of a treatment with 1-methylcyclopropene on antioxidant metabolism in pears during shelf-life. *Biology and Biotechnology of the Plant Hormone Ethylene III, Vendrell M et al. (Eds),* IOS Press. 443-444.

Laureys F, Dewitte W, Witters E, Van Montague M, Inze D, Van Onckelen H (1998). Zeatin is indispensable for the G2-M transition in tobacco BY-2 cells. *FEBS Letters.* **426:** 29-32.

Lee MG, Nurse P (1980). Complementation used to clone a human homologue of the fission yeast cell cycle control gene *cdc2*. *Nature.* **327:** 31-35.

Levine A, Tenhaken R, Dixon R, Lamb C (1994). H_2O_2 from the Oxidative Burst Orchestrates the Plant Hypersensitive Disease Resistance Response. *Cell.* **79:** 583-593.

Levine A, Pennell RI, Alverez ME, Palmer R, Lamb C (1996). Calcium-mediated apoptosis in plant hypersensitive disease resistance response. *Current Biology.* **6:** 427-437.

Linsmaier EM, Skoog F (1965). Organic growth factor requirement of tobacco tissue. *Plant Physiology.* **18:** 100-127.

Lohman KN, Gan S, Amasino RM (1994). Molecular analysis of natural leaf senescence in *Arabidopsis thaliana. Plant Physiology.* **92**: 322-328.

Lopez-Girona A, Funari B, Mondesert O, Russell P (1999). Nuclear localisation of Cdc25 is regulated by DNA damage and a 14-3-3 protein. *Nature.* **397:** 172-175.

Lopez-Girona A, Kanoh J, Russell P (2001). Nuclear exclusion of Cdc25 is not required for DNA damage checkpoint in fission yeast. *Current Biology.* **11:** 50.

M

Madeo F, Herker E, Maldener C, Wissing S, Lachelt S, Herlan M, Fehr M, Lauber K, Sigrist SJ, Wesselborg S, Frohlich KU (2002). A caspase-related protease regulates apoptosis in yeast. *Molecular Cell.* **9(4):** 911-917.

Magnaghi-Jaulin L, Groisman R, Naguibneva I, Robin P, Lorain S, Le Villain JP, Troalen F, Trouche D, Harel-Bellan A (1998). Retinoblasta protein represses transcription by recruiting a histone deacetylase. *Nature.* **391:** 601-605.

Magyar Z, Meszaros T, Miskolczi P, Deak M, Feher A, Brown S, Kondorosi E, Athanasiadis A, Pongor S, Bilgin M *et al* (1997). Cell cycle phase specificity of putative cyclin-dependent kinase variants in synchronised alfalfa cells. *Plant Cell.* **9:** 223-235

Magyar Z, Atanassova A, De Veylder L, Rombauts S, and Inze D (2000). Characterization of two distinct DP-related genes from *Arabidopsis thaliana. FEBS Letters.* **486:** 79–87.

Matsushime H, Ewen ME, Strom DK, Kato JY, Hanks SK, Roussel MF, Sherr CJ (1992). Identification and properties of an atypical catalytic subunit (p34PSK-J3/cdk4) for mammalian D type G1 cyclins. *Cell.* **71:** 323-334.

McCabe PF, Leaver CJ (2000). Programmed cell death in cultures. *Plant Molecular Biology.* **44:** 359-368.

McGrath RB, Ecker JR (1998) Ethylene signaling in *Arabidopsis*: events from the membrane to the nucleus. *Plant Physiology and Biochemistry.* **36:** 103-113.

McKibbin R, Halford NG, Francis D (1998). Expression of fission yeast cdc25 alters the frequency of lateral root formation in transgenic tobacco. *Plant Molecular Biology.* **36**: 601-612.

Mee Park J, Park C-J, Lee S-B, Ham B-K, Shin R, Paek K-H (2001). Overexpression of the tobacco *Tsi1* gene encoding an EREBP/AP2–type transcription factor enhances resistance against pathogen attack and osmotic stress in tobacco. *Plant Cell.* **13(5):** 1035-1046.

Mergermann H, Sauter M (2000). Ethylene induces epidermal cell death at the site of adventitious root emergence in rice. *Plant Physiology.* **124:** 609-614.

Meuller PR, Coleman TR, Kumagai A, Dunphy WG (1995). Cloning and functional-characterisation of myt1, a membrane associated inhibitory kinase that phosphorylates cdc2 on both thr14 and tyr15. *Molecular Biology of the Cell.* **6:** 1349-1349.

Meyerson M, Harlow E (1994). Identification of G1 kinase activity for cdk6, a novel cyclin D partner. *Molecular and Cellular Biology.* **14:** 2077-2086.

Meyn MS (1999). Ataxia-telangiectasia and cellular responses to DNA damage. *Cancer Research.* **55:** 5991-6001.

Mironov V, De Veylder L, Van Montagu M, Inze D (1999). Cyclin-dependent kinases and cell division in plants – the nexus. *Plant Cell.* **11:** 509-521.

Misawa M, Samejima H (1978). In *Frontiers of Plant Tissue Culture 1978.* Thorpe TA (Ed). University of Calgary, Calgary, Alberta, Canada. 353-362.

Mitchson JM (1971). The Biology of the Cell Cycle. Cambridge: Cambridge University Press.

Mittler R, Shulaev V, Lam E (1995). Coordinated activation of programmed cell death and defense mechanisms in transgenic tobacco plants expressing a bacterial proton pump. *Plant Cell.* **7:** 29-42.

Molina A, Volrath S, Guyer D, Maleck K, Ryals J, Ward E (1999). Inhibition of protoporphyrinogen oxidase expression in *Arabidopsis* causes a lesion-mimic phenotype that induces systemic acquired resistance. *Plant Journal.* **17:** 667-678.

Morgan DO (1995). Principles of CDK regulation. *Nature.* **374:** 131-134.

Morgan DO (1997). Cyclin-dependent kinases: engines, clocks and microprocessors. *Annual Review of Cell Developmental Biology.* **13:** 261-291.

Mullins ED, McCollum TG, McDonald RE (2000). Consequences on ethylene metabolism of inactivating the ethylene receptor sites in diseased non-climacteric fruit. *Postharvest Biology and Technology.* **19:** 155-164.

Murashige T, Skoog F (1962). A revised medium for rapid growth and bioassay with tobacco tissue cultures. *Plant Physiology.* **15:** 473-479.

N

Nagata A, Igarashi M, Jinno S, Suto K, Okayama H (1991). An additional homolog of the fission yeast *cdc25* gene occurs in humans and is highly expressed in some cancer cells. *New Biologist.* **3:** 959-967.

Nagata S (2000). Apoptotic DNA fragmentation. *Experimental Cell Research.* **256:** 12-18.

Nagata T, Okada K, Kawazu T, Takebe I (1987). Cauliflower mosaic virus 35S promoter directs S-phase specific expression in plant cells. *Molecular and General Genetics.* **207:** 242-244.

Nagata T, Nemoto Y, Hasezewa S (1992) Tobacco BY-2 cell line as the 'HeLa' cell line in the biology of higher plants. *International Review of Cytology.* **132:** 1-30.

Nagata T, Kumagai F (1999). Plant cell biology through the window of the highly synchronized tobacco BY-2 cell line. *Methods in Cell Science. 21:* 123-127

Nakagami H, Sekine M, Murakami H, Shinmyo A (1999). Tobacco retinoblastoma-related protein phosphorylated by a distinct cyclin-dependent kinase complex with Cdc2/cyclin D *in vitro*. *Plant Journal.* **18:** 243-252.

Nasmyth K (1996). At the heart of the budding yeast cell cycle. *Trends In Genetics.* **12:** 405-412.

Neljubow DN (1901). "Uber die horizontale nutation der stengel von Pisum sativum und einiger anderen". *Pflanzen Beitrage und Botanik Zentralblatt* **10:**128-139.

Ness PJ, Woolhouse HW (1980). RNA synthesis in Phaseolus chloroplasts. *Journal of Experimental Botany.* **31:** 235-245.

Nosseri C, Coppola S, Ghibelli, L (1994). Possible involvement of poly(ADP-ribose) polymerase in triggering stress-induced apoptosis. *Experimental Cell Research.* **212:** 367-373.

Novak B, Csilkasz-Nagy A, Gyorffy B, Nasmyth K, Tyson J (1998). Model scenarios for evolution of the eukaryotic cell cycle. *Philosophical Transactions of the Royal Society of London Series B - Biological Sciences.* **353:** 2063-2076.

Nurse P (1975). Genetic control of cell size at cell division in yeast. *Nature.* **256:** 547-551.

Nurse P, Thuriaux P (1977). Controls over the timing of DNA replication during the cell cycle of fission yeast. *Experimental Cell Research.* **107:** 365-375.

Nurse P, Thuriaux P (1980). Regulatory genes controlling mitosis in the fission yeast *Schizosaccharomyces pombe. Genetics.* **96:** 627-637.

Nurse P (1990). Universal control mechanism regulating onset of M-phase. *Nature.* **256:** 547-551.

Nutt LK, Pataer A, Pahler J, Fang B, Roth J, McConkey DJ, Swisher SG (2002). Bax and Bak promote apoptosis by modulating endoplasmic reticular and mitochondrial Ca2+ stores. *Journal of Biological Chemistry.* **277(11):** 9219-9225.

O

Oberhammer F, Frisch G, Schmied M, *et al.* (1993). Condensation of the chromatin at the membrane of an apoptotic nucleus is not associated with activation of an endonuclease. *Journal of Cell Science.* **104:** 317-326.

O'Connell MJ, Raleigh JM, Verkade HM, Nurse P (1997). Chk1 is a wee1 kinase in the G2 DNA damage checkpoint inhibiting cdc2 by Y15 phosphorylation. *EMBO Journal.* **16:** 545-554.

O'Conner L, Huang DCS, O'Reilly LA, Strasser A (2000). Apoptosis and cell division. *Current Opinion In Cell Biology.* **12:** 257-263.

O'Farrell PH (2001). Triggering the all-or-nothing switch into mitosis. *Trends in Cell Biology.* **11:** 512-519.

Ohtsubo N, Mitsuhara I, Koga M, Seo S, Ohashi Y (1999) Ethylene promotes the necrotic lesion formation and basic PR gene expression in TMV-infected tobacco. *Plant Cell Physiology.* **40(8):** 808-817.

Orchard CB, Evett C, Davis MS, Herbert RJ, Rogers HJ, Francis D (2003) Effect of ethylene on cell mortality during the cell cycle in the TBY-2 cell line. *Biology and Biotechnology of the Plant Hormone Ethylene III, Vendrell M et al. (Eds),* IOS Press. 335-339.

P

Parkinson JS, Kofoid EC (1992). Communication modules in bacterial signaling proteins. *Annual Review of Genetics.* **26:** 71-112.

Patil C, Walter P (2001). Intracellular signaling from the endoplasmic reticulum to the nucleus: the unfolded protein response in yeast and mammals. *Current Opinion In Cell Biology.* **13:** 349-355.

Patra, D and Dunphy, WG (1996). Xe-p9, a *Xenopus* Suc1/Cks homolog, has multiple essential roles in cell cycle control. *Genes and Development.* **10**: 1503-1515.

Peng C, Graves P, Thoma R, Wu R, Shaw A, Piwnica-Worms H (1997). Mitotic and G2 checkpoint control: regulation of 14-3-3 protein binding by phosphorylation of Cdc25C on ser-216. *Science.* **277:** 1501-1505.

Penninckx IAMA, Thomma BPHJ, Buchala A, Metraux J-P, Broekaert WF (1998). Concomitant activation of jasmonate and ethylene response pathways is required for induction of a plant defense. *Plant Cell.* **10:** 2103-2113.

Piggott JR, Rai R, Carter BL (1982). A bifunctional gene product involved in two phases of the yeast cell cycle. *Nature.* **298:** 391-393.

Pines J (1996). Cyclin from sea urchins to HeLas: making the human cell cycle. *Biochemical Society Transactions.* **24:** 15-33.

Plesse B, Fleck J, Genschik P (1998). The ubiquitin-dependent proteolytic pathway and cell cycle control. In "Plant cell division" (D. Francis, D. Dudits, and D. Inze, ed), pp. 145-163. London, Portland Press

Polymenis M, Schmidt EV (1999). Coordination of cell growth with cell division. *Current Opinion in Genetic Development.* **9:** 76-80.

Porat R, Weiss B, Cohen L, Daus A, Goren R, Droby S (1999). Effects of ethylene and 1-methylecyclopropene on the postharvest qualitites of Shamouti oranges. *Postharvest Biology and Technology.* **15:** 155-163.

Potuschak T and Doerner P (2001). Cell cycle controls: genome-wide analysis in *Arabidopsis. Current Opinion In Plant Biology.* **4:** 501-506.

Q

Quastler H, Sherman FG (1959). Cell population kinetics in the intestinal epithelium of the mouse. *Experimental Cell Research.* **17:** 749-758.

R

Raleigh JM, O'Connell MJ (2000). The G(2) DNA damage checkpoint targets both Wee1 and Cdc25. *Journal of Cell Science.* **113:** 1727-1736.

Ramirez-Parra F, Xio Q, Roniotti MR, Gutierrez C (1999). The cloning of plant E2F, a retinoblastoma-binding protein, reveals unique and conserved features with animal G1/S regulators. *Nucleic Acids Research.* **27:** 3527-3533.

Ramirez-Parra E, Gutierrez C (2000). Characterization of wheat DP, a heterodimerization partner of the plant E2F transcription factor which stimulates E2F-DNA binding. *FEBS Letters.* **486:** 73–78.

Rechsteiner M (1990). PEST sequences are signals for rapid intracellular proteolysis. *Seminars in Cell Biology..* **1:** 433-440.

Redig P, Shaul O, Inze DH, Van Montague M, Van Onckelen H (1996). Levels of endogenous cytokinins, indole-3-acetic acid and abscisic acid during the cell cycle of synchronised tobacco BY-2 cells. *FEBS Letters.* **391:** 175-180.

Reichheld JP, Chaubert N, Shen WH, Murray JAH (1996). Multiple A-type cyclins express sequentially during the cell cycle in *Nicotiana tabacum* BY-2 cells. *Proceedings of the National Academy of Sciences, USA.* **93:** 13819-13824.

Reid MS, Celikel FG (2003). Studies on the inhibition of ethylene action by 1-methylcyclopropene (1-MCP). In Biology and Biotechnology of the Plant Hormone Ethylene III. M. Vendrell et al. (Eds). IOS Press, 412-415.

Renaudin J-P, Doonan JH, Freeman D, Hashimoto J, Hirt H, Inze D, Jacobs T, Kouchi H, Rouze P, Sauter M *et al* (1996). Plant cyclins: a unified nomenclature for plant A-, B-, and D-type cyclins based on sequence organisation. *Plant Molecular Biology.* **32:** 1003-1018

Renaudin JP, Savoure A, Philippe H, Van Montagu M, Inze D, Rouze P (1998). Characterisation and classification of plant cyclin sequences related to A- and B-type cyclins. In *Plant Cell Division*, Francis D, Dudits D, and Inze D., ed., Portland Press, London

Rhind N, Russell P (1998). Tyrosine phosphorylation of Cdc2 is required for the replication checkpoint in *Schizosaccharomyces pombe*. *Molecular Cell Biology*. **18:** 3782-3787.

Riou-Khamlichi C, Huntley R, Jacqmard A, Murray JAH (1999). Cytokinin activation of *Arabidopsis* cell division through a D-type cyclin. *Science*. **283:** 1541-1544.

Rodriguez FI, Esch JJ, Hall AE, Binder BM, Schaller GE, Bleecker AB (1999) A copper co-factor for the ethylene receptor ETR1 from *Arabidopsis*. *Science*. **283:** 996-998.

Rombaldi CV, Silva JA, Wally L, Lucchetta L, Marini LJ, Zanuzo MR (2003). Characterisation of transgenic melons expressing an apple ACC oxidase antisense gene. *Biology and Biotechnology of the Plant Hormone Ethylene III, M. Vendrell et al. (Eds) IOS Press.*

Ros Barcelo A (1999). *In Situ* inactivation of the oxidase activity of xylem peroxidases by H_2O_2 in the H_2O_2-producing xylem of *Zinnia elegans*. *Journal of Plant Research*. **112:** 383-390.

Rouet-Mayer MA, Bureau JM, Laurieri C (1992). Identification and characterization of lipoxygenase isoforms in senescing carnation petals. *Plant Physiology*. **98:** 971-978.

Rudel T, Bokoch GM (1997). Membrane and morphological changes in apoptotic cells regulated by caspase-mediated activation of PAK2. *Science*. **276:** 1571-1574.

Rupes I (2002). Checking cell size in yeast. *Trends in Genetics*. **18:** 479-485.

Russell P and Nurse P (1986). *cdc25*$^+$ functions as an inducer in the mitotic control of fission yeast. *Cell*. **45:** 145-153.

Russell P and Nurse P (1987). Negative regulation of mitosis by *wee1*$^+$, a gene encoding a protein kinase homolog. *Cell*. **49**: 559-567.

Ryerson DE, Heath MC (1996). Cleavage of nuclear DNA into oligonucleosomal fragments during cell death induced by fungal infection or by abiotic treatments. *Plant Cell*. **8:** 393-402.

S

Sadhu K, Reed SI, Richardson H, Russell P (1990). Human homolog of fission yeast cdc25 is predominantly expressed in G1. *Proceedings of the National Academy of Sciences, USA*. **87:** 5139-5143.

Sakai H, Hua J, Chen QG, Chang C, Bleecker AB, Meyerowitz EM (1998) ETR2 is an ETR1-like gene involved in ethylene signaling in *Arabidopsis*. *Proceedings of the National Academy of Sciences, USA*. **74:** 5463-5467.

Sanchez P, de Torres Zabala M, Grant M (2000). AtBI-1, a plant homologue of Bax inhibitor-1, suppresses Bax-induced cell death in yeast and is rapidly upregulated during wounding and pathogen challenge. *Plant Journal*. **21:** 393-399.

Savitsky K, Bar-Shira A, Gilad S, Rotman G, Ziv Y, Vanagaite L, Tagle DA, Smith S, Uziel, et al., (1995). A single ataxia telangiectasia gene with a product similar to PI-3 kinase. *Science*. **268:** 1749-1753.

Schaller GE, Ladd AN, Lanahan MB, Spanbauer J, Bleecker AB (1995). The ethylene-response mediator ETR1 forms a disulfied-linked dimer. *Journal of Biological Chemistry* **270:** 12526-12530.

Segers G, Rouze P, Van Montagu M, Inze D (1998). Cyclin dependent kinases in plants. In *Plant Cell Proliferation and its Regulation in Growth and Development*, Bryant JA, Chiatante D., ed., Chichester, Wiley.

Seo S, Okamoto M, Iwai T, Iwano M, Fukui K, Isogai A, Nakajima N, Ohashi Y (2000). Reduced levels of chloroplast FtsH protein in tobacco mosaic virus-infected tobacco leaves accelerate the hypersensitive response. *Plant Cell*. **12:** 917-932.

Serek M, Sisler EC, Reid MS (1994). Novel gaseous ethylene binding inhibitor prevents ethylene effects in pottered flowering plants. *Journal for the American Society of Horticultural Science*. **119:** 1230-1233.

Shaul O, Mironov V, Burssens S, Van Montague M, Inze D (1996). Two *Arabidopsis* cyclin promoters mediate distinct transcriptional oscillation in synchronised tobacco BY-2 cells. *Proceedings of the National Academy of Sciences, USA*. **93:** 4868-4872.

Shimizu S, Narita M, Tsujimoto Y (1999). Bcl-2 family proteins regulate the release of apoptogenic cytochrome C by the mitochondrial channel VDAC. *Nature*. **399:** 483–487.

Sisler EC, Dupille E, Serek M (1996a). Effect of 1-methylcyclopropene and methylcyclopropane on ethylene binding and ethylene binding on cut carnations. *Plant Growth Regulation*. **18:** 79-86.

Sisler EC, Serek M, Dupille E (1996b). Comparison of cyclopropene, 1-methylcyclopropene, and 3,3-dimethyl-cyclopropene as ethylene antagonists in plants. *Plant Growth Regulation*. **18:** 169-174.

Smalle J, Haegman M, Kurepa J, Van Montagu M, Van Der Straeten D (1997). Ethylene can stimulate *Arabidopsis* hypocotyl elongation in the light. *Proceedings of the National Academy of Sciences, USA*. **94:** 2756-2761.

Smart CM, Hosken SE, Thomas H, Greaves JA, Blair BG, Syhuch W (1995). The timing of maize leaf senescence and characterisation of senescence-related cDNAs. *Physiologia Plantarum.* **93:** 673-682.

Soni R, Carmichael JP, Shah ZH, Murray JAH (1995). A family of cyclin homologs from plants differentially controlled by growth regulators and containing the conserved retinoblastoma protein interaction motif. *Plant Cell.* **7:**85-103

Sorrell DA, Combettes B, Chaubet-Gigot N, Gigot C, Murray JAH (1999). Distinct cyclin D genes show mitotic accumulation or constant levels of transcripts in tobacco Bright Yellow-2 cells. *Plant Physiology.* **119:** 343-351.

Sorrell DA, Francis D, Dickinson JR, Rogers HJ, Halford NG, Coe S, Grierson C (2001). Detecting plant cell cycle proteins which interact with fission yeast Cdc25 using the yeast 2-hybrid system. *Plant Molecular Biology Supplement.* **18:2** S34-27.

Sorrell DA, Marchbank AM, McMahon A, Dickinson JR, Rogers HJ, Francis D (2002). A *WEE1* homologue from *Arabidopsis thaliana. Planta.* **215(3):**518-522

Steffens JC, Hunt DF, Williams BG (1986). Accumulation of non-protein metal binding polypeptides (γ-glutamyl-cysteinyl)$_n$-glycine in selected cadmium-resistant tomato cells. *Journal of Biological Chemistry.* **261:** 13879-13882.

Stern B, Nurse P (1996). A quantitative model for cdc2 control of S phase and mitosis in fission yeast. *Trends In Genetics.* **12:** 345-350.

Stevens R, Mariconti L, Rosignol P, Pe rennes C, Cella R, Bergounioux C (2002). Two E2F sites in the *Arabidopsis* MCM3 promoter have different roles in cell cycle activation and meristematic expression. *Journal of Biological Chemistry.* **277:** 32978-32984.

Sveiczer A, Novak B, Mitchison JM (1996). The size control of fission yeast revisited. *Journal of Cell Science.* **109:** 2947-2957.

Sun YJ, Dilkes BP, Zhang CS, Dante RA, Cameiro NP, Lowe KS, Jung R, Gordon-Kamm WJ, Larkins BA (1999). Characterisation of maize (*Zea mays* L.) wee1 and its activity in developing endosperm. *Proceedings of the National Academy of Sciences, USA.* **96:** 4180-4185.

Susin SA, Lorenzo HK, Zamzami N, Marzo I, Snow BE, Brothers GM, Mangion J, Jacotot E, Costantini P, Loeffler M, Larochette N, Goodlett DR, Aebersold R, Siderovski DP, Penninger JM, Kroemer G (1999). Molecular characterisation of mitochondrial apoptosis-inducing factor. *Nature.* **397:** 441-446.

T

Takizawa CG, Morgan DO (2000). Control of mitosis by changes in the subcellular location of cyclin-B1-Cdk1 and Cdc25. *Current Opinion in Cell Biology.* **12:** 658-665.

Tanaka H, Arakawa H, Yamaguchi T, Shiraishi K, Fukada S, Matsui K, Takei Y, Nakamura Y (2000). A ribonucleotide reductase gene involved in a p53-dependent cell-cycle checkpoint of DNA damage. *Nature.* **404:** 42-49.

Teramoto H, Toyama T, Takeba G, Tsuji H (1995). Changes in expression of two cytokinin-repressed genes, *CR9* and *CR20*, in relation to aging, greening and wounding in cucumber. *Planta.* **196:** 387-395.

Thelen MP, Northcote DH. (1989). Identification and purification of a nuclease from *Zinnia elegans* L.: a potential marker for xylogenesis. *Planta.* **179:** 181-195.

Thomas H, Ougham HJ, Davis TGE (1992). Leaf senescence in non-yellowing mutant of *Festuca pratensis*: Transcripts and translation products. *Journal of Plant Physiology.* **139:** 403-412.

Thuriaux P, Nurse P, Carter B (1978). Mutants altered in the control co-ordinating cell division with cell growth in the fission yeast *Schizosaccharomyces pombe. Mol. Gen. Genet.* **161:** 215-220.

Travers KJ, Patil CK, Wodicka L, Lockhart DJ, Weissman JS, Walter P (2000). Functional and genomic analyses reveal an essential coordination between the unfolded protein response and ER-associated degradation. *Cell.* **101:** 249-258.

U

Umeda M, Bhalerao RP, Schell J, Uchimiya H, Koncz C (1998). A distinct cyclin-dependent kinase-activating kinase of *Arabidopsis thaliana. Proceedings of the National Academy of Sciences, USA.* **95:** 5021-5026.

Umeda M, Umeda-Hara C, Yamaguchi M, Hashimoto J, Uchimiya H (1999). Differential expression of genes for cyclin-dependent protein kinases in rice plants. *Plant Physiology.* **119:** 31-40.

Uren AG, O'Rourke K, Aravind LA, Pisabarro MT, Seshagiri S, Koonin EV, Dixit VM (2000). Identification of paracaspases and metacaspases: two ancient families of caspase-like proteins, one of which plays a key role in MALT lymphoma. *Molecular Cell.* **6:** 961-967.

V

Vander Heiden MG, Chandel NS, Li XX, Schumacker PT, Colombini M, Thompson CB (2000). Outer mitochondrial membrane permeability can regulate coupled respiration and survival. *Proceedings of the National Academy of Sciences, USA.* **97:** 4666-4671.

Vierstra RD (2003). The ubiquitin/26S proteasome pathway, the complex last chapter in the life of many plant proteins. *Trends in Plant Science.* **8(3):** 135-142.

Vogel JP, Woeste K, Theologis A, Kieber JJ (1998). Recessive and dominant in the ACC synthase 5 gene of *Arabidopsis* result in cytokinin-insensitivity and ethylene overproduction respectively. *Proceedings of the National Academy of Sciences, USA.* **95:** 4766-4771.

W

Wagstaff C, Leverentz MK, Griffiths G, Thomas B, Chanasut U, Stead AD, Rogers HJ (2002). Cysteine protease gene expression and proteolytic activity during senescence of *Alstroemeria* petals. *Journal of Experimental Botany.* **53:** 233-240.

Walworth N, Davey S, Beach D (1993). Fission yeast chk1 protein kinase links the rad checkpoint pathway to cdc2. *Nature.* **363:** 368-371.

Walbot V (1991). Maize mutants for the 21st century. *Plant Cell.* **3:** 851-856.

Wang H, Li J, Bostock RM, Gilchrist DG (1996). Apoptosis: A functional paradigm for programmed plant cell death induced by a host-selective phytotoxin and invoked during development. *Plant Cell.* **8:** 375-391.

Wang H, Fowke LC, Crosby WL (1997). A plant cyclin-dependent kinase inhibitor gene. *Nature.* **386:** 451.

Wang H, Oi QG, Schorr P, Cutler AJ, Crosby WI, Fowke LC (1998). ICK1, a cyclin-dependent protein inhibitor from *Arabidopsis thaliana* interacts with both cdc2a and CycD3, and its expression is induced by abscisic acid. *Plant Journal.* **15:** 501-510.

Wang K L-C, Li H, Ecker JR (2002). Ethylene biosynthesis and signaling networks. *The Plant Cell.* S131-151.

Watanbe Y, Fukada H (1995). Autolysis during tracheary element differentiation: analysis with inhibitors. *Plant Cell Physiology.* **36(Suppl.):** 87.

Watkins CB, Miller WB (2003). Implications of 1-methylcyclopropene registration for use on horticultural products. In *Biology and Biotechnology of the Plant Hormone Ethylene III. M. Vendrell et al. (Eds).* IOS Press, **385-390**.

Weaver LM, Himelblau E, Amasino RM (1997). Leaf senescence: gene expression and regulation. In: Setlow JK, ed. *Genetic Engineering.* Vol. 19. New York: Plenum Press, **215-234**.

Weinert T (1998). DNA damage checkpoints update: getting molecular. *Current Opinion in Genetic Development.* **8:** 185-193.

Weymann K, Hunt M, Uknes S, Nevenschwander U, Lawton K, Steiner H-Y, Ryals J (1995). Suppression and restoration of lesion formation in *Arabidopsis lsd* mutants. *Plant Cell.* **7:** 2013-2022.

Willmer EN (1965). Cells and tissues in culture. In *Biology and Physiology Volume 3.* Academic Press Inc, London.

Woeste KE, Ye C, Kieber JJ (1999). Two *Arabidopsis* mutants that overproduce ethylene are affected in the posttranscriptional regulation of 1-aminocyclopropane-1-carboxylic acid synthase. *Plant Physiology.* **119:** 521-529.

Woolhouse HW (1983). Toxicity and tolerances in the response to metals in plants. *Encyclopaedia of plant physiology,* Vol. 12C. In: *Physiological plant ecology. III. Chemical and biological environment.* Lange OL, Nobel PS, Osmond CB, Ziegler H (eds). Berlin: Springer-Verlag. 245-300.

X

Xe Z, Chen Z (2000). Harpin-induced hypersensitive cell death is associated with altered mitochondrial functions in tobacco cells. *Molecular Plant-Microbe Interactions.* **13:** 183-190.

Y

Yamaguchi M, Umeda M, Uchimiya H (1998). A rice homolog of CDK7/MO15 phosphorylates both cyclin-dependent protein kinases and the carboxyl-terminal domain of RNA polymerase II. *Plant Journal.* **16:** 613-619.

Yan N, Doelling JH, Falbel TG, Durski AM, Vierstra RD (2000). The ubiquitin-specific protease family from *Arabidopsis*. *At*UBP1 and 2 are required for the resistance to the amino acid analog canavanine. *Plant Physiology*. **124:** 1828-1843.

Yang SF (1980). Regulation of ethylene biosynthesis. *HortScience* **15:** 238-243

Yarbro JW (1992). Mechanism of action of hydroxyurea. *Seminars in Oncology*. **19:** 1-10.

Yoshida Y (1961). The nuclear control of chloroplast activity in Elodea leaf cells. *Protoplasma*. **54:** 476-492.

Young TE, Gallie DR, DeMason DA (1997). Ethylene-mediated programmed cell death during maize endosperm development of wild-type and shrunken2 genotypes. *Plant Physiology*. **115:** 737-751.

Young TE, Gallie DR (1999). Analysis of programmed cell death in wheat endosperm reveals differences in endosperm development between cereals. *Plant Molecular Biology* **39:** 915-926.

Young TE, Gallie DR (2000). Programmed cell death during endosperm development. *Plant Molecular Biology*. **44:** 283-301.

Yuan J, Shaham S, Ledoux S, Ellis HM, Horvitz HR (1993). The *C. elegans* cell death gene ced-3 encodes a protein similar to mammalian interleukin-1B-converting enzyme. *Cell*. **75:** 641-652.

Z

Zha J, Harada H, Yang E, Jockel J, Korsmeyer SJ (1996). Serine phosphorylation of death agonist BAD in response to survival factor results in binding to 14-3-3, not Bcl-X_L. *Cell*. **87:** 619-628.

Zhang K, Letham DS, John PCL (1996). Cytokinin controls the cell cycle at mitosis by stimulating the tyrosine dephosphorylation and activation of $p34^{cdc2}$-like H1 histone kinase. *Planta*. **200:** 2-12.

Zhou Y, Fowke LC, Wang H (2002). Plant CDK inhibitor studies of interactions with cell cycle regulators in the yeast two-hybrid system and functional comparisons in transgenic *Arabidopsis* plants. *Plant Cell Reporter*. **20:** 967-975.

Zhu Y, Carroll M, Papa FR, Hochstrasser M, D'Andrea AD (1996). DUB-1, a deubiquitinating enzyme with growth-suppressing activity. *Proceedings of the National Academy of Sciences, USA*. **93:** 3275-3279.

Zhu Y, Lambert K, Corless C, D'Andrea AD (1997). DUB-2 is a member of a novel family of cytokine-inducible deubiquitinating enzymes. *Journal of Biological Chemistry.* **272:** 51-57.

Appendix I – Media And Solutions

A.I.i. Bacterial Growth Media

2 x YT Media –

Per litre:

To 900ml of distilled water add:

Tryptone	– 16g
Yeast extract	– 10g
Sodium chloride (NaCl)	– 5g

Adjust to pH 7.0 with sodium hydroxide (NaOH), make to 1 litre, and autoclave.

A.I.ii. Tobacco BY-2 Media and Solutions

Tobacco BY-2 Stock Solutions –

55mM Myoinositol	-	5g in 500ml distilled H_2O
147mM Potassium dihydrogen orthophosphate (KH_2PO_4)	–	10g in 500ml distilled H_2O
3mM Thiamine hydrochloride (HCl)	–	100mg in 100ml distilled H_2O
0.45mM 2, 4-Dichlorophenoxyacetic acid (2, 4-D)	–	50mg in 500ml distilled H_2O 20mM sodium hydroxide (NaOH)
Aphidicolin	–	5mg dissolved in 1ml DMSO

Tobacco BY-2 Liquid Media –

Per litre:

To 900ml of distilled water add

Murashige and Skoog basal salts	– 3.2g
Sucrose	- 30g
Myoinositol stock solution	- 10ml
KH_2PO_4 stock solution	- 10ml
Thiamine HCl stock solution	- 1ml
2, 4-D stock solution	- 2ml

Adjust to pH 5.8, make to 1 litre, and autoclave.

Tobacco BY-2 Solid Media –

As above but with the addition of 0.8% agar

A.I.iii. Protein Extraction

Stock Solutions –

0.5M HEPES (pH 7.5)	–	39.05g dissolved in UHP water. Adjust to pH 7.5 and make up to 150ml. Store at 4°C.
1M β-glycerophosphate (glycerol-2-phosphate)	–	21.6g dissolved in 100ml of UHP water. Store at room temperature.
5M NaCl	–	58.44g dissolved in 200ml of sterile UHP water.
0.2M Sodium vanadate	–	1.839g of sodium orthovanadate dissolved in 50ml of sterile UHP water.
0.5mM PMSF (Phenylmethylsulfonylflouride)	–	87mg dissolved in 5ml absolute ethanol. 5x 1ml aliquots were placed into microcentrifuge tubes and stored at -20°C.

Lysis Buffer –

For 10ml –

50mM HEPES (pH 7.5)	–	1ml of 0.5M stock solution
100mM NaCl	–	200µl of 5M NaCl stock solution
10% Glycerol	–	1ml of 100% glycerol stock solution
60mM β-glycerophosphate (glycerol-2-phosphate)	–	600µl of 1M stock solution
1mM Sodium vanadate	–	50µl of 0.2M stock solution
0.5mM PMSF	–	50µl of 0.1M stock solution
Protease inhibitor tablet (Roche)	–	1

Add 7.1ml of sterile UHP water to make up to 10ml

A.I.iv. Western Blotting Solutions

Stock Solutions –

5x Running Buffer –

Per litre:

To 900ml of distilled H_2O add:

Tris	- 1.5%
Glycine	- 7.2%
SDS	- 0.5%

Resolving Gel Buffer –

Tris	– 113.55g
SDS	– 1.25g

Make to 500ml in distilled H2O. pH should be 8.9.

Stacking Gel Buffer –

Tris	– 18.15g
SDS	– 2.5g

Make to 500ml in distilled H_2O. pH should be 6.7

5x Electrophoresis Buffer –

Per litre:

To 900ml of distilled H_2O add:

Tris	– 60.55g
Glycine	– 144.1g
SDS	– 5g

Make to 1 litre in distilled H_2O. pH should be 8.8

5x SDS-PAGE Sample Buffer –

For 20ml:

Glycerol	– 10ml
SDS	– 1g
Bromophenol blue	– 10mg
Tris-HCl	– 9ml of 0.5M stock solution (pH6.8)
Dithiothreitol (DTT)	– 0.771g

Aliquot into microcentrifuge tubes and store at -20°C.

Tank Blotting Transfer Buffer –

Resolving Gel –

Protogel (accrylamide/bisaccrylamide 30% solution)	– 2.5ml
Resolving gel buffer	– 1.95ml
UHP water	– 3ml
Ammonium perisulphate	– 75µl
TEMED	– 7.5µl

Stacking Gel –

Protogel	– 0.65ml
Stacking gel buffer	– 1.25ml
UHP water	– 3.05ml
Ammonium perisulphate	– 50µl
TEMED	– 5µl

Destain Solution –

dH2O	– 500ml
Methanol	– 400ml
Acetic acid	– 100ml

Tris Buffered Saline (TBS) Solution –

Per litre:

To 900ml of deionised water add

Sodium chloride (NaCl)	- 8g
Potassium chloride (KCl)	- 0.2g
Tris	- 3g

pH to 7.4 with HCl and autoclave.

A.I.v. 3'-OH Detection Solutions

Phosphate Buffered Saline (PBS) Solution –

Per litre:

To 900ml of deionised water add

NaCl	- 8g
KCl	- 0.2g
Na_2HPO_4	- 1.44g
KH_2PO_4	- 0.24g

pH to 7.4 with HCl and autoclave.

A.I.vi. DNA Extraction Solutions

2x CTAB Buffer –

Tris (pH 8.0)	-	100mM
NaCl	-	1.4M
EDTA	-	20mM
CTAB	-	2%

TE Buffer (pH8.0) –

Tris (pH 8.0)	-	10mM
EDTA	-	1mM

A.II.vii. Gel Electrophoresis

Gel Electrophoresis Sample Running Buffer –

For 20ml:

Sterile dH2O	– 500µl
Glycerol	– 500µl
Bromophenol blue	– 10mg

Aliquot into microcentrifuge tubes and store at -20°C.

Gel Electrophoresis Tank Buffer –

For 50x Working Concentration:

Tris	-	242g
Glacial Acetic Acid	-	57.1ml
0.5M EDTA	-	100ml

pH should be 8.0.

Appendix II – Chapter 3 Experimental Data

This appendix gives all the experimental data for chapter 3 including statistical analysis of mitotic cell sizes.

A.II.i. Cell Cycle Data For Control (WT) (Figure 3.1 And 3.2)

The percentage values for control (WT) mitotic index (Fig. 3.1) and mortality index (Fig. 3.2) after a 24 h synchronization with aphidicolin. The results shown in the table are from consolidated data. Standard error for the control mitotic index is shown.

Time (h) After Release From Aphidicolin	Control (WT) Mitotic Index (%)	Control (WT) Mortality Index (%)	Standard Error For Control Mitotic Index (%)
0		3	
1	0	0	0
2	0	4.5	0
3	0	0	0
4	0	3	0
5	11	0	2
6	26	5.5	5
7	42	0	3
8	46	6	3
9	32	0	2
10	18	7.5	2
11	10	3.1	0.5
12	7	0	1
13	0	3.5	0
14	0	0	0
15	0	2	0

16	0	0	0
17	2	3.4	0.1
18	5	0	0.5
19	10	3.1	0.4
20	15	0	0.8
21	20	0	0.2
22	20	0	1
23	17	0	0.7
24	18	0	0.4
25	10	0	0.1

A.II.ii. Cell Cycle Data For Ethylene Treated Cells (Figure 3.1a And 3.2a)

The percentage values for ethylene treated mitotic index (Fig. 3.1a) and mortality index (Fig. 3.2a) after a 24 h synchronization with aphidicolin. The results shown in the table are from consolidated data. Standard error for the control mitotic index is shown.

Time (h) After Release From Aphidicolin	Ethylene Treated Mitotic Index (%)	Ethylene Treated Mortality Index (%)	Standard Error For Ethylene Mitotic Index (%)
0		0	
1	0	0	0
2	0	0	0
3	0	0	0
4	0	5	0
5	0	0	0.6
6	7.7	11.3	0.1
7	14	0	0.4
8	26.5	22	3.3
9	17.4	0	1.7

10	11.5	23	0.3
11	7	5.5	1.2
12	4.7	0	0.8
13	3.2	13	2
14	2.2	0	1
15	2.2	17.4	0.2
16	0.6	0	0.5
17	1.2	6.6	0.4
18	1.1	0	0.2
19	4.3	7.5	1
20	5.4	0	0.6
21	10.4	7.9	1.3
22	17.4	0	1.3
23	6.1	5.8	0.6
24		0	
25		0	

A.II.iii. Cell Cycle Data For Ethylene+Silver Nitrate Treated Cells (Figure 3.1b And 3.2b)

The percentage values for ethylene+silver nitrate treated mitotic index (Fig. 3.1b) and mortality index (Fig. 3.2b) after a 24 h synchronization with aphidicolin. The results shown in the table are from consolidated data. Standard error for the control mitotic index is shown.

Time (h) After Release From Aphidicolin	Ethylene + Silver Nitrate Treated Mitotic Index (%)	Ethylene + Silver Nitrate Treated Mortality Index (%)	Standard Error For Ethylene + Silver Nitrate Mitotic Index (%)
0		0	
1	0	0	0

2	0	0	0
3	0	0	0
4	0	1	0
5	1.1	0	0.6
6	4.2	0	0.5
7	7	0	0.7
8	16	0	1
9	16	0	1.2
10	10	4.5	2.7
11	5	1.9	1.2
12	3.7	0	1.3
13	6.4	2.5	1.2
14	8	0	2.3
15	4.4	8	0.9
16	3.3	0	0.5
17	1	0.6	0.4
18	1.1	0	0.6
19	0.3	0	0.1
20	2.9	0	2.2
21	7.7	3	0.6
22	11.3	0	0.9
23	11.9	4.5	0.6
24	4.6	0	0
25		7	

A.II.iv. Cell Cycle Data For Silver Nitrate Treated Cells (Figure 3.1c And 3.2c)

The percentage values for silver nitrate treated mitotic index (Fig. 3.1b) and mortality index (Fig. 3.2b) after a 24 h synchronization with aphidicolin. The results shown in the table are from consolidated data. Standard error for the control mitotic index is shown.

Time (h) After Release From Aphidicolin	Silver Nitrate Treated Mitotic Index (%)	Silver Nitrate Treated Mortality Index (%)	Standard Error For Silver Nitrate Mitotic Index (%)
0	0		0
1	0	0.33	0
2	0		0
3	0.167	0.17	0.167
4	0		0
5	0.67	7.49	0
6	0	7.67	0
7	0	5.83	0
8	3.67	3.67	1.33
9	15	4	0.67
10	18.91	7.17	0.63
11	12.5	5.67	1.83
12	5.33	1.5	1.33
13	3.67	2.17	0.67
14	2.5	1.17	0.83
15	0.83	1.33	0.167
16	0.83	1.33	0.167
17	0.33		0.33
18	0.167		0.167
19	0.67		0.67
20	0.5		0.167
21	2.67		1
22	5.67		2
23	8.167		2.167
24	9.67		2
25	8.83		0.167

A.II.v. Nuclear Fragmentation In Control (WT) And Ethylene Treated Cells

The percentage values for nuclear fragmentation (3'-OH termini generation) in control (WT) and ethylene treated cells.

Time (h) After Release From Aphidicolin	Nuclear Fragmentation In Control (%)	Nuclear Fragmentation In Ethylene Treated (%)
0	0	0
2	1	1
4	2	3
6	2	3
8	1	12
10	2	14

A.II.vi. Mitotic Cell Size Data (Figure 3.5)

The average mitotic cell areas and other details were taken from calculations resulting from the tables in the section below regarding statistical analysis of mitotic cell areas.

Cell Line / Treatment	Mitotic Cell Size (mM^2)	*n*	Standard Error
Control (WT)	3046	125	75.7
Ethylene	2562	51	122
Ethylene + Silver Nitrate	3310	126	88.4
Silver Nitrate	3115	57	123

A.II.vii. Statistical Analysis Of Mitotic Cell Areas

All statistical analysis was carried using Minitab 13® in conjunction with the Sigma Scan® measured mitotic cell areas.

A.II.vii.i. Control Mitotic Cell Areas

Below is a table of all mitotic cell areas measured for wild-type (control) mitotic cell areas using Sigma Scan ®.

2106.962	2708.576	3119.61	2616.401	2787.315	3540.777	1711.616	4856.296	2409.007
3989.942	4117.47	3915.857	2424.845	3212.535	2314.43	1298.48	3523.738	2490.674
3641.133	2044.736	3607.506	2509.214	3459.111	1773.241	1627.172	3101.445	2928.805
3901.37	1956.54	4192.531	2013.811	4041.359	3965.397	2503.134	3390.43	2701.745
3506.924	2125.502	4019.666	2407.506	3216.814	4476.787	2757.591	2174.892	3660.199
3759.505	3189.491	3831.113	1989.341	3090.936	2873.034	2687.258	2706.099	3426.759
5164.421	3291.95	3949.334	2240.195	2291.162	4574.217	4942.09	3091.912	2466.054
2284.031	3448.527	4937.211	2625.934	2746.632	2007.056	3418.202	2344.98	2860.199
2709.702	3089.81	3010.021	4477.163	1921.711	6701.595	2643.648	2445.112	2651.905
2785.438	2755.264	3514.28	4003.378	1929.518	2501.858	3186.789	2578.12	3243.986
2752.336	3034.941	3676.037	2931.056	2567.086	3290.373	1790.655	2378.232	2345.205
2914.243	3244.736	2692.588	2531.432	2051.942	3901.07	4719.084	1894.314	2862.976
3543.779	2843.31	3775.042	2766.673	3416.851	4145.693	3148.883	2256.859	2827.247
2216.176	2516.194	3009.8705	2929.18	3032.164	2641.396	3378.87	3480.503	

Using Minitab 13® the basic statistics, including the Anderson-Darling test for normality, were carried out on the above data set.

Descriptive Statistics

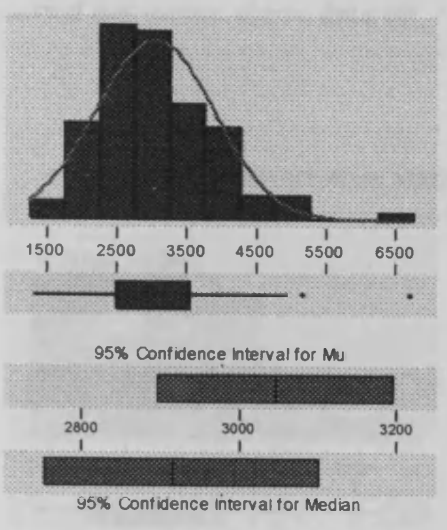

Variable: C1

Anderson-Darling Normality Test	
A-Squared:	1.052
P-Value:	0.009
Mean	3045.94
StDev	846.70
Variance	716902
Skewness	0.964681
Kurtosis	2.03004
N	125
Minimum	1298.48
1st Quartile	2478.36
Median	2914.24
3rd Quartile	3519.01
Maximum	6701.60

95% Confidence Interval for Mu	
2896.05	3195.84

95% Confidence Interval for Sigma	
753.16	966.98

95% Confidence Interval for Median	
2752.49	3100.96

The basic statistics on the control mitotic cell area data show the P-value for the Anderson-Darling normality test as 0.009. As this is below $P<0.05$ the data is not normally distributed (it is non-parametric).

A.II.vii.ii. Ethylene Treated Mitotic Cell Areas

Below is a table of all mitotic cell areas measured for ethylene-treated mitotic cell areas using Sigma Scan ®.

2015.913	3583.261	3295.2524	3278.4387	3078.852	3832.989	2334.021	1741.715	1595.872
1635.504	3477.125	3846.4252	2357.5905	2557.328	1287.296	4828.223	1604.278	1307.788
2742.578	3270.407	1598.9491	2480.0901	4094.352	1713.567	2405.479	1823.757	2045.165
2405.78	3088.534	2912.2162	2253.9313	1469.769	4489.773	3245.862	3635.729	
2953.8	2484.293	1589.4915	2780.1088	1923.513	2995.159	3188.215	2436.555	
1992.569	1222.068	2459.6735	1949.484	2896.453	1899.944	3250.816	1309.589	

Using Minitab 13® the basic statistics, including the Anderson-Darling test for normality, were carried out on the above data set.

Descriptive Statistics

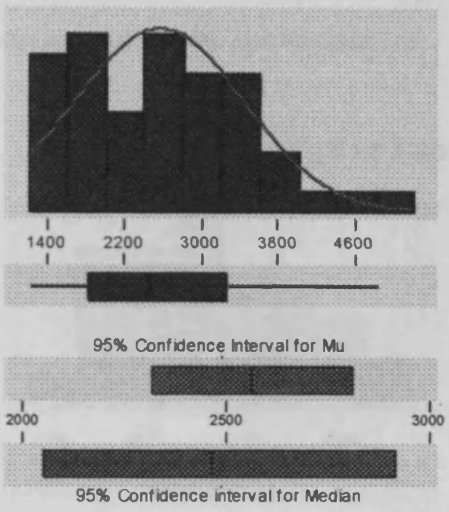

Variable: C2

Anderson-Darling Normality Test	
A-Squared:	0.465
P-Value:	0.244
Mean	2562.15
StDev	874.57
Variance	764878
Skewness	0.471835
Kurtosis	-3.3E-01
N	51
Minimum	1222.07
1st Quartile	1823.76
Median	2459.67
3rd Quartile	3245.86
Maximum	4828.22
95% Confidence Interval for Mu	
2316.17	2808.13
95% Confidence Interval for Sigma	
731.76	1087.16
95% Confidence Interval for Median	
2049.57	2912.19

The basic statistics on the ethylene-treated mitotic cell area data show the P-value for the Anderson-Darling normality test as 0.244. As this is above $P<0.05$ the data is normally distributed.

A.II.vii.iii. Silver Nitrate Treated Mitotic Cell Areas

Below is a table of all mitotic cell areas measured for silver nitrate-treated mitotic cell areas using Sigma Scan ®.

3250.896	3016.326	3911.803	3427.135	3457.009	3388.178	1806.868	2871.458	2878.589
2967.36	3787.052	3409.12	3705.536	2889.548	2709.476	3922.612	3204.954	
5201.992	2616.176	4339.951	4512.742	4903.659	3010.246	2909.439	2507.863	
2111.315	2632.014	4392.644	2140.139	4735.448	1326.178	2789.567	3274.761	

3932.82	3934.172	1816.476	2116.57	2043.385	1866.992	2452.468	2509.964	
2582.473	3585.288	2115.219	3224.47	1687.671	4298.893	2515.068	2991.631	
3085.907	2201.389	5148.583	4467.18	3813.924	2176.018	2744.605	2252.28	

Using Minitab 13® the basic statistics, including the Anderson-Darling test for normality, were carried out on the above data set.

Descriptive Statistics

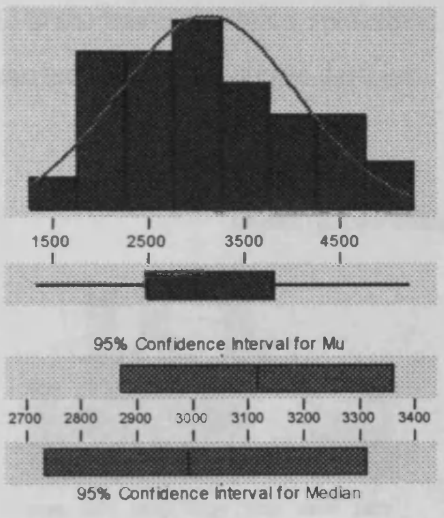

Variable: C3

Anderson-Darling Normality Test

A-Squared:	0.432
P-Value:	0.295
Mean	3115.29
StDev	925.22
Variance	856040
Skewness	0.408551
Kurtosis	-4.5E-01
N	57
Minimum	1326.18
1st Quartile	2480.17
Median	2991.63
3rd Quartile	3800.49
Maximum	5201.99

95% Confidence Interval for Mu

2869.79 3360.78

95% Confidence Interval for Sigma

781.12 1135.02

95% Confidence Interval for Median

2732.88 3312.63

The basic statistics on the silver nitrate-treated mitotic cell area data show the P-value for the Anderson-Darling normality test as 0.295. As this is above $P<0.05$ the data is normally distributed.

A.II.vii.iv. Ethylene And Silver Nitrate Treated Mitotic Cell Areas

Below is a table of all mitotic cell areas measured for ethylene and silver nitrate-treated mitotic cell areas using Sigma Scan ®.

2902.158	2074.01	2069.807	2122.049	1880.053	2335.598
3625.22	2712.179	1795.834	1434.04	1825.408	3161.043
2499.606	3494.84	2900.357	2895.327	1977.031	3876.675
3599.174	2209.345	1432.764	1937.774	3614.712	2906.887
2420.567	2751.06	2883.017	1785.1	3813.173	
2395.722	2290.261	2805.254	1555.339	2189.004	
1962.695	2649.202	2477.763	3834.791	2455.62	
1977.707	3292.325	2219.854	2398.724	4112.066	

Using Minitab 13® the basic statistics, including the Anderson-Darling test for normality, were carried out on the above data set.

Descriptive Statistics

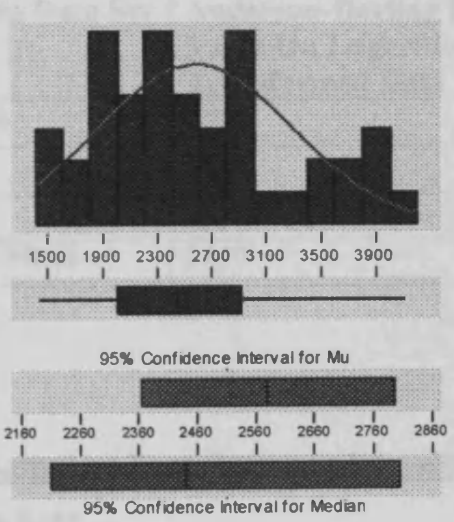

Variable: E+S

Anderson-Darling Normality Test

A-Squared:	0.678
P-Value:	0.072
Mean	2580.71
StDev	707.66
Variance	500789
Skewness	0.483467
Kurtosis	-6.2E-01
N	44
Minimum	1432.76
1st Quartile	2000.73
Median	2438.09
3rd Quartile	2905.70
Maximum	4112.07

95% Confidence Interval for Mu

2365.56	2795.86

95% Confidence Interval for Sigma

584.69	896.63

95% Confidence Interval for Median

2209.81	2802.83

The basic statistics on the ethylene + silver nitrate-treated mitotic cell area data show the P-value for the Anderson-Darling normality test as 0.072. As this is above $P<0.05$ the data is normally distributed.

A.II.vii.v. Comparison Of Control, Ethylene, Silver Nitrate, And Ethylene+Silver Nitrate Treated Mitotic Cell Areas

A.II.vii.v.i. Logarithmic Transformation Of Mitotic Cell Area Data Sets

Since control mitotic cell areas showed non-parametric distribution whilst mitotic cells areas of the treated cells were normally distributed, all mitotic cell area data sets were logarithmically transformed (Table 5; raw data not shown). This resulted in all data sets being normally distributed, enabling comparisons to be made against each other.

Mitotic Cell Area Data Set	Anderson-Darling P-Value On Logarithmically Transformed Data	Normally Distributed Yes/No
Control (Wild-Type)	0.990	Yes
Ethylene	0.301	Yes
Silver Nitrate	0.899	Yes
Ethylene and Silver Nitrate	0.640	Yes

A.II.vii.v.ii. 2 Sample t-Test Between Logarithmically Transformed Mitotic Cell Area Data Sets

The result of logarithmically transforming the mitotic cell area data sets into patterns of normal distribution meant that the data sets could be compared with each other. There are a number of parametric tests available to analysis normally distributed data sets. A two-sample t-test was used over ANOVA (Analysis of variance) as comparisons could be made between data sets with different *n*-value. A two-sample t-test was chosen over other t-tests as the data sets are considered independent (separate tobacco BY-2 cultures)

and the variances were shown to be equal using the F-test (P-value was greater than 0.05). A confidence interval of 95.0% and two-tailed tests (this uses the hypothesis that samples are not equal) were used when comparing mitotic cell area data. Table 6 gives the results of the two-sample two-tailed t-tests carried out to compare whether there was a statistical difference between the treated mitotic cell areas and control mitotic cell areas. Comparisons were also carried out between ethylene versus ethylene+silver nitrate, ethylene versus silver nitrate, and silver nitrate versus ethylene+silver nitrate.

Mitotic Cell Areas To Be Compared	**T-value and P-value**	**Degrees of Freedom**	**Significant Difference?**
Control versus Ethylene	T = 3.96 P= 0.000	174	Yes
Control versus Silver Nitrate	T = -0.32 P = 0.746	180	No
Control versus Ethylene+Silver Nitrate	T = 3.47 P = 0.001	167	Yes
Ethylene versus Silver Nitrate	T = -3.32 P = 0.001	106	Yes
Ethylene versus Ethylene+Silver Nitrate	T = -0.45 P = 0.655	93	No
Silver Nitrate versus Ethylene+Silver Nitrate	T = -3.08 P = 0.003	99	Yes

Appendix III – Chapter 4 Experimental Data

This appendix gives all the experimental data for chapter 4 including statistical analysis of mitotic cell sizes.

A.III.i. Cell Cycle Data For Control (WT) (Figure 4.2 And 4.3)

The percentage values for control (WT) mitotic Index (Fig. 4.2) and mortality Index (Fig. 4.3) after a 24 h synchronization with aphidicolin. The results shown in the table are the consolidated data from three readings per time point. Standard error, as calculated from the three replicates per time point, is also shown.

Time (h) After Release From Aphidicolin	Control (WT) Mitotic Index (%)	Control (WT) Mortality Index (%)	Standard Error For Control Mitotic Index (%)	Standard Error For Control Mortality Index (%)
0	0			
1	0.11	0.44	0.111	0.222
2	0.11	0.44	0.111	0.222
3	0.11	1.32	0.111	0.192
4	3.52	0.44	0.294	0.294
5	8.03	1.32	1.28	0.38
6	24.09	1.54	1.71	0.294
7	43.01	2.2	3.02	0.62
8	23.76	2.53	2.14	0.44
9	13.42	2.09	0.4	0.587
10	7.26	1.21	0.88	0.62
11	3.85	2.2	0.78	0.4
12	2.2	1.54	0.68	0.222

13	1.21	0.77	0.294	0.48
14	0.88	1.21	0.111	0.56
15	1.76	1.43	0.294	0.294
16	2.86	1.65	0.68	0
17	6.93	0.67	0.77	0.192
18	11.33	0.99	3.29	0
19	19.25	0.99	4.03	0.51
20	32.01	0.88	0.77	0.56
21	11.44	1.65	0.294	0.51
22	12.65	1.43	0.62	0.111

A.III.ii. Cell Cycle Data For 1-MCP Treated Cells (Figure 4.2a And 4.3a)

The percentage values for 1-MCP treated Mitotic Index (Fig. 4.2a) and Mortality Index (Fig. 4.3a) after a 24 h synchronization with aphidicolin. The results shown in the table are the consolidated data from three readings per time point. Standard error, as calculated from the three replicates per time point, is also shown.

Time (h) After Release From Aphidicolin	1-MCP Treated Mitotic Index (%)	1-MCP Treated Mortality Index (%)	Standard Error For 1-MCP Treated Mitotic Index (%)	Standard Error For 1-MCP Treated Mortality Index (%)
0	0			
1	0	0.33	0	0.111
2	0.33	0.77	0.192	0.4
3	0.33	1.21	0	0.294
4	3.33	0.67	0.84	0.19
5	13.09	1.87	0.4	0.48
6	18.7	0.22	0.4	0.111

7	42.57	0.33	1.26	0.19
8	28.33	0.44	1.26	0.222
9	18.81	0.67	0.77	0.38
10	11.77	0.22	0.867	0.111
11	8.69	0.44	0.587	0.294
12	5.28	0.88	0.192	0.222
13	2.53	1.1	0.4	0.222
14	2.97	0.77	0.192	0.294
15	1.76	1.21	0.111	0.73
16	2.31	0.55	0.192	0.222
17	4.07	0.44	0.587	0.294
18	8.8	1.87	0.867	0.111
19	5.39	0.55	0.587	0.222
20	22.22	0.77	0.867	0.62
21	9.57	0.44	0.51	0.222
22	7.04	0.67	0.48	0.38

A.III.iii. Cell Cycle Data For 1-MCP + Ethylene Treated Cells (Figure 4.2b And 4.3b)

The percentage values for 1-MCP + ethylene treated Mitotic Index (Fig. 4.2b) and Mortality Index (Fig. 4.3b) after a 24 h synchronization with aphidicolin. The results shown in the table are the consolidated data from three readings per time point. Standard error, as calculated from the three replicates per time point, is also shown.

Time (h) After Release From Aphidicolin	1-MCP + Ethylene Treated Mitotic Index (%)	1-MCP + Ethylene Treated Mortality Index (%)	Standard Error For 1-MCP + Ethylene Treated Mitotic Index (%)	Standard Error For 1-MCP + Ethylene Treated Mortality Index (%)
0	0			
1	0	0.33	0	0.192

2	0.2211	0.55	0.111	0.294
3	0.2211	1.33	0.222	0.333
4	1.43	1.76	0.111	0.294
5	4.73	1.87	0.222	0.4
6	21.67	1.43	0.587	0.8
7	41.14	0.55	3.53	0.222
8	34.54	0.55	0.867	0.222
9	19.8	0.67	0.693	0.383
10	12.76	0.67	0.294	0.192
11	5.17	0.44	0.294	0.222
12	2.09	0.67	0.294	0.192
13	0.55	0.67	0.222	0.192
14	0.2211	4.51	0.587	1.68
15	1.76	10.67	0.8	3.26
16	2.31	0.77	0.77	0.294
17	2.97	1.21	0.51	0.111
18	10.67	0.55	0.677	0.111
19	11	0.33	0.294	0.192
20	16.61	1.1	0.294	0.4
21	21.78	2.53	0.51	0.62
22	11	0.77	0.62	0.294

A.III.iii.i. Statistical Analysis of 1-MCP + Ethylene Cell Cycle Mortality Peak At 15 h

To see if there was a statistical difference between the 1-MCP/control (WT) mortality at 15 h and the 1-MCP + ethylene mortality peak at 15 h, statistical analysis was carried out. The data for control, 1-MCP, and 1-MCP + ethylene at 15 h after release from aphidicolin was all normally distributed. Therefore, a two sampled t-test was employed to see if there was a statistical difference between 1-MCP+ethylene and 1-MCP/control.

Mitotic Cell Areas	T-value and P-	Degrees of	Significant

To Be Compared	value	Freedom	Difference?
1-MCP+Ethylene versus Control	T = -2.85 P = 0.046	4	Yes
1-MCP+Ethylene versus 1-MCP	T = -2.86 P = 0.046	4	Yes

A.III.iv. Histone H4 Expression Level Data For 1-MCP Control (WT) (Figure 4.1)

The raw volume values for histone H4, 18S ribosomal RNA, and histone H4 corrected against 18S Ribosomal RNA (Fig. 4.1) in control (WT) for 1-MCP.

Time (h) after release from aphidicolin	Histone H4 Expression In Control (WT)	18S Ribosomal RNA Expression In Control (WT)	Corrected Histone H4 Expression In Control (WT)
0	65851	9168	7.18
1	68212	11248	6.06
2	63329	12678	5
3	62697	14340	4.37
4	58531	13988	4.18
5	50476	19050	2.65

A.III.v. Optical Density Readings For 1-MCP Treated And Control (WT) Over A 7 Day Period (Figure 4.4)

The growth (optical density) of 1-MCP treated and control (WT) cells over a seven day period. Data consolidated from 9 separate readings per time point (1-MCP) and from 3 separate readings per time point (control) are given in the table as well as standard error.

Day	Control (WT) Optical Density @ 550nm	Standard Error For Control (WT) Optical Density @ 550nm	1-MCP Treated Optical Density @ 550nm	Standard Error For 1-MCP Treated Optical Density @ 550nm
0	0.045	0	0.058	0.00083
1	0.092	0.00167	0.082	0.00183
2	0.147	0	0.151	0.00309
3	0.205	0.00441	0.209	0.00182
4	0.207	0	0.209	0.00056
5	0.215	0.00167	0.217	0.0241
6	0.215	0	0.218	0.00083

A.III.vi. Mitotic Index Readings For 1-MCP Treated And Control (WT) Over A 7 Day Period (Figure 4.5)

The mitotic index readings of 1-MCP treated and control (WT) cells over a seven day period. Data consolidated from 9 separate readings per time point (1-MCP treated) and from 3 separate readings per time point (control) are given in the table as well as standard error.

Day	Control (WT) Mitotic Index (%)	Standard Error For Control (WT) Mitotic Index	1-MCP Treated Mitotic Index (%)	Standard Error For 1-MCP Treated Mitotic Index
0				
1	0.11	0.111	0.48	0.185
2	7.26	0.192	6.75	0.527
3	4.73	0.4	7.92	0.303
4	3.19	0.294	4.14	0.353
5	2.64	0.192	3.63	0.208
6	2.53	0.294	2.02	0.137

A.III.vii. Mortality Index Readings For 1-MCP Treated And Control (WT) Over A 7 Day Period (Figure 4.6)

The mortality index readings of 1-MCP treated and control (WT) cells over a seven day period. Data consolidated from 9 separate readings per time point (1-MCP treated) and from 3 separate readings per time point (control) are given in the table as well as standard error.

Day	Control (WT) Mortality Index (%)	Standard Error For Control (WT) Mortality Index	*Atetr*^{4} Cl 1 Mortality Index (%)	Standard Error For *Atetr*^{4} Cl 1 Mortality Index
0				
1	0.88	0.222	7.26	1.12
2	1.32	0.192	7.81	0.757
3	1.65	0.333	4.36	0.633
4	2.42	0.62	10.49	0.49
5	3.08	0.294	6.99	0.593
6	0.77	0.294	6.23	0.563

A.III.iii.i. Statistical Analysis of Control (WT) and 1-MCP Mortality Over a 7 Day Period

To see if there was a statistical difference between the control (WT) mortality and 1-MCP mortality over a 7 day period, statistical analysis was carried out. Since control and 1-MCP mortality data were normally distributed, a two sampled t-test was employed to see if there was a statistical difference.

Mitotic Cell Areas To Be Compared	T-value and P-value	Significant Difference?
Control versus 1-MCP	T = -0.30 P = 0.768	No

A.III.viii. Mitotic Cell Size Data (Figure 4.7)

The average mitotic cell areas and other details were taken from calculations resulting from the tables in the section below regarding statistical analysis of mitotic cell areas.

Cell Line / Treatment	Mitotic Cell Size (mM^2)	*n*	Standard Error
Control (WT)	3046	125	75.7
1-MCP	3067	124	66.9
1-MCP + Ethylene	2991	92	86.6
Ethylene	2562	51	122

A.III.ix. Statistical Analysis Of Mitotic Cell Areas

All statistical analysis was carried using Minitab 13® in conjunction with the Sigma Scan® measured mitotic cell areas.

A.III.ix.i. Control Mitotic Cell Areas

Below is a table of all mitotic cell areas measured for wild-type (control) mitotic cell areas using Sigma Scan ®. The same data was used as that in the ethylene chapter since wild-type mitotic cell areas was seen to be consistent between synchrony experiments.

2106.962	2708.576	3119.61	2616.401	2787.315	3540.777	1711.616	4856.296	2409.007
3989.942	4117.47	3915.857	2424.845	3212.535	2314.43	1298.48	3523.738	2490.674
3641.133	2044.736	3607.506	2509.214	3459.111	1773.241	1627.172	3101.445	2928.805
3901.37	1956.54	4192.531	2013.811	4041.359	3965.397	2503.134	3390.43	2701.745
3506.924	2125.502	4019.666	2407.506	3216.814	4476.787	2757.591	2174.892	3660.199
3759.505	3189.491	3831.113	1989.341	3090.936	2873.034	2687.258	2706.099	3426.759
5164.421	3291.95	3949.334	2240.195	2291.162	4574.217	4942.09	3091.912	2466.054
2284.031	3448.527	4937.211	2625.934	2746.632	2007.056	3418.202	2344.98	2860.199
2709.702	3089.81	3010.021	4477.163	1921.711	6701.595	2643.648	2445.112	2651.905
2785.438	2755.264	3514.28	4003.378	1929.518	2501.858	3186.789	2578.12	3243.986
2752.336	3034.941	3676.037	2931.056	2567.086	3290.373	1790.655	2378.232	2345.205
2914.243	3244.736	2692.588	2531.432	2051.942	3901.07	4719.084	1894.314	2862.976
3543.779	2843.31	3775.042	2766.673	3416.851	4145.693	3148.883	2256.859	2827.247
2216.176	2516.194	3009.8705	2929.18	3032.164	2641.396	3378.87	3480.503	

Using Minitab 13® the basic statistics, including the Anderson-Darling test for normality, were carried out on the above data set.

Descriptive Statistics

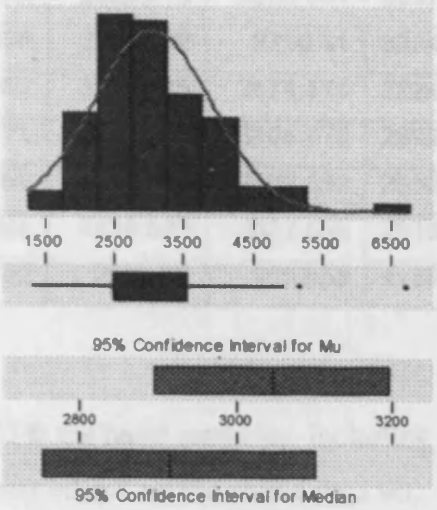

Variable: C1

Anderson-Darling Normality Test	
A-Squared:	1.052
P-Value:	0.009
Mean	3045.94
StDev	846.70
Variance	716902
Skewness	0.964681
Kurtosis	2.03004
N	125
Minimum	1298.48
1st Quartile	2478.36
Median	2914.24
3rd Quartile	3519.01
Maximum	6701.60
95% Confidence Interval for Mu	
2896.05	3195.84
95% Confidence Interval for Sigma	
753.16	966.98
95% Confidence Interval for Median	
2752.49	3100.96

The basic statistics on the control mitotic cell area data show the P-value for the Anderson-Darling normality test as 0.009. As this is below $P<0.05$ the data is not normally distributed (it is non-parametric).

A.III.ix.ii. 1-MCP Treated Mitotic Cell Areas

Below is a table of all mitotic cell areas measured for 1-MCP-treated mitotic cell areas using Sigma Scan ®.

3009.12	2520.323	2854.494	3538.375	2791.368	2652.956	2822.969	4842.409	3127.866
2931.207	2492.7	3238.807	3065.04	2498.18	2394.671	4538.863	1719.947	2718.033
3871.345	3538.675	3702.158	2549.672	2628.936	2350.535	3223.644	1994.971	3050.779
5222.218	3705.911	2896.679	3096.266	2957.703	3001.464	4052.092	2896.904	2858.397
3996.622	4156.202	2522.349	3511.953	1823.381	2829.499	3397.485	2663.914	2618.653
3666.429	3623.794	3194.37	2907.863	1737.587	3569	2004.804	2128.955	3749.897

4536.611	4395.646	3135.297	2596.059	3145.881	4159.054	1462.713	2571.965	3377.895
3218.915	3523.738	3339.313	3206.981	2037.906	1826.309	1772.941	2190.205	2692.888
4197.561	3797.936	2684.932	2750.31	3224.845	2894.877	3584.838	2540.589	2664.74
5272.584	3387.052	3286.545	2674.573	2224.582	2760.293	3693.976	4005.104	2655.958
3493.789	3903.171	3598.724	3104.673	2692.813	2147.044	2785.063	1948.733	3386.451
3170.126	3827.059	2634.866	2962.582	2352.937	2577.744	3865.115	2581.723	2961.156
3481.178	3238.882	3339.538	2337.099	2613.023	4506.737	4326.065	2518.596	
3665.603	3386.752	2381.76	2652.58	4150.647	2172.941	1895.815	2690.261	

Using Minitab 13® the basic statistics, including the Anderson-Darling test for normality, were carried out on the above data set.

Descriptive Statistics

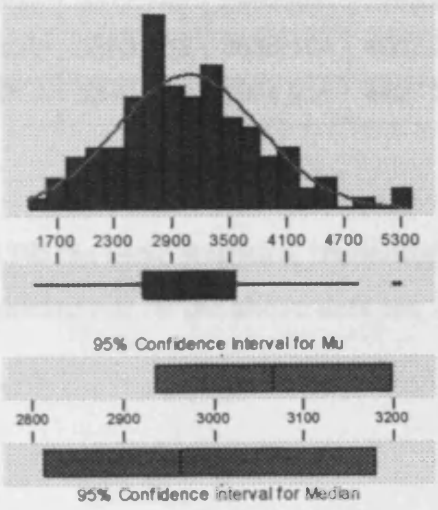

Variable: 1-MCP

Anderson-Darling Normality Test

A-Squared:	0.586
P-Value:	0.124
Mean	3066.95
StDev	744.90
Variance	554871
Skewness	0.473581
Kurtosis	0.247646
N	124
Minimum	1462.71
1st Quartile	2585.31
Median	2961.87
3rd Quartile	3538.60
Maximum	5272.58

95% Confidence Interval for Mu

2934.53 3199.36

95% Confidence Interval for Sigma

662.31 851.21

95% Confidence Interval for Median

2811.30 3179.08

The basic statistics on the 1-MCP-treated mitotic cell area data show the P-value for the Anderson-Darling normality test as 0.124. As this is above $P<0.05$ the data is normally distributed.

A.III.ix.iii. 1-MCP+Ethylene Treated Mitotic Cell Areas

Below is a table of all mitotic cell areas measured for 1-MCP+ethylene mitotic cell areas using Sigma Scan ®.

4946.219	3390.505	2289.06	2522.124	3350.422	3710.265	2289.36	3815.35
4400.976	2981.422	2499.156	2534.509	3182.961	1370.464	3662	2859.749
3612.835	2227.81	2448.039	2597.41	3171.102	1685.945	2132.933	3172.077
5047.851	2911.315	2311.128	3177.782	2078.439	2558.829	2456.896	2476.562
4480.39	3617.564	2727.491	4197.335	3759.204	4298.818	2476.412	2865.753
4562.732	1775.943	2772.002	2862.376	3294.877	4448.564	2229.762	2718.709
3899.643	1985.288	3455.282	2205.442	2358.341	2403.753	1968.099	4298.818
3913.38	1163.445	3953.537	3556.615	2827.698	4735.973	2459.373	4448.564
3827.21	2603.565	3135.898	3042.222	2327.866	2828.673	2286.208	2209.57
2034.528	2595.834	3312.742	2992.606	2763.595	2397.673	2898.48	2874.46
3461.362	2251.529	2563.783	3636.104	4052.318	2181.422	2439.107	
2310.677	4047.213	2349.859	3804.916	4427.322	2349.559	3299.306	

Using Minitab 13® the basic statistics, including the Anderson-Darling test for normality, were carried out on the above data set.

Descriptive Statistics

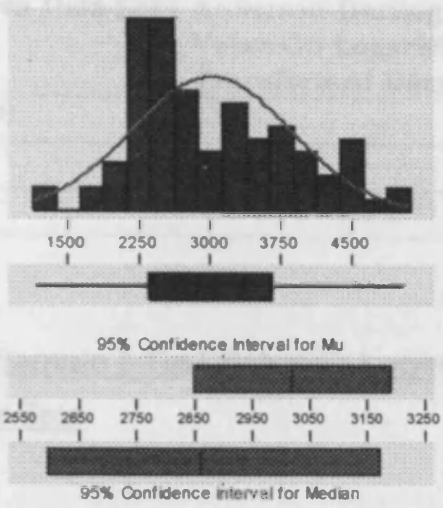

Variable: 1-MCP+E

Anderson-Darling Normality Test	
A-Squared:	1.400
P-Value:	0.001
Mean	3020.19
StDev	840.10
Variance	705767
Skewness	0.440811
Kurtosis	-4.5E-01
N	94
Minimum	1163.45
1st Quartile	2356.22
Median	2861.06
3rd Quartile	3642.58
Maximum	5047.85

95% Confidence Interval for Mu	
2848.13	3192.26
95% Confidence Interval for Sigma	
734.78	980.94
95% Confidence Interval for Median	
2595.80	3171.10

The basic statistics on the 1-MCP+ethylene-treated mitotic cell area data show the P-value for the Anderson-Darling normality test as 0.001. As this is below $P<0.05$ the data is not normally distributed (non-parametric).

A.III.ix.iv. Comparison Of Control, 1-MCP, And 1-MCP+Ethylene Treated Mitotic Cell Areas

A.III.ix.iv.i.. Logarithmic Transformation Of Mitotic Cell Area Data Sets

Since control mitotic cell and 1-MCP+ethylene areas showed non-parametric distribution whilst mitotic cells areas of the 1-MCP-treated cells were normally distributed, all mitotic cell area data sets were logarithmically transformed. This resulted in all data sets being normally distributed, enabling comparisons to be made against each other.

Mitotic Cell Area Data Set	Anderson-Darling P-Value On Logarithmically Transformed Data	Normally Distributed?
Control (Wild-Type)	0.990	Yes
1-MCP	0.509	Yes
1-MCP+Ethylene	0.099	Yes

A.III.ix.iv.ii. 2 Sample t-Test Between Logarithmically Transformed Mitotic Cell Area Data Sets

The result of logarithmically transforming the mitotic cell area data sets into patterns of normal distribution meant that the data sets could be compared with each other. There are a number of parametric tests available to analysis normally distributed data sets. A two-sample t-test was used over ANOVA (Analysis of variance) as comparisons could be made between data sets with different *n*-value. A two-sample t-test was chosen over other t-tests as the data sets are considered independent (separate tobacco BY-2 cultures) and the variances were shown to be equal using the F-test (P-value was greater than 0.05). A confidence interval of 95.0% and two-tailed tests (this uses the hypothesis that samples are not equal) were used when comparing mitotic cell area data. Table 5 gives the results of the two-sample two-tailed t-tests carried out to compare whether there was a statistical difference between the treated mitotic cell areas and control mitotic cell areas. A comparison was also carried out between 1-MCP and 1-MCP+ethylene.

Mitotic Cell Areas To Be Compared	T-value and P-value	Degrees of Freedom	Significant Difference?
Control versus 1-MCP	T = -0.42 P = 0.672	247	No
Control versus 1-MCP+Ethylene	T = -0.29 P = 0.776	217	No
1-MCP versus 1-MCP+Ethylene	T = 0.69 P = 0.493	216	No

Appendix IV – Chapter 5 Experimental Data

This appendix gives all the experimental data for chapter 5 including statistical analysis of mitotic cell sizes.

A.IV.i. Cell Cycle Data For *Atetr*^{e} Cl 1 And *Atetr*^{e} Cl 2 (Figure 5.2)

The percentage values for *Atetr*^{e} Cl 1 and *Atetr*^{e} Cl 2 mitotic index (Fig. 5.2) and mortality index after a 24 h synchronization with aphidicolin:

Time (h) after release from aphidicolin	*Atetr*^{e} Cl 1 Mitotic Index (%)	*Atetr*^{e} Cl 1 Mortality Index (%)	*Atetr*^{e} Cl 2 Mitotic Index (%)	*Atetr*^{e} Cl 2 Mortality Index (%)
0	0		0	
1	0	8.33	0	14.33
2	0	9	0.33	
3	0		0	10.33
4	0	9	0	
5	0		0	11.67
6	0	15.67	0.67	
7	0		2	12
8	0	16.33	3	
9	2.67		3.67	12.67
10	4.67	9.67	8.33	
11	11		7	11.33
12	7.67	11.33	5.67	
13	7		4	7.33
14	6.33		4.33	

A.IV.ii. Cell Cycle Data For *Atetr*^{e} Cl 1 And *Atetr*^{e} Cl 1 + Ethylene (Figure 5.3 And 5.4)

The percentage values for *Atetr*^{e} Cl 1 and *Atetr*^{e} Cl 1 + ethylene mitotic index (Fig. 5.3) and mortality index (Fig. 5.4) after a 24 h synchronization with aphidicolin:

Time (h) after release from aphidicolin	*Atetr*^{e} Cl 1 Mitotic Index (%)	*Atetr*^{e} Cl 1 Mortality Index (%)	*Atetr*^{e} Cl 1 + Ethylene Mitotic Index (%)	*Atetr*^{e} Cl 1 + Ethylene Mortality Index (%)
0	0		0	
1	0	10.33	0	12
2	0	13.33	0	12.33
3	0	15	0	9.67
4	0	6.67	0	12.67
5	0	14	0.67	18.67
6	1	20.33	1	9.67
7	2.33	25.67	1.33	19.33
8	11.67	13	3	14.33
9	13	27.67	13.33	18.67
10	15.67	18.67	12.33	13.67
11	20.67	13.67	13	12
12	10	19	14.33	16
13	12	20.67	11	11.33
14	8	16.33	11.33	15.33
15	5.67	17.33	11	13.33
16	5.67	16	7	14
17	5.33		7	
18	4.67	13.67	7.67	13.33
19	6	12.33	4.67	10.33
20	7	16.67	3.67	19.33
21	4.67	17.67	4.33	11
22	4.67	20	5	13
23	5	14.67	5.33	11.67

24	4.33	21.33	5.67	15
25	3	10.67	4	22.67
26	1.67	13.67	3.33	26.33
27	4.33	25.33	3.33	18.67
28	1.67	22.33	3	23.33
29	2	34	2	16
30	4	25.33	2.67	19.33
31	7.67		3.33	
32	10.67		4	
33	8	13.67	4.67	11
34	6.33	17.67	3.33	11
35	4.67		4	

A.IV.iii. Peroxidase Activity For *Atetr*^{e} Cl 1 And *Atetr*^{e} Cl 1 + Ethylene (Figure 5.5)

The peroxidase activity for *Atetr*^{e} Cl 1 and *Atetr*^{e} Cl 1 + ethylene measured using TMBZ-PS and a spectrophotometer at 655nm. The results shown in the table are the consolidated data from three readings per time point. Standard error as calculated from the three replicates per time point are also shown.

Time (h) after release from aphidicolin	*Atetr*^{e} Cl 1 Peroxidase Activity @ 655nm	*Atetr*^{e} Cl 1 Peroxidase Activity Standard Error	*Atetr*^{e} Cl 1 + Ethylene Peroxidase Activity @ 655nm	*Atetr*^{e} Cl 1 + Ethylene Peroxidase Activity Standard Error
1	0.36	0.00882	0.26	0.0115
3	0.55	0.00667	0.54	0.012
5	0.49	0.00882	0.51	0.0176

7	0.48	0.00333	0.42	0.012
9	0.58	0.00333	0.57	0.00333
11	0.56	0	0.54	0.00289
13	0.59		0.56	
15	0.6		0.6	
17	0.57		0.56	
19	0.55		0.52	
21	0.6		0.58	

A.IV.iv. Optical Density Readings For *Atetr*^{e} Cl 1 And Control (WT) Over A 7 Day Period (Figure 5.6)

The growth (optical density) of *Atetr*^{e} Cl 1 and control (WT) cells over a seven day period. Data consolidated from 9 separate readings per time point (*Atetr*^{e} Cl 1) and from 3 separate readings per time point (Control) are given in the table as well as standard error.

Day	Control (WT) Optical Density @ 550nm	Standard Error For Control (WT) Optical Density @ 550nm	*Atetr*^{e} Cl 1 Optical Density @ 550nm	Standard Error For *Atetr*^{e} Cl 1 Optical Density @ 550nm
0	0.045	0	0.053	0.00083
1	0.092	0.00167	0.085	0.0057
2	0.147	0	0.107	0.00265
3	0.205	0.00441	0.173	0.00206
4	0.207	0	0.204	0.00176
5	0.215	0.00167	0.217	0.00083
6	0.215	0	0.22	0

A.IV.v. Mitotic Index Readings For *Atetr*^{e} Cl 1 And Control (WT) Over A 7 Day Period (Figure 5.7)

The mitotic index readings of *Atetr*^{e} Cl 1 and control (WT) cells over a seven day period. Data consolidated from 9 separate readings per time point (*Atetr*^{e} Cl 1) and from 3 separate readings per time point (control) are given in the table as well as standard error.

Day	Control (WT) Mitotic Index (%)	Standard Error For Control (WT) Mitotic Index	*Atetr*^{e} Cl 1 Mitotic Index (%)	Standard Error For *Atetr*^{e} Cl 1 Mitotic Index
0				
1	0.11	0.111	1.47	0.126
2	7.26	0.192	4.67	0.44
3	4.73	0.4	3.34	0.307
4	3.19	0.294	5.13	0.255
5	2.64	0.192	4.4	0.176
6	2.53	0.294	2.31	0.124

A.IV.vi. Mortality Index Readings For *Atetr*^{e} Cl 1 And Control (WT) Over A 7 Day Period (Figure 5.8)

The mortality index readings of *Atetr*^{e} Cl 1 and control (WT) cells over a seven day period. Data consolidated from 9 separate readings per time point (*Atetr*^{e} Cl 1) and from 3 separate readings per time point (control) are given in the table as well as standard error.

Day	Control (WT) Mortality Index (%)	Standard Error For Control (WT) Mortality Index	*Atetr*^{r} Cl 1 Mortality Index (%)	Standard Error For *Atetr*^{r} Cl 1 Mortality Index
0				
1	0.88	0.222	7.26	1.12
2	1.32	0.192	7.81	0.757
3	1.65	0.333	4.36	0.633
4	2.42	0.62	10.49	0.49
5	3.08	0.294	6.99	0.593
6	0.77	0.294	6.23	0.563

A.IV.vii. Mitotic Cell Size Data (Figure 5.9)

The average mitotic cell areas and other details were taken from calculations resulting from the tables in the section below regarding statistical analysis of mitotic cell areas.

Cell Line	Mitotic Cell Size (mM^2)	*n*	Standard Error
Control (WT)	3046	125	75.7
Control (WT) + Ethylene	2562	51	122
Atetr^{r} Cl 1	4371	158	196
Atetr^{r} Cl 2	4629	13	258
Atetr^{r} Cl 1 + Ethylene	4523	155	217

A.IV.viii. Statistical Analysis Of Mitotic Cell Areas

All statistical analysis was carried using Minitab 13® in conjunction with the Sigma Scan® measured mitotic cell areas.

A.IV.viii.i. Control Mitotic Cell Areas

Below is a table of all mitotic cell areas measured for wild-type (control) mitotic cell areas using Sigma Scan ®. The same data was used as that in the ethylene chapter since wild-type mitotic cell areas was seen to be consistent between synchrony experiments.

2106.962	2708.576	3119.61	2616.401	2787.315	3540.777	1711.616	4856.296	2409.007
3989.942	4117.47	3915.857	2424.845	3212.535	2314.43	1298.48	3523.738	2490.674
3641.133	2044.736	3607.506	2509.214	3459.111	1773.241	1627.172	3101.445	2928.805
3901.37	1956.54	4192.531	2013.811	4041.359	3965.397	2503.134	3390.43	2701.745
3506.924	2125.502	4019.666	2407.506	3216.814	4476.787	2757.591	2174.892	3660.199
3759.505	3189.491	3831.113	1989.341	3090.936	2873.034	2687.258	2706.099	3426.759
5164.421	3291.95	3949.334	2240.195	2291.162	4574.217	4942.09	3091.912	2466.054
2284.031	3448.527	4937.211	2625.934	2746.632	2007.056	3418.202	2344.98	2860.199
2709.702	3089.81	3010.021	4477.163	1921.711	6701.595	2643.648	2445.112	2651.905
2785.438	2755.264	3514.28	4003.378	1929.518	2501.858	3186.789	2578.12	3243.986
2752.336	3034.941	3676.037	2931.056	2567.086	3290.373	1790.655	2378.232	2345.205
2914.243	3244.736	2692.588	2531.432	2051.942	3901.07	4719.084	1894.314	2862.976
3543.779	2843.31	3775.042	2766.673	3416.851	4145.693	3148.883	2256.859	2827.247
2216.176	2516.194	3009.8705	2929.18	3032.164	2641.396	3378.87	3480.503	

Using Minitab 13® the basic statistics, including the Anderson-Darling test for normality, were carried out on the above data set.

Descriptive Statistics

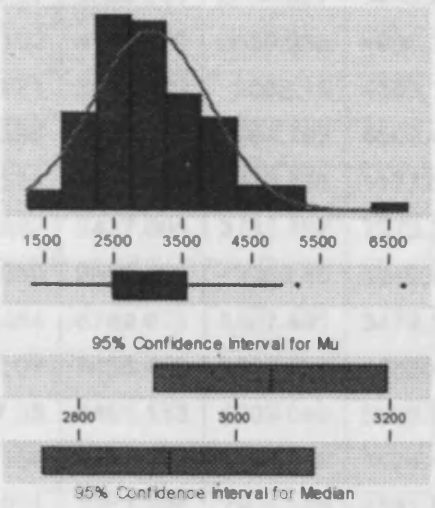

Variable: C1

Anderson-Darling Normality Test	
A-Squared:	1.052
P-Value:	0.009
Mean	3045.94
StDev	846.70
Variance	716902
Skewness	0.964681
Kurtosis	2.03004
N	125
Minimum	1298.48
1st Quartile	2478.36
Median	2914.24
3rd Quartile	3519.01
Maximum	6701.60
95% Confidence Interval for Mu	
2896.05	3195.84
95% Confidence Interval for Sigma	
753.16	966.98
95% Confidence Interval for Median	
2752.49	3100.96

The basic statistics on the control mitotic cell area data show the P-value for the Anderson-Darling normality test as 0.009. As this is below $P<0.05$ the data is not normally distributed (it is non-parametric).

A.IV.viii.ii. *Atetr*^{e} Cl 1 Mitotic Cell Areas

Below is a table of all mitotic cell areas measured for *Atetr*^{e} Cl 1 mitotic cells using Sigma Scan ®.

9215.388	5180.409	5752.824	4462.601	1150.985	1165.097	2112.742	3853.406
6526.328	4566.485	7858.81	6629.762	3041.546	2655.282	2043.235	2058.322
5769.413	2715.106	2992.907	4094.802	2869.356	4062.376	4106.962	6284.106
3548.959	2855.995	3830.888	3074.873	2307.825	4335.673	3861.963	2495.027
2967.386	1883.055	3859.486	3374.141	2789.491	5075.999	11690.3	1842.597
2765.322	1423.457	6066.429	1810.396	3963.37	2456.671	3110.978	3134.172
2923.926	1767.236	2412.31	6304.072	5063.239	2854.569	2902.608	3297.579

2319.309	3926.44	6891.424	9049.127	2853.293	2722.312	2146.669	3198.949
3153.162	4208.67	5696.904	2864.027	3493.263	976.018	6335.748	2371.552
3759.955	1775.192	4182.023	2659.936	4986.226	15479.9	1852.805	2916.57
8381.835	3410.921	3833.139	2062.15	4363.145	5043.948	3165.097	3698.33
9946.256	3986.339	4150.572	3344.793	4562.432	7175.38	2263.464	2841.509
6885.87	2561.531	5013.248	3366.786	11772.49	2406.155	7110.978	3005.292
5716.57	9682.492	2437.005	3743.892	7373.766	5855.207	2597.636	4731.394
3584.763	6996.059	2559.129	3089.36	6249.953	2085.194	2507.187	5742.166
3539.951	2927.454	6769.075	3527.491	3472.171	2070.707	4054.044	4275.924
6176.543	10422.07	5455.433	2814.862	14526.63	7379.171	8316.457	2282.229
1768.887	7077.05	4453.518	6209.045	6489.548	4773.879	2737.85	3281.366
3636.48	8651.154	1975.53	8317.058	1924.414	3495.515	5452.505	
2768.85	5656.971	3363.408	2305.348	4561.606	4588.553	6774.78	

Using Minitab 13® the basic statistics, including the Anderson-Darling test for normality, were carried out on the above data set.

Descriptive Statistics

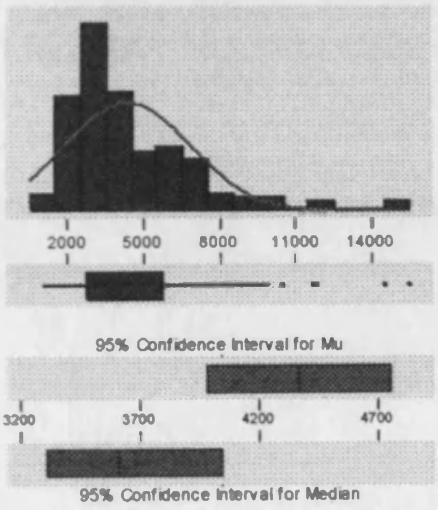

Variable: etr1 cl1

Anderson-Darling Normality Test	
A-Squared:	5.919
P-Value:	0.000
Mean	4370.98
StDev	2468.24
Variance	6092215
Skewness	1.71409
Kurtosis	3.92577
N	158
Minimum	976.0
1st Quartile	2734.0
Median	3610.6
3rd Quartile	5701.8
Maximum	15479.9
95% Confidence Interval for Mu	
3983.1	4758.8
95% Confidence Interval for Sigma	
2222.8	2775.1
95% Confidence Interval for Median	
3307.3	4040.1

The basic statistics on the *Atetr*^{e} Cl 1 mitotic cell area data show the P-value for the Anderson-Darling normality test as 0.000. As this is below P<0.05 the data is not normally distributed (non-parametric).

A.IV.viii.iii. *Atetr*^{e} Cl 2 Mitotic Cell Areas

Below is a table of all mitotic cell areas measured for *Atetr*^{e} Cl 2 mitotic cell areas using Sigma Scan ®.

2832.051	2155.376	5374.292	2555.451	3984.462
5281.366	2166.41	7040.796	4332.07	5054.081
3799.437	4206.943	5070.97	2464.327	7040.796
2827.773	6255.282	5374.292	4765.622	5070.97
3204.654	3316.57	3192.119	2640.871	2055.32
2346.707	3215.463	2144.868	1605.555	2821.092
2686.658	3673.26	6618.728	3035.091	
4086.395	3735.71	4410.659	7919.009	

Using Minitab 13® the basic statistics, including the Anderson-Darling test for normality, were carried out on the above data set.

Descriptive Statistics

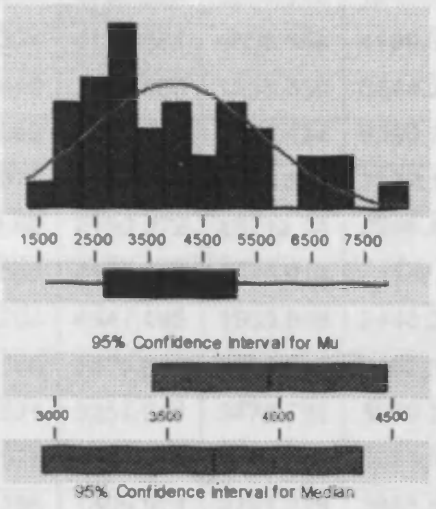

Variable: etr1 cl2

Anderson-Darling Normality Test	
A-Squared:	0.766
P-Value:	0.042
Mean	3956.88
StDev	1590.35
Variance	2529200
Skewness	0.751634
Kurtosis	-1.5E-01
N	38
Minimum	1605.55
1st Quartile	2675.21
Median	3704.48
3rd Quartile	5070.97
Maximum	7919.01
95% Confidence Interval for Mu	
3434.15	4479.62
95% Confidence Interval for Sigma	
1296.55	2057.51
95% Confidence Interval for Median	
2949.71	4365.12

The basic statistics on the *Atetr*^{e} Cl 2 mitotic cell area data show the P-value for the Anderson-Darling normality test as 0.042. As this is below $P<0.05$ the data is not normally distributed (non-parametric).

A.IV.viii.iv. *Atetr*^{e} Cl 1 + Ethylene Mitotic Cell Areas

Below is a table of all mitotic cell areas measured for *Atetr*^{e} Cl 1 + ethylene mitotic cell areas using Sigma Scan ®.

12218.5	3721.449	3836.592	2206.568	1698.555	8737.099	8048.564	16038.21
3438.469	3365.96	4607.694	1593.47	1884.031	2323.588	8614.674	5921.336
2851.792	5501.595	5286.17	2287.709	2499.231	3961.944	9421.655	3072.021
4019.891	7825.108	5637.53	4418.615	4056.821	4189.979	5209.983	6208.745
1944.305	8195.084	3796.96	8712.779	1504.447	4093.001	11589.79	5092.513
10185.93	3422.706	2624.658	1319.197	1584.162	3030.737	3189.116	4769.976

4844.136	8389.041	2239.445	1808.294	6144.417	6314.13	4731.319	2986.827
3260.274	4533.609	4105.686	2884.143	12000.08	5221.317	7032.089	1028.411
2504.71	5506.324	4137.887	4656.859	4199.662	4155.601	3654.795	989.2287
2103.734	6023.419	2554.476	1856.859	3444.023	11044.02	4758.491	6780.784
2139.914	3632.652	6966.936	6429.424	6290.711	4020.116	7276.938	3924.789
4379.734	4707.975	7181.91	4365.622	3122.162	3601.201	12557.93	2114.993
4135.935	6301.52	2150.272	13712.14	2255.433	10805.7	1608.857	1269.882
1478.476	5739.538	4176.168	4970.914	4147.57	4146.144	3108.05	4435.429
2139.463	5839.294	4547.195	1905.648	2446.238	1733.383	4575.418	4295.59
3316.42	6751.586	5875.699	1805.892	2102.683	7721.674	3214.111	
3623.119	3349.521	3251.041	3478.701	5580.259	2752.411	2049.24	
2174.517	3381.573	3876.825	3645.112	8023.344	4109.214	3216.288	
2678.101	1737.136	1469.994	2791.218	3656.896	2748.358	3400.488	
6508.688	6867.18	2636.817	5488.91	2020.266	3679.264	1885.532	

Using Minitab 13® the basic statistics, including the Anderson-Darling test for normality, were carried out on the above data set.

Descriptive Statistics

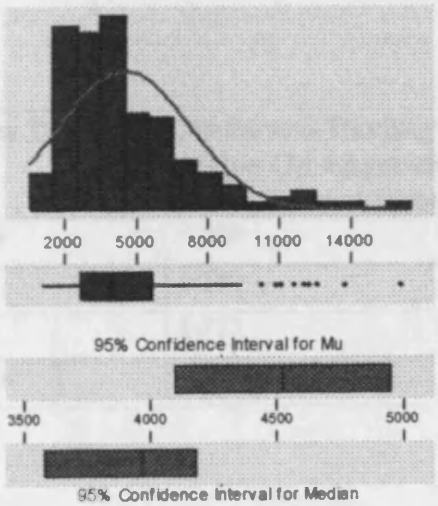

Variable: etr1 + E

Anderson-Darling Normality Test

A-Squared:	5.233
P-Value:	0.000
Mean	4523.60
StDev	2703.24
Variance	7307482
Skewness	1.56390
Kurtosis	2.92575
N	155
Minimum	989.2
1st Quartile	2624.7
Median	3961.9
3rd Quartile	5637.5
Maximum	16038.2

95% Confidence Interval for Mu

4094.7 4952.5

95% Confidence Interval for Sigma

2432.1 3042.9

95% Confidence Interval for Median

3579.8 4178.6

The basic statistics on the *Atetr*^{e} Cl 1 + ethylene mitotic cell area data show the P-value for the Anderson-Darling normality test as 0.000. As this is below P<0.05 the data is not normally distributed (non-parametric).

A.IV.viii.v. Comparison Of Control, *Atetr1*-Expressing, And *Atetr*^{e} Cl 1 + Ethylene Mitotic Cell Areas

A.IV.viii.v.i. Logarithmic Transformation Of Mitotic Cell Area Data Sets

Although all the mitotic cell area measurements taken for the above were non-parametric, data was logarithmically transformed so that comparisons could be made between *Atetr1* mitotic cell area measurements and those carried out for previous chapters. This resulted in all data sets being normally distributed, enabling use of the same statistical test used for previous comparisons of mitotic cell sizes.

Mitotic Cell Area Data Set	Anderson-Darling P-Value On Logarithmically Transformed Data	Normally Distributed?
Control (Wild-Type)	0.990	Yes
Atetr^{e} Cl 1	0.133	Yes
Atetr^{e} Cl 2	0.717	Yes
Atetr^{e} Cl 1 + Ethylene	0.721	Yes

AIV.viii.v.ii. 2 Sample t-Test Between Logarithmically Transformed Mitotic Cell Area Data Sets

As with the analysis of ethylene and 1-MCP treatments, a two-sample t-test was used over ANOVA (Analysis of variance) as comparisons could be made between data sets with different *n*-value. A two-sample t-test was chosen over other t-tests as the data sets are considered independent (separate tobacco BY-2 cultures) and the variances were shown to be equal using the F-test (P-value was greater than 0.05). A confidence interval of 95.0% and two-tailed tests (this uses the hypothesis that samples are not equal) were used when comparing mitotic cell area data. The table below gives the results of the two-sample two-tailed t-tests carried out to compare whether there was a statistical difference between control (WT) mitotic cell areas and the *Atetr1*-expressing cell lines. A comparison was also carried out between the two *Atetr1*-expressing cell lines and between *Atetr*^{e} Cl 1 and *Atetr*^{e} Cl 1 + ethylene.

Mitotic Cell Areas To Be Compared	**T-value and P-value**	**Degrees of Freedom**	**Significant Difference?**
Control versus *Atetr1* clone 1	T = -5.59 P = 0.000	249	Yes
Control versus *Atetr1* clone 2	T = -3.22 P = 0.002	47	Yes
Control versus *Atetr1* clone 1 + ethylene	T = -5.40 P = 0.000	232	Yes
Atetr1 clone 1 versus *Atetr1* clone 2	T = 0.48 P = 0.630	194	No
Atetr1 clone 1 versus *Atetr1* clone 1 + ethylene	T = -0.19 P = 0.851	311	No

Appendix V – Chapter 6 Experimental Data

This appendix gives all the experimental data for chapter 6 including statistical analysis of mitotic cell sizes.

A.V.i. Cell Cycle Data For *Spcdc25* 1* And EV1 (Figure 6.2 and Figure 6.4a)

The percentage values for *Spcdc25* 1* and EV1 mitotic index (Fig. 6.2) and mortality index (Fig. 6.5a) after a 24 h synchronization with aphidicolin:

Time (h) After Release From Aphidicolin	*Spcdc25* 1* Mitotic Index (%)	*Spcdc25* 1* Mortality Index (%)	EV1 Mitotic Index (%)	EV1 Mortality Index (%)
0	0		0	4
1	7.33	3.67	0	1.67
2	13.67	3	0.33	4.67
3	14.33	13.67	1	3.67
4	11.67	16.33	0.67	3.33
5	5.33	6	0.67	4.67
6	6.33	13.33	1	4.33
7	5.33	14.67	0.67	6
8	6	36.67	0.33	7
9	5.67	14	4.33	1.67
10	4	9.67	23.67	4.33
11	3.67	13	35.33	5
12	6	25.33	23.67	5.67
13	10.33	23.33	14.67	3.33
14	10.67	29.67	8	5.33
15	10	35.67	5.67	2
16	11.67	5.67	1.33	3

17	5.67	12.67	1.33	5.67
18	3.33	13	2	8
19	6	14.67	1.67	7
20	5.67	13.33	3	
21	4.67		4	3.67
22	7.33	5	4	2.33
23	7.67	8.67	2	3
24	7.33	9	6.33	
25			12	
26			6	

A.V.ii. Cell Cycle Data For *Spcdc25* 2* And Spcdc25 3* (Figure 6.3 and Figure 6.5a-b)

The percentage values for the mitotic index (Fig. 6.3) and mortality index (Fig. 6.5a-b) of *Spcdc25* 2* and *Spcdc25* 3* cells against time after the release from a 24 h synchronization with aphidicolin:

Time (h) After Release From Aphidicolin	***Spcdc25* 2* Mitotic Index (%)**	***Spcdc25* 2* Mortality Index (%)**	***Spcdc25* 3* Mitotic Index (%)**	***Spcdc25* 3* Mortality Index (%)**
0	0.67		1.33	
1	1	2	1.67	0.67
2	0.67	4.67	1.33	7.67
3	0	1	2.33	2
4	7	4.33	3.67	2.67
5	13.67	4.33	12.33	9.67
6	27.33	9	22.67	6.67
7	12	3.33	13	1.33
8	10.67	1.67	11.67	2.67
9	9	2	5	3

10	7.33	4.33	3	2
11	4.33	1	3	1.67
12	2	2	1.67	1
13	3	3	1.67	2
14	1.33	7.67	2	4
15	4	3.67	2.67	3.33
16	6	9	8.67	3.67
17	12.33	2	13.67	2.33
18	13.22	5	9.33	4.33
19	8	3	9.33	3.67
20	11	4.33	8.33	3
21	6.33	3.67	5	2
22	5	3.33	6	1
23	4.33	4	5.67	0
24	4.33	0.33	3.33	3.33

A.V.iii. Cell Cycle Data For EV2 (Figure 6.3 and Figure 6.5c)

The percentage values for EV1 mitotic index (Fig. 6.3) and mortality index (Fig. 6.5c) after a 24 h synchronization with aphidicolin:

Time (h) After Release From Aphidicolin	EV1 Mitotic Index (%)	EV1 Mortality Index (%)
0	0.67	
1	0.67	1.33
2	0	2
3	1	2
4	1	2.33
5	0	4

6	8.67	4.33
7	14.67	2.33
8	15.67	1.33
9	9.56	2.33
10	9.67	5.67
11	7	0.33
12	4.33	1.67
13	3	1
14	1	2
15	1.67	0.67
16	1.33	0.67
17	2.33	1.33
18	2.33	1.33
19	4.33	0.67
20	6.67	1.67
21	10.67	3
22	7	3.33
23	8.33	2.67
24	4.33	4.33

A.V.iv. Histone H4 Expression Level Data For *Spcdc25* 3* (Fig. 6.4)

The raw volume values for histone H4, 18S ribosomal RNA, and histone H4 corrected against 18S Ribosomal RNA (Fig. 6.4) in *Spcdc25* 3*.

Time (h) after release from aphidicolin	Histone H4 Expression In Spcdc25 3*	18S Ribosomal RNA Expression In *Spcdc25* 3*	Corrected Histone H4 Expression In Spcdc25 3*
0	5840.86	4121.22	1.417
1	11377.4	7232.24	1.573

2	11109.3	6162.46	1.803
3	2832.96	5827.91	0.486

A.V.v. Mitotic Cell Size Data (Figure 6.6)

The average mitotic cell areas and other details were taken from calculations resulting from the tables in the section below regarding statistical analysis of mitotic cell areas.

Cell Line	Mitotic Cell Size (mM^2)	*n*	Standard Error
Wild-type	3046	125	75.7
EV1	3009	82	95.7
EV2	3002	134	108
Spcdc25 1*	1805	140	56.3
Spcdc25 2*	2356	147	86.8
Spcdc25 3*	1848	156	53.9

A.V.vi. Mitotic Index Cell Cycle Data For Mevinolin Treatment Of EV2 (Figure 6.7a)

The percentage values for EV2 mitotic index ± mevinolin (Fig. 6.7a) after a 24 h synchronization with aphidicolin:

Time (h) After Release From Aphidicolin	EV2 Mitotic Index (%)	EV2 + Mevinolin Mitotic Index (%)	EV2 + Mevinolin Mitotic Index (%)
0	0	0	0
1	0	0	0

2	0	0	0
3	0	0	0
4	0.33	0	0
5	0	0.33	0
6	1.67	0.33	0.33
7	1.67	1.67	0.67
8	5	2	1.33
9	21	6.33	2.33
10	29	3.33	9.33
11	13.67	15.67	9.67
12	10.67	11.67	9

A.V.vii. Mitotic Index Cell Cycle Data For Mevinolin Treatment Of *Spcdc25* 3* (Figure 6.7b)

The percentage values for *Spcdc25* 3* mitotic index ± mevinolin (Fig. 6.7b) after a 24 h synchronization with aphidicolin:

Time (h) After Release From Aphidicolin	***Spcdc25* 3* Mitotic Index (%)**	***Spcdc25* 3* + Mevinolin Mitotic Index (%)**	***Spcdc25* 3* + Mevinolin Mitotic Index (%)**
0	0	0	0
1	0.33	0	0
2	0	0	0.33
3	0	0.33	0
4	0	0	0
5	0.33	0.67	0
6	2.33	4.33	1
7	9.67	11.67	11.67
8	21	18.33	20
9	19.67	13.33	19.67
10	12	9.67	10.67

A.V.viii. The Frequency Of Doublets In *Spcdc25* 1*, Spcdc25 3*, EV1, and EV2 (Figure 6.9)

The frequency of doublets (%) occurring in a 7 day batch culture of *Spdc25* 1*, *Spcdc25* 3*, EV1, and EV2 cell lines (Fig. 6.9).

Day	*Spcdc25* 1* Doublet Frequency (%)	*Spcdc25* 3* Doublet Frequency (%)	EV1 Doublet Frequency (%)	EV2 Doublet Frequency (%)
1	6.4	2.1	0	0
2	9.6	7.4	1	0
3	24.2	17.9	0	0
4	33.7	18.8	0	0
5	26.4	8.7	0	0
6	16.6	3.3	0	0
7	4.4	2.1	0	0

A.V.ix. Cell Cycle Data For *Spcdc25* 1* ± Ethylene (Figure 6.10)

The percentage values for *Spcdc25* 1* mitotic index and mortality index ± ethylene (Fig. 6.10) after a 24 h synchronization with aphidicolin.

Time (h) After Release From Aphidicolin	*Spcdc25* 1* Mitotic Index (%)	*Spcdc25* 1* Mortality Index (%)	*Spcdc25* 1* + Ethylene Mitotic Index (%)	*Spcdc25* 1* + Ethylene Mortality Index (%)
0				
1	0	1	0	2.33

2	0	2.67	0	2.33
3	0	2.67	0	0.67
4	0.33	3.67	0.33	3.33
5	0	14.33	0.33	4.67
6	1.67	4	2.67	5
7	3.67	4	15.33	4
8	16.33	35.33	20.33	10.67
9	11.33	48.33	11	10.67
10	8.67	17.33	6.33	20.33
11	8	4.33	5.67	2.67
12				

A.V.x. Statistical Analysis Of Mitotic Cell Areas

All statistical analysis was carried using Minitab 13® in conjunction with the Sigma Scan® measured mitotic cell areas.

A.V.x.i. Wild-Type Mitotic Cell Areas

Below is a table of all mitotic cell areas measured for wild-type mitotic cell areas using Sigma Scan ®. The same data was used as that in the ethylene chapter since wild-type mitotic cell areas was seen to be consistent between synchrony experiments.

2106.962	2708.576	3119.61	2616.401	2787.315	3540.777	1711.616	4856.296	2409.007
3989.942	4117.47	3915.857	2424.845	3212.535	2314.43	1298.48	3523.738	2490.674
3641.133	2044.736	3607.506	2509.214	3459.111	1773.241	1627.172	3101.445	2928.805
3901.37	1956.54	4192.531	2013.811	4041.359	3965.397	2503.134	3390.43	2701.745

3506.924	2125.502	4019.666	2407.506	3216.814	4476.787	2757.591	2174.892	3660.199
3759.505	3189.491	3831.113	1989.341	3090.936	2873.034	2687.258	2706.099	3426.759
5164.421	3291.95	3949.334	2240.195	2291.162	4574.217	4942.09	3091.912	2466.054
2284.031	3448.527	4937.211	2625.934	2746.632	2007.056	3418.202	2344.98	2860.199
2709.702	3089.81	3010.021	4477.163	1921.711	6701.595	2643.648	2445.112	2651.905
2785.438	2755.264	3514.28	4003.378	1929.518	2501.858	3186.789	2578.12	3243.986
2752.336	3034.941	3676.037	2931.056	2567.086	3290.373	1790.655	2378.232	2345.205
2914.243	3244.736	2692.588	2531.432	2051.942	3901.07	4719.084	1894.314	2862.976
3543.779	2843.31	3775.042	2766.673	3416.851	4145.693	3148.883	2256.859	2827.247
2216.176	2516.194	3009.8705	2929.18	3032.164	2641.396	3378.87	3480.503	

Using Minitab 13® the basic statistics, including the Anderson-Darling test for normality, were carried out on the above data set.

Descriptive Statistics

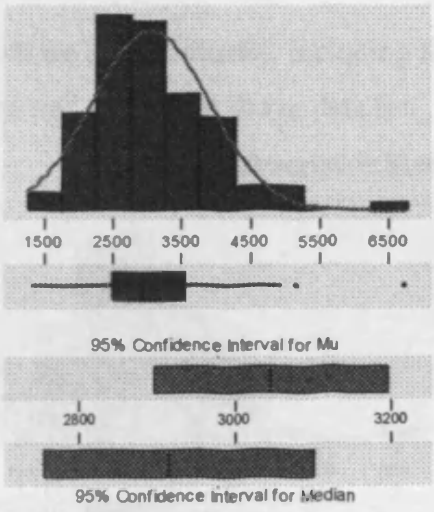

Variable: C1

Anderson-Darling Normality Test

A-Squared:	1.052
P-Value:	0.009
Mean	3045.94
StDev	846.70
Variance	716902
Skewness	0.964681
Kurtosis	2.03004
N	125
Minimum	1298.48
1st Quartile	2478.36
Median	2914.24
3rd Quartile	3519.01
Maximum	6701.60

95% Confidence Interval for Mu

2896.05 3195.84

95% Confidence Interval for Sigma

753.16 966.98

95% Confidence Interval for Median

2752.49 3100.96

The basic statistics on the control mitotic cell area data show the P-value for the Anderson-Darling normality test as 0.009. As this is below $P<0.05$ the data is not normally distributed (it is non-parametric).

A.V.x.ii. EV1 Mitotic Cell Areas

Below is a table of all mitotic cell areas measured for mitotic cells transformed with the *Spcdc25* empty vector, EV1. Measurements were taken using Sigma Scan ®.

3261.55	2740.552	2584.65	2370.351	3214.562	1542.879	2363.145
3206.23	2729.893	2874.611	4627.96	4072.884	3878.551	2790.767
2332.52	2911.09	2482.567	2559.88	2473.41	2918.521	2770.201
2936.536	4273.522	1716.87	1797.035	3848.752	4205.967	2190.655
6295.59	2229.762	1928.317	4048.64	3135.748	3244.361	1745.243
3529.142	1701.257	2000.6	3285.72	1897.992	2737.624	1950.16
4030.775	2189.829	2613.323	3557.741	3386.677	4324.639	2682.379
3664.327	3115.031	4403.978	3231.15	3331.957	3559.617	2799.55
2393.019	3505.348	3141.452	3694.352	2912.291	2917.696	2295.065
3158.716	2956.802	2315.782	3030.362	3381.648	3957.666	1796.209
2044.811	3657.872	1791.706	2286.583	3974.554	2305.874	
2760.743	5233.177	2734.622	4195.684	2689.735	3312.216	

Using Minitab 13® the basic statistics, including the Anderson-Darling test for normality, were carried out on the above data set.

Descriptive Statistics

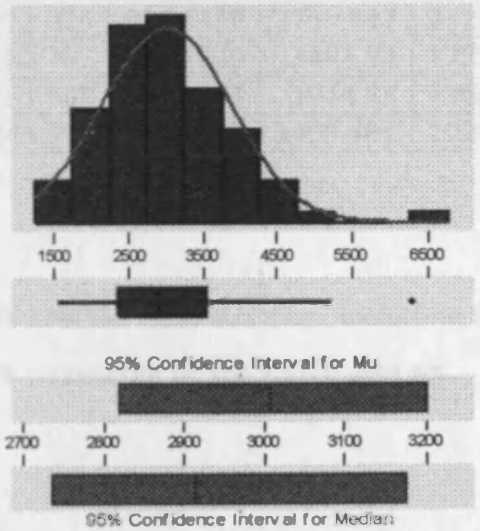

Variable: EV1

Anderson-Darling Normality Test	
A-Squared:	0.528
P-Value:	0.172
Mean	3009.04
StDev	866.85
Variance	751429
Skewness	0.850736
Kurtosis	1.53300
N	82
Minimum	1542.88
1st Quartile	2355.49
Median	2914.99
3rd Quartile	3536.29
Maximum	6295.59
95% Confidence Interval for Mu	
2818.57	3199.51
95% Confidence Interval for Sigma	
751.47	1024.42
95% Confidence Interval for Median	
2736.66	3174.02

The basic statistics on the EV1 mitotic cell area data show the P-value for the Anderson-Darling normality test as 0.172. As this above P<0.05, the data is normally distributed.

A.V.x.iii. *Spcdc25 1** Mitotic Cell Areas

Below is a table of all mitotic cell areas measured for *Spcdc25* 1* mitotic cell areas using Sigma Scan ®.

1682.792	2219.253	1879.977	1905.273	2475.061	2258.585	1023.757	2340.852
1156.164	1527.491	2482.117	1275.136	1048.002	1507.525	1616.438	2246.575
2050.891	2478.964	2426.046	1885.532	2348.208	1366.185	1916.082	2344.605
3554.513	1733.383	1585.663	1279.64	1738.788	1512.479	1048.152	3617.789
2472.434	2780.784	1693.826	1130.118	978.5701	1194.521	2361.944	3137.774
2293.488	2760.593	1637.981	1678.739	1053.631	1581.835	1740.064	1577.857
1770.163	2674.723	903.2839	1458.36	1636.93	2000.15	1911.803	1573.278
1299.606	2667.142	1224.695	2158.604	1735.485	1689.698	2237.718	1397.26
2043.01	4297.392	1771.74	1776.619	2270.144	1637.155	1367.611	932.0323
1548.508	1773.166	1440.721	2325.615	2830.024	1069.544	1674.385	988.8534
1154.738	2239.745	1517.808	1027.135	1088.685	1263.351	1488.159	2264.965
1386.977	1656.146	1859.786	2254.607	1605.78	1120.51	2993.207	1434.415
3711.315	1177.932	1763.933	2065.904	1420.304	1086.132	3218.315	915.2937
1055.883	2810.433	1155.564	1739.088	2661.362	1135.072	2442.109	1064.365
1031.263	923.025	936.5359	2759.017	2123.625	1717.771	2427.923	
1135.448	2482.792	860.1239	1495.74	1722.199	2549.597	1450.253	
1937.549	1251.567	1259.373	1944.38	1968.099	1271.008	974.4417	
1842.222	1245.562	1433.965	3409.495	2029.049	1994.445	1031.713	

Using Minitab 13® the basic statistics, including the Anderson-Darling test for normality, were carried out on the above data set.

Descriptive Statistics

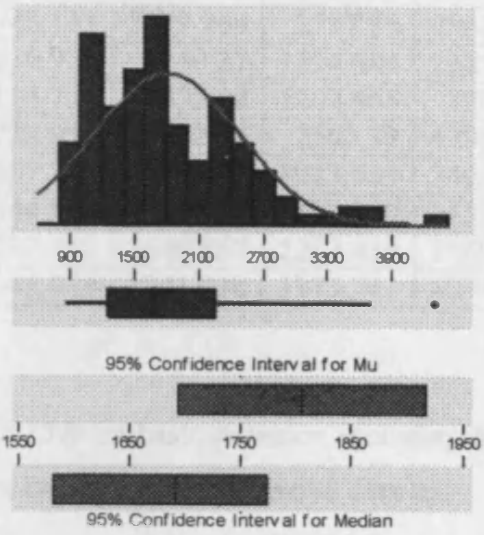

Variable: 1*

Anderson-Darling Normality Test	
A-Squared:	2.019
P-Value:	0.000
Mean	1804.85
StDev	666.24
Variance	443882
Skewness	0.986174
Kurtosis	1.07396
N	140
Minimum	860.12
1st Quartile	1285.27
Median	1691.76
3rd Quartile	2252.60
Maximum	4297.39
95% Confidence Interval for Mu	
1693.52	1916.18
95% Confidence Interval for Sigma	
596.28	754.95
95% Confidence Interval for Median	
1581.51	1773.44

The basic statistics on the mitotic cell area data show the P-value for the Anderson-Darling normality test as 0.000. As this is below $P<0.05$ the data is not normally distributed (non-parametric).

A.V.x.iv. EV2 Mitotic Cell Areas

Below is a table of all mitotic cell areas measured for EV2 mitotic cell areas using Sigma Scan ®.

1614.487	1629.949	3429.236	2014.262	2234.866	3486.057	2269.394	5871.796
1454.006	3303.809	3593.019	4463.877	2180.146	6697.767	4318.033	4886.695
2092.1	1786.902	1788.628	4886.62	2367.949	1362.432	3725.277	3972.978
2043.761	1673.935	1763.408	2928.279	2113.717	4404.203	6728.017	2209.871
2545.618	4273.147	2116.645	2977.744	1921.411	4410.734	5613.136	2374.104
1825.108	1313.642	3169.375	3536.799	2031.901	1970.876	3336.686	1946.031
4015.913	1853.106	3622.518	2078.439	2619.403	2136.986	1708.088	4418.69

1156.615	2926.628	1561.944	2433.327	5038.469	2038.656	2313.455	1657.046
2381.085	2449.24	2063.502	3295.403	5297.129	4164.759	2696.866	2027.397
2350.985	2748.133	5279.264	2597.26	2962.507	4195.309	3168.399	1950.835
2146.519	2216.926	2240.27	1524.564	2385.663	3392.682	2376.956	2918.972
4080.616	3114.731	1575.08	1302.458	2202.89	1945.731	2576.318	2059.523
2356.915	3728.955	1772.64	2560.33	4795.121	2462.376	4710.377	5539.801
3181.31	2567.311	3460.612	1923.513	3495.815	1849.953	5607.806	3892.212
5509.927	2344.305	3143.254	6398.349	3139.801	3082.98	972.9405	3153.913
4113.267	3337.512	3546.857	2237.418	3169.825	5644.736	4630.362	
2538.488	2046.988	3203.078	3373.241	3238.131	2873.935	2787.915	

Using Minitab 13® the basic statistics, including the Anderson-Darling test for normality, were carried out on the above data set.

Descriptive Statistics

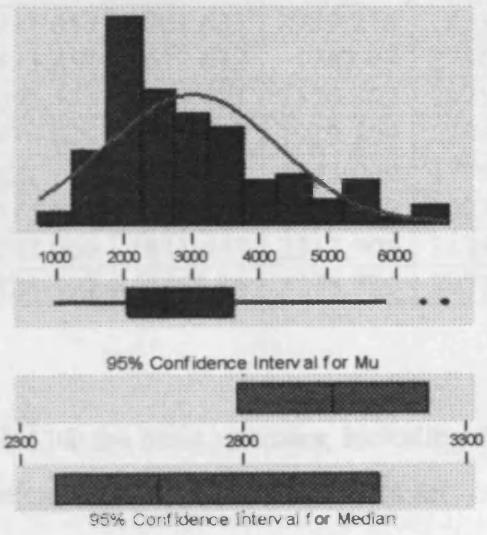

Variable: EV2

Anderson-Darling Normality Test	
A-Squared:	3.254
P-Value:	0.000
Mean	3002.37
StDev	1251.51
Variance	1566268
Skewness	0.980850
Kurtosis	0.403556
N	134
Minimum	972.94
1st Quartile	2056.39
Median	2808.33
3rd Quartile	3600.39
Maximum	6728.02
95% Confidence Interval for Mu	
2788.53	3216.22
95% Confidence Interval for Sigma	
1117.48	1422.35
95% Confidence Interval for Median	
2377.69	3109.06

The basic statistics on the EV2 mitotic cell area data show the P-value for the Anderson-Darling normality test as 0.000. As this is below $P<0.05$ the data is not normally distributed (non-parametric).

A.V.x.iii. *Spcdc25* 2* Mitotic Cell Areas

Below is a table of all mitotic cell areas measured for *Spcdc25* 2* mitotic cell areas using Sigma Scan ®.

4344.08	2729.217	1634.603	2301.895	1371.064	2263.164	1599.55	2240.12
4654.607	1534.322	2250.328	2113.417	1495.515	2338.75	1639.632	4887.371
2071.908	2068.305	1724.451	1996.622	1608.707	1879.452	1716.87	1180.784
7423.457	2438.431	1928.992	1559.767	2331.019	2464.027	1785.025	6769.225
2238.769	2020.342	1760.856	2993.883	3475.399	1726.253	2981.723	2790.392
2736.799	2588.929	1516.907	3768.812	4256.859	2329.142	1716.044	3382.548
1202.477	2126.928	1342.841	4279.227	2031.751	2454.87	1688.872	2907.262
1890.186	1602.552	1117.058	2805.404	1477.951	2614.449	2390.542	2369.3
1948.208	2128.579	1543.404	2171.815	4190.054	3159.017	2350.535	3519.535
1527.491	1584.462	1942.578	2982.023	4037.305	2130.006	1822.556	2068.831
1802.965	1789.004	1864.29	2312.704	3618.915	2124.977	1366.185	1999.775
1505.723	1911.653	1701.633	2939.238	1853.706	1988.891	1052.88	2047.138
3155.639	2833.252	1677.613	1742.09	2736.649	1723.325	1782.774	2162.432
3550.235	2053.443	1871.421	1356.802	1375.418	2333.871	2172.64	2418.24
3876.825	2374.629	1554.813	1919.309	2184.575	1545.356	1743.216	
3605.63	2121.449	3237.831	1543.029	1799.362	2400	2301.22	
2002.327	4474.611	1561.193	1485.082	2023.869	2853.819	1133.421	
1617.339	2143.066	1811.447	2313.905	3139.351	1899.719	1274.686	
6996.134	2328.392	1765.96	3278.739	3973.278	2260.011	975.943	

Using Minitab 13® the basic statistics, including the Anderson-Darling test for normality, were carried out on the above data set.

Descriptive Statistics

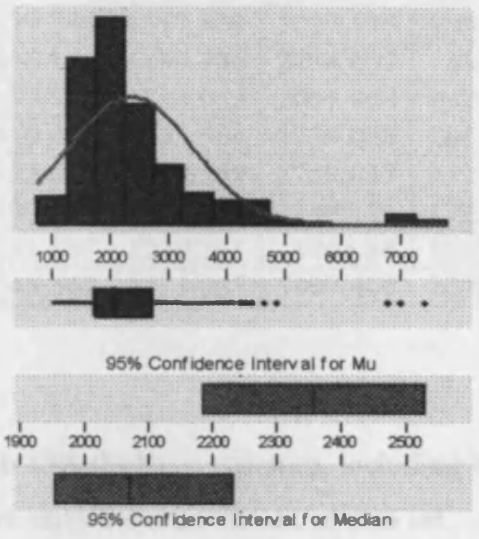

Variable: 2*

Anderson-Darling Normality Test	
A-Squared:	7.578
P-Value:	0.000
Mean	2356.34
StDev	1052.33
Variance	1107408
Skewness	2.24871
Kurtosis	6.92581
N	147
Minimum	975.94
1st Quartile	1716.87
Median	2071.91
3rd Quartile	2729.22
Maximum	7423.46
95% Confidence Interval for Mu	
2184.80	2527.87
95% Confidence Interval for Sigma	
944.23	1186.61
95% Confidence Interval for Median	
1953.72	2231.43

The basic statistics on the mitotic cell area data show the P-value for the Anderson-Darling normality test as 0.000. As this is below $P<0.05$ the data is not normally distributed (non-parametric).

A.V.x.vi. *Spcdc25* 3* Mitotic Cell Areas

Below is a table of all mitotic cell areas measured for *Spcdc25* 3*mitotic cell areas using Sigma Scan ®.

1682.792	2219.253	1879.977	1905.273	2475.061	2258.585	1023.757	2340.852
1156.164	1527.491	2482.117	1275.136	1048.002	1507.525	1616.438	2246.575
2050.891	2478.964	2426.046	1885.532	2348.208	1366.185	1916.082	2344.605
3554.513	1733.383	1585.663	1279.64	1738.788	1512.479	1048.152	3617.789
2472.434	2780.784	1693.826	1130.118	978.5701	1194.521	2361.944	3137.774
2293.488	2760.593	1637.981	1678.739	1053.631	1581.835	1740.064	1577.857
1770.163	2674.723	903.2839	1458.36	1636.93	2000.15	1911.803	1573.278
1299.606	2667.142	1224.695	2158.604	1735.485	1689.698	2237.718	1397.26

2043.01	4297.392	1771.74	1776.619	2270.144	1637.155	1367.611	932.0323
1548.508	1773.166	1440.721	2325.615	2830.024	1069.544	1674.385	988.8534
1154.738	2239.745	1517.808	1027.135	1088.685	1263.351	1488.159	2264.965
1386.977	1656.146	1859.786	2254.607	1605.78	1120.51	2993.207	1434.415
3711.315	1177.932	1763.933	2065.904	1420.304	1086.132	3218.315	915.2937
1055.883	2810.433	1155.564	1739.088	2661.362	1135.072	2442.109	1064.365
1031.263	923.025	936.5359	2759.017	2123.625	1717.771	2427.923	
1135.448	2482.792	860.1239	1495.74	1722.199	2549.597	1450.253	
1937.549	1251.567	1259.373	1944.38	1968.099	1271.008	974.4417	
1842.222	1245.562	1433.965	3409.495	2029.049	1994.445	1031.713	

Using Minitab 13® the basic statistics, including the Anderson-Darling test for normality, were carried out on the above data set.

Descriptive Statistics

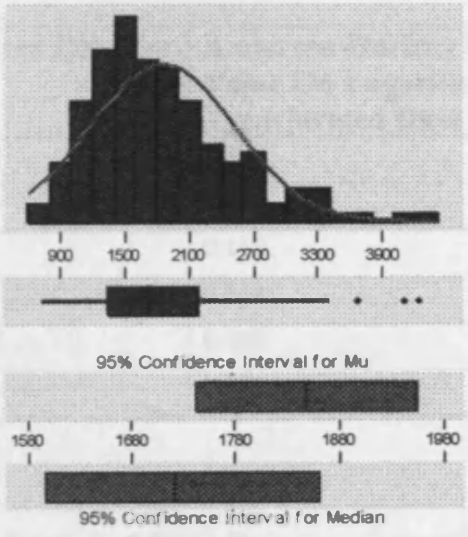

Variable: 3*

Anderson-Darling Normality Test	
A-Squared:	2.418
P-Value:	0.000
Mean	1847.97
StDev	673.70
Variance	453878
Skewness	1.01281
Kurtosis	1.09122
N	156
Minimum	731.32
1st Quartile	1353.86
Median	1721.67
3rd Quartile	2178.01
Maximum	4238.77
95% Confidence Interval for Mu	
1741.42	1954.52
95% Confidence Interval for Sigma	
606.33	758.06
95% Confidence Interval for Median	
1598.64	1861.76

The basic statistics on the mitotic cell area data show the P-value for the Anderson-Darling normality test as 0.000. As this is below $P<0.05$ the data is not normally distributed (non-parametric).

A.V.x.vii. Comparison Of WT, EV, And *Spcdc25*-Expressing Mitotic Cell Areas

A.V.x.vii.i. Logarithmic Transformation Of Mitotic Cell Area Data Sets

Since the majority of mitotic cell areas showed non-parametric distribution whilst EV1 mitotic cell areas were normally distributed, all mitotic cell area data sets were logarithmically transformed. This resulted in all but one data sets being normally distributed. Although this presents a problem with carrying out a two sampled t-test, I decided to keep the statistical test constant with all previous tests on mitotic cell sizes.

Mitotic Cell Area Data Set	Anderson-Darling P-Value On Logarithmically Transformed Data	Normally Distributed?
Wild-type	0.990	Yes
EV1	0.785	Yes
Spcdc25 1*	0.117	Yes
EV2	0.162	Yes
Spcdc25 2*	0.000	No
Spcdc25 3*	0.994	Yes

A.V.x.vii.ii. 2 Sample t-Test Between Logarithmically Transformed Mitotic Cell Area Data Sets

There are a number of parametric tests available to analysis normally distributed data sets. A two-sample t-test was used over ANOVA (Analysis of variance) as comparisons could be made between data sets with different *n*-value. A two-sample t-test was chosen over other t-tests as the data sets are considered independent (separate tobacco BY-2 cultures). A confidence interval of 95.0% and two-tailed tests (this uses the hypothesis

that samples are not equal) were used when comparing mitotic cell area data. The table below gives the results of the two-sample two-tailed t-tests carried out to compare whether there was a statistical difference between EV mitotic cell areas and *Spcdc25* mitotic cell areas. A comparison was also carried out between WT and EV lines.

Mitotic Cell Areas To Be Compared	**T-value and P-value**	**Degrees of Freedom**	**Significant Difference?**
EV1 versus *Spcdc25* 1*	T = 10.84 P = 0.000	137	Yes
WT versus *Spcdc25* 1*	T = 12.31 P = 0.000	199	Yes
EV2 versus *Spcdc25* 2*	T = 5.13 P = 0.000	279	Yes
WT versus *Spcdc25* 2*	T = 5.11 P = 0.000	270	Yes
EV2 versus *Spcdc25* 3*	T =10.53 P = 0.000	288	Yes
WT versus *Spcdc25* 3*	T =14.11 P = 0.000	278	Yes
WT versus EV1	T =0.39 P = 0.698	205	No
WT versus EV2	T =1.38 P = 0.167	234	No

A.V.x.vii.iii. Mann-Whitney Test Between Spcdc25 2* And EV2 Untransformed Mitotic Cell Area Data Sets

To ensure that there was a significant difference in mitotic cell sizes between *Spcdc25* 2* and its control cell line (EV2), a mann-whitney test was carried out on the untransformed data. Both data sets showed non-parametric distribution before logarithmic transformation (see above), enabling a comparison using mann-whitney to be carried out between them. Results indicated that there was a significant difference between *Spcdc25* 2* and EV2, the same result as the two sampled t-test.